

The Recovery of Microalgae Cells onto a Non-Porous Adsorbent

A thesis submitted to The University of Manchester in fulfilment of the requirements of the degree of Doctor of Philosophy in the Faculty of Science and Engineering.

AKINLABI ADEYEMI

SCHOOL OF CHEMICAL ENGINEERING AND ANALYTICAL SCIENCE

2017

I. Table of Contents

I. Table of Contents.....	3
II. List of Figures.....	7
III. List of Tables.....	16
IV. List of Symbols.....	18
V. List of Abbreviations.....	20
VI. Abstract.....	21
VII. Declaration.....	23
VIII. Copyright.....	24
IX. Confidentiality.....	24
X. Dedication.....	25
XI. Acknowledgements.....	26
1 Introduction.....	27
1.1 Brief Background and Motivation	27
1.2 Research Strategy	30
1.2.1 Literature Review	30
1.2.2 Research Objectives and Experimental Studies.....	31
1.3 Experimental Rational and Scope.....	32
1.4 Thesis Structure	33
2 Literature Review.....	35
2.1 Why Oleaginous Microbial Cells?	35
2.1.1 The Biological and Chemical Characteristics of Microalgae	39
2.1.2 The Potentials of Microalgal Biomass	41
2.1.3 Summary	44
2.2 Present Techniques of Harvesting Microalgae Cells and Extracting Lipids	45
2.2.1 Introduction.....	45
2.2.2 Strain Isolation and Selection	45
2.2.3 Cultivation (Suspended systems)	48
2.2.4 Harvesting	50
2.2.5 Lipids Extraction	58
2.2.6 Challenges and Prospects.....	68
2.2.7 Summary	70
2.3 Adsorption and Electrochemical Methods.....	71
2.3.1 Introduction	71
2.3.2 Adsorption Process.....	71

2.3.3	Adsorption for Microbial Applications.....	80
2.3.4	Electrochemical Process	86
2.3.5	The Arvia Process	91
2.3.5	Summary.....	93
3	Experimental Programme Overview	95
3.1	Nyex™ - The Adsorbent Material	95
3.2	Microalgae strain, growth conditions and cultivation.....	98
3.2.1	Microalgae Strain.....	98
3.2.2	Growth Conditions	99
3.2.3	Cultivation	100
3.3	Evaluation of Batch Recovery of Microalgae Cells onto Adsorbent	101
3.3.1	Adsorbent and Microalgae cells.....	101
3.3.2	Microalgae Cell Recovery from Suspension	101
3.3.3	Recovery of Microalgae Cells in the Arvia Y-cell	103
3.3.4	Effect of Growth Characteristics on Adsorption Recovery	104
3.3.5	Effect of pH on Adsorption Recovery.....	104
3.3.6	Acidic Properties of Nyex™ Particles.....	105
3.3.7	Measurement of the Zeta Potential of <i>Chlamydomonas reinhardtii</i>	105
3.3.8	Influence of the Acidic Properties of Nyex™	105
3.4	Adsorption Column Studies of Microalgae Cells Recovery	106
3.4.1	Downward flow mode	106
3.4.2	Upward and Submerged flows mode	107
3.4.3	Control studies.....	107
3.5	Adsorbent Regeneration, Reuse and Lipids Recovery	108
3.5.1	Equipment description	108
3.5.2	Preparation of Catholyte.....	108
3.5.3	Adsorbent Regeneration at different current densities	109
3.5.4	Reuse of Regenerated Adsorbent in Batch Mode	110
3.5.5	Effects of Constant Electrical Charge on Regeneration and Reuse	110
3.5.6	Effects of Constant Electrical Energy on Regeneration and Reuse.....	111
3.5.7	Reuse of Regenerated Adsorbent in a Fixed Bed Column	112
3.5.8	Effects of particle size variation of Nyex™ on cells recovery.....	113
3.5.9	Cell wall rupture and Lipid recovery tests.....	114
3.6	Analytical Techniques	115
3.6.1	Absorbance Measurement by Spectrophotometer	115
3.6.2	Cell Counting by Haemocytometer	116
3.6.3	Other Analytical Techniques considered.....	118

3.7 Error Analysis.....	119
3.8 Calibration Curves.....	121
3.9 Summary.....	121
4 Results and Discussions.....	123
4.1 Evaluation of Batch Recovery of Microalgae Cells onto Adsorbent.....	123
4.1.1 Introduction.....	123
4.1.2 Influence of Contact Time	123
4.1.3 Influence of Initial Concentration of Microalgae Suspension	125
4.1.4 Influence of the Intensity of Agitation	127
4.1.5 Influence of Microalgae Cell Size.....	129
4.1.6 Influence of Media Change on Cell Viability and Recovery	131
4.1.7 Adsorption Isotherms and Capacities.....	134
4.1.8 Microalgae Recovery in the Arvia Y-cell.....	141
4.1.9 Summary	146
4.2 Understanding the mechanisms of adsorption; Zeta Potential and pH effects..	147
4.2.1 Introduction	147
4.2.2 Effect of Growth Characteristics on the Adsorption of Microalgae Cells....	147
4.2.3 Effect of pH on the recovery of microalgae cells using Adsorption.....	150
4.2.4 Proposed Mechanisms for Cell Recovery from Suspension	156
4.2.5 Summary	161
4.3 Adsorption Column Studies of Microalgae Cells Recovery	162
4.3.1 Introduction	162
4.3.2 Effect of Flow Rate.....	163
4.3.3 Effect of Bed Depth.....	164
4.3.4 Effect of the Initial Feed Concentration	165
4.3.5 Fixed-Bed Scenarios and Performance Comparison.....	166
4.3.6 Performance Comparison of Upward and Downward Flows.....	168
4.3.7 Performance Comparison of Submerged and Conventional Fixed Bed....	171
4.3.8 Anomalous behaviour of Microalgae Cell Recovery in the Fixed Bed.....	173
4.3.9 Control Studies	180
4.3.10 Summary	182
4.4 Adsorbent Regeneration, Reuse and Lipids Recovery.....	184
4.4.1 Introduction	184
4.4.2 Reuse of Regenerated Adsorbent at Varied Current Densities in Batch....	185
4.4.3 Evaluation of Adsorption Recovery Performance of Nyex™ ‘Variants’.....	186
4.4.4 Effects of Electrical Charge and Energy on Regeneration and Reuse.....	190
4.4.5 Reuse of Regenerated Adsorbent in a Fixed Bed Column	192

4.4.6	Effects of Nyex™ particles size variation on cells recovery	196
4.4.7	Effects of Electrochemical Regeneration on Adsorbed Microalgae Cells ..	200
4.4.8	Lipid Recovery Analysis.....	205
4.4.9	Summary	207
5	Modelling the Recovery of Microalgae Cells in a Fixed Bed Column	209
5.1	Introduction	209
5.2	Fixed bed process models	210
5.2.1	The Bohart-Adams Model	211
5.2.2	The Bed Depth Service Time (BDST) Model.....	213
5.2.3	The Thomas Model.....	214
5.2.4	The Clark Model	215
5.2.5	The Modified Dose Response (MDR) Model.....	217
5.3	Data and Error Analysis	219
5.4	Results and Discussions	219
5.4.1	Non Linear Analysis.....	219
5.4.2	Linear Analysis	226
5.5	Adaptation of the Logistic Functionality of Bed Column Models	238
5.6	Summary	243
6	Conclusions and Future Perspectives	245
6.1	Conclusions	245
6.2	Future Perspectives	248
6.2.1	Recovery of Variety of Microalgae Strains	248
6.2.2	Choice of Adsorbent Material.....	249
6.2.3	Effects of electrode materials/catholyte.....	249
6.2.4	Development of a protocol to estimate total lipids released.....	250
6.2.5	Dual use of technique for bioremediation.....	250
6.2.6	Energy and cost implications	251
	References.....	251

II. List of Figures

Figure 1:1: The total primary energy share by fuel usage in 1973 and 2013 (IEA, 2015) .27	.27
Figure 1:2: World CO ₂ emissions from fuel combustion from 1971 to 2013 by fuel [Mt of CO ₂] (IEA, 2015).28	.28
Figure 2:1: Share of bioenergy in the world primary energy mix (IEA, 2009)36	.36
Figure 2:2: The classification of biomass sources.36	.36
Figure 2:3: Nearly 1 billion people do not have enough food to lead a healthy active life (Brown, 2012)37	.37
Figure 2:4 Biorefinery concept for microalgae biomass.44	.44
Figure 2:5: Schematic diagram of the stages for lipid recovery from microalgae cells.45	.45
Figure 2:6: Schematic of stages involved in strain isolation and selection (Mutanda <i>et al.</i> , 2011).47	.47
Figure 2:7: Plan view of an open raceway pond. Microalgae suspension is introduced after the paddlewheel, and completes a cycle as it is being mechanically aerated with CO ₂ . Biomass are harvested before the paddlewheel to repeat the cycle again (Brennan and Owende 2010).49	.49
Figure 2:8: Basic design of a horizontal tubular photobioreactor. The two main sections include the airlift system and solar collector; the airlift system allow for the transfer of oxygen out of the system and transfer of carbon dioxide into the system in addition to providing a means to harvest the biomass. The solar collector provides a platform for the microalgae cells to grow by giving a high surface area to volume ratio (Brennan and Owende, 2010).50	.50
Figure 2:9: Schematic representation of proposed mechanism involved in the bioflocculation of <i>Chlorella vulgaris</i> cells using <i>Ankistrodesmus falcatus</i> as the flocculating microalgae cell (Salim <i>et al.</i> , 2011).53	.53
Figure 2:10: Schematic comparing conventional (dead end) and Tangential flow filtration systems (Stevens <i>et al.</i> , 2013).55	.55
Figure 2:11: Schematic of flotation method combined with flocculation (Gerardo <i>et al.</i> , 2015)56	.56
Figure 2:12: Grouping of the cell disruption methods (Günerken <i>et al.</i> , 2015).59	.59
Figure 2:13: High pressure homogenization (Patravale <i>et al.</i> , 2004)60	.60

Figure 2:14: Schematic diagram of the proposed organic solvent extraction mechanisms. Pathway shown at the top of the cell: mechanism for non-polar organic solvent. Pathway shown at the bottom of the cell: mechanism for non-polar/polar organic solvent mixture. ● lipids, ○ non-polar organic solvent, ◇ polar organic solvent (Halim <i>et al.</i> , 2012).	63
Figure 2:15: Schematic of in situ biomass transesterification (Rawat <i>et al.</i> , 2013).	67
Figure 2:16: The schematic of a breakthrough curve showing the movement of the mass transfer zone through the adsorbent bed as a result of throughput (Taty-Costodes <i>et al.</i> , 2005).	77
Figure 2:17: The recovery of microalgae cells from suspension with nanomaterials (Cerff <i>et al.</i> , 2012).	82
Figure 2:18 Simplified model of the electric double-layer at a charged interface in aqueous solution and representation of zeta potential (Malvern, 2001).	84
Figure 2:19: Harvesting procedures for attached growth system (Johnson and Wen, 2010).	86
Figure 2:20: Schematic diagram for batch electroflocculation reactor system (Gao <i>et al.</i> , 2010b)	88
Figure 2:21: Overview of regeneration techniques for spent activated carbon (Sheintuch and Matatov-Meytal, 1999).	92
Figure 3:1: The structure of graphite (Sliwinska-Bartkowiak <i>et al.</i> 2012)	95
Figure 3:2: Scanning Electron Micrograph of Nyex™ flake particles.	96
Figure 3:3: Microscopic image of Chlamydomonas reinhardtii cells (Tsukii, 1995).	99
Figure 3:4: Flask containing microalgae suspension that has attained stationary phase.	101
Figure 3:5 Schematic diagram depicting the Arvia Y-cell.	104
Figure 3:6 Schematic diagram for the experimental setup for the fixed bed studies showing downward flow mode.	106
Figure 3:7 Schematic diagram of batch electrochemical zone within the Arvia Y-cell.....	109
Figure 3:8; A triolein standard curve indicates the fluorescence intensity measured against varying concentrations of triolein after staining with a Nile Red dye.	116
Figure 3:9: A haemocytometer grid showing Neubauer rulings.	118
Figure 3:10: Schematic of cells behaving like a capacitor in the presence of electric field (Poppleton, 2008).	119

Figure 4:1 The residual cell density after adsorption of microalgae cells from suspension onto Nyex™. Initial microalgae suspension concentration of approximately 3,000,000 cells/ml (●) 1,500,000 cells/ml (■) and 750,000 cells/ml (▲).....	124
Figure 4:2: The percentage recovery of microalgae cells from suspension onto Nyex™. Initial microalgae suspension concentration of approximately 3,000,000 cells/ml (●), 1,500,000 cells/ml (■) and 750,000 cells/ml (▲).	125
Figure 4:3; The amount of microalgae cells adsorbed ($\times 10^4$ cells/ml) and percentage recovery of cells from suspensions after mixing a measured mass Nyex™ with varying initial concentration of microalgae suspension.	126
Figure 4:4; The accumulated cell density ($\times 10^4$ cells/ml) and percentage recovery of microalgae cells from suspension when a measured mass of Nyex™ is reused with fresh batch microalgae suspension until the Nyex™ surface is considered saturated.	127
Figure 4:5; Residual cell density of microalgae suspensions after mixing with a measured mass of Nyex™ in a number of centrifuge tubes at various intensity of agitation.....	128
Figure 4:6; Percentage recovery of microalgae cells from suspensions after mixing with a measured mass of Nyex™ in a number of centrifuge tubes at various intensity of agitation.	128
Figure 4:7; The size distribution of <i>Chlamydomonas reinhardtii</i> , <i>Chlorella vulgaris</i> , and <i>Chlorella luteoviridis</i> obtained from measuring the size of random microalgae cells with the aid of a microscopic graticule device and ImageJ software.....	130
Figure 4:8; The percentage recovery and average cell size of <i>Chlamydomonas reinhardtii</i> , <i>Chlorella vulgaris</i> , and <i>Chlorella luteoviridis</i> when Nyex™ was brought in contact with the microalgae strains' suspensions.	130
Figure 4:9; Microscopic images of microalgae cells (A) in their original TAP media and (B) suspended in deionised water.....	132
Figure 4:10; The residual cell density of microalgae cells in TAP and Deionised Water media after mixing the suspensions with 10 g of Nyex™ particles.	132
Figure 4:11; The Initial and Final pH of the suspension media of microalgae cells in TAP and Deionised Water media.....	133
Figure 4:12; Pictorial image of the supernatant of (A) the deionised water media and (B) the TAP media after adsorption.	134
Figure 4:13; Linearised Langmuir adsorption isotherms (at low and high cell concentrations) for the microalgae cells recovered onto the surface of the adsorbent.....	135
Figure 4:14; Linearised Freundlich adsorption isotherm for the microalgae cells recovered from suspension onto the surface of the adsorbent.....	135

Figure 4:15; Comparison of the predicted Langmuir and Freundlich curves with the experimental curve for the adsorption of microalgae cells onto Nyex™ particles.	137
Figure 4:16; Calibration curve relating the concentration of microalgae suspension in mg/ml against the microalgae suspension density in cells/ml.	138
Figure 4:17; Separation factors for microalgae cells onto Nyex™ particles at a range of initial concentrations and a temperature of 21°C.....	140
Figure 4:18; Design graph for the mass of adsorbent required to recover a given percentage of microalgae cells at initial concentration 2.0×10^6 cells/ml, for different volumes of suspension.	141
Figure 4:19; The percentage recovery of microalgae cells in the Arvia Y-cell over 3 adsorption cycles and a control experiment in the absence of Nyex™ particles.....	142
Figure 4:20; Images of froth lifting Nyex™ particles from the adsorption zone of the Arvia Y-cell.....	142
Figure 4:21; Images of froth lifting microalgae cells from the adsorption zone.	143
Figure 4:22; Images of the effect of the addition of antifoam to microalgae suspension to prevent the formation of froth.....	143
Figure 4:23; The percentage recovery (estimated on the basis of optical density measurements) of a number of control experiments in the Arvia reactor in the absence of Nyex™ particles with/without the addition of antifoam.	144
Figure 4:24; Images of the effect of the washing the suspension and resuspending the cells in deionised water.	144
Figure 4:25; The percentage recovery of washed microalgae suspension and a number of control experiments in the Arvia Y-cell in the absence of Nyex™ particles with/without washing.....	145
Figure 4:26; (A) unbroken microalgae cells before being placed into the Arvia Y-cell. (B) broken microalgae cells after air was passed to the suspension in the Arvia Y-cell.	146
Figure 4:27: Growth curve for <i>Chlamydomonas reinhardtii</i>	148
Figure 4:28: The residual cell density in the supernatant of a microalgae suspension at different growth stages after mixing with Nyex™ particles.	149
Figure 4:29: The percentage recovery and pH of suspension after mixing with Nyex™ at various suspension pH.	151
Figure 4:30: The mixture of microalgae cells suspension and Nyex™ after adsorption at different suspension pH is left to settle for 60 minutes. From left to right, suspension pH varies from 3 – 11.....	152



- Figure 4:31: microscopic images of a mixture of microalgae cells  and NyexTM particles  after adsorption and a settlement time of 30 minutes for (A) blank haemocytometer, and cell suspension (B) without NyexTM (C) at pH 3 (D) at pH 4 (E) at pH 5 (F) at pH 7 (G) at pH 7.7 (H) at pH 9 (I) at pH 10 and (J) at pH 11. 155
- Figure 4:32: Acidic properties of NyexTM particles in deionised Water (DW) showing variation in media pH when the adsorbent is added to deionised water (DW), before (■) and after (■) mixing at different intensities of agitation. 156
- Figure 4:33: The concentration of cells adsorbed after a measured mass of NyexTM was mixed with microalgae cells suspension at different intensities of agitation. Controls include: MxNN - Mixing, No Adsorbent; NMxNN - No Mixing, No Adsorbent; NMx+N-No Mixing, Adsorbent present. 157
- Figure 4:34: Zeta potential of *C. reinhardtii* at various suspension pH..... 159
- Figure 4:35: Changes in the suspension of microalgae cells at various pH where suspension medium at pH 11 had more cells sediment. The red oval shows cell flocculation and sedimentation. 161
- Figure 4:36: Breakthrough curves for the recovery of cells using NyexTM particles at various flowrates with conditions ($Q = 5, 10, 40$ mL/min, $h = 20$ cm, $C_o = 0.2$ OD). 163
- Figure 4:37: Breakthrough curves for the recovery of cells using NyexTM particles for different bed heights at conditions ($h = 5, 10, 20$ cm, $C_o = 0.2$ OD, $Q = 5$ mL/min)..... 164
- Figure 4:38: Breakthrough curves for cell recovery using NyexTM particles at varying initial concentration (IC) with conditions ($C_o = 0.1, 0.4$ OD, $Q = 10$ mL/min, $h = 20$ cm). 165
- Figure 4:39: Breakthrough curve for cell recovery cells using NyexTM at flow conditions ($h = 20$ cm, $C_o = 0.3$ OD, $Q = 10$ mL/min) for upward and downward flow modes..... 169
- Figure 4:40: Pictorial image of floc formation, including cells and flocs settling in a bed for upward flow mode..... 170
- Figure 4:41: Pictorial images of a NyexTM bed being lifted for upward flow mode. The third picture clearly shows the bed height had expanded considerably beyond its initial level. 171
- Figure 4:42: Breakthrough curves for the recovery of microalgae cells using NyexTM particles at flow conditions ($h = 20$ cm, $C_o = 0.3$ OD, $Q = 10$ mL/min) for submerged and conventional bed configurations. 172
- Figure 4:43: Breakthrough curves for the recovery of microalgae cells using NyexTM particles at two suspension concentrations (IC = 0.1 and 0.4 OD) with the feed concentrations re-measured (C_i) throughout the experiment..... 173

Figure 4:44: Normalised breakthrough curve for the recovery of microalgae cells using Nyex™ particles. Concentration data are presented as measured OD/re-measured suspension OD.....	174
Figure 4:45: Total cells adsorbed for the experimental and “typical” breakthrough curves.	175
Figure 4:46: Pictorial images of cell accumulation on (A) top aspect of the column, (B) along the tubing, (C) on the column wall, and (D) cell aggregation.....	176
Figure 4:47: Breakthrough curve for the recovery microalgae cells using Nyex™ particles at the flow conditions ($h = 5$ cm, $C_o = 0.43$ OD, $Q = 20$ mL/min) in the downward flow mode.	177
Figure 4:48: Breakthrough curve for the recovery of microalgae cells using Nyex™ particles at the flow conditions ($h = 30$ cm, $C_o = 0.4$ OD, $Q = 40$ mL/min) in the downward flow mode.	178
Figure 4:49: Pictorial image of bed blockage, showing that liquid above the bed is not able to pass downward through the column.	179
Figure 4:50: Pictorial image showing build-up of suspension (from left to right) in the column as a result of a potential bed blockage.	179
Figure 4:51: Breakthrough curves for the recovery AV 17 dye using Nyex™ particles at the flow conditions ($h = 20$ cm, $C_o = 0.3$ OD, $Q = 10$ mL/min) in the upward and downward modes of flow.	180
Figure 4:52: Breakthrough curves for the recovery of microalgae cells using Nyex™ particles at the flow conditions ($h = 20$ cm, $C_o = 0.3$ OD, $Q = 10$ mL/min) in the downward flow mode for a variety of materials.	181
Figure 4:53: The total adsorbed cells and percentage recovery, on adsorbent reuse, after batches of adsorbent were subjected to various regeneration current densities.	186
Figure 4:54: The residual cell density of microalgae suspensions after using variants of Nyex™ particles to recover microalgae cells.....	187
Figure 4:55: The percentage recovery and normalised fraction of variants of Nyex™ particles after being used to recovery microalgae cells suspension.	187
Figure 4:56: The accumulated adsorbed cells over each adsorption cycle after using ‘Spent’ and ‘Regenerated’ Nyex™ particles to recover microalgae cells.....	188
Figure 4:57: The fractional percentage recovery for each adsorption cycle after using ‘Spent’ and ‘Regenerated’ Nyex™ particles to recover microalgae cells.	188

- Figure 4:58: The total adsorbed cells onto the regenerated Nyex™ particles after mixing with microalgae suspension. Regenerated adsorbent is based on constant electrical charges but variable energy consumption, as shown on the secondary axis.....190
- Figure 4:59: The total adsorbed cells onto the regenerated Nyex™ particles after mixing with microalgae suspension. Regenerated adsorbent is based on constant electrical energy but variable electrical charges.....191
- Figure 4:60: The percentage recovery of cells onto the regenerated Nyex™ particles after mixing with microalgae suspension. Regenerated adsorbent is based on constant charges passed but variable energy consumption.....192
- Figure 4:61: Breakthrough curves for the recovery of microalgae cells using fresh and regenerated Nyex™ particles at flow conditions ($h=20\text{cm}$, $C_o= 0.3 \text{ OD}$, $Q = 10 \text{ mL/min}$).193
- Figure 4:62: Breakthrough curves for the recovery of microalgae cells using fresh, electrochemical treated fresh and regenerated Nyex™ particles at flow conditions ($h = 20\text{cm}$, $C_o = 0.3 \text{ OD}$, $Q = 10 \text{ mL/min}$).194
- Figure 4:63: Breakthrough curves for dye adsorption using fresh, regenerated, loaded (Spent&Rinsed) Nyex™ particles at conditions ($h = 5 \text{ cm}$, $C_o = 0.3 \text{ OD}$, $Q = 10 \text{ mL/min}$).195
- Figure 4:64: The total cells adsorbed and percentage recovery when cells were recovered from suspension using different size fractions of the Nyex™ particles.196
- Figure 4:65: The total cells adsorbed and percentage recovery when cells were recovered from suspension using different size fractions of the Nyex™ particles.197
- Figure 4:66: Microscopic images of microalgae suspension samples on haemocytometer before adsorption (A) and after adsorption procedure with Nyex™ particles with size less than $160 \mu\text{m}$ (B), unwashed (C) and washed (D) variants. Green and red oval shapes show some microalgae cells and Nyex™ particles on the haemocytometer slides respectively.198
- Figure 4:67: Elution of adsorbed microalgae cells from a bed of Nyex™ that (A) was not regenerated and (B) a regenerated Nyex™ bed.....200
- Figure 4:68: Microscopic images of microalgae cells (A) in their original suspension, stained (B) before adsorption (C), eluted and stained after adsorption (D) after electrochemical treatment. Green and Red oval shapes show living and inactivated (dead) microalgae cells respectively.....201
- Figure 4:69: Scanning Electron Micrograph of fresh Nyex™ particles before adsorption.202
- Figure 4:70: Scanning Electron Micrograph of adsorbed microalgae cells on the Nyex™ particles after adsorption.....203

Figure 4:71: SEM of microalgae cells on the Nyex™ surface after regeneration shows dimple at point of contact with the adsorbent which could be due to movement of electrons.	203
Figure 4:72: SEM of microalgae cells on the Nyex™ surface after regeneration shows what appears to be release of intracellular material due to cell lysis.	204
Figure 4:73: SEM of a microalgae cell on the Nyex™ surface after regeneration of the adsorbent shows what appears to be the result of cell lysis.	204
Figure 4:74: Fluorescence intensity of batch samples of Nyex™ particles loaded with microalgae cells after being in contact with a variety of solvents.	205
Figure 4:75: Normalised Fluorescent intensity of batch samples of Nyex™ particles loaded with microalgae cells after being regenerated at different current densities and in contact with hexane.	206
Figure 5:1; Experimental and modelled breakthrough characteristics of recovery of microalgae cells onto Nyex™ particles at ($h = 20$ cm, $C_o = 0.2$ OD, $Q = 5$ mL/min).	220
Figure 5:2: Experimental and modelled breakthrough characteristics of recovery of microalgae cells onto Nyex™ particles at ($h = 10$ cm, $C_o = 0.2$ OD, $Q = 5$ mL/min).	221
Figure 5:3: Experimental and modelled breakthrough characteristics of recovery of microalgae cells onto Nyex™ particles at ($h = 5$ cm, $C_o = 0.2$ OD, $Q = 5$ mL/min).	223
Figure 5:4: Experimental and modelled breakthrough characteristics of recovery of microalgae cells onto Nyex™ particles at ($h = 20$ cm, $C_o = 0.2$ OD, $Q = 10$ mL/min).	224
Figure 5:5: Experimental and modelled breakthrough characteristics of recovery of microalgae cells onto Nyex™ particles at ($h = 20$ cm, $C_o = 0.4$ OD, $Q = 10$ mL/min).	226
Figure 5:6: Linearised Bohart-Adams and Thomas models to predict breakthrough characteristics of recovery of microalgae cells onto Nyex™ particles at ($h = 20$ cm, $C_o = 0.2$ OD, $Q = 5$ and 10 mL/min).	228
Figure 5:7: Linearised Bohart-Adams and Thomas models to predict breakthrough characteristics of recovery of microalgae cells onto Nyex™ particles at ($h = 5$ and 10 cm, $C_o = 0.2$ OD, $Q = 5$ mL/min).	229
Figure 5:8: Linearised Bohart-Adams and Thomas models to predict breakthrough characteristics of cell recovery at ($h = 20$ cm, $C_o = 0.4$ OD, $Q = 10$ mL/min).	229
Figure 5:9: Linearised Clark to model breakthrough characteristics of recovery of cells onto Nyex™ particles at ($h = 20$ cm, $C_o = 0.2$ OD, $Q = 5$ and 10 mL/min).	231
Figure 5:10: Linearised Clark to model breakthrough characteristics of recovery of cells onto Nyex™ particles at ($h = 5$ and 10 cm, $C_o = 0.2$ OD, $Q = 5$ mL/min).	231

Figure 5:11: Linearised Clark to model breakthrough characteristics of recovery of cells onto Nyex™ particles at ($h = 20$ cm, $C_o = 0.4$ OD, $Q = 10$ mL/min).....	232
Figure 5:12: Linearised MDR to model breakthrough characteristics of recovery of cells onto Nyex™ particles at ($h = 20$ cm, $C_o = 0.2$ OD, $Q = 5$ and 10 mL/min).	233
Figure 5:13: Linearised MDR to model breakthrough characteristics of recovery of cells onto Nyex™ particles at ($h = 5$ and 10 cm, $C_o = 0.2$ OD, $Q = 5$ mL/min).	234
Figure 5:14: Linearised MDR to model breakthrough characteristics of recovery of cells onto Nyex™ particles at ($h = 20$ cm, $C_o = 0.4$ OD, $Q = 10$ mL/min).	234
Figure 5:15: Service time against bed height at 40% saturation of the Nyex™ particles by the microalgae cells.	236
Figure 5:16: Service time against bed height at 70% saturation of the Nyex™ particles by the microalgae cells.	236
Figure 5:17: Breakthrough characteristics for recovery of microalgae cells onto Nyex™ particles at ($h = 10$ cm, $C_o = 0.2$ OD, $Q = 5$ mL/min), predicted with the original and adapted Bohart-Adams models.	239
Figure 5:18: Breakthrough characteristics of recovery of microalgae cells onto Nyex™ particles at ($h = 20$ cm, $C_o = 0.2$ OD, $Q = 10$ mL/min), predicted with the original and adapted Bohart-Adams models.	240
Figure 5:19: Breakthrough characteristics of recovery of microalgae cells onto Nyex™ particles at ($h = 20$ cm, $C_o = 0.4$ OD, $Q = 10$ mL/min), predicted with the original and adapted Bohart-Adams models.	240
Figure 5:20: Breakthrough characteristics of cell recovery onto Nyex™ particles ($h = 10$ cm, $C_o = 0.2$ OD, $Q = 5$ mL/min), predicted with the original and adapted Clark models.	241
Figure 5:21: Breakthrough characteristics of cell recovery onto Nyex™ at ($h = 20$ cm, $C_o = 0.2$ OD, $Q = 10$ mL/min), predicted with the original and adapted Clark models.	242
Figure 5:22: Breakthrough characteristics of cell recovery onto Nyex™ particles at ($h = 20$ cm, $C_o = 0.4$ OD, $Q = 10$ mL/min), predicted with the Original and adapted Clark models.	242

III. List of Tables

Table 2.1: Lipid contents of various oleaginous microbial organisms.....	38
Table 2.2: Comparison of microalgae with other biodiesel feedstocks (Chisti, 2007; Mata <i>et al.</i> , 2010)	42
Table 2.3: Oil contents of some microalgae strains (Chisti, 2007).....	48
Table 3.1: Laser diffraction particle size and nitrogen adsorption (BET) analysis of Nyex™ characterisation (Nkrumah-Amoako <i>et al.</i> , 2014).	97
Table 3.2: Elemental analysis on graphite basal and edge planes using Energy Dispersive X-Rays (Nkrumah-Amoako <i>et al.</i> , 2014).	98
Table 3.3: Concentrations of acidic surface functional groups on Nyex™ particles using Boehm titration (Asghar <i>et al.</i> , 2012).	98
Table 3.4; The time required for each electrical energy at corresponding current density to maintain a constant electrical charge.....	111
Table 4.4.1: Isotherm parameters for microalgae cells-Nyex™ system at 21°C.	136
Table 4.4.2: indicates the classification of isotherm curves generated from the calculated R_L values:	139
Table 4.3: Comparison between column performances based on breakthrough times and other parameters such as percentage recovery and bed capacity.	167
Table 4.4: The total adsorbed cells and bed capacity for figures 8.14 and 8.15.....	178
Table 5.1: Experimental and model parameters for the recovery of microalgae cells onto Nyex™ particles at ($h = 20$ cm, $C_o = 0.2$ OD, $Q = 5$ mL/min).....	220
Table 5.2: Experimental and model parameters for recovery of microalgae cells onto Nyex™ particles at ($h = 10$ cm, $C_o = 0.2$ OD, $Q = 5$ mL/min).....	222
Table 5.5.3: Experimental and model parameters for recovery of microalgae cells onto Nyex™ particles at ($h = 5$ cm, $C_o = 0.2$ OD, $Q = 5$ mL/min).	223
Table 5.4: Experimental and model parameters for recovery of microalgae cells onto Nyex™ particles at ($h = 20$ cm, $C_o = 0.2$ OD, $Q = 10$ mL/min).....	224
Table 5.5: Experimental and Model parameters for recovery of microalgae cells onto Nyex™ particles at ($h = 20$ cm, $C_o = 0.4$ OD, $Q = 10$ mL/min).....	226
Table 5.6: Parameter comparison of linear and non-linear Bohart-Adams to model the breakthrough characteristics of recovery of microalgae cells onto Nyex™ particles.....	230

Table 5.7: Parameter comparison of linear and non-linear Thomas to model the breakthrough characteristics of recovery of microalgae cells onto Nyex TM particles.	230
Table 5.8: Parameter comparison of linear and non-linear Clark to model the breakthrough characteristics of recovery of microalgae cells onto Nyex TM particles.	232
Table 5.9: Parameter comparison of linear and non-linear MDR to model the breakthrough characteristics of recovery of microalgae cells onto Nyex TM particles.	235
Table 5.10: BDST model parameters and the experimental and predicted service times to model the breakthrough characteristics of cell recovery at 40% bed saturation.	237
Table 5.11: BDST model parameters and the experimental and predicted service times to model the breakthrough characteristics of cell recovery at 70% bed saturation.	237
Table 5.12: Bohart-Adams parameters in the original, and adapted forms to predict breakthrough characteristics of cells recovery onto Nyex TM particles.	241
Table 5.13: Clark parameters in the original and adapted forms to predict breakthrough characteristics of cell recovery onto Nyex TM particles.	243

IV. List of Symbols

a	Langmuir empirical constant	mg/g
A, B	Bed depth service time model constants	
α	Slope of the modified dose response model	
b	Langmuir constant	L/mg
C, C_t	Liquid phase concentration at time (t)	mg/L
C_b	Breakthrough concentration	mg/L
C_e	Liquid phase equilibrium concentration	mg/L
C_0	Initial liquid phase concentration	mg/L
C_r	Recovered microalgae cells concentration	mg/L
C_s	Saturation concentration	mg/L
δC	Differential concentration	mg/L
δV	Differential volume element	L
δZ	Differential bed height	cm
d_p	Diameter of adsorbent particle	m
D_L	Axial dispersion effect	m ² /s
ε	Percentage deviation	
I	Electric current	A
I	The Clark model constant	
K	Microbial equilibrium constant	(m ³ /cells)
K_f	Freundlich capacity factor,	(mg/g)(L/mg) ^{1/n}
K_L	Langmuir constant	L/g
K_{BA}	Bohart- Adams model constant	L/min.mg
K_T	Thomas model constant	L/min.mg
k_1	First-order adsorption rate constant	min ⁻¹
k_2	Second-order adsorption rate constant	g/mg.min
L	Mass velocity of adsorbent	g/m ² .min
μ	Viscosity of suspension	kg/s.m
M	Mass of adsorbent	g
n	Freundlich isotherm exponent	
N_0	Bohart-Adams bed capacity	mg/L
σ_M	Standard error	
σ_y	Standard deviation	
p	Density of adsorbent particle	kg/m ³
P	Power	W
q	Adsorbed capacity of bed	mg/g

q_e	Adsorbed phase equilibrium concentration	mg/g
q_m	Maximum adsorbed phase concentration	mg/g
q_o	Thomas model bed capacity	mg/g
q_r	Residual adsorptive capacity	mg/g
q_t	Total cells adsorbed	mg
q_z	Microalgae adsorbent capacity in a column	(cells/g)
Q_c	Electric charge	C
Q	Volumetric flowrate of fluid	L/min
r	The Clark model constant	1/min
R^2	Correlation coefficient	
S	Initial adsorption rate constant	mg/g.min
t	Time	min
t_b	Breakthrough time	min
t_z	Mass transfer zone time	min
U	Superficial fluid velocity	m/s
U_e	Electrophoretic mobility	$m^2/s.V$
V	Volume of solution	L
V_{av}	Average potential difference	V
V_b	Breakthrough volume of packed bed	L
V_{sat}	Saturation volume of packed bed	L
χ	Permittivity of suspension	F/m
X	Amount of microalgae cells fed into the column	mg
ζ	Zeta potential	mV
Z	Bed height	m
Z_o	Critical bed height	m

V. List of Abbreviations

BA	- Bohart-Adams
BDST	- Bed depth service time
BTC	- Breakthrough curve
BH	- Bed heights
CF	- Conventional fixed bed
CO ₂	- Carbon dioxide
ETC	- Electrochemical treatment
GHGs	- Greenhouse gases
HA	- Hectare
IEA	- International Energy Agency
IEP	- Isoelectric point
MDR	- Modified dose response
OD	- Optical density
SB	- Submerged bed
SEM	- Scanning electron micrograph
SSE	- Sum of the squared errors
TAP	- Tris-Acetate-Phosphate
ZP	- Zeta potential

The Recovery of Microalgae Cells onto a Non-Porous Adsorbent

VI. Abstract

The threats of global warming attributed to fossil fuel combustion, combined with increasing energy demands and a growing population, have generated interests in diversifying the world energy mix. Biofuels from microalgae offer a sustainable renewable option and do not suffer the sustainability issues associated with early forms of bioenergy. However, research efforts of nearly 5 decades have not resulted in any significant gains and have motivated further investigation into novel techniques. The dilute nature of microalgae suspensions often requires dewatering and drying, which adds to energy intensity and costs associated with recovery processes. Curiously, the conventional recovery techniques do not consider the characteristic tendency of microalgae cells for surface attachment. This behaviour of cells, coupled with the discovery of a non-porous adsorbent material, Nyex™ particles, has brought to the fore an exciting prospect. This has motivated the underpinning question behind this research; does the non-porous characteristic of the Nyex™ particles presents an opportunity to recover microalgae cells from suspension using an adsorption technique?

Using *Chlamydomonas reinhardtii* as a model microalgae strain, preliminary batch studies revealed a rapid recovery of the cells onto the Nyex™ particles; nearly 90% recovery was attained within one minute, which depends on suspension concentration. At a correlation coefficient, $R^2 = 0.99$, the Freundlich isotherm was found to give a better description of batch systems than the Langmuir isotherm, which suggests that cell coverage onto the Nyex™ particles may not be a simple monolayer adsorption. Although a low adsorptive capacity of 0.55 mg/g was measured, the equilibrium parameter ($1/n$) of about 0.6 was well within the range for favourable adsorption (i.e. 0 - 1). Further studies undertaken suggest that the recovery of cells could be driven by a hydrophobic-hydrophobic interaction, electrostatic forces of attraction and the flocculating behaviour of the Nyex™ particles.

Fixed bed studies showed that the lack of pores led to an early breakthrough. However, findings demonstrated that unlike most column studies, the bed capacity was a more valuable parameter to assess the column performance. Unexpectedly, depressed breakthrough curves, where bed exhaustion never attained $C_t/C_0 = 1.0$, were observed. Nonetheless, the modified dose response (MDR) model was found to predict the experimental bed capacity to a greater degree of accuracy than other models. Furthermore, this research exploited the logistic features of the Bohart-Adams and the Clark models to adapt them to the experimental data. The adapted models significantly improved the accuracy of predictions with R^2 values > 0.99 for the depressed breakthrough curves.

The conductive nature of Nyex™ particles was explored to electrochemically regenerate the adsorbent and reuse it to recover more cells. A current density of 32 mA.cm⁻² was sufficient to inactivate the cells, regenerate the adsorbent and attain a maximum percentage recovery. Interestingly, scanning electron micrograph showed that the membranes of the adsorbed cells were ruptured, during Nyex™ regeneration, potentially leading to lipid release. The maximum lipids extracted into a hexane solvent was estimated as 30 µg/mL at a current density of 64 mA.cm⁻².

Overall, the potential to recover microalgae cells onto a non-porous adsorbent has been demonstrated. The prospect of rupturing membranes of adsorbed cells offers the opportunity to use this technique to recover microalgae cells for potential biofuel applications. The results obtained from this research can serve as the impetus to further exploit this novel procedure. Future work should consider high lipid producing varieties of microalgae strains, develop a robust protocol to account for all forms of lipids released and undertake an energy and cost analysis to develop the technology further.

VII. Declaration

I declared that no portion of the work referred to in the thesis has been submitted in support of an application for another degree or qualification of this or any other university or other institute of learning.

Signed: _____

Name: Akinlabi Adeyemi

VIII. COPYRIGHT STATEMENT

- i. The author of this thesis (including any appendices and/or schedules to this thesis) owns certain copyright or related rights in it (the “Copyright”) and s/he has given The University of Manchester certain rights to use such Copyright, including for administrative purposes.
- ii. Copies of this thesis, either in full or in extracts and whether in hard or electronic copy, may be made only in accordance with the Copyright, Designs and Patents Act 1988 (as amended) and regulations issued under it or, where appropriate, in accordance with licensing agreements which the University has from time to time. This page must form part of any such copies made. Page 10 of 25 Presentation of Theses Policy.
- iii. The ownership of certain Copyright, patents, designs, trademarks and other intellectual property (the “Intellectual Property”) and any reproductions of copyright works in the thesis, for example graphs and tables (“Reproductions”), which may be described in this thesis, may not be owned by the author and may be owned by third parties. Such Intellectual Property and Reproductions cannot and must not be made available for use without the prior written permission of the owner(s) of the relevant Intellectual Property and/or Reproductions.
- iv. Further information on the conditions under which disclosure, publication and commercialisation of this thesis, the Copyright and any Intellectual Property and/or Reproductions described in it may take place is available in the University IP Policy (see <http://documents.manchester.ac.uk/DocuInfo.aspx?DocID=24420>), in any relevant Thesis restriction declarations deposited in the University Library, The University Library’s regulations (see <http://www.library.manchester.ac.uk/about/regulations/>) and in The University’s policy on Presentation of Theses

IX. Confidentiality

The results reported in this research may be of commercial applications for Arvia Technology Limited. Due to intellectual property rights and commercial confidentiality of this work, this thesis is restricted for general access in the library.

X. Dedication

I dedicate this PhD thesis to my amazing mother, Muibat Agbeke Adeyemi, who has made incredible and selfless sacrifices for me to attain my aspirations. May you live long to reap the fruits of your immeasurable efforts, Aameen.

XI. Acknowledgements

All praise and thanks belong to Him, Who has guided me, and never could I have found guidance, were it not for His grace...

Words are not sufficient to capture my gratitude and immense appreciation to Professor Colin Webb for the motivation, his indefatigable support and incredible understanding throughout this research work. I am also thankful for his availability at all times since the beginning of this PhD work. I have learnt a great deal from you far and beyond the academic skills and knowledge imparted, but as well as the social skills that I strongly believe I require to achieve future goals. My heart also goes to my co-supervisors Dr Jon Pittman of Faculty of Life Sciences and Dr Nigel Brown of Arvia Technology for their support to carry out this project. I would also like to show my immense appreciation to Dr Edward Roberts of University of Calgary who gave me the rare privilege to undertake this novel research.

I would like to thank the various teams in different laboratories in the School of Chemical Engineering and Analytical Science, School of Materials and the Faculty of Life Sciences for providing me with the assistance in developing the analytical techniques to use their equipment. I owe immense appreciation to all my astounding teachers, lecturers and mentors who have greatly influenced me and taught me the basic knowledge since my primary school days. What would have become of me without your unique contributions to my life?

To my siblings, family and friends, you make my world meaningful by your presence in my life and I appreciate you all in your irreplaceable ways. Special mention of my sweetheart, my beautiful and adorable daughter, Maimoonah Oyinkansola, May Allaah make you righteous, make you grow in a good manner and make you kind to your parents and to every soul that crosses your path, Aameen. I love you dearly!

I would like to thank the Arvia Technology Limited and its staff for the material, financial and technical support to undertake this research. I am most indebted to the Petroleum Development Technology Fund (PTDF), Nigeria for providing the scholarship and the logistics support to make my dream come true.

1 Introduction

1.1 Brief Background and Motivation

The threats posed by global warming attributable to the combustion of fossil fuels have frequently raised concerns over the sustainability of fossil fuels. Global warming is believed to be driven by emission to the atmosphere, of anthropogenic greenhouse gases (GHGs) from fossil fuel usage. In addition, the desire for a better life by a growing global population, expected to reach 8.5 billion over the next decade, requires ever more energy. Worldwide energy use is expected to grow by one-third by 2040 (IEA, 2015). With the present energy mix and energy forecast scenarios, such demands can only realistically be met through the combustion of fossil fuels, leading to even more emissions.

The International Energy Agency (IEA) in its “2015 Key World Energy Statistics” revealed that fossil fuels still accounted for 81.4% of total primary energy supply. As revealed in figure 1.1, the superiority of fossil fuel in the share of global energy supply, dates back to more than 4 decades ago when it accounted for 86.7% of total supply (IEA, 2015). This scenario will most likely remain as it is through to the foreseeable future.

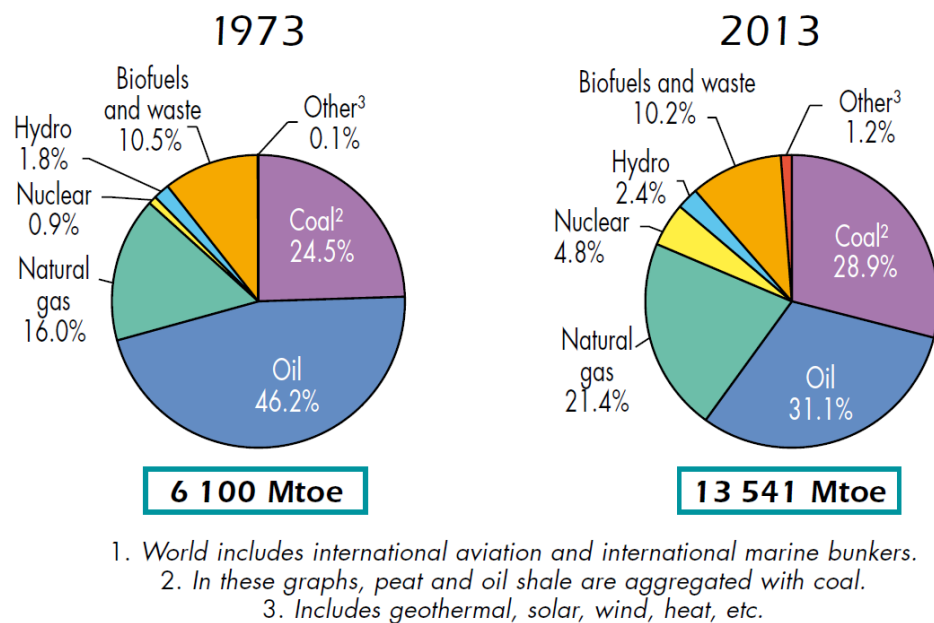


Figure 1.1: The total primary energy share by fuel usage in 1973 and 2013 (IEA, 2015)

Expectedly, carbon dioxide (CO₂) emissions as a result of fossil fuels combustion is 99.6% of world CO₂ emissions by fuel usage. As depicted in figure 1.2, the CO₂

emissions by fuel usage in 2013 has more than doubled since records began in 1971. It is thought that as of 2011, about 63% of annual emissions of anthropogenic GHGs were due to fossil fuel combustion (Edenhofer *et al.*, 2014).

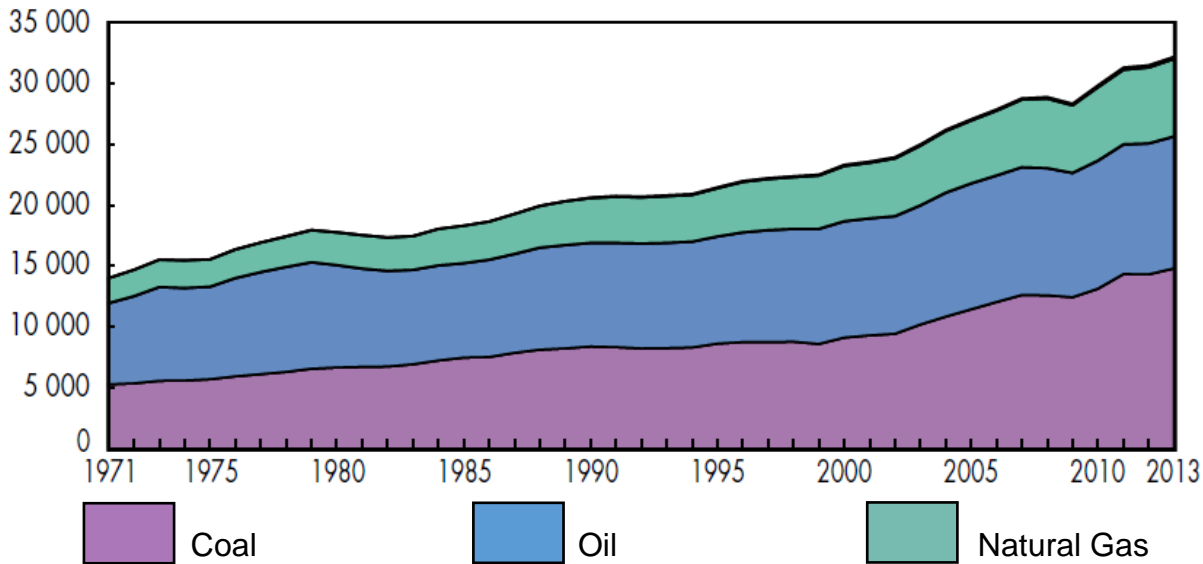


Figure 1:2: World CO₂ emissions from fuel combustion from 1971 to 2013 by fuel [Mt of CO₂] (IEA, 2015).

Meeting future energy demands requires a number of strategies that include;

- better deployment of renewables
- improved supply and distribution efficiency,
- heat and power recovery initiatives,
- more fuel-efficient vehicles,
- more efficient electrical equipment and heating and cooling devices to mention but a few (Edenhofer *et al.*, 2014).

Deployment of renewables can be pivotal towards the provision of sustainable energy that also guarantees the security of energy supply. It also ensures that GHGs emissions to the atmosphere are maintained at levels that minimize the negative effects of global warming. Bioenergy offers a valuable alternative for meeting the growing demand of energy consumption of an increasing population whilst minimising the environmental footprint of such energy use. Amongst the various bioenergy options, biofuel from microalgae is thought to have the best chance of replacing liquid fuels from fossil fuels (Chisti, 2008a; Chisti and Yan, 2011). This is as a result of its relative capacity to accumulate more biofuel precursors in comparison to other biomass sources like vegetable, palm and rapeseed oils.

Besides, biofuels from food and agricultural crops are considered to have sustainability issues namely security of food supply and, competition for arable land and fresh water.

However, the prospect of producing biofuels from microalgae has largely been disappointing; nearly 5 decades of intensive research has yielded little success in commercial scale production of biofuels from microalgae. One of the main challenges faced by microalgae biofuels is the inherent dilute nature of microalgal suspensions. The application of conventional routes require concentration of the microalgae suspension to form a paste, which may sometimes entail a 2-stage dewatering process depending on the extraction process involved. It is believed that to make commercial production of biofuels from microalgae economically competitive, the following options have to be considered, namely;

- novel methods of microalgae cultivation and cell recovery,
- wet extraction that does not require an initial dewatering stage to be involved and
- the microalgae suspension should be utilised within a biorefinery concept so that more valuable products can be derived from the resulting microalgae biomass.

The variety of microalgae strains imply that a number of novel techniques can be developed to suit the characteristics of such strains. Interestingly, the innate preference of some of microalgae strains for surface attachment has rarely been exploited as an opportunity to develop a recovery technique based on adsorption technology. Ironically, similar to other conventional recovery techniques for microalgae cells, adsorption is one of the established methods for wastewater treatment. The insouciance towards adsorption could stem from the fact that most conventional adsorbents are highly porous and, while this might mean good adsorption, it also poses problems in the recovery and processing of the microalgae cells.

As a consequence, the research work presented in this thesis considers the natural tendency of microalgae cells for surface attachment as a potential opportunity to develop a technique to recover them from suspension. The uniqueness of this research work is hinged on a novel non-porous adsorbent, NyexTM, which recovers

adsorbates on its external surface. Its lack of porosity makes it a low capacity adsorbent, but its high electrical conductivity makes it a preferred material for the purpose of electrochemical regeneration. These characteristics have led to the development of a single stage process known as the Arvia Process. It is a novel technology, which combines adsorption and electrochemical methods to provide a wastewater treatment system. In the process, organic pollutants adsorbed onto the Nyex™ particles, can be destroyed to form CO₂ and water, during electrochemical regeneration. The restoration of the adsorbent capacity using this method makes it both environmentally friendly and cost effective. The process has led to the spin out of a company, Arvia Technology, and has found successful application in the removal/ treatment of contaminants such as atrazine, chlorinated effluents, organic dyes and nuclear wastes (Brown *et al.*, 2004; Brown and Roberts, 2007; Asghar *et al.*, 2012; Brown *et al.*, 2013).

The preference of microalgae cells for surface attachment coupled with the non-porous characteristics of Nyex™ particles, has brought to the fore an exciting interest in undertaking this research. Thus, the overarching question being asked in this research is; does the non-porous characteristic of the Nyex™ particles presents an opportunity to recover microalgae cells from suspension using an adsorption technique for potential biofuel applications? Knowing that the Nyex™ is conductive, an electrochemical method could be employed to regenerate the adsorbent particles. Hence, the effects of regenerating a non-porous adsorbent loaded with microalgae cells is also of interest in this research work.

1.2 Research Strategy

1.2.1 Literature Review

To provide answer(s) to the research question, a critical review of the literature was undertaken to establish the gap(s) in field of recovery techniques for microalgae cells on one hand and adsorption and electrochemical methods on the other hand.

This was carried out under three main headings, namely;

➤ Why Oleaginous Microalgae Cells

This was carried out to appreciate the potentials and interests in microalgae biofuels as well as the historical background involving research and development initiatives.

In addition, the biological and chemical composition of microalgae cells was studied with a view to show how such characteristics make microalgal cells a good candidate for biofuel applications.

➤ **Present techniques to harvest microalgae cells and extract lipids**

This was undertaken to look at the various stages involved in extracting lipids from microalgae cells which entails; strain selection, cultivation, recovery/harvesting methods, and extraction/cell disruption mechanisms. More specifically, the advantages and shortcomings of these techniques were studied. This revealed that adsorption has received little attention as a recovery technique and thus there is a need to investigate it.

➤ **Theory of adsorption and electrochemical methods**

From the review of existing recovery/harvesting techniques, it was apparent that all of them were directly from wastewater techniques. However, the adsorption process is the least considered wastewater technique for recovering microalgae cells. Although electrochemical methods are being applied to recover microalgae cells or as a disinfection treatment, its use to regenerate an adsorbent loaded with microalgae cells has not been carried out. Coupled with the inherent propensity of microalgae cells to attach to surfaces and the availability of a non-porous adsorbent, the need to investigate adsorption as a recovery technique was established. This led to the research questions being addressed by the research reported in this thesis.

1.2.2 Research Objectives

Based on the findings from the literature review, a number of research objectives were developed to proffer answers to the research questions previously stated in section 1.1. These research objectives also served as the platform on which experimental investigations were carried out. Details and the scope of the experimental studies are outlined in Chapter 3. To find answers to these research questions, the objectives developed include;

1. Evaluate the adsorption equilibrium characteristics of the Nyex™/microalgae cells system to establish the adsorptive capacity.
2. Investigate the process conditions and factors influencing the Nyex™/microalgae cells adsorption system in order to elucidate on the

probable mechanism(s) governing the recovery of microalgae cells onto Nyex™ particles.

3. Examine the recovery of microalgae cells onto Nyex™ particles within a continuous fixed bed column.
4. Scrutinise the suitability of existing mathematical models to predict the dynamic behaviour of cell recovery within a continuous fixed bed column.
5. Study the electrochemical regeneration of the Nyex™ particles loaded with microalgae cells and examine the electrochemical effects on the membranes of adsorbed microalgae cells for potential release of lipids.

1.3 Experimental Rationale and Scope

➤ Batch Studies

Preliminary studies involving the recovery of microalgae cells onto the adsorbent solid were undertaken in a batch system. This was carried out to understand the adsorption characteristics and equilibrium/isotherms. These studies also facilitated investigating the factors and conditions affecting microalgae cells recovery. More importantly, the findings from the batch studies provided some understanding to proffer probable mechanism(s) governing cell recovery onto the adsorbent.

➤ Fixed Bed Column Studies

This was undertaken to study the dynamics involved in the recovery of microalgae cells for a continuous process, specifically in a fixed bed column. A number of mathematical models was then considered to enable the prediction of such a system. The model parameters are useful tools to facilitate the scale up of microalgae cell recovery for industrial applications.

➤ Adsorbent Regeneration and Membrane Cell Rupture

This involved using electrochemical methods to regenerate the adsorbent with the aim of investigating the effects of the process both on the adsorbent and the adsorbed microalgae cells. More importantly, whether the membrane/wall of the adsorbed microalgae cells can be ruptured during the electrochemical regeneration of the adsorbent was of significant interest.

1.4 Thesis Structure

The thesis presented here is a culmination of the literature review and experimental studies carried out to report the credibility or otherwise of hypotheses proposed in this research work.

The thesis has been organised into 6 chapters. Chapter 2 was dedicated to the literature survey carried out at the start of the research work with the aim of identifying the gap(s) in the field of knowledge as explained in section 1.2.1. Chapter 3 highlights the detailed experimental programme implemented to undertake this research.

Chapter 4 comprises findings from experimental trials carried out in the batch system in order to authenticate the veracity of the claim that microalgae cells can be recovered using the adsorbent of interest. It also comprises the outcomes from investigations undertaken in the continuous mode within a fixed bed column. In addition, this Chapter contains results obtained from electrochemical studies carried out to investigate the regeneration of the adsorbent, rupture of the microalgae cell wall and the potential recovery of lipids for biofuel applications.

Chapter 5 consists of mathematical models employed to describe the recovery of microalgae cells in a continuous fixed bed system.

Finally, Chapter 6 concludes the thesis with key findings relating to the research questions posed at the start of this research work as well as considerations for future work.

2 Literature Review

2.1 Why Oleaginous Microalgae Cells?

The use of renewables is of global interest and has motivated a number of countries, especially the eight biggest economies (the G8), to support and promote enabling legislations (Subhadra and Grinson, 2011). For instance, the European Union introduced a binding target among member states of 10% biofuel energy in transport by 2020 (DECC, 2011). In addition, the United Kingdom has a legally binding goal of 80% emissions reduction by 2050. In 2014, the UK achieved 7% of its energy demand from low carbon sources and 20% of electricity generation was from renewables. For the first time in the UK, in the 2nd quarter of 2015, more electricity was generated from renewables than from coal (DECC, 2016). Commendably, similar legislation and policies have been and continue to be put forward in Brazil, China, India and the US, thus suggesting a significant shift in the energy sector (Subhadra and Grinson, 2011). For instance, bioethanol has become a household option in Brazil, replacing more than 40% of the gasoline that would otherwise be used (Goldemberg *et al.*, 2003; Henniges and Zeddies, 2004; Goldemberg, 2008).

Renewable energy from biomass, also referred to as bioenergy, can be defined as, “material that stores solar energy as a result of photosynthesis which can be used as a feedstock in the production of fuels and alternatives for petrochemical and other energy intensive products” (IEA, 2009; Hanova *et al.*, 2010). Currently, bioenergy is the largest contributor to renewables; making up to 77% of renewable energy in the world’s primary energy mix (IEA, 2009). As evident in figure 2.1, bioenergy accounts for about 10% of the energy mix; a percentage share that has remained the same for more than 4 decades (Hanova *et al.*, 2010; Jones and Mayfield, 2012; IEA, 2015).

Of the different forms of bioenergy, traditional wood burning still accounts for the majority but the most rapidly growing sector is biofuels production. Depending on the material source, biofuels can be classified into 3 generations (see figure 2.2). First generation biofuels, for instance bioethanol and biodiesel from crops, are developed technologies that have attained economic levels of production. This includes corn, sugarcane and sugar beet bioethanol; soybean, rapeseed and animal

fat biodiesel (Demirbaş, 2001; Ratledge and Cohen, 2008; Brennan and Owende, 2010).

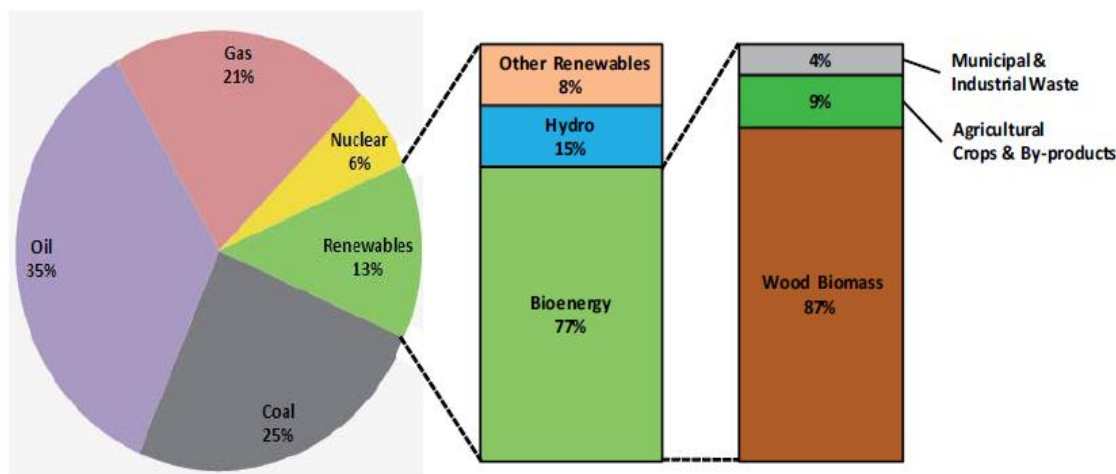


Figure 2:1: Share of bioenergy in the world primary energy mix (IEA, 2009)

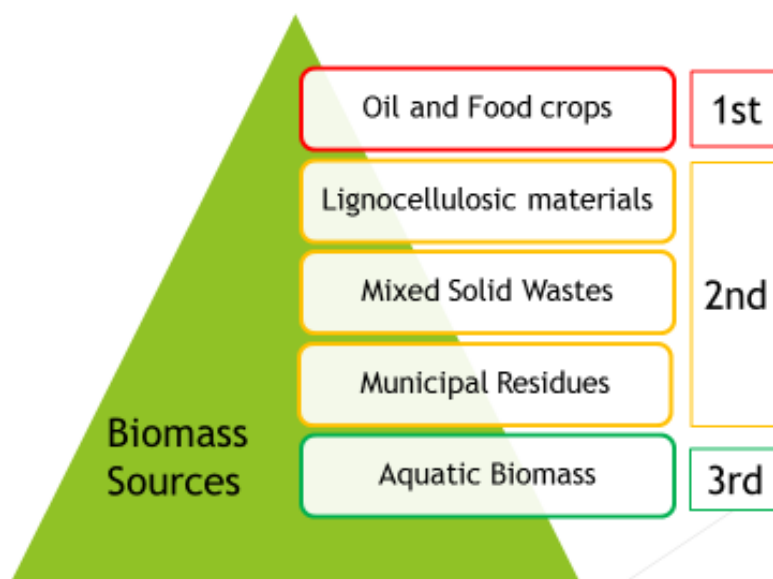


Figure 2:2: The classification of biomass sources.

Second generation biofuels are “non-food” technologies which use thermochemical and biochemical pathways to convert lignocellulosic materials (grass, straw and wood), mixed solid wastes and municipal residues to generate heat and electricity. They can also be converted to ethanol, butanol and syndiesel. Although production of second generation biofuels at economic scale still remains limited; a number of pilot and demonstration facilities have been successfully proven (Chisti, 2007; Greenwell *et al.*, 2010; Brennan and Owende, 2010; Naik *et al.*, 2010).

However, concerns over the sustainability of the first and second generation biofuels have been raised. These include but are not limited to (Goldemberg *et al.*, 2008; Rosegrant, 2008; Azapagic and Perdan, 2010; Rawat *et al.*, 2013);

- Security of food supply (see figure 2.3)
- Competition for arable land and release of CO₂ when virgin land is cultivated
- Competition for fresh water and water pollution

Rosegrant (2008) reported that increases in biofuel demand accounted for 30% of the increase in the weighted average of grain prices from the year 2000 to 2007. It was noted that the biggest impact was on maize prices for which high demand for biofuel use was estimated to account for 39% of the increase in real prices.



Figure 2:3: Nearly 1 billion people do not have enough food to lead a healthy active life (Brown, 2012)

These challenges of early generation biomass resources highlight the necessity for alternative feedstocks with potential for better productivity and reduced sustainability issues. This is the principal stimulus for the attraction in oleaginous microbial organisms (Chisti, 2007; Meng *et al.*, 2009; Papanikolaou and Aggelis, 2011; Demirbas, 2011; Wahlen *et al.*, 2013; Wan *et al.*, 2015). The latter can be microalgae, yeasts, fungi or bacteria that accumulate oil, otherwise known as microbial lipids (see Table 2.1). The lipids comprise, but are not limited to, neutral lipids, sterols, hydrocarbons, free fatty acids, and polar fractions (such as

phospholipids, sphingolipids, glycolipids). Neutral lipids, mainly in the form of triacylglycerols (TAGs), are formed and accumulated as a form of carbon storage. TAGs are stored in densely packed lipid bodies that are located in the cytoplasm, for instance globules in microalgae cells (Hu *et al.*, 2008; Olsson *et al.*, 2012; Rawat *et al.*, 2013).

The oil bearing characteristic is not common to all species of microbial organisms, hence, those with the capacity to accumulate oil have to be identified (Araujo *et al.*, 2011). It is a distinctive feature of an unbalanced metabolism where microbial cells can convert substrates, such as carbon dioxide, sugars and organic acids to create new cells and accumulate lipids (Chisti, 2010). Whilst some species can accumulate reasonable levels of lipids, fascinatingly, some require stressors such as nutrient deprivation or photo-oxidative stress to double or triple lipid synthesis (Rawat *et al.*, 2013; Chen *et al.*, 2015). However, studies have shown that such an increase in lipid content is usually inversely proportional to the biomass productivity (Boussiba *et al.*, 1987; Pittman *et al.*, 2011).

Table 2.1: Lipid contents of various oleaginous microbial organisms.

Strain	Microbial type	Lipid content (%w/w)	References
<i>Cryptococcus curvatus</i>	Yeast	58-60	(Wahlen <i>et al.</i> , 2013)
<i>Rhodotorula glutinis</i>	Yeast	72	(Ratledge and Cohen, 2008)
<i>Botryococcus braunii</i>	Microalgae	25-75	(Ratledge and Cohen, 2008)
<i>Dunaliella Salina</i>	Microalgae	42-45	(Chen <i>et al.</i> , 2015)
<i>Rhodococcus Opacus</i>	Bacteria	51	(Wahlen <i>et al.</i> , 2013)

There is a distinction between yeasts, bacteria, fungi, and algae. The latter are typically phototrophic organisms, considered to be sunlight-driven cell factories that can utilize carbon dioxide as a source of carbon to accumulate biofuels and biofuel precursors, while the others are heterotrophic microbes that require some fixed carbon source for the synthesis of new cells. Some microalgae can also be heterotrophic, while others are mixotrophic, that is, possessing the ability to photosynthesise and also make use of exogenic organic nutrients (Brennan and Owende, 2010). Sunlight and carbon dioxide being “freely” available make

microalgae a preferred choice amongst microbial organisms for the synthesis of biological materials such as lipids (Meng *et al.*, 2009; Singh *et al.*, 2011; Wahlen *et al.*, 2013; Tan *et al.*, 2015).

2.1.1 The Biological and Chemical Characteristics of Microalgae Cells

Algae are microscopic primitive plants that are known to be amongst the oldest living organisms. They are also sometimes classified as thallophytes, which are simple plants that have no leaves, stems, or roots but contain chlorophyll as a primary photosynthetic pigment (Brennan and Owende, 2010; Satyanarayana *et al.*, 2011). Microalgae utilize essential elements such as nitrogen, phosphorous, iron, potassium and photosynthesise sugars by fixing carbon dioxide, to grow and multiply (Ratledge and Cohen, 2008). They can grow in different aquatic environments that include freshwater, saline and brackish water depending on the strain (Aragón *et al.*, 1992; Lin *et al.*, 1998; Pittman *et al.*, 2011; Wiley *et al.*, 2011; Boelee *et al.*, 2011).

Algae include cyanobacteria (blue-green algae), macroalgae (seaweed) and microalgae (unicellular eukaryotic microorganisms) (USDOE, 2010). According to Brennan and Owende (2010), microalgae are unicellular and simple multicellular organisms which include both eukaryotic and prokaryotic species. Unlike the prokaryotic cells, the eukaryotic cells have organelles that regulate their cell functions thereby allowing them to reproduce and survive (Brennan and Owende, 2010). The eukaryotes are mainly macroalgae and some microalgae that can be classified in a variety of ways depending on their pigmentation, cell density, surface charge and cell morphology, which includes appendages, shape and size (Henderson *et al.*, 2008). The high chlorophyll content in some species give them their green pigmentation and they are therefore known as green algae.

There are three principal groups of microalgae; dinoflagellates; green algae (Chlorophyceae); and diatoms (Bacillariophyceae). Other classifications based on pigmentation include; red algae (Rhodophyta), blue green algae, golden algae (Chrysophyceae) and brown algae (Brennan and Owende, 2010; Singh and Olsen, 2011; Singh *et al.*, 2011). Green algae are either ellipsoidal, globular or spherical in shape, and some possess flagella which facilitate movement of the cells (Henderson *et al.*, 2008; Phukan *et al.*, 2011). The green algae are the most studied strains

largely due to their ease of isolation, faster growth and ubiquity in various natural habitats (Hu *et al.*, 2008; Henderson *et al.*, 2008). The surface charge of algae, depending on age of growth medium, is typically negative within a pH range of 4 and 10, which is responsible for their stability when in suspension. The isoelectric point, when surface charge is zero, is around pH 3 – 4 for most microalgae species (Henderson *et al.*, 2008; Xia *et al.*, 2015). The size of microalgae varies widely, depending on the species, from ca. 2 μm for the globular *Chlorella luteoviridis*, to ca. 70 μm for the linear *Spirulina platensis* (Clément *et al.*, 1980; Borowitzka, 1992).

Chisti (2007) estimated that the biomass of microalgae, based on minimal nutritional requirements, has a molecular formula approximated as $\text{CO}_{0.48}\text{H}_{1.83}\text{N}_{0.11}\text{P}_{0.01}$. The chemical composition of algae largely varies depending on the species but typically comprises carbohydrate, protein and lipids (Chisti, 2007). The cell walls of algae contain polysaccharides which account for a high proportion of the carbon present in algae cells (Packer, 2009). Carbohydrates in microalgae can be in the form of glucose, sugar, starch and other polysaccharides (USDOE, 2010). A number of microalgae, for example red algae, employ starch for energy storage while some, for example diatoms, store carbohydrates such as fucoidin, laminaran, or mannitol as food reserves. Microalgae are also a valuable source of essential vitamins, namely, Vitamins A, B₁, B₂, B₆, B₁₂, C, E, nicotinate, biotin, folic acid and pantothenic acid. Pigments such as chlorophyll, carotenoids and phycobiliproteins are also present in microalgae (Borowitzka, 1992; Chini Zittelli *et al.*, 1999; Lubián *et al.*, 2000; Curtain, 2000; Spolaore *et al.*, 2006; Henriques *et al.*, 2007; Rawat *et al.*, 2013).

It is worthy of note that macroscopic algae are known to have a low lipid content but also have a high carbohydrate that is convertible to various biofuels (USDOE, 2010; John *et al.*, 2011). Unlike these macroalgae, microalgae are typically high lipid organisms and can have oil contents ranging from 60 – 80% by dry weight (Chisti, 2008a, 2008b). Lipids also exist as hydrocarbons which are produced in large quantities only by *Botryococcus brauni* reaching up to 80% by dry weight under stressed environmental conditions (Anirban *et al.*, 2002; Liu *et al.*, 2013). Interestingly, these long chain hydrocarbons (C₂₃ – C₄₀) are similar to those found in fossil crude oil (Largeau *et al.*, 1980; Frenz *et al.*, 1989; Anirban *et al.*, 2002).

The building blocks for the formation of lipids in algae cells are fatty acids. The latter can be in either saturated or unsaturated form, where the unsaturated fatty acids vary in the number and position of double bonds on the carbon chain. Ultimately, the structures of these fatty acids determine the properties of any resulting biofuel products (Knothe, 2005). For instance, biodiesel produced from saturated fats tend to have a higher cetane number and superior oxidative stability but poor low-temperature characteristics. However, those produced from feedstocks with high levels of polyunsaturated fatty acids have good cold-flow properties but have instability problems during prolonged storage (Hu *et al.*, 2008).

2.1.2 The Potentials of Microalgal Cells

The lipid composition of microalgae in the form of TAGs and hydrocarbons is a prime motivation for their potential application in the biofuel industry. For instance, biodiesel is formed when a chemical reaction, transesterification, takes place between TAGs and alcohol in the presence of a catalyst to produce mono-alkyl fatty acid esters (Hu *et al.*, 2008). The polysaccharides present in the microalgae cells are also potential feedstocks for conversion to biofuels, notably ethanol (USDOE 2010; Singh and Olsen, 2011; Tan *et al.*, 2015).

It is widely believed that biofuels from microalgae are renewable and sustainable energy and have the unique potential to substitute fossil fuels without the sustainability issues that early generation biofuels have encountered (Chisti, 2007). Proponents claim that biofuels from microalgae will not compete for arable land or water unlike the early generation biofuels. This is because they require less land area to grow as well as being able to use brackish or saline water and agricultural or industrial waste effluents (Chisti, 2008a; 2010). More importantly, as depicted in table 2.2, the oil yield (litre per hectare) is much higher than the oil yield of the best oil crops (Chisti, 2008a; Rittmann, 2008).

A number of other advantages which have been put forward include but are not limited to:

- microalgae multiply very rapidly; in the exponential growth phase, microalgae biomass doubling intervals can be as small as 3.5 hours,
- cultivation is feasible throughout the year,

- carbon dioxide from power plant flue gas or other industrial emissions can be recycled to growth ponds or chambers,
- cultivation in wastewater can serve a twofold purpose of bioremediation of wastewater,
- the use of herbicides and pesticides is not required during cultivation
- higher photosynthetic efficiency than terrestrial crops,
- biomass that remains after extraction can be converted to valuable biofuels or value-adding chemicals (Chisti, 2007; Hu *et al.*, 2008; Brennan and Owende, 2010; Subhadra and Grinson, 2011).

Table 2.2: Comparison of microalgae with other biodiesel feedstocks (Chisti, 2007; Mata *et al.*, 2010)

Plant source	Oil content (% oil by wt. in biomass)	Oil yield (L oil/ha year)	Land use (m² year/kg biodiesel)	Biodiesel productivity (kg biodiesel/ha year)
Corn/Maize	44	172	66	152
Hemp	33	363	31	321
Soybean	18	636	18	562
Jatropha	28	741	15	656
Camelina	42	915	12	809
Rapeseed	41	974	12	862
Sunflower	40	1070	11	946
Castor	48	1307	9	1156
Palm oil	36	5366	2	4747
Microalgae¹	30	58,700	0.2	51,927
Microalgae²	50	97,800	0.1	86,515
Microalgae³	70	136,900	0.1	121,104

1 – Low Oil Content; 2 – Medium Oil Content; 3 – High Oil Content

On the other hand, dissenting opinions cast doubt on the feasibility of the role of microalgae bioenergy in the future energy mix. This is largely due to disquiets over exaggerated claims and highly academic projections on producing biofuels from microalgae (Walker, 2009; Hanova *et al.*, 2010). For instance, Reijnders (2008) argued that when petroleum inputs during the microalgae biofuel life cycle are

considered, it is highly likely to result in a negative energy balance. He further suggested that in scenarios where a positive energy balance is achieved, sugar cane and oil palms have higher net energy yield than microalgae (Reijnders, 2008, 2009). Van Beilein (2010) argued that the use of carbon dioxide from flue gas emissions would require that cultivation ponds or photobioreactors are near power plants; the latter are usually situated in or close to population centres. Consequently, he reasoned that such flat areas would compete with land required for housing and agriculture. Some critics further argued that the use of brackish water to culture microalgae cells may still require fresh water to regularly dilute the increase in salt concentration due to evaporation (van Beilen, 2010). It has also been contentious that biofuels from microalgae may not be economically viable without the biorefinery concept (see figure 2.4) which ensures that other valuable products such as astaxanthin, agar, lutein and β – carotene are produced alongside the biofuels (Pienkos and Darzins, 2009; Zhong *et al.*, 2010; Subhadra and Grinson, 2011; Trzcinski *et al.*, 2012; Gerardo *et al.*, 2015).

In addition, with combustion being a well-developed technology, it is possible to burn the microalgae biomass to generate heat and/or electricity rather than extracting lipids. The challenge with combustion is that biomass moisture content has to be less than 50% dry weight (McKendry, 2002) and in general also requires pre-treatments such as drying, chopping and grinding (Brennan and Owende 2010). Furthermore, the reported calorific values of algal biomass which vary from 14.65 MJ/kg for *chlorella vulgaris* (Ghayal and Pandya, 2013) to 19.5 MJ/kg for *Ulva lactuca* (Bruhn *et al.*, 2011), is considerably lower than that of algal biodiesel reported to be 41 MJ/kg (Xu *et al.* 2006). Hence, combustion of the biomass requires bulk handling of materials with low calorific value whilst the biodiesel has higher value that is worth the bulk handling of the liquid transport fuel. Ultimately, the choice between direct combustion and lipids extraction would boil down to desired use of the end product.

Nonetheless, there is considerable agreement over the potentials of microalgae biomass and their unique advantage over the early generations of biomass. Having said that, further techno-economic analysis and life cycle assessments are required to explore the existing options and viable scenarios. Importantly, consistent

research and development initiatives into new methods are required to offer insights that can guarantee the successful commercialisation of biofuels from microalgae.

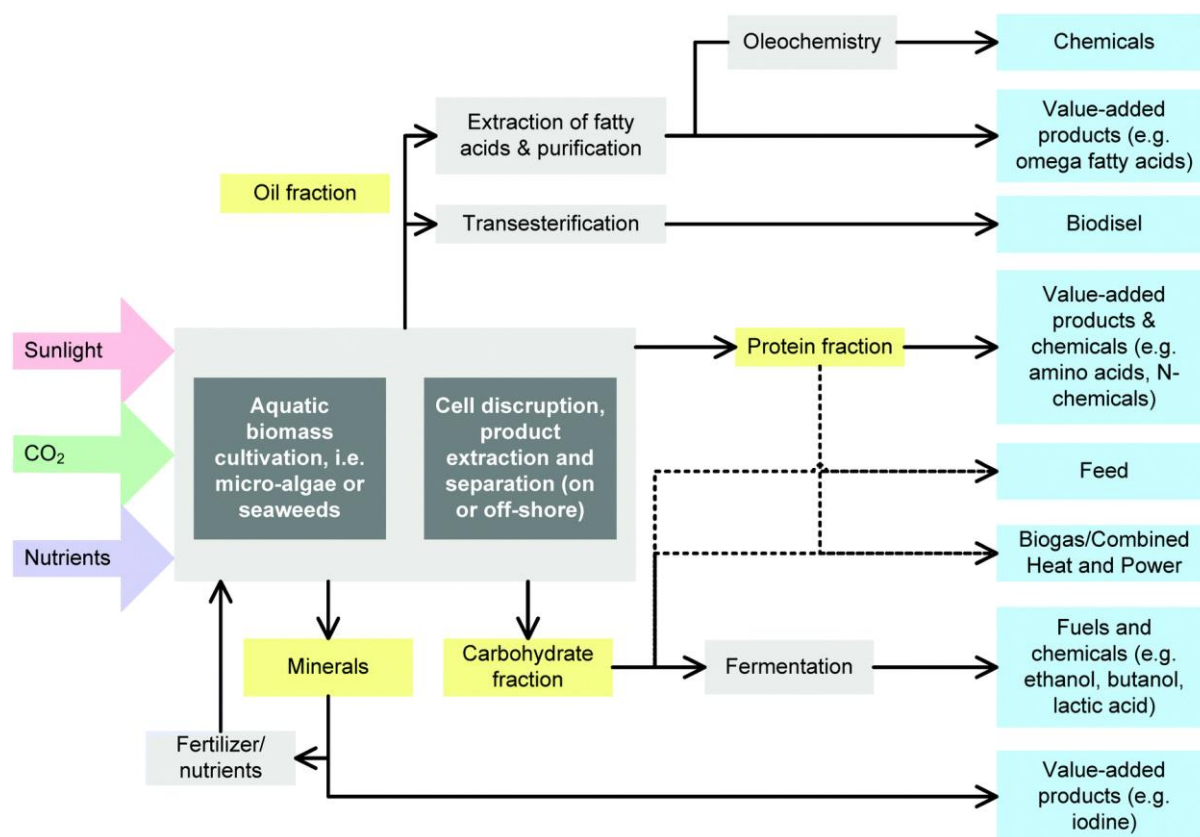


Figure 2:4 Biorefinery concept for microalgae biomass (Koutinas et al., 2014).

2.1.3 Summary

This section highlights the motivation behind investigating oleaginous microalgae cells for biofuel applications. Bioenergy accounts for 77% of renewable energy in the world's primary energy mix. However, the sustainability issues with early biofuel resources such as food crops and lignocellulosic wood limit their advancement to replace fossil fuels.

Hence, interest has shifted towards the use of microalgae cells as they can be easily grown in waste media. The preference for microalgae, amongst other microbial cells, stems from their capability to freely fix CO₂ and use sunlight to accumulate biological biofuel precursors such as lipids. Their exponential growth rate as well as their much better oil yield has led to the belief that they can replace fossil fuels. However, concerns have been raised over exaggerated claims with regards to the extent of lipids accumulation in microalgae cells.

Despite differing opinions, there is an optimistic perception about the potentials of biofuels from microalgae as well as their unique advantages over early generations of biofuels. However, further research and development initiatives into novel methods are required to offer innovative solutions to the challenges faced in the commercialisation of biofuels from microalgae.

2.2 Present Techniques of Harvesting Microalgae Cells and Extracting Lipids

2.2.1 Introduction

The extraction of lipids and other intracellular materials typically involves 4 stages (see figure 2.5), namely; (1) strain selection, (2) cultivation, (3) harvesting, (4) cell rupturing/extraction. This section discusses each stage, the advantages as well as the challenges faced by each aspect of the process chain are also reviewed.



Figure 2.5: Schematic diagram of the stages for lipid recovery from microalgae cells.

2.2.2 Strain Isolation and Selection

As illustrated in figure 2.6, this is a bioprospecting stage whose significance is in the identification and collection of potential high lipid producing microalgal strains. Bioprospecting comprises searching and collecting distinctive microalgal species across different aquatic environments to exploit them for potential applications such

as biofuels recovery (Araujo *et al.*, 2011; Mutanda *et al.*, 2011). It is a vital phase in isolating robust strains of microalgae in order to achieve efficient biofuel production. For instance, *Botryococcus braunii* has been reported to have an oil content which reaches 75% dry cell weight but this is associated with low biomass productivity (see Table 2.3). Strains such as *Chlorella*, *Isochrysis*, *Nannochloropsis*, *Dunaliella*, *Nannochloris* spp., on the other hand, have oil levels between 20 and 50% but better biomass productivities (Frenz *et al.*, 1989; Lubián *et al.*, 2000; Chinnasamy *et al.*, 2009; Tang *et al.*, 2011).

Ideally, growth physiology, strain robustness and metabolite production are the three major areas considered in the screening of microalgal strains. Growth physiology includes a number of factors that affect biomass productivity. These factors include but are not limited to growth temperature, salinity, availability of micronutrients and pH. The environmental conditions are to be considered in a way that mimics the natural habitats of the microalgal strains. For example, strains grown in less saline media are likely to accumulate more lipids as a result of the nutrient deprived conditions that enhances lipids accumulation (Rodolfi *et al.*, 2009).

Screening for metabolites entails the determination of the cellular composition of intracellular materials such as lipids. This also comprises lipid profiling, which permits a distinction between polar, neutral and other types of lipids (Khoomrung *et al.*, 2013). Depending on the strains, microalgae accumulate different types of lipids, hydrocarbons and other complex oils. However, some oils produced by microalgae are not suitable for biodiesel but most of the extracted oil can be converted (Hu *et al.*, 2008). The criteria for selection is often based on a number of parameters such as growth rate, lipid quality and quantity, adaptability to environmental changes and nutrient uptake rates (USDOE, 2010).

The robustness of strains takes into account factors such as community stability, culture consistency and vulnerability to predators present in the environment. The cultivation of microalgae in new environments is usually challenging as a result of the time it takes the cells to acclimatise to changes in their environment. Typically, lab-scale simulations of mass culture conditions are performed before outdoor mass cultures are considered (Amaro *et al.*, 2011; Araujo *et al.*, 2011; Rashid *et al.*, 2014).

In addition, the type of downstream technique required to recover the microalgae cells from suspension as well as extract the lipids embedded within the cell membranes also determines the type of microalgal strain to be selected. Ultimately, the isolation and selection of a strain will depend on its intended use. A balance between the aforementioned criteria is usually considered before a decision is made on which type of microalgal strain to select (Araujo *et al.*, 2011; Chen *et al.*, 2015).

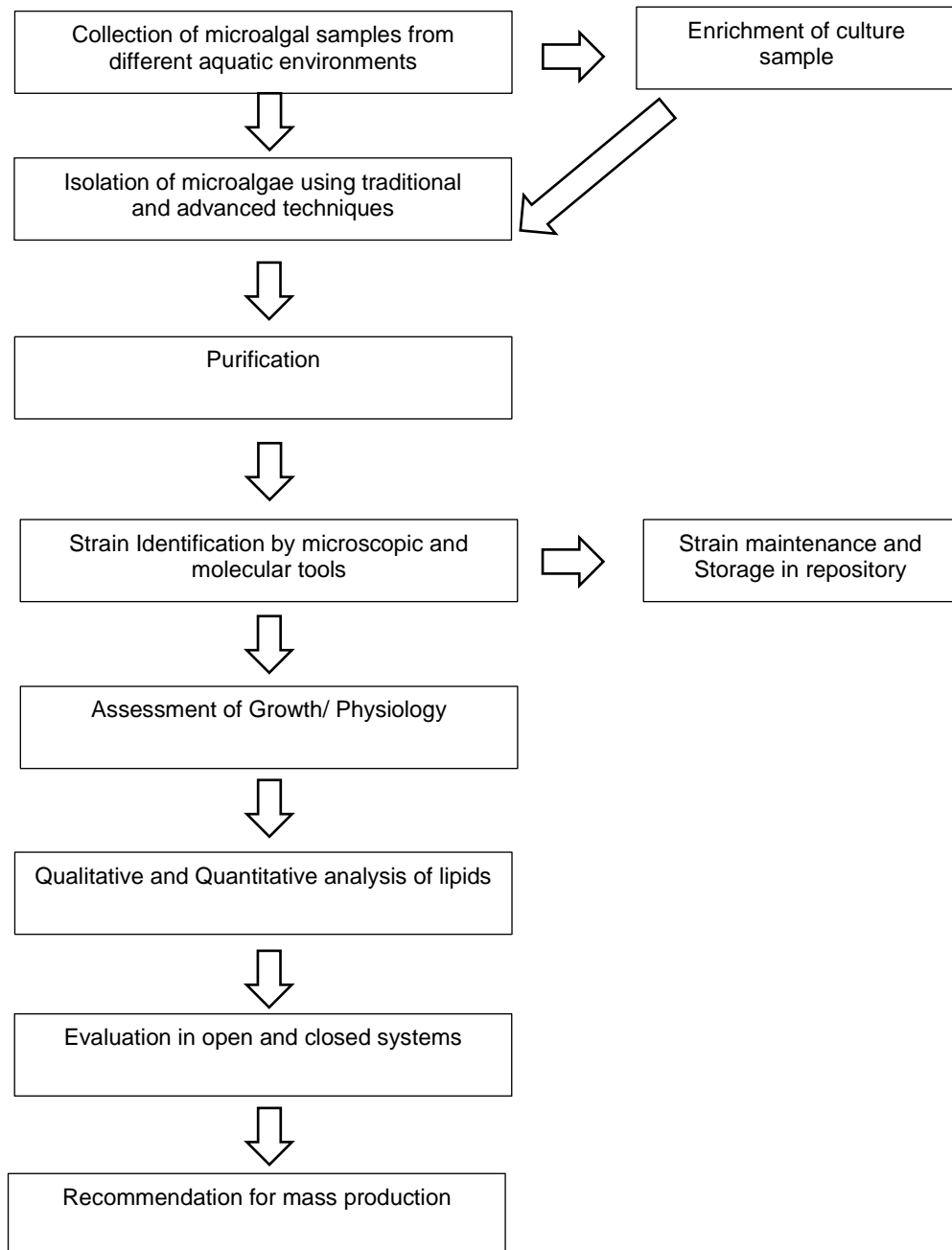


Figure 2:6: Schematic of stages involved in strain isolation and selection (Mutanda *et al.*, 2011).

Table 2.3: Oil contents of some microalgae strains (Chisti, 2007)

Microalgae strain	Oil content (% dry wt.)
<i>Botryococcus braunii</i>	25-75
<i>Chlorella sp.</i>	28-32
<i>Cryptocodinium cohnii</i>	20
<i>Cylindrotheca sp.</i>	16-37
<i>Dunaliella primolecta</i>	23
<i>Isochrysis sp.</i>	25-33
<i>Monallanthus salina</i>	> 20
<i>Nannochloris sp.</i>	20-35
<i>Nannochloropsis sp.</i>	31-68
<i>Neochloris oleoabundans</i>	35-54
<i>Nitzschia sp.</i>	45-47
<i>Phaeodactylum tricornutum</i>	20-30
<i>Schizochytrium sp.</i>	50-77
<i>Tetraselmis sueica</i>	15-23

2.2.3 Cultivation (Suspended systems)

Open ponds and photobioreactors are the leading cultivation systems utilized for the production of photoautotrophic microalgae biomass. These configurations are artificial production structures that are designed with the aim of replicating the natural aquatic conditions to achieve optimum growth (Pulz, 2001; Brennan and Owende, 2010; Rawat *et al.*, 2013; Gonçalves *et al.*, 2015).

In open pond configurations, also known as raceways, phototrophic microalgae photosynthesize using energy from sunlight, fix carbon dioxide from the atmosphere and assimilate nutrients from the environment (Chisti, 2007; Pienkos and Darzins, 2009). Raceways are closed loop recirculation channels which are usually oval-shaped. Mixing and circulation of the medium are required to prevent sedimentation and to stabilize microalgae growth and productivity; which can be achieved using a paddlewheel (see figure 2.7). This system is easy to operate and maintain, involves low capital costs and energy usage. However, monocultures are almost impossible

to achieve due to contamination, while biomass productivity is poor, utilisation of carbon dioxide and sunlight is also poor (Chisti, 2010; Milledge and Heaven, 2012).

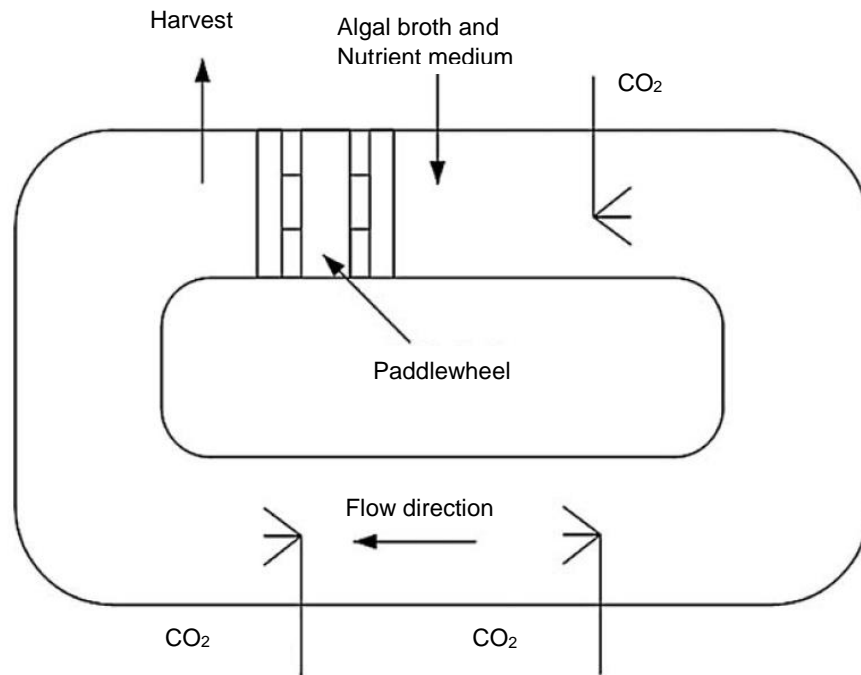


Figure 2:7: Plan view of an open raceway pond. Microalgae suspension is introduced after the paddlewheel, and completes a cycle as it is being mechanically aerated with CO_2 . Biomass are harvested before the paddlewheel to repeat the cycle again (Brennan and Owende 2010).

A closed photobioreactor system is usually made up of an array of plastic tubes or straight glass that are designed such that the sun rays are captured by the tubular array (Chisti, 2007). The tubular arrays can be aligned horizontally, vertically or as a helix. Closed photobioreactors can be configured as column, flat plate and tubular shapes (figure 2.8). A closed photobioreactor does not have some of the shortcomings inherent in the open pond systems. However, they are more expensive, difficult to scale up, and can accumulate oxygen (Pulz, 2001; Davis *et al.*, 2011; Chen *et al.*, 2011).

A hybrid production system is a two-stage cultivation set-up that aims to combine the complementary advantages of the open ponds and closed photobioreactor systems as well as minimising their disadvantages (Schenk *et al.*, 2008). It entails an initial growth stage in a closed photobioreactor where conditions are controllable to minimise contamination and enhance monoculture. The second stage is targeted at exposing the microalgae cells to nutrient stresses to improve synthesis of the

desired intracellular material such as lipids (Brennan and Owende, 2010; Rawat *et al.*, 2013).

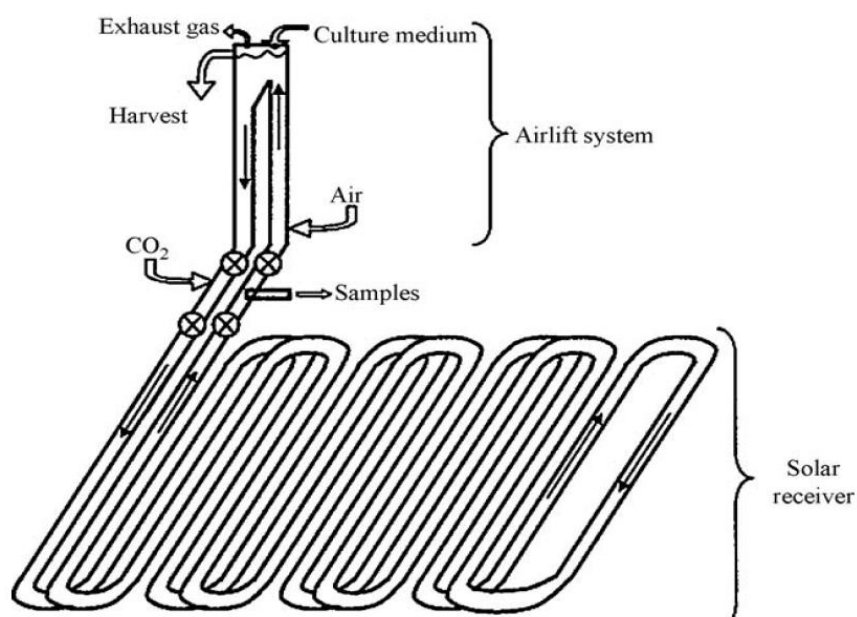


Figure 2:8: Basic design of a horizontal tubular photobioreactor. The two main sections include the airlift system and solar collector; the airlift system allow for the transfer of oxygen out of the system and transfer of carbon dioxide into the system in addition to providing a means to harvest the biomass. The solar collector provides a platform for the microalgae cells to grow by giving a high surface area to volume ratio (Brennan and Owende, 2010).

It has been reported that microalgae cells can be grown without light energy and on organic carbon sources such as sugars in fermenters in a system referred to as heterotrophic cultivation (Miao and Wu, 2006; Rashid *et al.*, 2014). Additionally, some strains can photosynthesise as well as ingest organic carbon sources for growth in a metabolic process called mixotrophic production (Chen *et al.*, 2011). An advantage of such production systems is that sunlight energy is not a limiting factor for growth.

2.2.4 Harvesting

The harvesting of microalgae biomass represents one of the most important stages in the process train for biodiesel production. Yet, the dilute nature inherent in microalgae cultures makes it one of the most difficult steps before lipid extraction can be achieved. The low specific gravity, small size and negative surface charges of the microalgae cells lead to stable suspensions which add to the difficulty of harvesting (Uduman *et al.*, 2010; Milledge and Heaven, 2012; Barros *et al.*, 2015;

Gerardo *et al.*, 2015). Depending on the end use of the algae biomass, a 2 step harvesting stage, classified as primary and secondary harvesting, is usually required to concentrate the microalgae culture to achieve 15 – 20% solids (Shelef *et al.*, 1984; Pragya *et al.*, 2013). Co-incidentally, most of the physical harvesting techniques developed to treat wastewater have been adapted to recover microalgae biomass from suspension. The density, motility, shape, size, surface charge and the importance of the target products determine the choice of harvesting technique to be employed (Henderson *et al.*, 2010; Brennan and Owende, 2010; Uduman *et al.*, 2010; USDOE, 2010). A number of these techniques are reviewed below:

2.2.4.1 Flocculation

Flocculation results in the formation of flocs which are formed by the neutralization of the negative surface charges of the microalgae cells. The negative surfaces are as a result of the dissociation of functional groups found on the cell membrane surfaces as well as the metabolic excretion of algogenic organic matter (Bernhardt *et al.*, 1991; Henderson *et al.*, 2008). The formation of flocs enhances the formation of large agglomerates thereby simplifying solid-liquid separation (Tenney *et al.*, 1969; Salim *et al.*, 2011; Vandamme *et al.*, 2013). Flocculation can be induced by the addition of chemicals known as flocculants which can be further divided into organic and inorganic flocculants.

Inorganic flocculants include aluminium sulphate (alum), ferric chloride and lime, which are multivalent metal salts. The use of such multivalent salts causes microalgae flocculation either by a charge neutralization mechanism or by reducing the surface charge, so long as the cells are small and nearly spherical (Molina Grima *et al.*, 2003; Uduman *et al.*, 2010; Wiley *et al.*, 2011). In a detailed literature survey conducted by Shelef *et al.*, (1984), it was concluded that a suitable pH is vital for effective microalgae flocculation to be achieved and that aluminium sulphate has a superior flocculating ability in comparison to ferric sulphate.

Organic flocculants are polymeric flocculants that may include ionic or non-ionic species and natural or synthetic polymers (Tenney *et al.*, 1969; Vandamme *et al.*, 2014). Cationic and anionic flocculants are examples of ionic species of polymeric flocculants although it was reported that cationic flocculants were more effective (Shelef *et al.*, 1984; Beach *et al.*, 2012). The use of these organic polymers

increases floc size and enhances microalgae settling as a result of their bridging power (Danquah *et al.*, 2009; Cheng *et al.*, 2011). The mechanism of flocculation by organic flocculants has been described as a combination of particle bridging and charge neutralization that largely depends on the charge density and the chain length of the polymers (Uduman *et al.*, 2010). A key advantage of employing polymeric flocculants is that a lower optimal dose is required to achieve effective flocculation and this can be accomplished at low pH levels (Tenney *et al.*, 1969; Shelef *et al.*, 1984).

The high ionic strength of media found in marine microalgae cultures implies that either organic flocculants are not effective or higher doses of inorganic flocculants are required in such high saline conditions (Sukenik *et al.*, 1988; Vandamme *et al.*, 2011; Hu *et al.*, 2013). Interestingly, the combination of organic and inorganic flocculants in such media resulted in improved flocculation and a lower dosage of inorganic flocculants being required (Sukenik *et al.*, 1988; Danquah *et al.*, 2009a). A study on how the use of chemicals might impact the quality of the final product, biofuels in this case, is yet to be undertaken. For instance, the utilization of these chemicals may not be suitable when the microalgae biomass is used in aquaculture. Hence, a detailed investigation of the effects, if any, of using such chemicals on the extracted lipids and/or the biomass will be useful. An alternative to the use of flocculants is to induce flocculation by pH change in a concept referred to as autoflocculation (González-Fernández and Ballesteros, 2012; Salim *et al.*, 2013; Gerardo *et al.*, 2015). This can be prompted by the use of alkalis such as calcium and sodium hydroxides to raise the pH of the culture media (Uduman *et al.*, 2010).

Bioflocculation of microalgae cells with autoflocculating microbes has been proposed as an alternative to chemical flocculation (see figure 2.9). Autoflocculating microbes could be microalgae (Lee *et al.*, 2009; Salim *et al.*, 2012), bacteria (Gutzeit *et al.*, 2005; Vandamme *et al.*, 2013), fungi or diatoms (Zhou *et al.*, 2013). For instance, some microalgae species could be in a symbiotic association with the filamentous fungi, *Aspergillus oryzae*. In such relationships, the microalgae cells through photosynthesis fix CO₂ to produce organic carbon thereby promoting the growth of the filamentous fungi. The latter in turn could entrap the microalgae through the hyphae produced by the fungi. This association could lead to the formation of fungi–algae pellets, therefore resulting in the efficient microalgae

harvesting (Zhou *et al.*, 2013). In some other cases, microbes such as bacteria, under nutrient depletion stress, excrete extracellular polymeric substances that promote binding of the microalgae cells thereby promoting flocculation (Salim *et al.*, 2011). Nonetheless, the potential for this novel approach remains largely at laboratory scale and the ease of full scale up and its cost efficiency remain unproven. Besides, as is typical of other flocculation means, it is preferred only as a pre-concentration step.

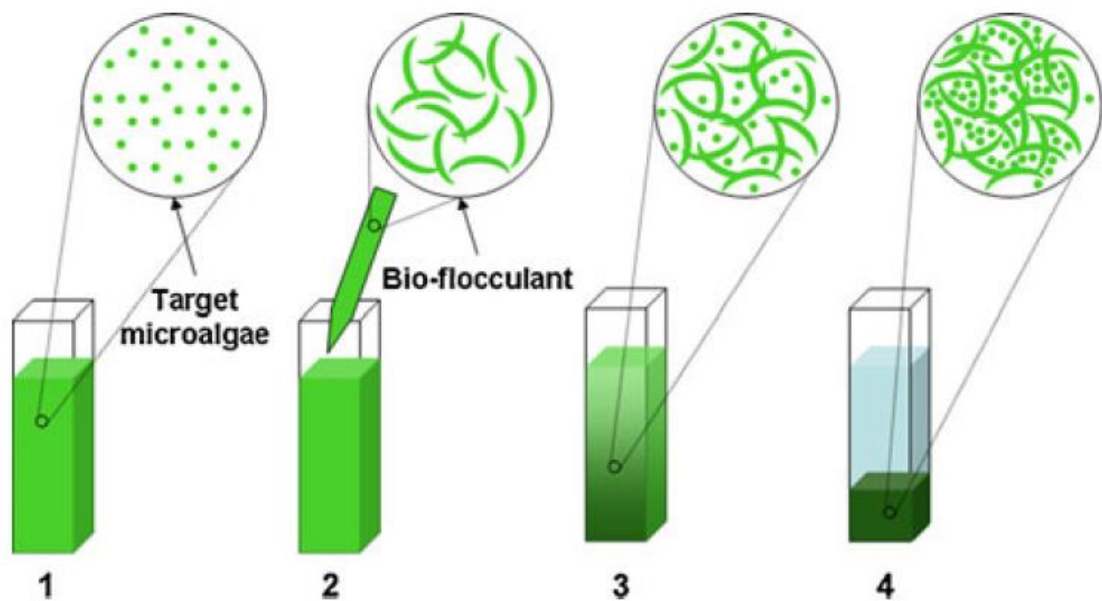


Figure 2:9: Schematic representation of proposed mechanism involved in the bioflocculation of *Chlorella vulgaris* cells using *Ankistrodesmus falcatus* as the flocculating microalgae cell (Salim *et al.*, 2011).

2.2.4.2 Gravity Sedimentation

This technique is often used in complement with flocculation to enable the separation of flocculated microalgae biomass from the liquid culture with the help of gravity (Yahi *et al.*, 1994). It is an inexpensive and widely used harvesting technique for biomass in wastewater treatment plants and is often applicable to open ponds (raceways) cultivation systems (Brennan and Owende, 2010; Singh *et al.*, 2011; Wiley *et al.*, 2011). However, it is a slow process that requires either the use of flocculants or for the microalgae to be relatively large ($> 70\mu\text{m}$) such as *spirulina platensis* thereby limiting its singular use in the industry (Greenwell *et al.*, 2010; Uduman *et al.*, 2010). Greenwell *et al.* (2010) opined that the method may not be suitable in high-temperate environments as much of the biomass produced may deteriorate during the time-consuming harvesting process.

2.2.4.3 Centrifugation

Centrifugation is a separation process which depends on the effect of centrifugal forces to separate suspended solids from liquids (Heasman *et al.*, 2000; Pragya *et al.*, 2013). It is a technique founded on the size of particle as well as the density difference between the media components. It is believed that the behaviour of the smallest particles in the media has the largest influence on efficiency of separation (Uduman *et al.*, 2010). Centrifugation is a rapid, very reliable and favoured technique to recover microalgae cells. Moraine *et al.* (1980) reported that centrifugation reliably recovered microalgae cells attaining between 80%–90% percentage recovery, depending on the speed, in less than 5 min (Pandey *et al.*, 2013). However, the process can be energy intensive, as a result, the capital and operating costs of running a centrifuge can be high (Molina Grima *et al.*, 2003; Brennan and Owende, 2010; Wiley *et al.*, 2011). Brennan and Owende (2010) also observed that a reason for the high operating costs may be due to the freely moving parts of the equipment, thus resulting in high maintenance requirements.

An appraisal of the technique estimated that centrifugation can consume *circa* 3000 kWh/ton dry algal biomass, which may restrict its application for microalgae biofuel (Wiley *et al.*, 2011). In addition, Barros *et al.* (2015) stated that centrifugation is an effective dewatering process, but exposure of cells to high gravitational and shear forces can damage cell structure. Be that as it may, it is a proven method but preferably utilized to recover highly valuable metabolites and to produce extended shelf life slurries for hatcheries and nurseries in aquaculture (Molina Grima *et al.*, 2003).

2.2.4.4 Filtration

Filtration systems are based on a solid-liquid separation involving the use of semi-permeable media to act as barriers (Danquah *et al.*, 2009). These barriers, whose pores are smaller than the cells, retain the latter whilst allowing selective passage of water and other soluble substances (Brennan and Owende, 2010). The most simple amongst the different modes of filtration is the dead-end filter (Greenwell *et al.*, 2010). As illustrated in figure 2.10, the suspension flows in a perpendicular direction to the filter medium. It entails the use of packed bed filters to concentrate microalgae biomass so that the filter beds retain the solids within the filter medium (Satyanarayana *et al.*, 2011). One of the forms of dead-end filtration is the surface

filter where solids are collected on the filter medium as a thin film or cake (Uduman *et al.*, 2010). A conventional filtration process is quite appropriate for large microalgae ($> 70\mu\text{m}$) such as *spirulina platensis* when operated under pressure or vacuum. However, amongst the main drawbacks of these methods are the operating costs and high capital in order to avoid blinding of filters. Ultrafilters and membrane microfilters are potential alternatives to conventional filters for the harvesting of small celled microalgae (Zhang *et al.*, 2010). The cost of membrane replacement and pumping are the major drawbacks that tend to limit their applications (Molina Grima *et al.*, 2003). Depending on the volume of the culture to be handled, microfiltration is less expensive than centrifugation for small-scale volumes while the latter may be more cost-effective for larger scale production (Molina Grima *et al.*, 2003). In addition, some types of dead end filtration such as pressure or vacuum filters failed to recover small-celled microalgae species such as *Chlorella* and *Dunaliella* (Brennan and Owende, 2010).

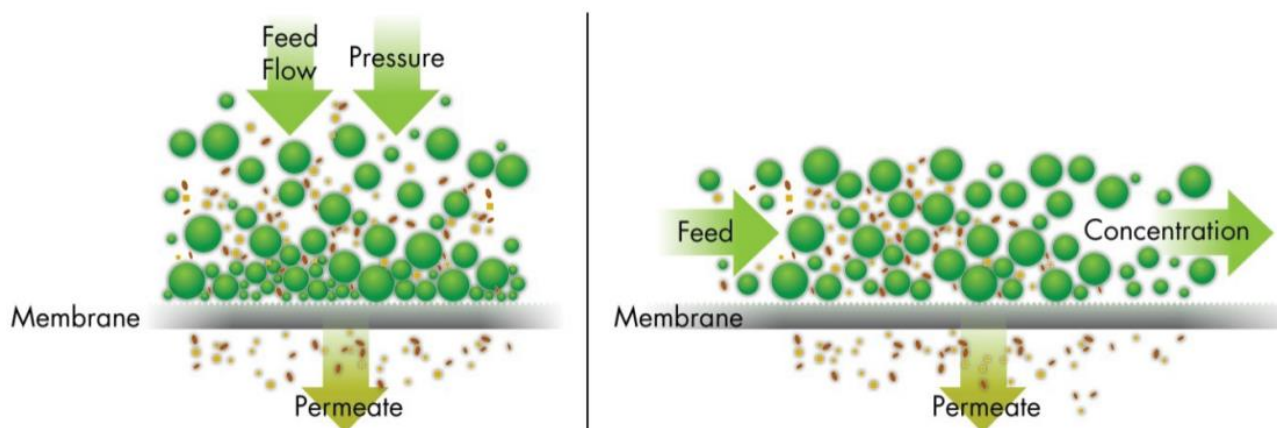


Figure 2:10: Schematic comparing conventional (dead end) and Tangential flow filtration systems (Stevens *et al.*, 2013).

In tangential filtration (cross-flow filtration) as the name suggests, flow is at a tangent to the membrane surface, while the retentate is recirculated across the membrane (Danquah, *et al.*, 2009). This keeps the cells in suspension, which reduces the build-up of filter cake thereby minimising fouling (Barros *et al.*, 2015). It is a technique that utilizes semi-permeable membranes with pore sizes ranging between a few Angstroms to microns (Gerardo *et al.*, 2015). The pore size of the membrane determines its classification as microfiltration, ultrafiltration, nanofiltration and reverse/forward osmosis (Gerardo *et al.*, 2015). Many studies reported are still lab-

scale in nature, and demonstration at large scale is atypical. Furthermore, energy consumption and cost estimates still needs to be established. Sharma *et al.*, (2013) reported that tangential filtration is too expensive to be considered for low-value products such as biofuels.

2.2.4.5 Flotation

Flotation is technology based on the premise that naturally buoyant cells are able to float upwards considerably more rapidly than they would sediment (Kim *et al.*, 2005). It is a method of separation that involves the use of air or gas bubbles, which attach to the solid particles to effectively reduce their density and enable them to float (Uduman *et al.*, 2010). Such attachments can improve the movement of microalgae biomass to the aqueous surface where they are accumulated as froth for easy removal. In some studies, flocculants are introduced into the microalgae suspension to increase the size of cell aggregates (see figure 2.11), which enhances the likelihood of a collision between the cells and bubbles. However, this can prove problematic as flocs become too large, thereby increasing the likelihood of detaching, thus requiring more bubble attachments.

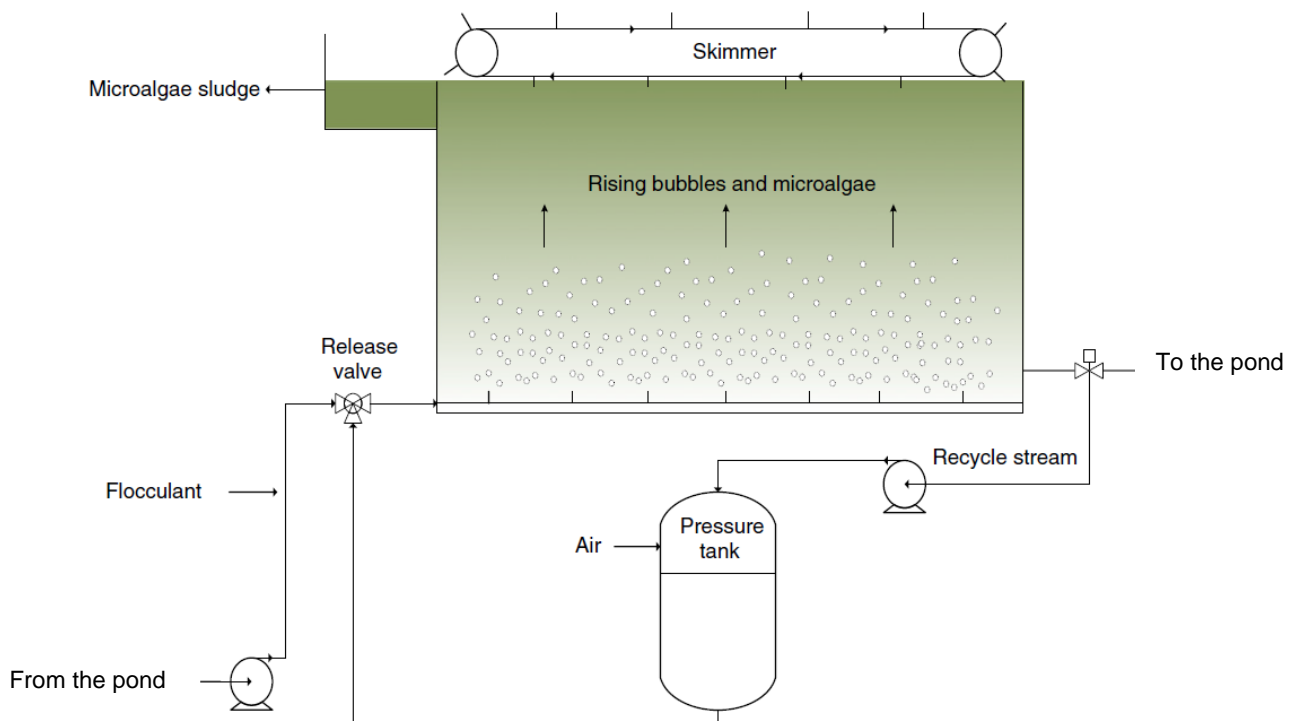


Figure 2:11: Schematic of flotation method combined with flocculation (Gerardo *et al.*, 2015)

The particles size and the ability of the bubbles to capture the particles are essential parameters of this technique (Barros *et al.*, 2015). Relatively small particles decrease the probability of collision and adhesion of the particles to the bubbles (Uduman *et al.*, 2010). Dissolved air flotation (DAF) and dispersed air flotation (DiAF) are the two main flotation techniques (Cheng *et al.*, 2011; Zhang *et al.*, 2012). Their main difference lies with the size of bubbles generated and the bubble generation mechanism. While bubble sizes range from 10 to 100µm with a mean diameter of 40 µm for dissolved air flotation; the size of bubbles are much bigger in dispersed air flotation ranging from 700 to 1500 µm (Uduman *et al.*, 2010; Rawat *et al.*, 2013; Gerardo *et al.*, 2015).

Scenedesmus quadricauda and *Chaetoceros* species are some of the strains whose cells were successfully recovered using dispersed air flotation and dissolved air flotation respectively (Uduman *et al.*, 2010). However not all types of strains require bubble attachment methodology. *Spirulina platensis* biomass were recovered utilizing their natural flotation characteristic without the aid of gas or air bubbles. This species with other types of cyanobacteria such as *Anabaena* and *Microcystis* possess gas vesicles which makes it problematic to harvest such species by sedimentation or centrifugation. Although 2% sodium chloride was added to the culture media to enhance the flotation activity of *Spirulina platensis*, this study demonstrated the possibility of harvesting some certain species of microalgae with gas vesicles without the need to generate air or gas bubbles (Kim *et al.*, 2005).

Generally, the flotation technique appears to be a technically sound method of harvesting. However, energy requirements of flotation methods are considered to be high as a result of the high pressures needed to supersaturate water with air bubbles (Brennan and Owende, 2010; Uduman *et al.*, 2010; Gerardo *et al.*, 2015). Other methods of creating micron-sized bubbles are being exploited, these include microflotation, vacuum gas, and froth flotation (Gerardo *et al.*, 2015). Their differences lie in the methods by which the bubbles are generated in the bulk liquid. Studies on the approaches are still in the early stages and more research is required to prove their efficiency at large scale.

2.2.5 Lipids Extraction

Lipids can be extracted from a microalgae biomass in different physical states, namely; as dried powder, concentrate or disrupted concentrate (Hanova *et al.*, 2010; Mercer and Armenta, 2011). These physical states largely depend on the pre-treatment pathway for the microalgae biomass. As the lipids are trapped in the cell wall of most algae strains, lipid extraction entails exposing the biomass to an extraction solvent to extract the lipids from the cellular matrices (Kanda and Li, 2011). The thickness of the cell wall and the size of the cell are critical properties of the microalgae strain that must be considered during the design and development of an extraction process (Halim *et al.*, 2012).

An ideal lipid extraction technology should possess the following properties;

- (1) a high level of specificity to extract lipids only and minimize co-extraction of non-lipid contaminants such as carbohydrates and proteins, and
- (2) To effectively extract lipids from either a concentrate or disrupted concentrate wet biomass feedstock to reduce energy requirements to dry (Pienkos and Darzins, 2009; Brennan and Owende, 2010; Halim *et al.*, 2012).

Extraction techniques that have been studied to elute lipids from microalgae biomass feed include but are not be limited to; cell disruption, solvent extraction, supercritical fluid extraction, sub-critical water extraction and direct esterification (Frenz *et al.*, 1989; Herrero *et al.*, 2006; Henriques *et al.*, 2007; Cooney *et al.*, 2009; Pragma *et al.*, 2013).

2.2.5.1 Cell Disruption Techniques

Disruption of cell walls prior to extraction is sometimes required as the cell walls and tissue structure form daunting barriers for the eluting solvents. As depicted in figure 2.12, the cell disruption techniques can be grouped into mechanical and non-mechanical methods. The former involves the application of mechanical forces, which include solid-shear forces (bead milling, high speed homogenisation), energy transfer through waves (sonication, microwave), liquid shear forces (high pressure homogenization) and heat (autoclaving) (Lee *et al.*, 2010; Mata *et al.*, 2010; Mercer and Armenta, 2011; Günerken *et al.*, 2015).

Cell homogenization is a technique of rupturing cell walls, which entails forcing the microalgae biomass through an orifice. This results in a prompt pressure change

and a high shearing action on the microalgae cell (Günerken *et al.*, 2015). Figure 2.13 is another configuration of cell homogenisation equipment where the impact of the accelerated microalgae suspension on the stationary valve surface causes cell disruption (Patravale *et al.*, 2004). In bead milling, microalgae cells are packed with small beads inside a vessel that can be agitated at high speeds. This also results in cell wall disruption. The degree of disruption is dependent on the strength of the cell walls, the composition, shape, and size of the beads, as well as the contact time between the beads and the microalgae cells (Rashid *et al.*, 2014; Günerken *et al.*, 2015).

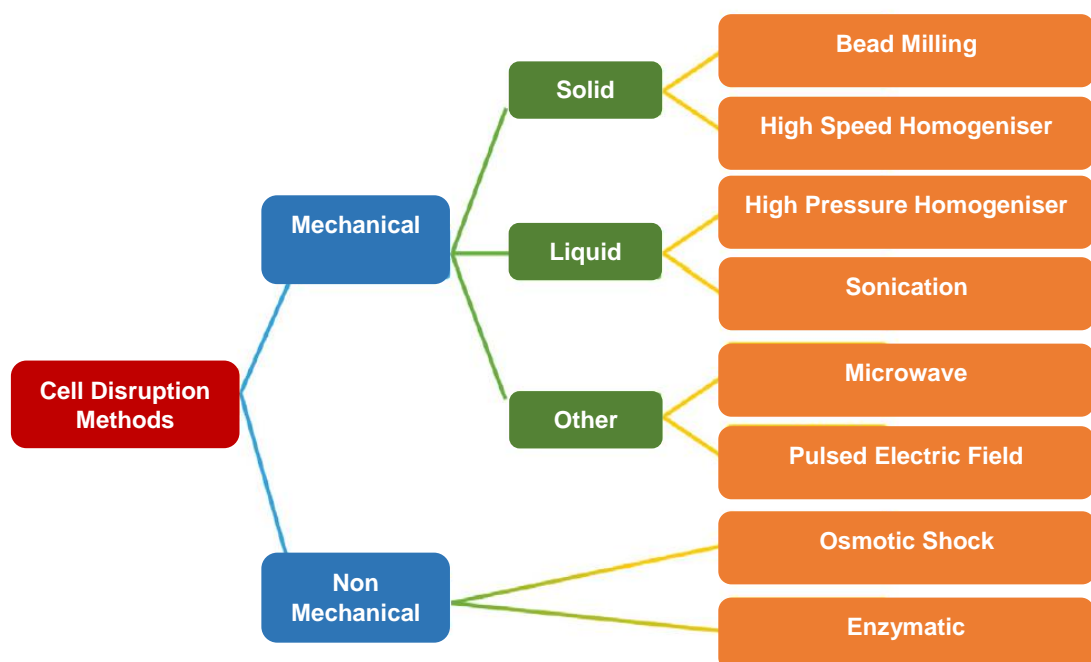


Figure 2:12: Grouping of the cell disruption methods (Günerken *et al.*, 2015).

Pressing involves rupturing the microalgae cells by subjecting dry microalgae biomass to high pressure (Mercer and Armenta, 2011). The use of ultrasonic waves to create bubbles in a solvent is referred to as sonication. The bubbles created are allowed to burst near the microalgae cell walls thereby producing shock waves throughout the solvent to rupture the microalgae cells (Wiley *et al.*, 2011). Lipids are then released from the ruptured cells into the solvent which can then be recovered using hexane as the eluting solvent.

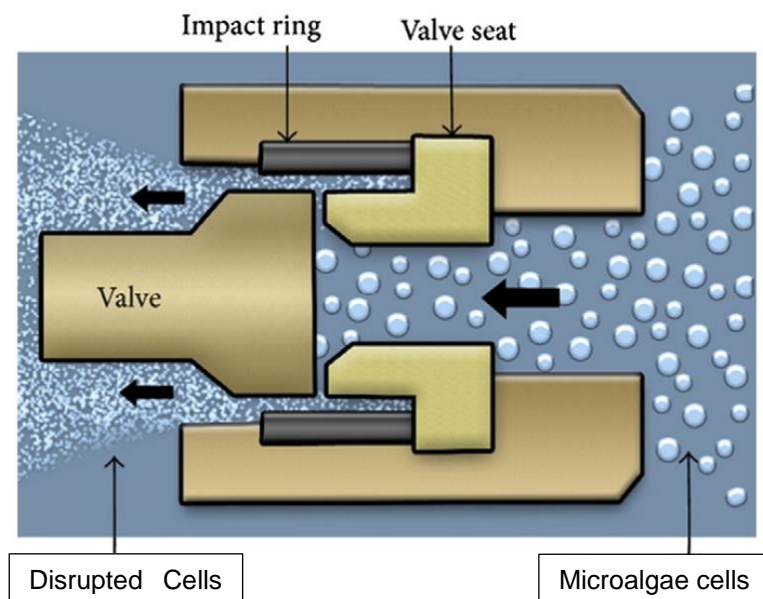


Figure 2:13: High pressure homogenization (Patravale *et al.*, 2004)

Microwave cell disruption techniques require that the microalgae cells are exposed to a shock from high frequency waves (Prochazkova *et al.*, 2013; Khoomrung *et al.*, 2013). While the use of high temperature and pressure to rupture the microalgae cell walls is known as autoclaving (Cooney *et al.*, 2009; Lee *et al.*, 2010 Mercer and Armenta, 2011). High intensity electric field pulse (HELP) utilises an external electric field to generate electrical potential across the cell wall/membrane. This leads to electromechanical compression thereby causing formation of pores in the cell wall/membrane (Barbosa-Canovas *et al.*, 1999).

A number of studies have been carried out to identify the most effective method of mechanical cell disruption. Prabakaran and Ravindran (2011) used *Chlorella* sp., *Nostoc* sp., and *Tolypothrix* sp. to compare the effectiveness and efficacy of autoclaving, bead milling, microwave, osmotic shock, sonication, and non-disruption methods. Prabakaran and Ravindran (2011) observed that high lipid content was extracted from all the species with sonication while the microwave method showed the highest extraction efficiency for *Tolypothrix* sp. Thus, the study concluded that sonication appears to be the simplest and most efficient of the cell disruption techniques investigated for the microalgae strains considered (Prabakaran and Ravindran, 2011).

In the same vein, a comparative study of autoclaving, bead-milling, microwave, sonication, and 10% sodium chloride solution was carried out using *Botryococcus* sp., *Chlorella vulgaris* and *Scenedesmus* sp (Lee *et al.*, 2010). Ironically, in this

study, sonication had either a lower or at best a comparable lipid extraction efficiency with other methods considered. Interestingly, microwave was observed to be the most efficient disruption technique for all the three microalgae species (Lee *et al.*, 2010). Lee *et al.* (2010) concluded that the microwave technique is straightforward and the most efficient disruption technique for microalgae cells. These studies may have differing conclusions, yet they share some similarities. In the two studies, microwave was found to be consistently effective.

A common observation from the two studies was that the application of cell disruption techniques minimised the amount of solvent required to elute the lipids. Furthermore, the use of these disruption techniques may help to offset the requirements to undertake solvent extraction on wet biomass at elevated temperature and pressure (USDOE, 2010). However, cell disruption techniques such as bead milling and pressing are more effective when the biomass is dried prior to extraction. However, the drawbacks of these mechanical methods include but are not limited to (Lee *et al.*, 2010; Mata *et al.*, 2010; Prabakaran and Ravindran, 2011; Günerken *et al.*, 2015);

- 1) technology proven only at laboratory scale,
- 2) high energy demands making it unfavourable for biofuel applications,
- 3) further cooling required due to heat generation,
- 4) initial drying of microalgae biomass is required,
- 5) denaturing of the lipids released due to temperature increase and chemical conversion,
- 6) Formation of very fine cell debris thereby requiring an additional downstream process,
- 7) Rupturing of cell walls/membranes is highly dependent on strain type.

Non-mechanical cell disruption techniques include enzymatic cell lysis (Lee *et al.*, 2010; Rawat *et al.*, 2013). This entails the use of lytic enzymes such as lipases, glucanases, glycosidases, and peptidases. The mechanism of cell lysis is based on the binding of enzymes to specific molecules in the cell wall/membrane to hydrolyse the bonds that result in the degradation of the cell wall/membrane. Osmotic shock is also a non-mechanical cell disruption technique that causes microalgae cells to burst and release their contents by exposing the cells to a sudden lowering of

osmotic pressure (Mata *et al.*, 2010; Mercer and Armenta, 2011). Non-mechanical cell disruption techniques are generally considered to be more benign to the cells and have higher selectivity to the product of interest in comparison to the mechanical methods. Nonetheless, some of the reported drawbacks include but are not limited to long process times, lower production capacity, product inhibition, high cost and non-suitability of some enzymes for microalgae cell wall/membrane disruption (Cooney *et al.*, 2009; Brennan and Owende, 2010; Mercer and Armenta, 2011; Günerken *et al.*, 2015).

2.2.5.2 Organic Solvent Extraction

The basic principles governing the organic solvent extraction of lipids from microalgae biomass is that “like dissolves like” (Bligh and Dyer, 1959). When a microalgae biomass is exposed to a non-polar organic solvent, the proposed mechanism for lipid extraction by organic solvents, as shown in figure 2.14, can be explained as one involving 5 different steps namely (Halim *et al.*, 2012);

- (1) the cytoplasm where the lipids are trapped is penetrated by the organic solvents through the cell membrane,
- (2) the neutral lipids and the organic solvent interacts using similar van der Waals forces of attraction,
- (3) an organic solvent/lipids complex is formed,
- (4) the organic solvent/lipids complex diffuses across the cell membrane driven by the concentration gradient, and
- (5) the organic solvent/lipids complex then diffuses across the static organic solvent film surrounding the cell into the bulk non – polar organic solvent environment.

However the use of non-polar organic solvents may result in the non-extraction of some the neutral lipids. This occurs when some neutral lipids occur as a complex with polar lipids which are facilitated by the strong hydrogen bonds to proteins in the cell membrane. Hence, polar organic solvents such as isopropanol and methanol are required to disrupt the lipid-protein association (Halim *et al.*, 2012).

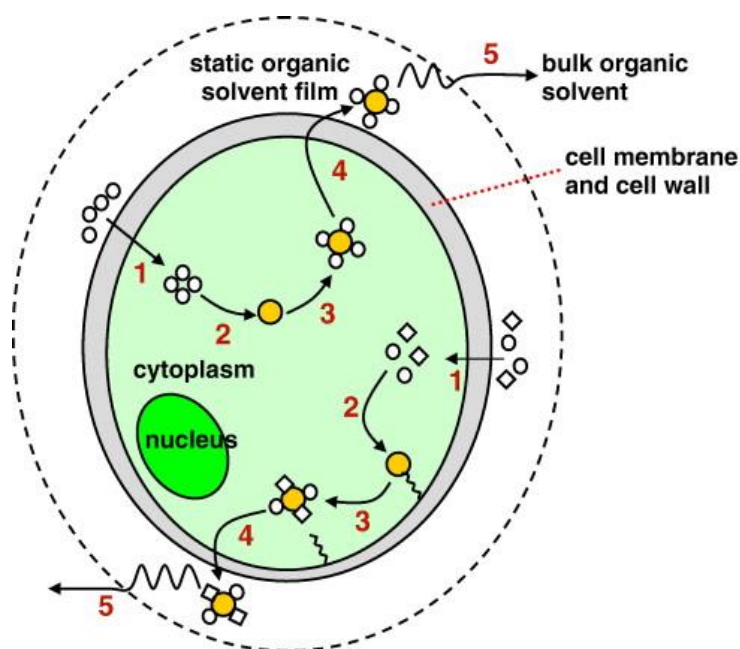


Figure 2:14: Schematic diagram of the proposed organic solvent extraction mechanisms..

● lipids, ○ non-polar organic solvent, ◇ polar organic solvent (Halim *et al.*, 2012).

An extraction process that is well-known in the application of the organic co-solvent mixtures technique is the Bligh and Dyer method (Iverson *et al.*, 2001). The Bligh and Dyer method entails the use of a miscible co-solvent mixture of methanol and chloroform (Cooney *et al.*, 2009). As explained earlier, the neutral lipids, mainly the hydrophobic lipids dissolve in the chloroform while the methanol dissolves the membrane-associated lipid complexes that are polar (Kates and Work, 1972). Afterwards, water is added to the co-solvent mixtures to induce a biphasic separation so that an organic phase (mixture of polar and non-polar organic mixtures) will contain primarily the polar and neutral lipids, while an aqueous phase (polar organic solvent and water mixtures) will mainly consist of non-lipid contaminants such as carbohydrates and proteins. The organic phase can then be decanted and evaporated to produce dry crude lipids for further processing (Cooney *et al.*, 2009; Halim *et al.*, 2012).

However, a limitation of the Bligh and Dyer method is that chloroform has a low selectivity for neutral lipids, thus, eluting pigments and non-lipid contaminants (Fajardo *et al.*, 2007). Furthermore, chloroform and methanol are known to be toxic solvents. Hence, alternative combinations that have been proposed include hexane/ethanol (Cartens *et al.*, 1996) and hexane/isopropanol co-solvent mixtures (Nagle and Lemke, 1990). Although hexane is less efficient in lipids extraction from

microalgae cells, its superior selectivity for neutral lipids, less toxicity and reduced affinity towards non-lipid contaminants and pigments makes it a preferred choice over chloroform (Schäfer, 1998). It is also worthy of note that the Bligh and Dyer method was reported to perform well mostly for samples that comprise less than 2% lipids but is less effective for samples whose lipid content exceeds 2% (Iverson *et al.*, 2001).

An obvious failing of solvent extraction is the need to use dried biomass to achieve an efficient extraction (Mercer and Armenta, 2011). This is due to the formation of a solvent shell around the lipids by the water present in a wet biomass which creates some difficulty for the organic solvents in extracting the lipids (Cooney *et al.*, 2009). Mechanical cell disruption may be helpful to ensure that organic solvents can fully penetrate biomass in order to make contact and extract the lipids (Lee *et al.*, 2010). Otherwise, solvent extraction may be undertaken at elevated temperatures and pressures to propel the solvents through the cell membrane but may lead to an extra cost for extraction due to additional energy needs (USDOE, 2010). Furthermore, the use of solvents at a large scale can incur more costs as a result of concerns over risk and safety associated with handling large quantities of organic solvents (Greenwell *et al.*, 2010; Mercer and Armenta, 2011). These challenges have made it difficult to scale up the solvent extraction into a viable industrial process, hence, it largely remains a laboratory scale technique (Cooney *et al.*, 2009).

2.2.5.3 Accelerated Solvent Extraction

Accelerated solvent extraction is the use of single organic solvents at elevated temperature and pressure to improve solvent extraction. The method is anchored on the principle that the utilization of solvents at temperature and pressure above their boiling point will ensure that; (1) the carrying capacity of solvents to elute lipids from the microalgae is greatly increased at high temperatures and (2) faster transport of organic solvent is achieved at high pressure which leads to the ease with which the solvent access the pores in the biomass matrix (Richter *et al.*, 1996). Usually for this technique, extraction of lipids from the cell matrix can take place at temperature range from 50 – 200°C and pressures between 50 – 300 psi within a time frame of between 5 – 10 minutes.

A study shows that this method can extract up to 90% of the lipids from microalgae biomass depending on the solvent employed (USDOE, 2010). A potential advantage of this technique is that less volume of solvent may be required to extract the lipids compared to when the solvents are employed without the elevated temperatures and pressures (Schäfer, 1998). Nonetheless, the main disadvantage of this is that biomass must be dried which leads to additional energy requirement for the process. More so, the use of solvents at elevated temperature and pressure adds to the energy intensity of the extraction process and may not be economically feasible at an industrial scale.

2.2.5.4 Supercritical Fluid Extraction

The method is based on using some chemicals, that can behave as both a gas and a liquid, at temperatures and pressures above their critical points such that their solvating power is enhanced (Herrero *et al.*, 2006; Couto *et al.*, 2010). From a number of chemicals such as carbon dioxide (CO₂), ethane, methanol, pentane and water proposed for this method, carbon dioxide is the most preferred choice. The preference for CO₂ lies with its relatively low critical temperature (31.1°C) and pressure (72.9 atm), low toxicity and chemical inertness (Herrero *et al.*, 2006; Mercer and Armenta 2011). At first, the CO₂ is heated and compressed above its critical point, attaining the liquid–gas state, before it is added to the harvested microalgae biomass, to act like a solvent (Cheung, 1999).

The advantages of this procedure include; (1) the ability to produce highly purified solvent-free lipid extracts, (2) separation and extraction is rapid as the product and solvent are easily separated as soon as the temperature and pressure of the system is below atmospheric conditions, and (3) the use of carbon dioxide from industrial waste counteracts greenhouse gas effects (Cooney *et al.*, 2009; Mercer and Armenta, 2011; Halim *et al.*, 2012). Extraction of lipids from microalgae strains such as *Cryptocodinium cohnii*, *Spirulina platensis*, *Botryococcus braunii* and *Skeletonema* have been reported (Couto *et al.*, 2010; Tan *et al.*, 2015).

Cooney *et al.* (2009) suggested that a dried biomass is required for this technique. However, a laboratory study investigated supercritical carbon dioxide (SCCO₂) extraction using dried and wet biomass of *Chlorococcum* sp. Interestingly, the results obtained showed that a higher final yield was extracted from the wet biomass

than the dry biomass. The study suggested that water aided extraction due to its swelling of the cellular matrix and its usual function as a polar co-solvent (Halim *et al.*, 2011). This observation is in contrast to Cooney *et al.* (2009) assertion as well as the common view that water acts as a barrier to extraction of lipids from microalgae cells. What appears logical is that the outcome of this study is only peculiar to supercritical carbon dioxide extractions. This is because the same study also observed that hexane extraction from wet biomass resulted in less lipid yield than the dried biomass (Halim *et al.*, 2011).

In as much as supercritical carbon dioxide extractions appear to be an emerging green technology, prohibitive costs of installation of extraction pressure vessels as well as high energy requirements for heating and fluid compression remain the principal hindrances for scaling up this extraction method for biofuel applications (Cooney *et al.*, 2009; Halim *et al.*, 2012, Rawat *et al.* 2013).

2.2.5.5 Sub-critical Water Extraction

When accelerated solvent extraction method is carried out with water as the solvent, the procedure is referred to as pressurized low polarity water extraction, preferably known as sub-critical water extraction (Herrero *et al.*, 2006). In the this procedure, polarity of water decreases as pressure increases with the effect that the solvent power of water is modified (Soto Ayala and Luque de Castro, 2001). The implication is that water can extract compounds that would otherwise not solubilize in water (Mercer and Armenta, 2011). Similar to accelerated solvent extraction, the advantages of this method include; (1) the extraction time is rapid, (2) the quality of the extract is enhanced, (3) the eluted lipids and water are easily separated immediately the process system is cooled to room temperature (as the mixture of water and lipids becomes immiscible) (4) the dewatering stage can be eliminated as water is the solvent, and (5) it is an environmentally clean process (Herrero *et al.*, 2006; Cooney *et al.*, 2009).

Nonetheless, there is dearth of literature regarding the performance of this method to extract lipids from microalgae. A number of studies have claimed to successfully extract oil from plants and other products such as carotenoids and antioxidants from microalgae. However, the technique suffers from the high energy load required to heat and pressurise the system which affects the ease of scale up of the process

(Cooney *et al.*, 2009). Cooney *et al.* (2009) also opined that commercial applications to extract lipids may prove to be energy intensive due to the need to install large cooling systems to reduce the temperature of the product so as to prevent product degradation.

2.2.5.6 *In situ* microalgae biomass transesterification

Transesterification is a chemical reaction often used to convert raw microalgal lipid (triacyleglycerols/free fatty acids) into biodegradable, non-toxic and renewable biodiesel, also known as fatty acid methyl esters (Singh *et al.*, 2008). The reaction takes place as an equilibrium, hence a supply of alcohol in excess is required to ensure the equilibrium shifts towards the biodiesel product and improves the rate of reaction (Li *et al.*, 2011). However, as depicted figure 2.15, it is possible to convert the lipids while still trapped in the biomass without the need for an initial lipid extraction.

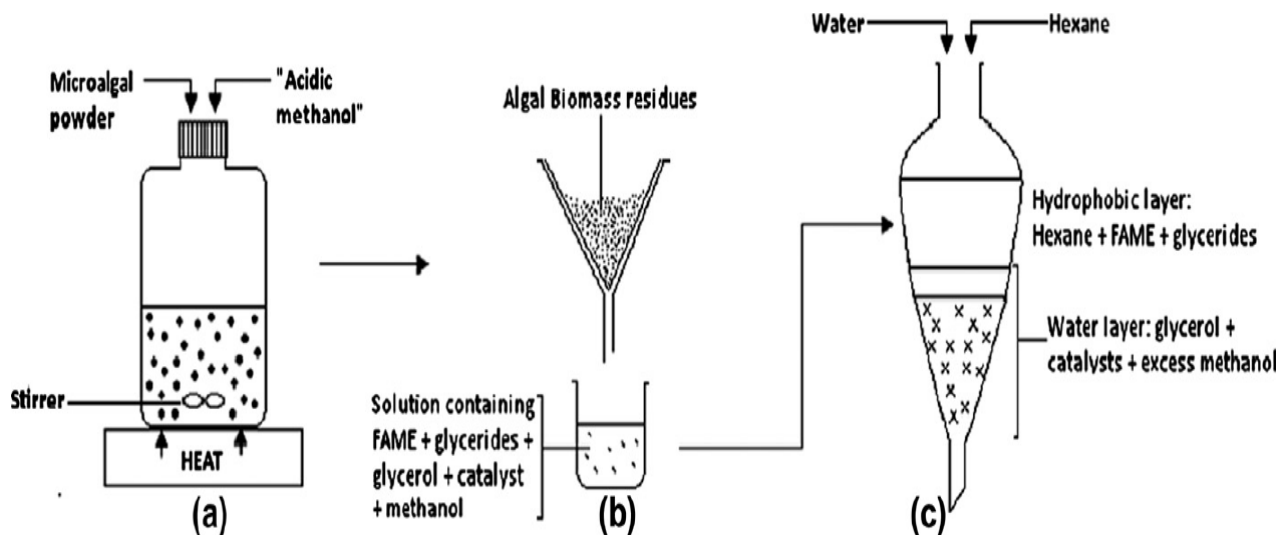


Figure 2.15: Schematic of *in situ* biomass transesterification (Rawat *et al.*, 2013).

According to Rawat *et al.*, 2003, Figure 2.15 can be explained as involving 3 different steps namely; (a) The vessel is allowed to stand for complete reaction. (b) The reaction mixture can be filtered and the residues washed by re-suspending in methanol to recover any product traces (c) Water and Hexane are added to aid the separation of the hydrophilic components of the extract, and further extraction of the product respectively.

Lepage and Roy (1984) were the first to apply this method on human milk and adipose tissue by-passing the extraction of fatty acids. In their application for biofuel application, Harrington and D'Arcy-Evans were reported to be the first researchers to establish the technique for biodiesel production from a sunflower seed feedstock (Lepage and Roy, 1984). It is a one-step procedure where an alcohol (for example methanol) in the presence of an acid catalyst (for example acetyl chloride) is added to the microalgae biomass and heated to a temperature of 100°C for one hour under sealed conditions (Lepage and Roy, 1984). Another study later discovered that the duration of reaction can be reduced to 10 minutes when hexane is added to the reaction phase and a dried microalgae biomass is utilized (Rodríguez-Ruiz *et al.*, 1998). It was also reported that the presence of a less polar solvent (for instance toluene) in the alcohol modifies the reaction medium polarity and as such increases the efficiency of the reaction (Carvalho and Malcata, 2005).

Some of the reported merits of this technique include (Cooney *et al.*, 2009);

- (1) more efficient recovery of lipids, 15-20% above conventional extraction pathways,
- (2) removal of the necessity to utilize antioxidants to protect unsaturated lipids,
- (3) minimises the amount of downstream processing required to produce biodiesel.

Nonetheless, some of the shortcomings reported for this procedure include (a) the need to increase the volume of alcohol for complete conversion, (b) temperature sensitivity, (c) moisture content of the microalgae biomass has a negative effect on biodiesel yield, and (d) drying of the biomass adds to the energy requirement. Further research is also required to investigate the effects of process parameters such as reaction time and temperature on the properties of the biodiesel formed (Cooney *et al.*, 2009; Mercer and Armenta, 2011; Günerken *et al.*, 2015).

2.2.6 Challenges and Prospects

The Aquatic Species Program established in 1970 by the United States Department of Energy was among the earliest attempts to develop biofuels from microalgae (Sheehan, 1998; Jarvis, 2008). One of the main conclusions of a report produced after the winding down of the program was that it was not economically feasible to produce biodiesel from microalgae as the cost of production would be double the

cost of a comparable production of petroleum diesel (Sheehan, 1998). Despite various remarkable efforts in research and development, production of microalgae biofuel at a competitive economic scale is still very limited. At present, a number of companies attempting economic scale production of biofuels from microalgae include but not limited to Neste Oil, Algenuity, Renewable Energy Group, Cellana and Sapphire Energy Inc to mention but few. Whether these companies are operating at competitive production and for how long they can afford to remain in business is unknown. This is not unconnected to the challenges of replicating successes discovered in the laboratory into long term commercial production ((Singh and Gu, 2010; Chisti and Yan, 2011).

The dilute nature of microalgae cultures makes it difficult to recover microalgae cells let alone to extract the biofuels/biofuel precursors such as lipids. Small celled strains, typically 2 – 10 μm , have densities almost equal to their suspension media. Coupled with their highly negative surface charges, the cells are quite stable in suspension. Hence, either a primary or secondary dewatering procedure or a combination of both in most cases is required. In addition, a number of extraction processes require an initial drying of the biomass, thus increasing the cost and energy requirements for biofuel recovery (Brennan and Owende, 2010; Halim *et al.*, 2012; Pienkos and Darzins, 2009). Furthermore, the initial drying of the biomass has been associated with risks of biomass loss during transportation of the biomass (Brennan and Owende, 2010). The existing conventional harvesting and extraction techniques are energy intensive and account for up to 20-30% of the total production costs (Brennan and Owende, 2010).

Recent research and development efforts have been directed towards by-passing the need to dry the algae biomass before the lipids can be extracted as well as avoiding the need to harvest/dewater the microalgae biomass. For instance, Dierkes *et al.* (2012) investigated explosive decompression, using CO_2 , butane or propane, of *Haematococcus pluvialis* cells still in suspension for concurrent cell disruption and lipid extraction. An extraction efficiency of between 80–100% of the lipids was reported. Likewise, McMillan *et al.* (2013) employed laser technologies to rupture membranes of cell suspensions and reported that rapid cell membrane disruption was achieved in comparison with other conventional cell disruption technologies. In the same vein, Yoo *et al.* (2014) used a method that entails coating the cell

membranes with cationic polymer to disrupt their local electrostatic equilibrium due to the membranes being in contact with tertiary-amine cations. It was reported that simply shaking the microalgae suspension afterwards, resulted in the rupturing of the cell membranes.

These efforts attest to the genuine interest directed towards microalgae biofuel. Regardless of this, significant research efforts are still desirable for some of these promising emerging approaches, while existing conventional techniques need further refinements.

2.2.7 Summary

This section reviews the stages involved in the recovery of microalgae cells and their intracellular materials. The significance of each stage, from identification of a particular microalgae strain to the recovery of the embedded materials such as lipids, was thoroughly discussed.

Open ponds and closed photobioreactors are established cultivation systems being utilised in the production of microalgae biomass. However, each of these systems has their unique problems which has led to the design of hybrid systems. The latter aims to combine the complementary advantages of those two systems. As will be discussed in the next chapter, novel systems are being investigated due to the challenges still being experienced with the well-known cultivation systems.

The recovery/harvesting of the cells is one of the most important stages. The dilute nature of microalgae suspensions requires concentration/dewatering before any other downstream processes can be applied. While conventional techniques discussed in this chapter have been successfully used to recover microalgae biomass, the energy implications of those techniques have limited their use to experimental laboratory trials. The same can be said of the lipid extraction stage, where a lot of studies have demonstrated the use of cell disruption/extraction techniques, but commercialisation to full scale remains limited.

One of main problems is that the biofuel products are not considered as high value product, for example, β -carotene. Added to this, is the reality that microalgae biofuel will have to compete with fossil fuels and/or other renewable energy options. The

implication is that the net energy balance and associated costs involved have to be competitive in commercial production.

Despite the various efforts highlighted in this chapter, there is still a need to embark on more research effort to develop the existing techniques. However, it is clear that alternative, novel processes, also need to be explored if any significant breakthroughs are to be achieved in the microalgae biofuels industry.

2.3 Theory of Adsorption and Electrochemical Methods

2.3.1 Introduction

The conventional techniques of recovery that have been developed to recover microalgae cells from suspension are also directly applied in water treatment processes. Despite the similarity in these techniques, the objectives of dewatering algae suspensions are quite dissimilar from wastewater treatment technologies. In the former, the aim is to concentrate the biomass for further processing which includes but is not limited to the extraction of lipids. Hence, care must be taken to avoid contamination during the dewatering process. Various research efforts (as reviewed in section 2.2) have been carried out to investigate the application of these techniques for biofuel purposes.

Ironically, adsorption and electrochemical methods, despite being wastewater treatment options, have not received significant attention as most other technologies for biofuel applications. Without a doubt, recovering microalgae cells and/or the intracellular materials trapped within the membrane after an adsorption process may truly pose a substantial problem. Nonetheless, adsorption as a method of recovery of cells onto an adsorbent material provides an opportunity. This is because microalgae strains possess the natural tendency to attach to surfaces; a property that none of the existing conventional techniques make use of.

Hence, the objective of this section is to review the literature on the application of adsorption and electrochemical processes especially for microbial cells.

2.3.2 Adsorption Process

Adsorption is a mass transfer procedure of recovering materials (also known as adsorbate) from the liquid or gas phase onto a suitable solid phase material known as the adsorbent. In adsorption, adsorbates from the bulk fluid diffuse to the solid

adsorbent surface to form a distinctive adsorbed phase (Tchobanoglous *et al.*, 2003). The use of adsorption has found application in (Crini and Badot, 2010);

- (i) separation and purification of liquid or gas mixtures,
- (ii) drying of liquids and gases
- (iii) purification of water
- (iv) wastewater treatment
- (v) removing (trace) constituents from liquid or gas mixtures
- (vi) purification and separation of biological and pharmaceutical substances
- (vii) biotechnology industry.

Adsorption exploits the readiness of the component of interest to bind to the surface of the solid particles (Tchobanoglous *et al.*, 2003). In the midst of a number of water treatment technologies, adsorption is considered to be one of the best options as a result of its ease of operation, simplicity of design and high efficiency. This is because the use of adsorption results in the reduction of Biological Oxygen Demand (BOD), Chemical Oxygen Demand (COD), colour and odour from wastewater. These are problems, to an extent, resistant to biological degradation. In addition, other physio-chemical treatments method such as coagulation, filtration and sedimentation are not effective in removing them. One of the limitations of adsorption is its being a non-destructive method that entails a phase change of pollutants, thereby resulting in additional problem of sludge disposal. Activated carbon is the most extensively used adsorbent, which has found applications as early as the 1900s to treat drinking water (Faust and Aly, 1998; Tchobanoglous *et al.*, 2003; Hammer, 2008).

However, activated carbon is expensive and non-selective. Various studies that have been undertaken to replace activated carbon have resulted in the development of zeolites, silica gels, commercial ion exchange resins, biomass, biopolymers, chitosan and nanoparticles to mention but a few. In addition, sometimes the various adsorbents have specific applications, for example in colour removal, metal extraction and fluoride removal (Crini and Badot, 2010).

In biotechnology applications, adsorption is one of the ways to achieve immobilization of cell systems such as algae. Immobilization involves the use of support materials to retain microbial biomass. It has been reported that application

of immobilized systems can be found in culturing of metabolite products, metal and organic pollutants removal and nutrient removal to mention but a few (Klein and Ziehr, 1990; Cassidy *et al.*, 1996; Moreno-Garrido, 2008).

Furthermore, some studies have categorised adsorption into two types; physisorption and chemisorption. Physisorption is a non-specific loose binding of the adsorbate to the adsorbent as a result of van der Waals type interactions. In physisorption, multi-layered adsorption is possible and can be disrupted by increases in temperature or pressure decreases (Sing, 1995; Rouquerol *et al.*, 2013). However, chemisorption entails a more specific attachment between the adsorbate and the adsorbent particles akin to a chemical bond. This type of adsorption is not easily reversible (Coughlin *et al.*, 1968; Rivera-Utrilla *et al.*, 2001).

2.3.2.1 Modes of Solute Removal in an Adsorption System

The adsorbent material, Nyex™ can be employed in removing the solute (adsorbate), in this study microalgae cells, by either

- i) mixing the solid adsorbent with the suspension/solution to be treated within a batch process followed by filtration or sedimentation of the spent adsorbent, or
- ii) allowing the solution/suspension to flow through a bed of solid adsorbent packed within a column which can be operated as a fixed, fluidised or spouted bed (Tchobanoglous *et al.*, 2003).

The two of modes are used for different purposes; for example, the batch is useful to estimate the capacity of the adsorbent while the bed column helps to explore the operational behaviour for industrial applications (McKay 1995; Crini & Badot 2010). One of the most important pieces of information for a batch evaluation of an adsorption process is the capacity of the adsorbent particles for the solute of interest. This is because different adsorbent materials have a varied capacity for different solute particles.

Adsorptive capacity represents the amount of adsorbate that can be recovered per unit mass of the adsorbent. Generally, the higher the adsorptive capacity the better, however, a low adsorptive capacity does not necessarily imply a bad adsorbent as other considerations such as ease of adsorbent regeneration may influence the

choice of adsorbent to use (Brown *et al.*, 2004). More importantly, is the fact that such a knowledge (adsorptive capacity) is key in any potential scale up of the adsorption process. Knowing the adsorptive capacity can help in making a decision over the potential use of a particular adsorbent. In the research reported in this thesis, the adsorbent/adsorbate system was NyexTM/microalgae cells.

The amount of adsorbate taken up by an adsorbent is a function of

- the concentration and characteristics of the adsorbent,
- the concentration and characteristics of the adsorbate,
- the temperature of the system (Faust & Aly 1998; Tchobanoglous *et al.* 2003; Crini & Badot 2010).

In most cases, the temperature of the system is kept constant, such that when the other two are graphed at equilibrium, the resulting plot is referred to as an adsorption isotherm. In rare cases, solid adsorbent concentration is kept constant to produce graph known as adsorption isosteres (Tchobanoglous *et al.*, 2003).

2.3.2.2 Adsorption Isotherms

Adsorption isotherms can be developed by varying the amounts of either the adsorbate or the adsorbent which are exposed to a fixed amount of the adsorbent and adsorbate respectively. Typically, experiments are carried out in a batch unit and a minimum time is allowed for the adsorbate and adsorbent to “equilibrate”. For a batch system which contains a known amount of a solid adsorbent and a known concentration of the solution to be treated, a mass balance after a mass transfer process at equilibrium can be expressed in words as;

$$\text{Quantity adsorbed} = \text{Initial quantity of adsorbate} - \text{Final quantity of adsorbate} \quad (2.1)$$

Equilibrium is attained when the rate of adsorption of solute onto to the adsorbent surface equals the rate of desorption of solute from the surface. The driving force is the difference between the amount of solute adsorbed to the solid phase and the amount of adsorbable solute in the liquid phase at a particular concentration (McKay, 1995; Hammer, 2008). At equilibrium, this difference is expected to be zero. However in real systems, this may not be the case but at least the driving force should tend to zero so that the amount of solute being taken from the liquid phase becomes insignificant.

The statement from equation (2.1) can be symbolically represented as;

$$q_e M = V C_o - V C_e \quad (2.2)$$

Where q_e = concentration of the adsorbed phase after equilibrium, mg(adsorbate)/g(adsorbent)

M = amount of adsorbent, g

V = Volume of the liquid in the batch system, L

C_o = initial concentration of adsorbate in solution, mg/L

C_e = final equilibrium concentration of adsorbate in solution, mg/L

Equation (2.2) can be re-written as;

$$q_e = \frac{V}{M} (C_o - C_e) \quad (2.3)$$

Based on equation (2.3), a number of adsorption isotherms describing the attachment of adsorbate have been developed which include Langmuir, Freundlich, and Brunauer, Emmet and Teller (Bitton and Marshall, 1980; George and Davies, 1988; Tchobanoglous *et al.*, 2003; Crini and Badot, 2010).

The Langmuir model was developed based on the following assumptions;

- the adsorbent surface has a fixed number of sites accessible to the adsorbate,
- only monolayer adsorption is possible and,
- adsorption is reversible.

It has been defined mathematically as;

$$\frac{x}{M} = \frac{abC_e}{1+bC_e} = q_e \quad (2.4)$$

Where $\frac{x}{M}$ = mass of adsorbate adsorbed per unit mass of adsorbent, measured in, mg(adsorbate)/g(adsorbent). This term is the same as q_e in equation (2.3) above.

a and b are empirical constants.

C_e = equilibrium concentration of the adsorbate in solution after adsorption, mg/L

The empirical constants of the Langmuir isotherm can be determined by plotting (C_e/q_e) versus C_e after the linearized form of equation (2.4) has been established which can be given as:

$$\frac{C_e}{q_e} = \frac{1}{ab} + \frac{1}{a} C_e \quad (2.5)$$

Where $\frac{1}{a}$ and $\frac{1}{ab}$ can be estimated from the slope and the y – intercept of the graph respectively.

While the Langmuir isotherm is generally the most commonly used, for water and wastewater systems the Freundlich isotherm is often preferred, particularly where the adsorbent is activated carbon. This is generally because the Freundlich isotherm describes the data better if the adsorbate is at lower concentrations as is usually the case in water and wastewater systems (Mohan and Pittman Jr, 2007; Hammer, 2008).

The Freundlich isotherm is mathematically defined as;

$$q_e = K_f C_e^{1/n} \quad (2.6)$$

Where K_f = Freundlich capacity factor, $(mg/g)(L/mg)^{\frac{1}{n}}$

$1/n$ = Freundlich intensity parameter.

The constants in the Freundlich isotherm can be estimated by plotting $\log(q_e)$ against $\log C_e$ after the linearised form of equation (2.6) has been established which is given as;

$$\log(q_e) = \log K_f + 1/n \log C_e \quad (2.7)$$

Whereas some of these classical adsorption isotherms were developed for soluble/gaseous species, a number of works have also reported their application to the adsorption of microbial cells from suspension (Bitton and Marshall, 1980; George and Davies, 1988; Kim *et al.*, 2009). Bitton and Marshall (1980) depicted the initial reversible reaction between the adsorbent and the microbial cell as;



Equation 2.8 symbolises the formation and potential dissociation of cell – adsorbent complexes/aggregates.

For a reversible process that is governed by monolayer adsorption, the Langmuir isotherm can be applied to describe the rate of adsorption and desorption at equilibrium in a mathematical form as (Bitton and Marshall, 1980);

$$\frac{q}{q_z} = \frac{K_L C_e}{1 + K_L C_e} \quad (2.9)$$

Where C_e = equilibrium concentration of the microbial cells (cells/m³), q = number of adsorbed microbial cells per unit mass of adsorbent (cells/g), q_z = adsorbent capacity (cells/g), K_L = equilibrium constant (m³/cells).

2.3.2.3 Breakthrough curves

An S-shaped graph of concentration against time, also referred to as a breakthrough curve, is often used to evaluate the performance of an adsorption process in a column. The steepness of the curve indicates the efficiency of the adsorbent bed (Borba *et al.*, 2006). Figure 2.16 illustrates a typical breakthrough curve, which shows the movement of a mass transfer zone (MTZ) along the adsorbent bed. As suspension is allowed to flow through the bed, it initially comes in contact with the first layers of the adsorbent.

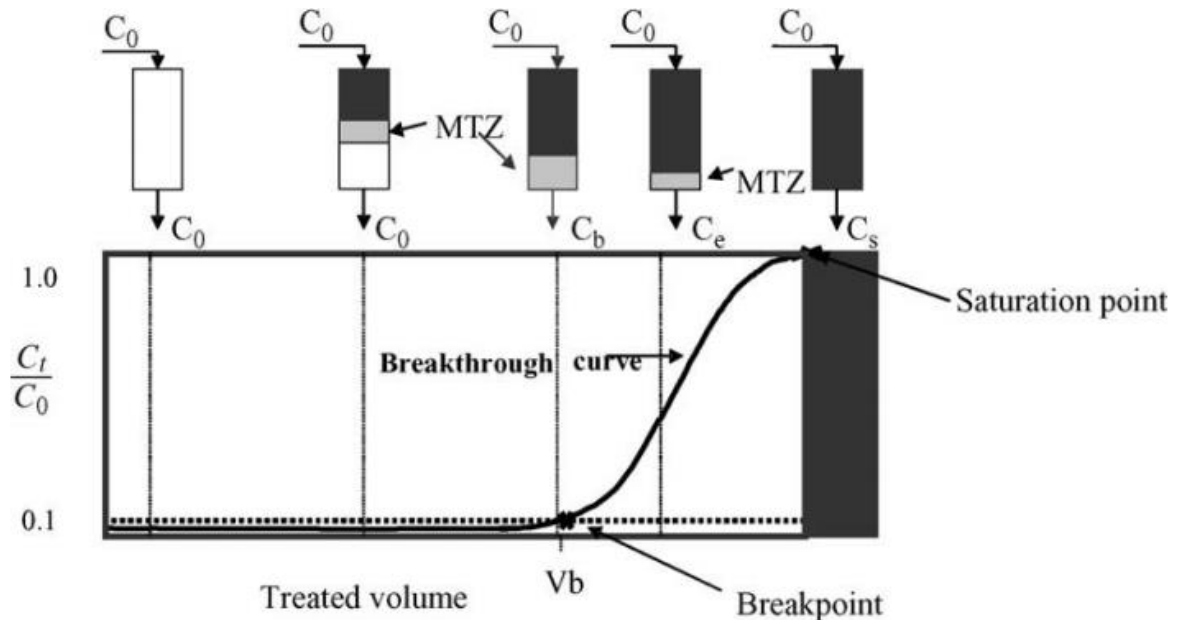


Figure 2:16: The schematic of a breakthrough curve showing the movement of the mass transfer zone through the adsorbent bed as a result of throughput (Taty-Costodes *et al.*, 2005).

The adsorbate is recovered onto any available adsorption sites. In a short time, the adsorbent near to these layers is saturated (or spent) so that the suspension penetrates further through the bed. The region of the bed where adsorption is taking place is referred to as the mass transfer zone (MTZ). The MTZ shifts along the length of the bed, such that initially, the effluent emerging may be free of the adsorbate. The break point occurs when the MTZ just “breaks through” the bed so that it is possible to measure some concentration of the adsorbate in the effluent (McKay, 1981; Tchobanoglous *et al.*, 2003; Taty-Costodes *et al.*, 2005; Faust and Aly, 1998).

Breakthrough is often considered to have occurred at the time the effluent concentration reaches 5 percent of the feed concentration. Although, depending on the nature of the downstream process, the breakthrough concentration can be the maximum allowable or minimum detectable adsorbate concentration in the effluent. A breakthrough time for 50% of the initial adsorbate concentration has been reported elsewhere (Goel *et al.* 2005). After the breakthrough time, the capacity of the bed to adsorb reduces sharply, as a result, the time taken to reach breakthrough is considered as the service time of the bed (Tchobanoglous *et al.*, 2003). As the breakthrough proceeds, the adsorbate concentration in the effluent gradually increases up to the inlet suspension concentration. At this time, the bed is considered to be exhausted and no more adsorption occurs as depicted in figure 2.16. Some authors reported that the exhaustion of the bed is said to occur when between 90 - 95 percent of the feed concentration is measurable. The longer the breakthrough/exhaustion time, the more efficient and economically favourable the adsorbent bed (Ko *et al.*, 2000; Tchobanoglous *et al.*, 2003; Maji *et al.*, 2007).

The breakthrough curves are usually expressed as normalised concentrations against volume of effluent (V) or time taken (t) or even sometime bed volume for a particular bed height (Crini and Badot, 2010). The normalised concentration is defined as a ratio of the effluent concentration at a given time (C_t) to the initial influent/feed concentration (C_o), which can then be expressed as $\frac{C_t}{C_o}$.

Knowing the volumetric flow rate (Q), the volume of effluent passed at any given time (t), can be estimated from equation 2.10;

$$V = Qt \quad (2.10)$$

Where Q is measured in mL/min, t (min) and V (mL).

For the purpose of the research reported in this thesis, the total amount of cells recovered, q_t , in the column can be estimated over the entire time it took the bed to be 'exhausted'. This quantity can be derived through integrating the recovered microalgae cells (C_r) against time (t). The recovered microalgae cells (C_r) is the difference between the inlet and effluent concentrations of the cell suspensions. So that,

$$q_t = QA = Q \int_{t=0}^{t=t} C_r dt \text{ (mg)} \quad (2.11)$$

Alternatively, q_t can be estimated from the breakthrough curve, given as

$$q_t = QA = Q \int_{t=0}^{t=t} \left(1 - \frac{C}{C_o}\right) dt \text{ (mg)} \quad (2.12)$$

The integral aspect of equation 2.12 can be solved by the approximate numerical equation of the trapezium rule, using the observed data of the breakthrough curves. Where 'A' is an integral function representing the area of the breakthrough curve as shown in figure 2.16.

The total adsorbed capacity of the bed, q , for the recovery of cells in the column can be estimated by the equation 2.13;

$$q = \frac{q_t}{M} \text{ (mg/g)} \quad (2.13)$$

Where M , is the quantity of adsorbent in the column.

The amount of cells fed into the system (X , mg) can be estimated from the equation;

$$X = C_o Qt \quad (2.14)$$

The bed efficiency, measured in terms of percentage recovery of cells onto the Nyex™ bed (PR), can be estimated by;

$$PR (\%) = \frac{q_t}{X} \times 100 \quad (2.15)$$

2.3.3 Adsorption for Microbial Applications

2.3.3.1 Cell Recovery from Suspension

The first recognised work on the interaction between solid surfaces and microbial organisms was the pioneering study of Claude ZoBell in 1935, who discovered the surface modifying characteristics due to microbial adhesion (Bitton and Marshall, 1980). Microorganisms including bacteria and viruses are quite small so that in aqueous systems, they are considered to behave as 'living' colloidal particles. So that it is possible to explain their attraction and attachment to surfaces in terms of adsorption/adhesion similar to what scientists use for typical colloids (Rosenberg and Kjelleberg, 1986; George and Davies, 1988; A Ozkan and Berberoglu, 2013).

For instance, George and Davis (1988) used activated charcoal cloth (ACC) to adsorb bacteria, *Escherichia coli* and yeast, *Saccharomyces cerevisiae*. With the aid of universal tubes, suspensions of the microbes and the adsorbent were mixed using a rolling machine. Scanning electron microscope (SEM) micrograph were utilized to show that reduction in cell concentration was solely due to adsorption of the microbes onto the solid particles. Based on these results, the authors suggested that the ACC may be a relevant material for biotechnology application such as cell immobilisation in continuous fermentation systems, effluent treatment and bacterial removal in medical applications (George and Davies 1988).

Furthermore, Rivera-Utrilla *et al.* (2001) investigated surface modification of activated carbon and its effect on adsorption of bacteria and aqueous lead. One of the significant outcomes was that activated carbon that had adsorbed bacteria was shown to adsorb more aqueous lead ions in comparison to a "pure" activated carbon. An explanation given for this observation was that the surface charge density of such activated carbons became more negative in a wider range of pH due to the bacteria adsorbed. The authors attributed the enhanced capacity of activated carbon to adsorb positively charged species to the increased adsorbent-adsorbate electrostatic interactions (Rivera-Utrilla *et al.*, 2001).

In agreement with Sirmerova *et al.*, (2013), the study of microalgae adhesion to solid materials has received significantly less attention in comparison to other microbial cells. The work of Hartog was amongst the first study to report the attachment of algae, known as *haptophytes*, to large stones and rock surfaces (Hartog, 1959).

It was Baker and Evans in 1973 who stated that algal groups possess adhesive surfaces which are due to the secretion of mucilaginous substances (Bitton and Marshall, 1980).

Based on the literature survey reported in this thesis, Curtain and Snook is thought to have pioneered the exploitation of the hydrophobic adhesion of *Dunaliella* to develop a recovery technique established on the principle of adsorption. They recovered *Dunaliella salina*, a halo tolerant microalgae strain, onto a hydrophobic surface (Curtain and Snook, 1983). In a rare application of using the adsorption to recover the microalgae cells from suspension, the authors revealed that (1) the hydrophobicity of *Dunaliella salina* cell membrane increases at higher saline conditions due to dominant presence of non-polar groups, thereby, enabling their rapid adsorption onto adsorbent materials with similar hydrophobic surfaces, and (2) a suitable solvent was contacted with the adsorbed algae to achieve the dual functions of cell disruption and β -carotene extraction (Curtain and Snook, 1985; Curtain *et al.*, 1986; Curtain, 2000). However, their studies failed to establish adsorptive capacity, shed light on the factors influencing such adsorption, examine mathematical models describing adsorption mechanisms as well as investigate the conditions for a continuous operation.

Recently, magnetic separation technology as a recovery technique is being developed to exploit the adherence of nanoparticles to microalgae cell surfaces (Li *et al.*, 2009; Xu *et al.*, 2011; Cerff *et al.*, 2012). However, the nanoparticles are considered to behave more as flocculants after attaching to the cell surfaces (Wan *et al.*, 2015; Lee *et al.*, 2015). They can be used in bare forms or coated with silica or cationic polyelectrolyte (Hu *et al.*, 2013; Lin *et al.*, 2015). The concentrated aggregates resulting from the nanoparticles and microalgal cells can be separated from the medium by decantation after a permanent magnet is placed near the mixture centrifuge tube (see figure 2.17).

Recovery efficiency of nearly 100% has been reported in the literature, which largely depends on factors that affect adsorption processes. These factors include effect of stirring, media pH, dose and size of nanoparticles as well as the type of algae strain and the base material of the nanoparticles (Xu *et al.*, 2011, Wan *et al.* 2015).

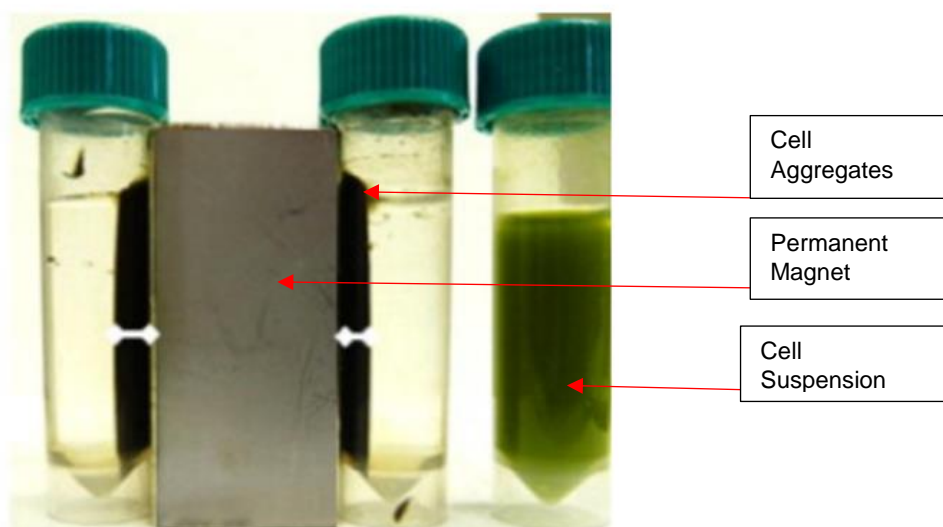


Figure 2:17: The recovery of microalgae cells from suspension with nanomaterials (Cerff *et al.*, 2012).

A number of studies have reported that the Langmuir model better describes the adsorption characteristics between the cells and the magnetic nanoparticles (Xu *et al.*, 2011, Cerff *et al.*, 2012, Hu *et al.* 2013). One of the apparent advantages of this technology to recover cells from suspension is the practicability of regeneration and reuse of the nanoparticles. Though, some of the drawbacks include but may not be limited to (Wan *et al.*, 2015; Lee *et al.*, 2015; Toh *et al.*, 2016);

- I. the high cost of magnetic nanoparticles,
- II. some of the nanomaterials have been reported to be unstable
- III. present methods of regenerating/reusing magnetic nanoparticles require substantial amount of strong acid and alkali for pH control,
- IV. a number of studies has recovered microalgae cells under a synthetic mineral salt medium,
- V. studies reported have been limited to batch experiments in vials or flasks,
- VI. toxicity of nanoparticle towards microalgae cells.

2.3.3.2 Zeta potential

Suspensions are one of the colloidal systems where solid particles (dispersed phase) are dispersed in a liquid (dispersion medium). Such systems tend to carry electric charges. Microalgae cells in their media behave like colloidal suspensions

largely due to the negative charges on their surfaces, which also makes them stable in suspension (Ives 1959; Edzwald 1993; Malvern 2001; Henderson *et al.* 2008a).

In an aqueous medium, a charged particle is neutralized by an “inner layer” of counter ions, often in an excess quantity. An outer layer of ions which are less firmly associated to the charged particle surrounds the “inner layer”. The formation of this double layer of ions around the charged particle is referred to as “the electric double layer” where the inner layer is called “the Stern layer”. The latter is considered to be immobile and the outer layer is referred to as “the diffuse layer” which allows the diffusion of ions depending on the influence of electrical forces and thermal motion (Mitchnick, 2012). As shown in Figure 2.18, the slipping plane is a notional boundary within the diffuse layer. The ions within the boundary move when the charged particle moves while the ions outside the boundary do not move with the particle. Zeta potential is a measure of the electrokinetic potential at the slipping plane, also referred to as the shear plane. It is also a measure of the surface charges of the stable particles in suspension (Hunter *et al.*, 2013).

Particles with large ZP repel each other so that the tendency to coalesce is greatly reduced. Generally, particles with a ZP of more than +30 or -30 mV are considered to be stable (Malvern, 2001). The measurement of the ZP makes it possible to answer the question; is the electrical charge on the material particle positive or negative? Importantly, the pH of the suspension is a significant factor that determines its ZP. In actual fact, it is useless to quote a measured value of the ZP if the suspension pH is unknown.

The origin of surface charges on particles in polar media could be due to a number of reasons such as the; differential loss of ions from the crystal lattice, adsorption of charged particles, ionization of surface groups (Leermakers *et al.*, 2005). It is understood that the negative charge of the microalgae cell surface is a result of the dissociation of functional groups found on the cell membrane surfaces as well as the metabolic excretion of algogenic organic matter [AOM]. AOM comprises neutral and charged polysaccharides, nucleic acids, proteins, lipids and small molecules. Interestingly, polysaccharides have been reported to make up to 80–90% of the total excreted AOM. The AOM has carboxyl and/or amino groups, which when in contact

with a polar medium, for example water, undergo ionisation or dissociation thereby leading to negatively charged surfaces (Henderson *et al.*, 2010).

The negative surfaces of microalgae cells are responsible for their stability in suspension, and one of the challenges of a harvesting technique is how to overcome this problem. The stability is the main reason, sometimes, flocculation of the suspension is employed prior to the use of other forms of mechanical separation techniques (Sukenic *et al.*, 1988; Bernhardt *et al.*, 1991; Wan *et al.*, 2015). Specifically, flocculants are used to neutralize the negative surface charges to enhance floc formation. The flocs can then coalesce to form larger particles, which then sediment and are collected at the bottom of the suspension (Uduman *et al.*, 2010).

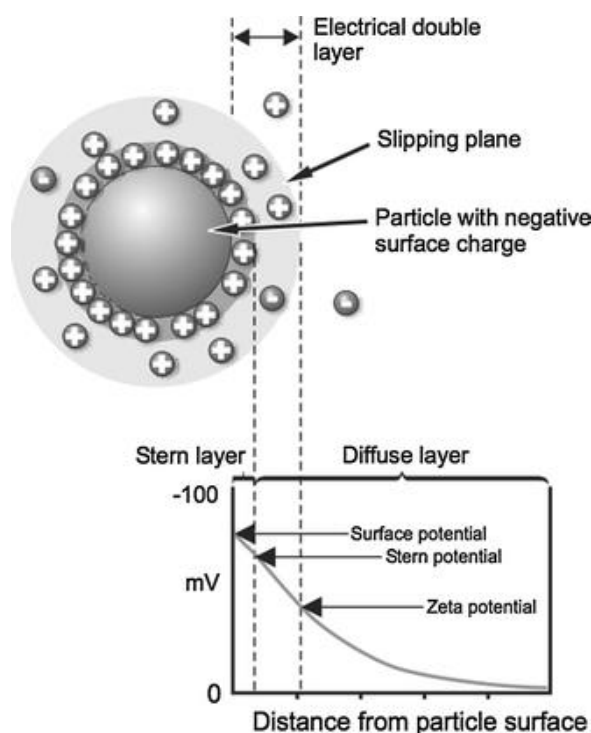


Figure 2:18 Simplified model of the electric double-layer at a charged interface in aqueous solution and representation of zeta potential (Malvern, 2001).

Furthermore, a number of studies reported that the microalgae cell characteristics are influenced by their growth conditions. Properties such as the zeta potential (ZP), average cell size and tendency to agglomerate depend on the growth phase of the microalgae cells (Danquah *et al.*, 2009; Wu *et al.*, 2012; Salim *et al.*, 2013; Lee *et al.*, 1998). Danquah *et al.* (2009) characterised the growth phases of two different microalgal strains. They showed that during the exponential growth phase, the High Growth Rate Phase (HGRP), the ZP of the microalgae cells was more

electronegative than in the stationary phase, which was considered as the Low Growth Rate Phase (LGRP). They suggested that the highly electronegative ZP makes the microalgae cells in the HGRP very stable in suspensions.

The higher electronegativity in the HGRP was attributed to high intracellular metabolic rate of the cells at this stage of growth. Another study suggested that the decrease in the absolute value of ZP throughout the growth phases was caused by the decline in the surface functional group concentrations (Zhang *et al.*, 2012). Likewise, it was reported that cell sizes in the HGRP were smaller in comparison with the LGRP. The reason for this observation was due to the lower electronegative ZP in LGRP. This was because of cells being less stable, thus able to coalesce to form larger groups of cells (Danquah *et al.*, 2009). To paraphrase, the decrease in the absolute value of ZP led to a decrease in the repulsive electrostatic forces between each cell thus leading to improved aggregation of the small cells.

2.3.3.3 Attached Growth System

This is a concept based on growing microalgae cells as a benthic system, which entails cultivation of microalgae cells on a supporting material. It is based on the premise that some microalgae strains prefer to attach to surfaces rather than remain in suspension. A number of studies have reported immobilised microalgae systems either for biofuel production or for environmental remediation purposes. Johnson and Wen (2010) tested different materials as supports in a growth chamber to cultivate *Chlorella sp.* It was reported that virtually all the cells settled on the surface of the materials and the cells in suspension were insignificant. As soon as the attached algal cells produced a thick “mat” on the support surface, it was scraped off to recover the algae biomass. Interestingly, the substrate was placed back into the growth chamber so that the remaining algal cells attached on the surface were used as resident inoculum for the next growth phase (see figure 2.19).

A comparison of the attached growth culture and suspension culture system showed that more algae biomass was produced in the former. Also, since the scraping technique was used to harvest biomass from the attached growth culture system, there was no need for any further harvesting technique such as centrifugation which would otherwise be required for suspension culture systems (Johnson and Wen, 2010).

Similarly, algae biofilm reactors designed on the basis of cultivating microalgae as biofilms have been reported (Roeselers *et al.*, 2008; Christenson and Sims, 2012).

Some of the advantages espoused for attached growth systems include;

- (i) higher density of microalgae biomass compared to suspended systems,
- (ii) efficient water saving potential as used culture can be recycled,
- (iii) energy saving due to non-requirement of further dewatering process.

However, the potential for monoculture growth, ease of full scale up and its robustness to cultivate varieties of microalgal strains remain to be proven.

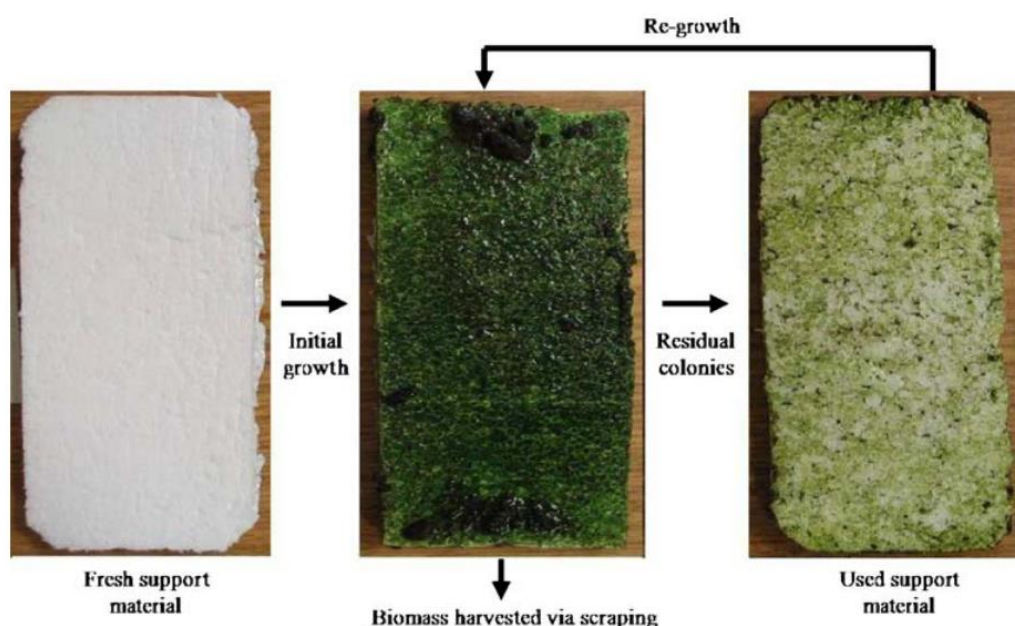


Figure 2:19: Harvesting procedures for attached growth system (Johnson and Wen, 2010).

2.3.4 Electrochemical Process

The electrochemical processes entail a chemical reaction achieved due to electron transfer between electrodes of an electrochemical cell and species in solution (Hibbert, 1993). The reaction occurs only after energy is applied across the cell, so that electrons enter the system through the negatively charged electrode (cathode), and leaves through the positively charged electrode (anode). Furthermore, an electrolyte is required within the system to conduct electricity, which generates the ions that flow to and from the electrodes when energy is applied. As electrochemical reaction occurs, species at the cathode undergo reduction whilst those at the anode undergo oxidation (Eberson, 1982; Garnett and Treagust, 1992; Perez, 2004).

The electrochemical methods are options for industrial players seeking a more economical and environmentally friendly treatment process. It offers a favourable alternative, which is finding increasing applications in treatment processes such as metal ion removal and recovery, and organic contaminants removal from industrial wastewaters (Campbell *et al.*, 1994; Bazan and Bisang, 2004; Rajkumar and Palanivelu, 2004; Laine and Cheng, 2007). It is considered to be energy efficient, environmentally friendly and cost effective due to absence of waste and harmful chemicals. However, limitations of the process include formation of toxic products as well as risk of electrode corrosion (Gheraout *et al.*, 2011). It is a method which can be applied in various forms which include but are not limited to electrocoagulation, electro-flotation and as a disinfection technique (Mollah *et al.*, 2004; Feng *et al.*, 2004; Kraft, 2008; Inman *et al.*, 2012).

2.3.4.1 Electrochemical methods to concentrate microalgae cells

As illustrated in figure 2.20, electro-coagulation and flocculation are electrochemical methods that use electrolytic cells to recover microalgae cells from suspension. They are based on the concept of using a sacrificial anode such as Aluminium (Al) and Iron (Fe) electrodes. These electrodes generate metal ions that induce the coagulation of the microalgae cells through the neutralisation of the negative charges on the cell surface (Mollah *et al.*, 2004; Xu *et al.*, 2010; Gao *et al.*, 2010a). The quantity of electricity passed through the electrolytic solution determines the quantity of metal ions formed. The method comprises three phases;

- I. Dissolution of the sacrificial anode to form coagulants due to the formation of aluminium or iron ions; they hydrolyse to form polymeric aluminium or iron hydroxides,
- II. Destabilisation of cells, and
- III. Flocculation of destabilised cells to form aggregates.

Vandamme *et al.*, (2011) conducted a study where inert Titanium dioxide was the cathode, and a comparison between aluminium and iron as the anode was investigated. Results obtained showed that 95% of *Chlorella vulgaris*, a freshwater specie, and 80% of *Phaeodactylum tricornutum*, a marine specie were recovered from their suspension media. They reported that the power consumption of this technique was an order- and 2 orders- of magnitude lower than centrifugation

technique when applied to *Chlorella vulgaris* and *Phaeodactylum tricornutum* respectively. Aluminium was also found to perform better than iron in terms of recovery efficiencies of the hydroxides formed as well as the lower current efficiency of the iron electrodes (Gao *et al.*, 2010a; Vandamme *et al.*, 2011).

This method in comparison to centrifugation, sedimentation tank with flocculation and flotation with flocculants, was found to be relatively cheaper in terms of total cost which includes investment, energy required and maintenance. Specifically, the total cost for separating 1 m³ of microalgae suspension using electro-flocculation was estimated as \$0.11/m³, while sedimentation with flocculants could cost as much as \$0.25/m³ and centrifugation would cost nearly 5 times the cost of electro-flocculation (Poelman *et al.*, 1997). In addition, power consumption ranging from 0.3 kWh/m³ to 2 kWh/m³ has been reported for electro-flocculation compared to centrifugation with a power consumption of up to 8 kWh/m³ (Milledge and Heaven, 2012). Furthermore, It was also observed that Aluminium concentration in the biomass was less when compared to using Alum to flocculate the cells (Poelman *et al.*, 1997; Uduman *et al.*, 2011).

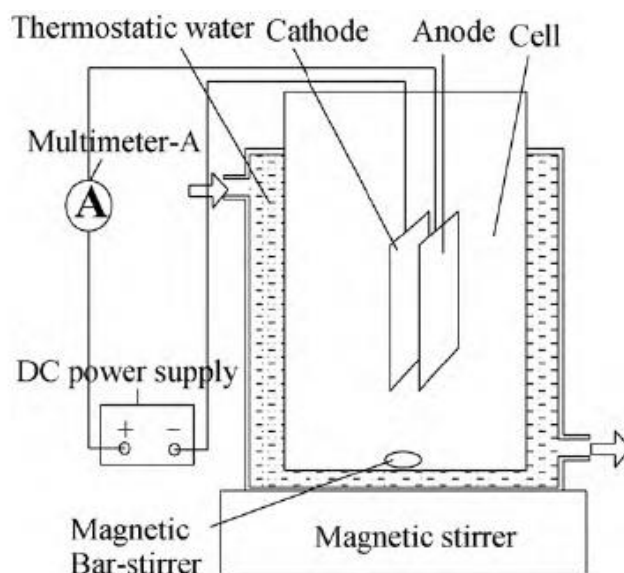


Figure 2:20: Schematic for batch electroflocculation reactor system (Gao *et al.*, 2010b).

Alternatively, electro-flotation which involves employing the gases (Oxygen and Hydrogen) generated at the electrodes during electrolysis to carry the microalgae flocs to the surface of the medium is another variation of this technique (Xu *et al.*, 2010; Tumsri and Chavalparit, 2011). This is similar to flotation technique previously

described in section 2.2.4 but in the absence of any mechanical equipment to generate the bubbles.

However it is worthy of note that the literature seems confused with regards to differences between electroflocculation and electro-flotation, and several authors interchange terms like electro-coagulation and electro-flocculation in a rather befuddling manner. While some papers regard the use of a sacrificial anode as an electro-coagulation process (Azarian *et al.*, 2007; Gao *et al.*, 2010b; Uduman *et al.*, 2010), some refer to the process as electro-flocculation (Alfafara *et al.*, 2002; Xu *et al.*, 2010). While sometimes the use of inert electrodes is referred to as an electro-flotation process (Alfafara *et al.* 2002, Uduman *et al.* 2010). There is a need for some clarity. Based on the literature survey in this thesis, it does appear that the gases released during an electrochemical reaction are the reason behind this ambiguity. To avoid electro-flotation and ensure electro-flocculation, some form of agitation of the medium (see figure 2.20) is applied to encourage sedimentation rather than flotation of the microalgae cells. The main advantage of using electrochemical methods to recover microalgae cells from suspension is hinged on the absence of any chemical usage.

Some of the drawbacks of this method include but may not be limited to (Mollah *et al.*, 2004; Alfafara *et al.*, 2002; Uduman *et al.*, 2010; Ghernaout *et al.*, 2011);

- I. The need to periodically replace the 'sacrificial anodes'.
- II. Formation of toxic chlorinated organic compounds/halomethanes depending on the microalgae suspension composition.
- III. Formation of an impermeable oxide film at the cathode may affect the performance of the electrochemical cell. Periodic mechanic cleaning of the electrodes for a large scale, continuous process would no doubt be difficult.
- IV. Where the cost of electricity is high, operating costs of ECF/EF may be high.

2.3.4.2 Electrochemical Method for Water Treatment

Electrochemical treatment of water is one of the treatment methods employed to combat pathogenic microorganisms to prevent infectious diseases. The bactericidal action of electrochemical disinfection is considered to be a robust, cost-effective and environmental friendly option of disinfection, in comparison to chlorination, ClO₂, UV radiation and ozonation. In this method of disinfection, electrodes including at least

an anode and a cathode are introduced either directly into the contaminated water, or through a bypass pipe. A direct current voltage is then applied between the electrodes, causing the electrolysis of the water (Stoner *et al.*, 1982; Patermarakis and Fountoukidis, 1990; Martínez-Huitle and Brillas, 2008; Y. Han *et al.*, 2008).

Diao *et al.* (2004) studied bactericidal action of electrochemical (EC) disinfection of *Escherichia coli* in comparison to other tests with chlorine, ozone and hydroxyl ($\bullet\text{OH}$) radicals produced by Fenton reaction. The authors reported that EC was decidedly effective to disinfect wastewater. With the aid of a scanning electron microscope (SEM), they revealed that dissimilar forms of damage in the surface morphology and structure of the cells, which depends on the varied forms of disinfection. The SEM, however, showed some similarity in the micrograph of the *E. coli* cells disinfected by the Fenton reaction and the EC method. *E. coli* cells treated with both methods were observed to have leaked a considerable amount of intracellular materials.

The killing mechanisms of both methods were thought to be similar, which entailed the formation of hydroxyl radicals. The radicals were believed to be mainly responsible for germicidal effect and were more powerful than chloride ions. On the other hand, SEM micrograph of disinfected cells by chlorination and ozone did not show such leakage of intracellular materials (Diao *et al.*, 2004). Another study investigated a similar comparison study using *E. coli*, *Staphylococcus aureus* and *Bacillus subtilis* as representative microbial organisms. In agreement with results obtained by Diao *et al.* (2004), the authors showed, using SEM micrograph, that surface damage of the microbial cells was more apparent in the electrochemical system (Li *et al.*, 2011).

Furthermore, studies have been carried out by Matsunaga *et al.* (1992 and 1994) on *E. coli* cells using granular activated carbon (GAC) and activated carbon fibres (ACF) as electrodes in a disinfectant electrochemical reactor. Matsunaga *et al.* (1992) explained that electrochemical oxidation of *E. coli* cells led to a decreased respiratory activity of the cells thereby causing cell death. The amount of cells killed was found to be a function of the cell concentration on the GAC, bacterial cell wall, bacterial membrane structures, amount of potential applied, and electrical conductivity (Matsunaga *et al.*, 1992, 1994).

Additionally, earlier works have also confirmed that microbial organisms can be inactivated when water is disinfected by electrochemical methods (Stoner *et al.*, 1982; Patermarakis and Fountoukidis, 1990). Specifically, Stoner *et al.* (1982) observed that about 40 species of microbial organisms such as viruses, bacteria and algae were successfully treated during the electrochemical disinfection of water. The disinfection mechanisms can be due to the generation of hypochlorite/hypochlorous acid, ozone or hydrogen peroxide disinfecting species within the system.

The advantages of EC methods are evident; no storage, transport and dosage of chemical disinfectants are needed. The effect of disinfection by electrochemical means can be altered depending on the on-site demand (Kraft, 2008). However, one of the limitations of the EC method as widely applied is in the evolution of gases during electrolysis of water. These gases/bubbles generated can adhere to and carry the microbial cells to the surface, out of reach of electrochemical disinfection. The consequence lies in the difficulty of inactivating such cells. In addition, the use of electrolytes within the electrochemical system results in the formation of toxic chlorinated organic compounds/halomethanes, which largely depends on the suspension/water composition (Mollah *et al.*, 2004). Furthermore, EC methods treat the whole volume of water, which results in relatively high energy costs.

2.3.5 The Arvia Process

Powdered or granular activated carbons, after adsorption, are either incinerated or disposed of when they become exhausted. Alternatively, regeneration of the adsorbents can be done as it is the most economically viable and environmentally benign route. Regeneration involves recovering the adsorption efficiency of the exhausted adsorbent to undertake further adsorption. As illustrated in figure 2.21, regeneration can be achieved through a number of methods including extraction, pressure swing, thermal desorption or thermal reactivation, biological reactivation or electrochemical processes (Sheintuch and Matatov-Meytal, 1999; Han *et al.*, 2008).

In the industry, thermal regeneration of the activated carbon is the commonly employed despite its shortcomings such as being energy and cost intensive, possible results in about 10% loss of the adsorbent material and most times requires an off-site regeneration process. Electrochemical regeneration was developed as a

response to the need to reduce operating cost, material loss and high energy requirements associated with some of the other regeneration techniques (Han *et al.*, 2008).

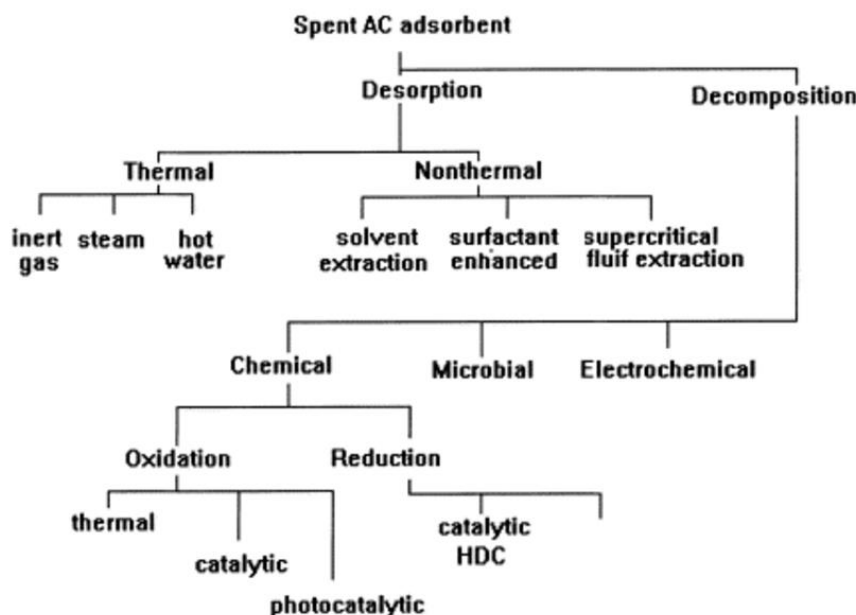


Figure 2:21: Overview of regeneration techniques for spent activated carbon (Sheintuch and Matatov-Meytal, 1999).

In an electrochemical regeneration, spent carbon is reactivated within an electrochemical cell in order to destroy or desorb the adsorbate. This technique is regarded as a very effective and favourable regeneration method, whose mechanism involves electro- destruction and/or desorption of adsorbed organic pollutants before the adsorption capacity is restored. However, when an electrochemical method was applied to spent activated carbon, lengthy regeneration periods, between 6 and 48 hours were experienced, as adsorption and desorption of organics from activated carbons are often determined by intra-particle diffusion (Narbaitz and Cen, 1994; Weng and Hsu, 2008). Thus, making electrochemical regeneration of activated carbon generally unattractive.

Interestingly, a novel graphite intercalation compound with tradename, Nyex™, was discovered. Nyex™ particles are considered to be relatively cheap carbon, non-porous with no internal surface area and are a highly conductive material. The non-porous characteristics of the adsorbent implies that adsorbates are accumulated on its external surface. As a consequence, Nyex™ has a low surface area, which does not make it a high capacity adsorbent material in comparison to activated carbon.

Even so, its high electrical conductivity makes it a preferred adsorbent material for the purpose of electrochemical regeneration.

The combined characteristics of the material as an adsorbent and its high electrical conductivity led to the invention of a single stage process known as the Arvia Process. In the process, organic pollutants are adsorbed onto the external surface of the Nyex™ particles, and during the electrochemical regeneration of the latter, the adsorbed organic pollutants are destroyed to form CO₂ and water. The regeneration capability of the electrochemical aspect of the process makes the methodology both environmentally friendly and cost effective.

The Arvia process has been successfully employed in the removal/ treatment of water contaminants such as atrazine, chlorinated effluents, organic dyes and microorganisms and has found application in the nuclear industry (Brown *et al.*, 2004; Brown and Roberts, 2007; Mohammed *et al.*, 2011; Asghar *et al.*, 2012; Conti-Ramsden *et al.*, 2012; Conti-Ramsden *et al.*, 2013; Brown *et al.*, 2013; Nkrumah-Amoako *et al.*, 2014). The achievements attained in the laboratory were successfully replicated at demonstration scale and led to the commercialisation of the process, and spin out of a company called, Arvia Technology Limited.

2.3.6 Summary

This section reviews the literature on the application of adsorption and electrochemical techniques for microalgae cells. Despite adsorption being a widely known and established method, there is little interest in its application as a technique to recover microalgae cells. This appears to be as a result of the porous nature of conventional adsorbents, which poses difficulties in the further processing of such adsorbed cells. Nonetheless, the innate preference of microalgae cells for surfaces is known and has been utilised in cell immobilisation and wastewater treatment applications. Recent efforts to use nanoparticles to recover cells as well as develop attached cultivation systems are highly commendable, but still limited as discussed in this chapter.

The use of electrochemical methods to recover microalgae cells, in electro-flocculation or electro-flotation, was also discussed. However, issues with the need to periodically replace the ‘sacrificial anodes’ and formation of an impermeable oxide film at the cathode suggests that more research are still required. Furthermore, the

use of electrochemical methods to disinfect microbial organisms is well understood. However, such processes disinfect the entire volume of water, which results in a relatively high energy cost despite the low levels of microbial removal.

Due to the varied nature of microalgae cells, thousands have been isolated, it does seem that no singular method can be universally applicable to the recovery of cells and its intracellular materials. In addition to the previous chapters, the need to further research, especially novel techniques, on all process chains of microalgae biofuel production has been laid bare.

The availability of a non-porous adsorbent, has brought to the fore an exciting interest to undertake research on the potential use of adsorption as a technique to recover microalgae cells from suspension. The next chapter focusses on the experimental programme developed and undertaken to answer the overarching question being asked in this research; does the non-porous characteristic of the Nyex™ particles present an opportunity to recover microalgae cells from suspension using an adsorption technique for potential biofuel applications?

3 Experimental Programme Overview

3.1 Nyex™ - The Adsorbent Material

Nyex™ is a non-porous graphite intercalated compound (GIC) adsorbent particle. Graphite is a conductive carbon material, whose structure comprises layers of graphene parallel to the basal plane of a hexagonal lattice of carbon atoms as illustrated in Figure 3.1 (Noel and Santhanam, 1998; Sliwinska-Bartkowiak *et al.*, 2012). Van der Waal's forces hold the layers in place; a bond significantly weaker than the strong covalent bonds of the carbon-carbon atoms. The Van der Waals forces between the layers ensures that species can be inserted between graphene layers of the graphite (Ubbelohde, 1979).

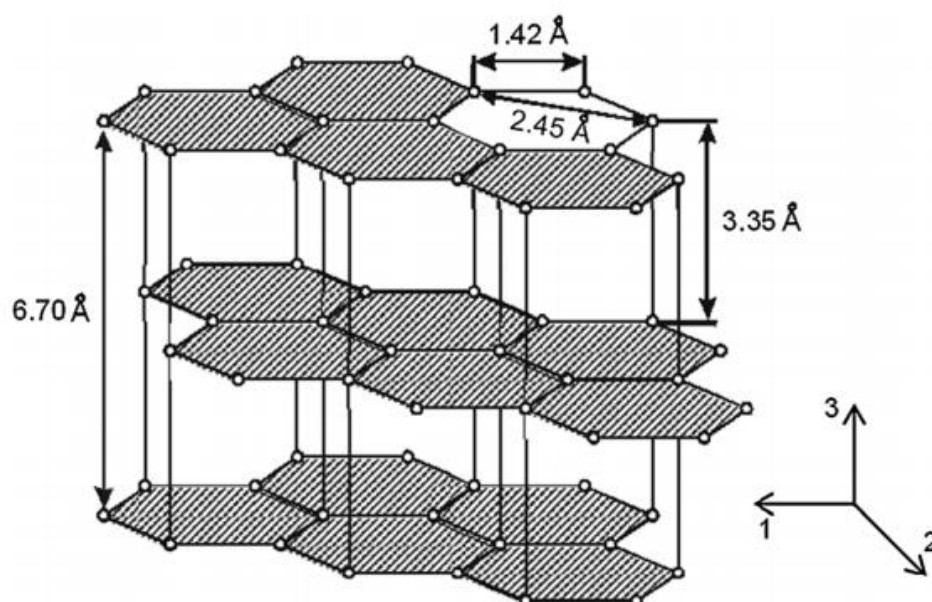


Figure 3:1: The structure of graphite (Sliwinska-Bartkowiak *et al.* 2012)

It is possible to react graphite with a range of intercalants to form a graphite intercalated compound with varying properties (Belash *et al.*, 1989). The distinct feature of graphite in comparison to other materials, which also react with intercalants is the ability of these compounds to have a regular ordering of constant graphene layers between two monolayers of intercalant; a phenomenon known as staging (Conte, 1983; Chen *et al.*, 2003). The graphite intercalated compounds are prepared using a number of techniques, which include vapour phase, liquid phase and electrochemical reactions (Charlier *et al.*, 1989). A wide range of these compounds are manufactured using various intercalants such as compounds of alkali metals which include Potassium, Caesium and Lithium (Maeda *et al.*, 1988)

as well as utilising Lewis acid intercalants such as bromide, fluoride and strong Bronsted acids such as HNO_3 and H_2SO_4 (Maeda *et al.*, 1985; Belash *et al.*, 1989; Chung, 2002). Interestingly, the presence of acidity confer the material with a unique electrical conductivity characteristics on their basal plane (Fischer, 1980).

These compounds have found applications as thermoelectric materials in thermal energy storage, in power sources, for example electrodes and batteries, and in intumescent strips on fire doors, which expand to seal the door should a fire break out (Furidin, 1998; Wang *et al.*, 2014; Nitta *et al.*, 2015). Their use as adsorbent materials is limited, although, graphite oxide a similar compound to graphite intercalated compounds was reportedly used as an adsorbent. Hartono *et al.* (2009) reported a study where graphite oxide particles were used to adsorb humic acid from an aqueous solution (Hartono *et al.*, 2009). Another study also investigated the adsorption of lead from wastewater using the same adsorbent (Olanipekun *et al.*, 2014). Furthermore, the use of exfoliated graphite intercalated compounds as adsorbents was reported to recover heavy oils (Vieira *et al.*, 2006) and organic pollutants from wastewater (Goshadrrou and Moheb, 2011).

The form of graphite intercalated compound employed in the research reported in this thesis is the graphite bi-sulphate manufactured from graphite flakes. Concentrated sulphuric acid intercalants which were used to produce this material, was supplied by Arvia Technology with the tradename of Nyex™ (see figure 3.2).

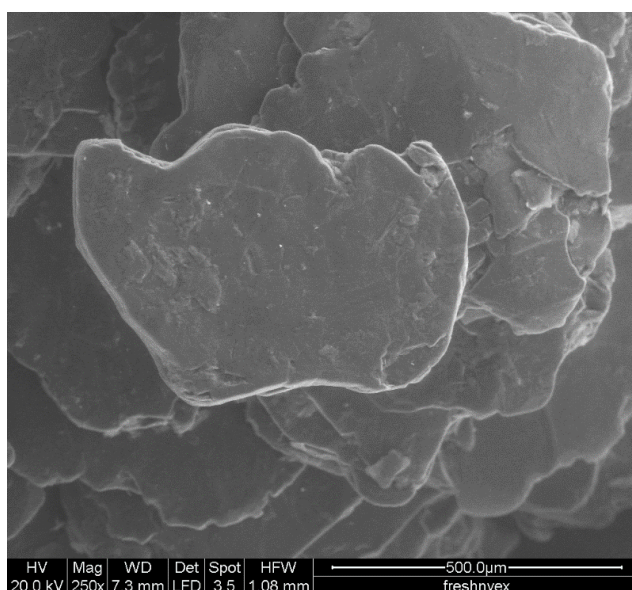


Figure 3:2: Scanning Electron Micrograph of Nyex™ flake particles.

Nyex™ particles are a type of altered graphite compounds with molecules intercalated between graphene sheets in the graphite lattice. These intercalates, which could be anionic or cationic, bring about an improvement of the existing characteristics of the adsorbent which include adsorptive capacity and electrical conductivity (Nkrumah-Amoako *et al.*, 2014).

As shown in Table 3.1, a mercury porosimetry study revealed the absence of internal pores in the Nyex™ material, resulting in a low surface area *circa* 1 m²/g (compared with activated carbon with a surface area range of 600–1200 m²/g). However, the non-porous nature of the adsorbent ensures rapid kinetics, due to the lack of diffusion into pores; a rate limiting factor for porous activated carbon (Noel and Santhanam, 1998). The Nyex™ flakes have a mean particle diameter of about 500 µm (particle size ranging from 100 to 1000 µm), with a carbon content of more than 90% (see Table 3.2). It has a particle density of 2.2 g/cm³ as well as a packed bed electrical conductivity of 0.8 S/cm.

Table 3.1: Laser diffraction particle size and nitrogen adsorption (BET) analysis of Nyex™ characterisation (Nkrumah-Amoako *et al.*, 2014).

BET surface area (m²/g)	Pore volume (cm³/g)	Pore diameter (Å)	Particle density (g/cm³)	Mean particle diameter (µm)
1.0	0.0038	138	2.22	500

The surface structure comprises flat layer basal planes and fragmented/dislocated edge planes. The basal planes comprise carbon atoms with mainly non-polar properties. The edge planes comprise chemisorbed surface functional groups, which have been reported to influence its capacity to adsorb (Li *et al.*, 2002; Quinlivan *et al.*, 2005; Hartono *et al.*, 2009). These functional groups are believed to be acidic oxygen containing functional groups, with a large proportion being phenolic hydroxyl groups and lower concentrations of carboxyl and carbonyl groups (Nkrumah-Amoako *et al.* 2014). It has also been established that electrochemical application treatment possibly affects surface chemistry (Proctor and Sherwood, 1983). Table 3.3 shows the composition of the functional groups present on the surface of the adsorbent. These functional groups also confer the acidity properties Nyex™ particles have been known for.

Table 3.2: Elemental analysis on graphite basal and edge planes using Energy Dispersive X-Rays (Nkrumah-Amoako *et al.*, 2014).

Elemental Analysis (wt %)	Basal Plane	Edge Plane
Carbon	88	93
Oxygen	9	5
Others	3	2

Table 3.3: Concentrations of acidic surface functional groups on Nyex™ particles using Boehm titration (Asghar *et al.*, 2012).

Carboxylic	Lactonic	Phenolic	Basic	Total acidic
53.9	45.2	0.9	0	100

The specific type of adsorbent used in the research reported in this thesis is Nyex™ 1102, which was supplied by Arvia Technology Ltd. Nyex™ 1102 particles were washed several times with deionised water to remove the fine particles. The washed Nyex™ 1102 was filtered to minimize the moisture content. The moisture content of the wet Nyex™ 1102 was taken into account before it was used in each of the experimental studies reported in this thesis.

3.2 Microalgae strain, growth conditions and cultivation

3.2.1 Microalgae Strain

The model strain of microalgae used for the research reported in this thesis is *Chlamydomonas reinhardtii*. *C. reinhardtii* is a unicellular green microalgae possessing two flagella with an average size of approximately 7 µm in diameter (see figure 3.3). It is not a high lipid producer, nonetheless, nitrogen and sulphur deprived *C. reinhardtii* showed enhanced total lipid content. The ability to influence the metabolism of *C. reinhardtii* by nutrient stress makes it a microalgae of interest in biofuel applications (Hu *et al.*, 2008). Furthermore, *C. reinhardtii* was shown to thrive in municipal wastewater with a lipid content akin to other microalgae species with high lipid yield. It is believed that for sustainable production of microalgae biofuel, growing microalgae in sewage effluents will play a significant role (Hoffmann, 1998;

Pittman *et al.*, 2011). It is one of the most studied eukaryotic microalgae strains and its ease of cultivation makes it frequently used for laboratory studies (Grossman *et al.*, 2007; Merchant *et al.*, 2007; Hu *et al.*, 2008; USDOE, 2010). As a result, *C. reinhardtii* was considered as the main model microalgal strain for the purpose of achieving the afore-mentioned research objectives.



Figure 3.3: Microscopic image of *Chlamydomonas reinhardtii* cells (Tsukii, 1995).

Occasionally, two other microalgal strains were considered depending on the objective(s) of the experimental studies. They include *Chlorella luteoviridis* and *Chlorella vulgaris*. *Chlorella* is a unicellular, spherical immotile green microalgae with a size as low as 2.0 μm in diameter. *Chlorella* cells are devoid of flagella and occur in both fresh and salt water (Scragg *et al.*, 2003; Phukan *et al.*, 2011). *Chlorella* genres are particularly tolerant to sewage effluent conditions exhibiting high growth rate in such media and some have rich lipid content (USDOE, 2010; Pittman *et al.*, 2011). *Chlorella vulgaris* is one of the common Indian species grown in fresh water and wastewater (Phukan *et al.*, 2011). Biotechnology applications of *Chlorella* include as a food supplement, food additive and in face and skin care products (Kay and Barton, 1991; Spolaore *et al.*, 2006).

3.2.2 Growth Conditions

Chlamydomonas reinhardtii, *Chlorella vulgaris* and *Chlorella luteoviridis* were grown in a Tris-Acetate-Phosphate (TAP) medium. The TAP medium was prepared to replicate the growth conditions in natural systems of algae cells.

It was prepared by mixing 25 mL of TAP salt solution (made of 15 g L⁻¹ NH₄Cl to give a final concentration of 7.0 mM, 4 g L⁻¹ MgSO₄·7H₂O to give a final concentration of 8.30 mM, and 2 g L⁻¹ CaCl₂·2H₂O to give a final concentration of 4.50 mM), 0.375 mL of potassium phosphate solution pH 7.0 (containing 288 g L⁻¹ K₂HPO₄ and 144 g L⁻¹ KH₂PO₄ to give a final concentration of 1 mM phosphate), 1 mL of Hutner's trace elements mixture and 1 mL of glacial acetic acid (to give a final concentration of 18 mM), buffered to pH 7.2 with 20 mM Tris base (Tris(hydroxymethyl)-aminomethan) and made to 1000 mL with de-ionized water (Harris, 1989). Hutner's trace elements are made up of the following final concentration of metals: 184 μM B (as H₃BO₃), 6.8 μM Co (as CoCl₂), 6.3 μM Cu (as CuSO₄), 17.9 μM Fe (as FeSO₄), 25.6 μM Mn (as MnCl₂), 6.2 μM Mo (as (NH₄)₆Mo₇O₂₄), 0.27 μM Na (as Na₂EDTA salt) and 76.5 μM Zn (as ZnSO₄).

The TAP medium was then autoclaved at 121°C for 20 minutes to prevent contamination during cultivation.

3.2.3 Cultivation

A volume of 1 mL of microalgal suspensions for each of the species was measured and inoculated into 200 mL of TAP media contained in a conical flask/plastic culture flask. The inoculation was carried out in a laminar flow cabinet to prevent contamination of the culture. The cultures were cultivated in a growth cabinet which was at an average temperature of 22°C and relative humidity of 46%. The conditions monitored in the growth cabinet were such that the cultures were continuously illuminated at 100 μmol⁻¹ photons m⁻² s⁻¹ by white fluorescent lamps for 16 hours and subjected to darkness for 8 hours. The cultures were shaken at 140 rpm using a Stuart Orbital Shaker to ensure that all the cells could uptake nutrients from the growth media. Each microalgae species was grown in three replicates. The growth of the cells was monitored daily by taking a volume of 1 mL samples and its absorbance at 680 nm was measured using a Jenway Genova Spectrophotometer as described in section 5.5.1. The microalgae suspensions that attained the stationary growth phase, figure 3.4, were then brought in contact with NyexTM particles to carry out recovery studies either in the batch or continuous column modes. The recovery experimental studies using adsorption are explained in detail in the coming chapter.



Figure 3:4: Flask containing microalgae suspension that has attained stationary phase.

3.3 Evaluation of Batch Recovery of Microalgae Cells onto Adsorbent

3.3.1 Adsorbent and Microalgae cells

The wet Nyex™ and microalgae strains employed, including their growth media and conditions, to carry out this research work were discussed in sections 3.1 and 3.2.

3.3.2 Microalgae Cell Recovery from Suspension

An initial analysis of the microalgae suspensions was undertaken before adsorption as described in sections 3.6.1 and 3.6.2. Afterwards, a batch experiment was carried out in which 30 mL of a suspension of *Chlamydomonas reinhardtii* was placed in a 50 mL cylindrical tube. 10 g of Nyex™ was weighed and added to the suspension. The mixture was shaken at 300 rpm using a Heidolph UNIMAX 1010 shaker for a specified period of time. The adsorbent in the mixture was allowed to settle, for about one minute, before samples of the supernatant were taken for analysis of unrecovered cells. The latter is the cell count after adsorption estimated as described in section 3.6.2, and converted to give the residual cell density of the suspension using equation 3.5. The difference between the initial and the residual cell density indicates the amount of cells recovered onto the adsorbent surface.

3.3.2.1 Influence of Contact Time

The microalgae suspension was made up to 3 batches of varying initial concentrations. The adsorption experiment was carried out as stated in section 3.3.2 where 10 g of washed Nyex™ was added to the suspension and agitated at 300 rpm using the shaker for 60 minutes. Samples of the supernatant were taken at regular time intervals to measure the residual cell density of the supernatant as previously described.

3.3.2.2 Influence of Intensity of Agitation

The adsorption experiments were carried out for 20 minutes (estimated equilibrium time based on section 3.3.2.1) at different speeds between 50 and 450 rpm on the shaker. A control experiment was undertaken which entailed a batch suspension in the absence of Nyex™ particles and it was placed on the shaker to ensure mixing at 300 rpm.

3.3.2.3 Influence of Initial Concentration of Microalgae Suspension

The effect of the initial concentration on the amount of microalgae cells recoverable onto the adsorbent was also studied. Different concentrations of the suspension were made up by diluting the original microalgae stock (at initial volumes between 3 ml and 30 ml) to a final volume of 30 ml diluted suspensions using deionised water. 10 g of washed Nyex™ was then added and shaken at 200 rpm on the shaker for 20 minutes. The resulting data was employed to construct the adsorption isotherms and estimate the adsorptive capacity of the Nyex™/*C. reinhardtii* system.

3.3.2.4 Influence of Microalgae Cell Size

Microalgae cells, depending on the strain, have sizes that can range from a few to many micrometres. An investigation into how this might affect the recovery efficiency of the microalgae cells from suspension was carried out. A measure of the size distribution of *C. reinhardtii*, *Chlorella vulgaris*, and *Chlorella luteoviridis* was undertaken using a microscopic graticule device and ImageJ software. This showed that *C. vulgaris* has an average size of 4.5 µm and *C. luteoviridis* has an average size of 3.9 µm and *C. reinhardtii* has an average size of 7.1 µm. Based on section 3.3.2, an adsorption procedure was carried out to recover cells from suspensions and their recovery efficiencies were compared.

3.3.2.5 Influence of Media Change on Cell Viability and Recovery

The microalgae suspension was centrifuged and re-suspended in deionised water to wash the cells. This was achieved by placing a measured volume of the suspension into 3 cylindrical tubes. These were placed in a centrifuge (Centrifuge 5702R supplied by Eppendorf AG Hamburg) and the samples were spun at 4.0 rpm for 5 minutes at 15°C. The supernatant was decanted and the resulting microalgae paste was resuspended in deionised water and placed in the centrifuge again. This procedure was repeated twice and the resulting suspension was used for cell viability and adsorption recovery studies.

First, the effect of washing, centrifuging and re-suspending on the viability of cells was also studied. Samples of the unwashed cells in their original media and washed suspensions in deionised water were pipetted onto a glass slide and enclosed with a cover slip. Drops of oil emulsion were placed on the slides to aid resolution. The slides were then visualised under a light inverted microscope (LEICA DMR) at a 1000x magnification to view the microalgae cells. The microscope images of the cells were taken using a SPOT Xplorer 4MP camera.

Thereafter, adsorption studies were undertaken to study the effects, if any, of media change on the recovery efficiency of the microalgae cells. The adsorption procedure as described in section 3.3.2 was carried out with microalgae cells in their original media as well as with washed microalgae cells, re-suspended in deionised water.

3.3.3 Recovery of Microalgae Cells in the Arvia Y-cell

The Arvia Y-cell is a piece of equipment that has been optimised to remove adsorbate from solutions such that the spent Nyex™ can be electrochemically restored in the regeneration zone of the equipment. For the work reported in this chapter, only the adsorption stage was investigated. The Arvia Y-cell was constructed using Poly Vinyl Chloride (PVC) material. It consists of an anode made of a graphite plate and a cathode constructed from a perforated '316' stainless steel plate 1 mm thick and perforated with holes of 3 mm diameter.

Its mode of operation for the adsorption stage entails placing the effluent/suspension to be treated in the adsorption zone. A known amount of Nyex™ is added while air is injected at the bottom of the Y-cell through nozzles to circulate the adsorbent and

generate mixing with the effluent. An air flow rate is set such that the Nyex™ is completely fluidized. The mixing is allowed to continue and samples of the supernatant are taken at regular time intervals to analyse the amount of microalgae cells remaining in suspension. Figure 3.5 depicts, schematically, the Arvia Y-cell.

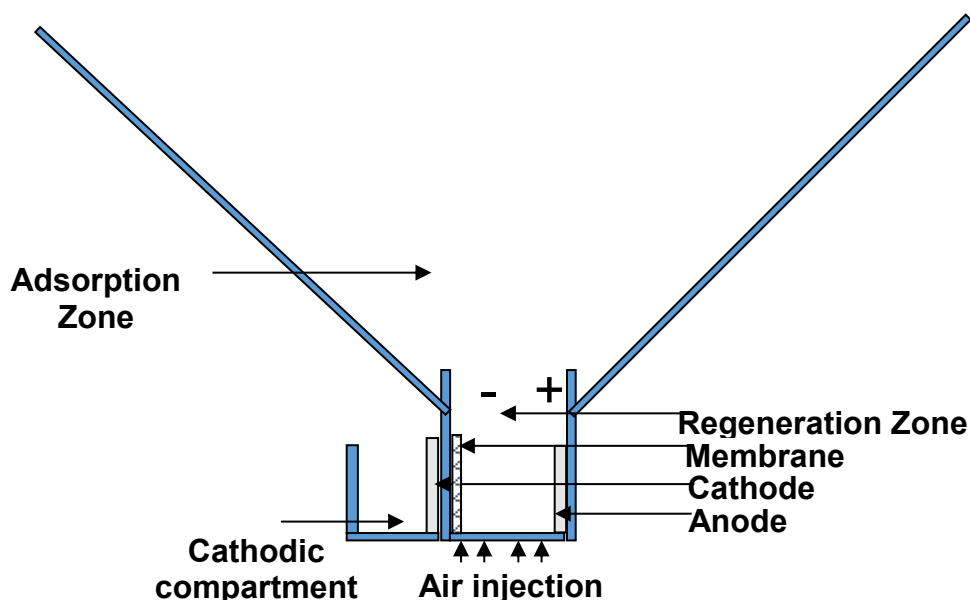


Figure 3:5 Schematic diagram depicting the Arvia Y-cell.

3.3.4 Effect of Growth Characteristics on Adsorption Recovery

A suspension of *Chlamydomonas reinhardtii* was cultured in 500 mL of Tris-Acetate-Phosphate (TAP) media in a 1L bottle. 1 mL of suspension was taken before placing the bottle in a growth chamber, and its optical density measured. Samples were then taken daily to monitor the growth phase of the cells.

Samples of suspensions were then collected during the exponential and stationary growth phases. 30 mL of each suspension was placed into a 50 mL centrifuge tube and suspensions examined in triplicates. 10 g of wet Nyex™ was added and the mixtures shaken at 200 rpm for 20 minutes. The adsorbent in the mixture was then allowed to settle for about 1 minute before samples of the supernatant were taken for analysis of unrecovered microalgae cells as previously described.

3.3.5 Effect of pH on Adsorption Recovery

The pH of suspensions were varied in a number of different centrifuge tubes using 0.5M/1.0M hydrochloric acid and 0.5M/1.0M sodium hydroxide. Using a magnetic

stirrer to ensure uniform mixing of the suspensions, drops of either the acid and/or alkali were added to the suspensions. The pH was measured and monitored using a pH meter so that batches of the suspensions with pH values ranging from 3 to 11 were made up.

A batch experiment was carried out in which 30 mL suspensions at pH values ranging from 3 – 11 as well as the original suspension pH (7.7), were placed in a cylindrical tube. 10 g of wet Nyex™ (30% moisture content) was weighed and added to the suspensions and the mixture was agitated at 200 rpm for 20 minutes. The adsorbent in the mixture was then allowed to settle for about 1 minute before samples of the supernatant were taken for analysis of the unrecovered cells.

3.3.6 Acidic Properties of Nyex™ Particles

30 mL of deionised water was placed in 3 conical flasks and the initial pH was measured. 10 g of wet Nyex™ was then added and the resulting mixture pH was also measured. Each mixture was shaken at different intensities of 100 rpm, 200 rpm and 300 rpm for 20 minutes. The pH of the resulting supernatant was then measured and taken as the pH of the Nyex™ particles (Pudipeddi *et al.*, 2016).

3.3.7 Measurement of the Zeta Potential of *Chlamydomonas reinhardtii*

Batches of the suspensions with pH values ranging from 3 to 11 were made up as highlighted in section 3.3.5. The zeta potential measurements of the suspensions were obtained using a Malvern ZetaSizer 2000 (Malvern, UK). The ZetaSizer 2000 works by measuring the electrophoretic mobility (U_e) of a particle and then converts it to zeta potential (ζ) based on the Smoluchowski model as shown in equation 3.1, where μ and ε symbolise the viscosity and permittivity of the suspension respectively.

$$U_e = \frac{\kappa \zeta}{\mu} \quad (3.1)$$

At an algae cell particle size of 3.2 μm or more, the use of the Smoluchowski equation was appropriate for *Chlamydomonas reinhardtii* (Hadjoudja *et al.*, 2010). Results of the zeta potentials were obtained in triplicate.

3.3.8 Influence of the Acidic Properties of Nyex™

The adsorption experiment was carried out as stated in section 3.3.1 where 10 g of wet Nyex™ was added to 30 mL of microalgae suspension. Experiments lasted for

20 minutes and were carried out at speeds of 50 to 400 rpm on the shaker. A number of control experiments were carried out which entailed a batch system where; (i) no Nyex™ was added to the suspension and it was allowed to stand in a vertical position without any form of mixing, (ii) no Nyex™ was added to the suspension and it was placed on the shaker to ensure mixing and (iii) 10 g of Nyex™ was added to the suspension and it was placed in a vertical position without any form of mixing. Samples of the supernatant were taken to determine the residual cell concentrations as described in section 3.6.2.

3.4 Adsorption Column Studies of Microalgae Cells Recovery

3.4.1 Downward flow mode

Experiments were conducted using a Perspex column of 1.4 cm internal diameter and 40 cm length. The column was packed with Nyex™ particles and was operated in a downward flow mode. A schematic diagram of the column is shown in Figure 3.6.

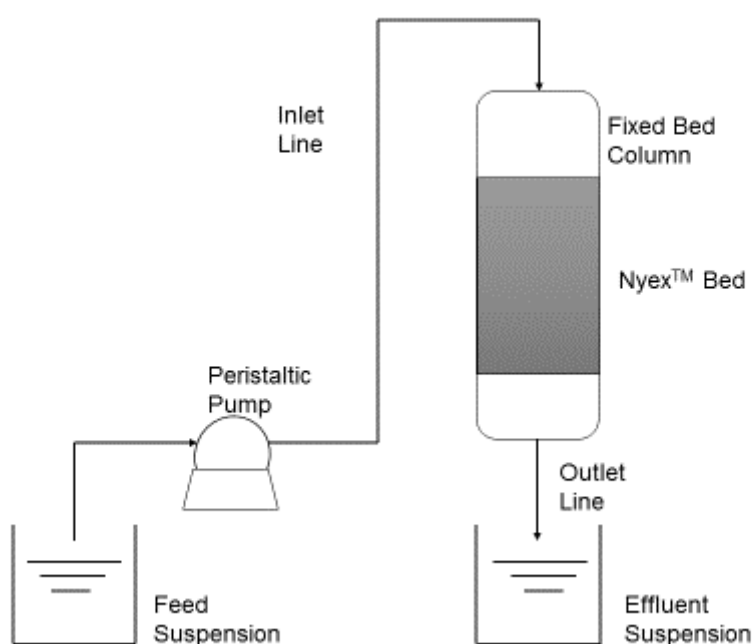


Figure 3:6 Schematic diagram for the experimental setup for the fixed bed studies showing downward flow mode.

Adsorbent retaining sieves were placed in the lower part of the column to prevent escape of the Nyex™ particles. The Nyex™ bed was wetted by filling the column with deionised water and retaining a thin film of the water at the top layer of the bed. The aim of this was to expel any trapped air within the Nyex™ bed before the start

of the experiment (Goel *et al.*, 2005). This also improved distribution of the suspension throughout the bed. The suspension feed flow rate was supplied and sustained throughout the experiment with the aid of a variable flow peristaltic pump (Model 520 supplied by Watson Marlow). The inlet flowrate was checked, periodically, by collecting samples of suspension into a measuring cylinder for a given time, while the effluent flowrate was not restricted.

The effects of process parameters viz; adsorbent bed height ($h = 5 - 20$ cm, $C_o = 0.2$ OD, $Q = 5$ mL/min) feed flow rate ($Q = 5 - 40$ mL/min, $h = 20$ cm, $C_o = 0.2$ OD) and suspension feed concentration ($C_o = 0.1 - 0.4$ OD, $Q = 10$ mL/min, $h = 20$ cm) were investigated to understand the performance of the NyexTM bed for the adsorption of cells in a column. Due to some observations evident from the above process parameters, microalgae cells were also recovered at process conditions of ($h = 30$ cm, $C_o = 0.4$ OD, $Q = 40$ mL/min).

3.4.2 Upward and Submerged flows mode

In an additional set of experiments, the bed was operated in an upward flow mode and its performance was compared to the downward mode at the same operating conditions ($h = 20$ cm, $C_o = 0.3$ OD, $Q = 10$ mL/min). Further experiments involved the bed being operated in a submerged mode, which essentially means that throughout the experiment, the bed was immersed in the microalgae suspension. This was achieved by controlling the effluent flowrate through the use of a second peristaltic pump. The effluent flowrate was set to a lower flowrate than the inlet such that a steady and controlled flooding of the bed would occur whilst avoiding an overflow of the bed.

3.4.3 Control studies

- (i) A number of control experiments were also conducted using an acid violet (AV) 17 dye. The latter was a powdered anionic tri-phenyl methane (TPM) dye, a solution of which was prepared by dissolving it in a hot deionised water. The dye was provided by Kemtex Educational Supplies under the tradename of Kenanthrol Violet with a dye content of 22%, the balance being inorganic salts. The adsorption of the dye solution by the NyexTM bed was carried out in both downward and upward flow modes at operating conditions ($h = 20$ cm, $C_o = 0.3$ OD, $Q = 10$ mL/min).

- (ii) The adsorption of cells in the column was also studied with different materials in the bed, namely; coarse and fine glass beads, and coarse industrial sand. In the downward flow mode at operating conditions ($h = 10$ cm, $C_o = 0.3$ OD, $Q = 10$ mL/min).

The concentration of cells in the feed and effluent were spectrophotometrically estimated through the use of a UV-vis spectrophotometer as described in section 3.6.1. The effluent was sampled at pre-determined time intervals to monitor the breakthrough curve. Each experiment was allowed to continue until a constant effluent concentration of the cells was evident. All the experiments were carried out at room temperature without any pH adjustments. The total cells recovered in the column was estimated from equation 2.11.

3.5 Adsorbent Regeneration, Reuse and Lipids Recovery

3.5.1 Equipment description

The adsorbent regeneration was undertaken in the regeneration zone of an Arvia Y-cell. The latter works as an adsorption system as described in section 3.3.3 and a schematic of its electrochemical regeneration zone is shown below in figure 3.7. The Y-cell was constructed using a Poly Vinyl Chloride (PVC) material. The regeneration zone comprises an anode in the form of a graphite plate and a cathode constructed from a perforated '316' stainless steel plate 1 mm thick and perforated with holes of 3 mm diameter. The active area of both electrodes is 25 cm². Both electrodes were provided by Arvia Technologies Ltd. The membrane separating the two electrodes is a micro porous polyethylene membrane (Daramic 350) supplied by Daramic. A cathodic compartment is fitted around the cathode electrode to accommodate the electrolyte (catholyte) solution. The latter is required to ensure that the cathodic side of the electrochemical cell remains acidic, otherwise, it may have a detrimental effect on the membrane.

3.5.2 Preparation of Catholyte

The electrolyte solution is 0.3% (w/w) sodium chloride (NaCl) acidified with hydrochloric acid (HCl_(aq)) to achieve acidic pH (about pH 2). It was prepared by adding 3 g of NaCl to a 1000 mL standard flask with 500 mL of deionised water, and the resulting solution was mixed to dissolve the NaCl crystals. A volume of 5 mL of

37% $\text{HCl}_{(\text{aq})}$ was then added to the solution and the mixture was shaken to ensure uniformity of the contents. The mixture was then emptied into a 1000 mL standard flask where it was made up to the mark by adding deionised water.

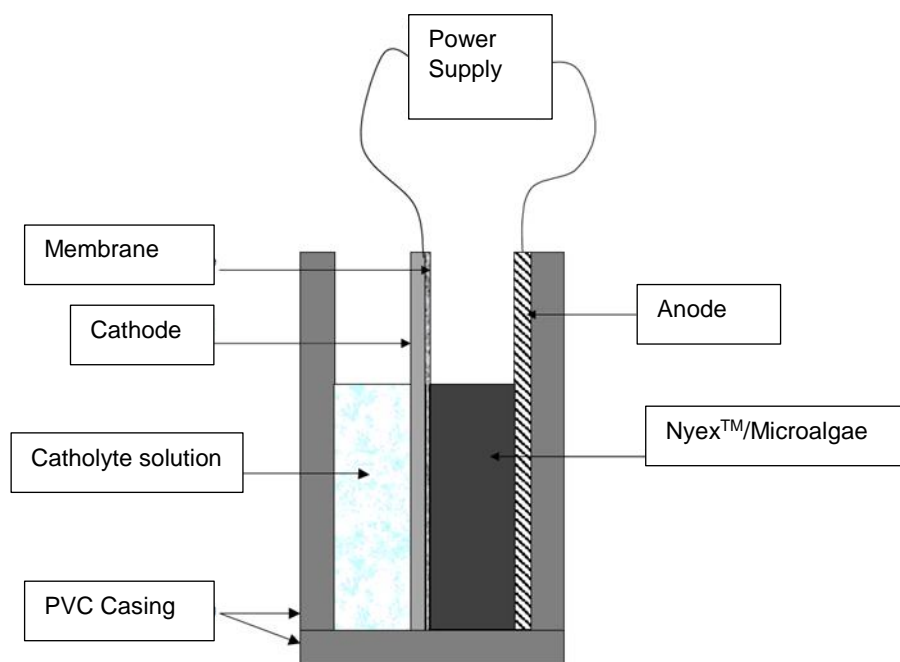


Figure 3:7 Schematic diagram of batch electrochemical zone within the Arvia Y-cell.

3.5.3 Adsorbent Regeneration at different current densities

Initial adsorption entailed adding 10 g of the Nyex™ particles to 30 mL of *Chlamydomonas reinhardtii* suspension in a 50 mL cylindrical tube. The mixture was shaken at the optimum speed of 300 rpm for a mixing time of 20 minutes using a Heidolph UNIMAX 1010 shaker. After adsorption, the adsorbent particles in the mixture were allowed to settle, and unrecovered microalgae cells in the supernatant were analysed as previously described in section 3.6.2.

The loaded (with microalgae cells) Nyex™ particles were placed in the anode compartment of the electrochemical cell, and in the presence of the electrolyte in the cathodic compartment. Power leads connected to the electrodes were connected to a DC power supply that provides a known amount of current to the electrochemical cell for the regeneration of the Nyex™ particles for some pre-determined time. There was no mixing/flow in the cell and the only 'mixing' in the system was due to the gas bubbles generated at the electrodes, which was insufficient to fluidise the adsorbent particles.

Specifically, the electrochemical regeneration of the Nyex™ particles was carried out by passing various currents between 0.1 and 2 A corresponding to current densities between 4 mA cm⁻² and 80 mA cm⁻² for 30 minutes. It was previously reported that about 20 mins was sufficient to inactivate bacteria cells depending on the current density (Hussain 2011). The applied current was held constant and, the initial and final voltages across the electrochemical cell were noted.

3.5.4 Reuse of Regenerated Adsorbent in Batch Mode

The electrochemically regenerated adsorbent particles were collected and reused to recover microalgae cells in a batch system in a similar fashion as described in section 3.5.3. The unrecovered microalgae cells from suspension were analysed as previously described. Based on the reuse of the regenerated adsorbent, the optimum current density was selected from the range used in section 3.5.3. As a consequence, the regenerated adsorbent particles from the optimum current density were reused for another four adsorption cycles.

To shed further light on the effects of electrochemical regeneration of Nyex™ particles, four variants of Nyex™ particles were also considered. They were; unused Nyex™ (Fresh Nyex), electrochemically regenerated loaded Nyex™ (Regenerated); unused but electrochemically treated Nyex™ (ETC treatment); and Nyex™ that has been used to adsorb microalgae cells but not regenerated (Loaded). These variants of Nyex™ particles were used to recover microalgae cells from suspension as described in section 3.5.3.

3.5.5 Effects of Constant Electrical Charge on Regeneration and Reuse

The effects of electrical charge and energy were investigated in order to help understand the process strategy for regenerating adsorbents at reasonably low energy consumption. It would also provide some insight as to the mechanisms of adsorbent regeneration and reuse. The electrical charge can be calculated from the equation;

$$Q = It \quad (3.2)$$

Where Q is the electrical charge passed in coulombs, I is the corresponding current in Amps and t is the length of time the current is passed in seconds.

In section 3.5.3, the amount of current passed at equal times gives rise to variation in the electrical charge passed. To maintain a constant electrical charge for different

current densities, the time required to achieve it was worked out and is presented in Table 5.4. The implication is that the electrical energy of the DC supply would be different for each current density. The electrical energy was calculated from the equation below;

$$E = QV_{av} \quad (3.3)$$

Where E is the electrical energy measured in kJ, V_{av} is the average potential difference across the electrodes measured in voltage.

The loaded adsorbents were electrochemically regenerated at the current densities and times as listed in Table 3.4 in order to maintain constant electrical charge and allowing changes in the electrical energy. The regenerated adsorbents were reused as previously described in section 3.5.3.

Table 3.4; The time required for each electrical energy at corresponding current density to maintain a constant electrical charge.

Current (A)	Current Density (mA cm ⁻²)	Time (sec)	Electrical Charge (C)	Potential Difference (V)	Electrical Energy (kJ)
0.4	16	3600	1440	4.6	6.624
0.8	32	1800	1440	7	10.08
1.2	48	1200	1440	8.35	12.024
1.6	64	900	1440	10.25	14.76
2.0	80	720	1440	8.75	12.6

3.5.6 Effects of Constant Electrical Energy on Regeneration and Reuse

Similarly, the electrical energy was maintained constant at 6.624 kJ to investigate the effect(s) of the electrical charge passed at different current densities. A constant electrical energy, from equation 3.3, is possible by ensuring that a calculated amount of electrical charge was passed as listed in Table 3.5. To achieve this, the time required for the adsorbent regeneration at each current density to give an electrical charge that maintained the electrical energy was calculated from equation 3.2. The loaded adsorbents were electrochemically regenerated at the current

densities and times as listed in Table 3.5 to investigate the effects of keeping the electrical energy constant and allowing changes in the electrical charge. The regenerated adsorbents were reused as described in section 3.5.3.

Table 3.5: The time required for each electrical charge at corresponding current density to maintain a constant electrical energy.

Electrical Energy (kJ)	Potential Difference (V)	Electrical Charge (C)	Current (A)	Time (sec)	Current Density (mA cm ⁻²)
6.624	4.4	1505	0.4	3763	16
6.624	6.3	1051	0.8	1314	32
6.624	6.6	1004	1.2	837	48
6.624	10.5	631	1.6	394	64
6.624	11	602	2.0	301	80

3.5.7 Reuse of Regenerated Adsorbent in a Fixed Bed Column

Initial adsorption entailed placing samples of the Nyex™ particles to a predetermined bed height to recover microalgae cells in a Fixed Bed Column. The column was set up as previously described in section 3.4.1. The suspension feed flow rate was supplied and sustained throughout the experiment with the aid of a variable flow peristaltic pump (Watson Marlow 520 peristaltic pump) in a downward flow mode. Samples of the effluent were taken to analyse for microalgae cells that break through the bed as described in in 3.6.1.

After adsorption, the loaded (with microalgae cells) Nyex™ particles were placed in the anode compartment of the electrochemical cell, in the presence of the electrolyte at the cathodic compartment. The electrochemical regeneration of the Nyex™ particles was undertaken as described in in section 3.5.3. The electrochemically regenerated adsorbent particles were collected and reused as described above.

For control studies, unused Nyex™ (Fresh) and unused but electrochemically treated Nyex™ (ETC treatment) were used to recover microalgae cells from

suspension. In addition, a control study involving the use of AV 17 dye crystals as the adsorbate in the column was undertaken with unused Nyex™ (Fresh), electrochemical regenerated Nyex™ (initially loaded with dye crystals and regenerated) and used Nyex™ but not regenerated (Loaded).

In each of the studies, the process parameters used for adsorbent bed height, suspension feed flow rate and feed concentration were 20 cm, 10 mL/min and 0.3 OD respectively.

3.5.8 Effects of particle size variation of Nyex™ on cells recovery.

The electrochemical regeneration of Nyex™ particles results in the degradation of the larger particles, thereby causing formation of a higher level of fines. The presence of Nyex™ fines is an unwanted situation in the adsorption of organics, hence, the need to always wash the fresh batch of Nyex™ particles before the adsorption procedure.

To study the effects of the Nyex™ fines on microalgae cell recovery, the original batch of unwashed adsorbents was separated into different size fractions. This was achieved by using sieves of different mesh sizes with a sieve shaker. Specifically, Nyex™ particles were separated into the following size fractions viz, $N \leq 710$, $125 \leq N \leq 354$, $160 \leq N \leq 354$, $355 \leq N \leq 709$ and $N \geq 710$. Where 'N' denotes Nyex™ particles size range. Measured masses of each of the adsorbent size fractions were used to recover microalgae cells in a batch test adsorption similar to that described in section 3.5.3.

As a control investigation, the original batch of unwashed adsorbents and the washed adsorbents (that had been used throughout this research study) was also employed in batch adsorption tests to recover microalgae cells from suspension.

The amount of unrecovered microalgae cells were analysed as described in section 3.6.2. The settling characteristics and more importantly the colourisation of the microalgae suspension by the size fraction variants was observed and noted.

3.5.9 Cell wall rupture and Lipid recovery tests

3.5.9.1 Observation of Microalgae cells after Nyex™ regeneration

After regeneration of loaded Nyex™ particles, samples of the adsorbents were taken and analysed for cell wall rupture and released lipids, if any. The cell wall rupture was analysed by inspecting samples of regenerated Nyex™ particles under a Scanning Electron Microscope (Quanta 200 ESEM) at different magnifications. This was relevant in order to physically verify whether the electrochemical regeneration of the adsorbents led to the rupture of the walls of the adsorbed microalgae cells.

Furthermore, microalgae cells were eluted from the electrochemically regenerated adsorbents. The elution was achieved by agitating samples of regenerated Nyex™ particles in deionised water. The suspension was then stained with trypan blue, a dye vital in staining microbial cells to selectively identify dead/inactivated cells. It is based on the concept that viable cells do not take up the impermeable dye, unlike the dead cells. Samples were taken from the mixture using a pipette onto a haemocytometer for microscopic viewing of the cells at a magnification of 1000x. Microalgae cells eluted from adsorbents, not electrochemically regenerated, were also put through the same procedure as a control study.

3.5.9.2 Lipid Recovery Analysis

For lipid quantification, samples of regenerated Nyex™ particles were 'rinsed' with different solvents namely; deionised water, ethanol and hexane (supplied by Sigma Aldrich). This was to identify the appropriate solvents to 'wash off' any lipids released onto the adsorbent. Measured samples of regenerated adsorbent were agitated with 5 ml of the solvents and shaken at 200 rpm for 5 minutes. Samples of the resulting supernatant were collected using syringes with a 0.45 micron nylon filter to remove traces of Nyex™ particles. The filtrate was then transferred into Eppendorf tubes and stained with Nile Red solution (50 µg ml⁻¹). The mixture was agitated and incubated at room temperature for about 10 minutes. The contents were then transferred into a glass cuvette for fluorescence analysis. An LS55-Fluorescence spectrometer (supplied by Perkin Elmer: Software is WinLab from Perkin Elmer) whose excitation and emission was set at 530 nm and 575 nm respectively was utilized to measure the fluorescence of the mixtures. The fluorescence intensity is an indirect method of measuring any lipids present (Huang

et al., 2009). Using a triolein standard curve, the amount of lipid present in the solution was quantified.

3.5.9.3 Triolein Standard Curve using Nile Red Method

The method used for quantifying lipid content involves staining the lipids with a dye called Nile Red. It is a quick and straightforward method, which can be used to detect lipids in a sample and also lipids within a microalgae cell. The dye attaches to the lipids such that they fluoresce and can therefore be detected and quantified using a fluorimeter ((Huang *et al.*, 2009).

A standard curve was obtained by dissolving triolein (a naturally occurring lipid) in chloroform 1:1 (v:v). This was achieved by preparing a stock containing 10 mg mL⁻¹ triolein. The triolein stock was further diluted in deionised water to achieve 100 µg mL⁻¹. This was then utilised to replicate the appropriate concentrations of triolein in Eppendorf tubes (between 0 and 100 µg mL⁻¹ in 3 replicates). The Eppendorf tubes were agitated to create micelles before adding 10 µL of 50 µg mL⁻¹ Nile Red (purchased from Invitrogen) and heated at 40°C for 5 minutes in the dark. The Nile Red solution was prepared according to a protocol outlined elsewhere (Greenspan *et al.*, 1985). The Eppendorf tube was further agitated before the samples were transferred to glass cuvettes for fluorescence analysis described above. Figure 3.8 shows strong correlation ($R^2 = 0.9901$) between fluorescence intensity and triolein concentrations, which can be used to quantify lipid presence in a sample.

3.6 Analytical Techniques

3.6.1 Absorbance Measurement by Spectrophotometer

This is an indirect method to monitor the growth and biomass concentration of microalgae cells. It can also be used to measure the amount of microalgae cells remaining after a harvesting process (Thatipamala and Hill, 1991; Prathalingam *et al.*, 2006). The equipment used in this research was a Jenova Genway Spectrophotometer and the absorbance of samples was measured at a wavelength of 680 nm. The wavelength at 680 nm was chosen because microorganisms contain various macromolecules that can absorb light which include cytochromes (400-500 nm), DNA (254 nm) and proteins (280 nm). Hence, it was suggested choosing wavelength around 600 nm would ensure that the absorbance measured was a

reflection of the biomass concentration (Winsconsin, 2013). Before samples were analysed, a blank zero reading was taken which entailed zeroing the reading corresponding to absorbance of a de-ionised water sample in a cuvette. The sample to be analysed was then filled into the cuvette and the reading indicates the absorbance of the sample.

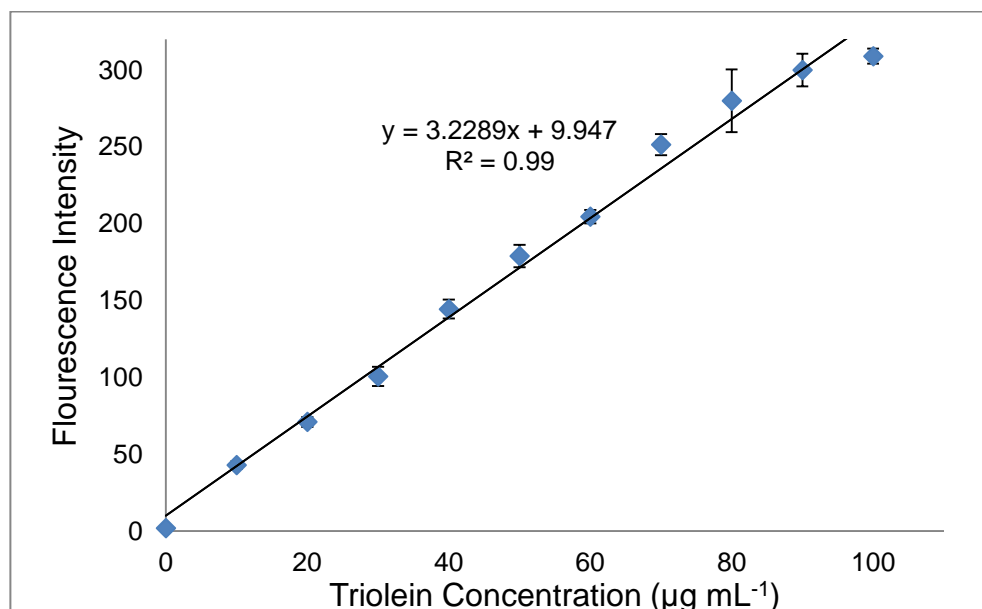


Figure 3:8; A triolein standard curve indicates the fluorescence intensity measured against varying concentrations of triolein after staining with a Nile Red dye.

3.6.2 Cell Counting by Haemocytometer

The presence of NyexTM particles in the suspension, after an adsorption procedure in a batch system, makes it extremely difficult to use a spectrophotometer to estimate the residual cell density; the amount of microalgae cells remaining in a suspension after recovery studies. This is because the adsorbent particles interfere with the light emitted by scattering such that any absorbance reading is the result of the combined effects of the cells and NyexTM particles. An attempt to use a control sample of NyexTM particles in deionised water does not serve a useful purpose because the amount of fines present in different batches varies considerably. Worse still, larger NyexTM particles sometimes disintegrate in a non-uniform and unpredictable manner in suspension after exposure to some form of agitation.

As a consequence, a more direct, albeit tedious, procedure of cell counting by a haemocytometer was considered (Christensen *et al.*, 2005; Prathalingam *et al.*, 2006). This would ensure that the biomass concentration of the microalgae cells

before and after an adsorption process could be determined. The difference between the initial and residual cells in suspension, after an adsorption procedure, is an indication of the amount of cells recovered onto the Nyex™ particles. A haemocytometer comprises a counting chamber and its cover slip that is used to estimate the number of cells per unit volume of a suspension.

The haemocytometer used in the research reported in this thesis was “the Reichter Improved Neubauer double cell” (obtained from Bright Line, USA). The counting chamber and its cover slip was thoroughly cleaned using ethanol solution (70% concentration) and slightly moistened to ensure that the cover slip can be firmly fixed to the counting chamber. A sample of cell suspension was pipetted at the edge of the cover slip and allowed to flow under the cover slip by capillary action. The haemocytometer grid (see figure 3.9) was then visualised under a light inverted microscope at a 400x magnification (based on the ease of recognising the cells) in order to count the cells.

As shown in figure 3.9, the microalgae cells were counted in the four large corner squares. The total count of cells was then divided by the volume of the large squares over which the cells were counted. This gives the biomass (cell) concentration in the original sample in cells mm⁻³. Since there are 1,000 cubic mm per ml, the biomass (cell) concentration is then converted to cells ml⁻¹ by multiplying cells mm⁻³ by 1000.

Equation 3.4 elucidates this, Cell concentration in the original sample (cells ml⁻¹) =

$$\frac{\text{number of cells counted on the haemocytometer}}{(\text{area of squares over which cells were counted})(\text{depth of chamber})} \times 1000 \quad (3.4)$$

For the study reported in this thesis, equation 5.4 can be rewritten as,

$$\frac{\text{number of cells counted}}{(4 \text{ mm}^2)(0.1\text{mm})} \times 1000 \quad (3.5)$$

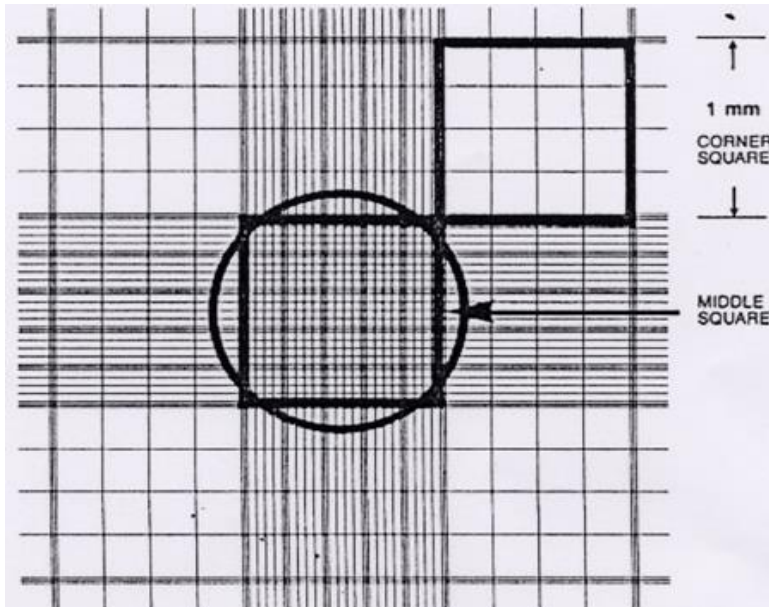


Figure 3:9: A haemocytometer grid showing Neubauer rulings.

3.6.3 Other Analytical Techniques considered

A number of techniques were also considered to carry out sample analysis before and after an adsorption procedure. They included the chlorophyll extraction and capacitance measurement techniques.

3.6.3.1 Chlorophyll Extraction

Chlorophyll extraction can be used to indirectly measure biomass concentration. It entails the use of a solvent such as ethanol or acetone to extract chlorophyll pigments from cell pellets (Henriques *et al.*, 2007). The total chlorophyll, $\mu g/ml$, in the extracts can be measured as a sum of chlorophyll a + chlorophyll b.

$$\text{Chlorophyll a } (\mu g/ml) = (13.95 \times A_{665nm}) - (6.88 \times A_{649nm}) \quad (3.6)$$

$$\text{Chlorophyll b } (\mu g/ml) = (24.96 \times A_{649nm}) - (7.32 \times A_{665nm}) \quad (3.7)$$

Where A_{649nm} and A_{665nm} are absorbance measurements. Unlike the absorbance measurement of the microalgae suspension, the Nyex™ particles can be removed from the suspension during the centrifugation stage of the chlorophyll extract procedure. However, the adsorption procedure leaves a greyish colouration in the samples. This also interferes with the green colour extracts from the cell pellets, which then affects measurement readings. Thereby making it unsuitable to use to indirectly measure biomass concentration after an adsorption procedure.

3.6.3.2 Capacitance Measurement

The capacitance measurement technique works on the concept that an electric field polarises a viable cell membrane surface (Gencer and Mutharasan, 1979; Huang *et al.*, 1992; Fehrenbach *et al.*, 1992). This is possible because the cell membrane can control the flow of ions in a live cell. Such that a polarised cell behaves like a capacitor, thus, the capacitance measured of a microalgae suspension is a function of viable biomass concentration. The advantage of this procedure is that solid particles (for instance such as Nyex™), either permeable or impermeable to ions, do not have the ability to create a capacitor-like arrangement of ions; a phenomenon possible with live cells (see figure 3.10). This appears to be a straightforward and less tedious, however, the cost (£20,000) of purchasing the equipment 'solely' for this research could not be justified.

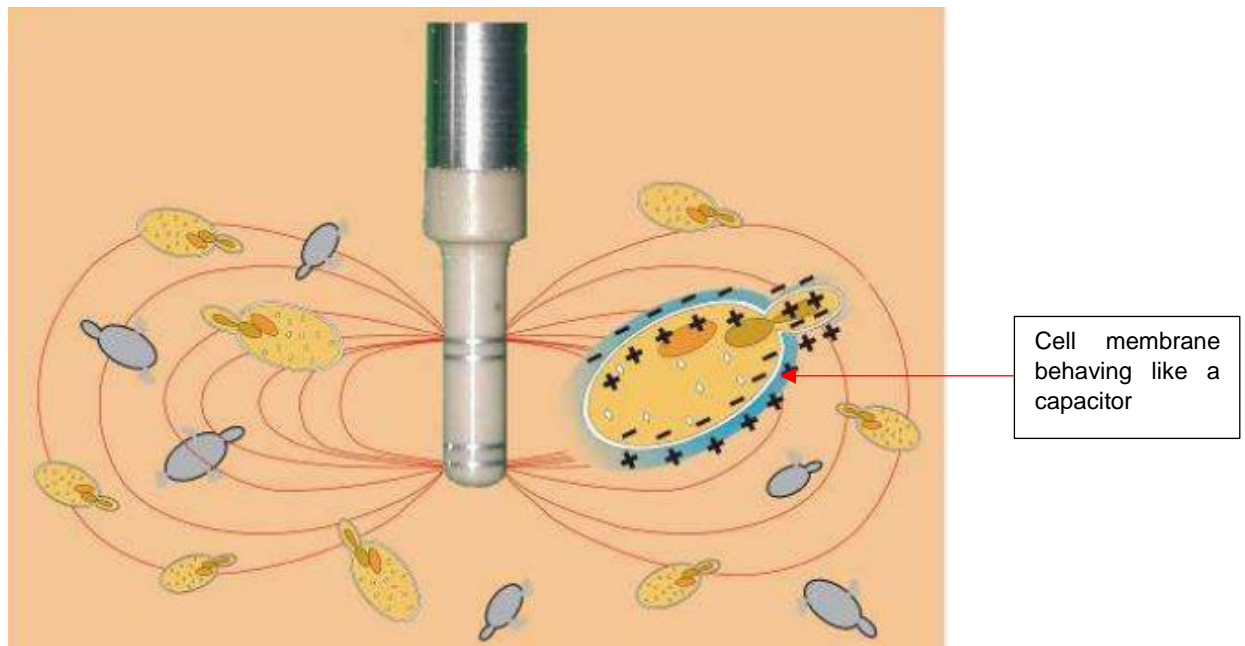


Figure 3:10: Schematic of cells behaving like a capacitor in the presence of electric field (Poppleton, 2008).

3.7 Error Analysis

The errors in the data in this study could be due to room temperature variability, the media pH (microalgae suspension and deionised water), the accuracy of the analytical methods considered in the research work as well as human errors. These errors were minimised by conducting multiple trials of experiments, for instance in triplicates and sometimes entire experiments were repeated.

The error in the experimental trials were estimated through calculation of the mean and the standard deviation from obtained triplicates, from a given measured quantity (y). The mean is defined as:

$$\bar{y} = \frac{1}{N} \sum_i^N y_i \quad (3.8)$$

Where N is the number of multiple trials (in triplicates) for the quantity and y_i is the i th measurement.

The standard deviation, σ_y , is given by;

$$\sigma_y = \left[\frac{1}{N} \sum_{i=1}^N (y_i - \bar{y})^2 \right]^{1/2} \quad (3.9)$$

The standard error, σ_M , is given by;

$$\sigma_M = \frac{\sigma_y}{\sqrt{N}} \quad (3.10)$$

In the research reported in this thesis, the standard error is presented as error bars on the graph plotted from the observed data. The graph plotted where error bars are inserted, as presented in the coming chapters 6 – 10, implies that experiments were undertaken in triplicate.

Where the fitness of a model to the experimental data was required, the correlation coefficient, sum of squared error and percentage deviation were considered and were used as statistical parameters to indicate model suitability. Their expressions are given as;

Correlation coefficient, R^2

$$R^2 = \frac{\sum_{i=1}^N (y_e - \bar{y}_c)_i^2}{\sum_{i=1}^N (y_c - \bar{y}_e)^2 + \sum_{i=1}^N (y_c - y_e)^2} \quad (3.11)$$

Sum of squared errors, SSE

$$SSE = \sum_{i=1}^N (y_e - y_c)_i^2 \quad (3.12)$$

Percentage deviation, ε

$$\varepsilon = \frac{y_e - y_c}{y_e} \times 100 \quad (3.13)$$

Where y_e and y_c are experimental and calculated values respectively.

3.8 Calibration Curves

As a result of the indirect methods used to estimate cell biomass, absorbance (in optical density [O.D]) and cell counts (in cells/ml), calibration curves were plotted in order to report some data on a mass basis (mg of the cell biomass). The calibration curves plotted are presented in the sections where they are utilised.

3.9 Summary

A detailed description of the key materials, namely NyexTM particles (the adsorbent) and *Chlamydomonas reinhardtii* (model microalgae strain), the methods and analytical techniques employed/considered in this research were discussed. The analysis carried out to quantify the errors present in experimental data was also highlighted. The subsequent chapter include discussion of observations/results obtained from the laboratory studies as well as modelling of experimentation data.

4 Results and Discussions

4.1 Evaluation of Batch Recovery of Microalgae Cells onto Adsorbent

4.1.1 Introduction

This section of the thesis presents results of experimental data obtained from mixing suspensions of microalgae cells recovery with Nyex™ particles in a batch system. The characteristics and dosage of adsorbent as well as the temperature of the system influence the amount of adsorbate accumulated onto the adsorbent (Faust and Aly, 1998; Tchobanoglous *et al.*, 2003). From the resulting experimental data, the Langmuir and Freundlich models were employed to describe the equilibrium relationship between the Nyex™ particles and the microalgae cells and its equilibrium concentration in solution in the batch process. They were considered as a result of their reasonable accuracy and relative simplicity. (Oss *et al.*, 1988; Chern and Chien, 2002; Crini and Badot, 2010). The adsorption characteristics between the Nyex™ particles and the microalgae cells are discussed below;

4.1.2 Influence of Contact Time

The rate at which microalgae cells were recovered onto the adsorbent was found to be quite similar regardless of the initial concentration. As shown in figure 4.1, within 1 minute of bringing the suspension in contact with the Nyex™ particles, an instant decrease in the concentration of microalgae cells was noticeable irrespective of the initial concentration of the microalgae suspension. As shown in figure 4.2, the percentage recovery of the cells onto the adsorbent, within 1 minute of mixing the samples, was 53%, 63% and 89% at initial concentrations of 3,000,000 cells/ml, 1,500,000 cells/ml and 750,000 cells/ml respectively. The rapid recovery of microalgae cells onto the Nyex™ surface is not uncharacteristic of the adsorbent. Earlier studies have revealed that similar behaviour was observed and this was linked to the fact that adsorption takes place on the external surface of the adsorbent (Brown and Roberts, 2007; Mohammed *et al.*, 2011; Asghar *et al.*, 2012). Specifically, Conti-Ramsden *et al.* (2012) reported a comparable substantial drop in the initial concentration of ethanethiol gas with the use of Nyex™ (Conti-Ramsden *et al.*, 2012). Additionally, Brown *et al.* (2004) also stated that 88% of equilibrium

capacity was achieved within 2 minutes of contacting Nyex™ particles with a crystal violet dye solution (Brown, *et al.*, 2004).

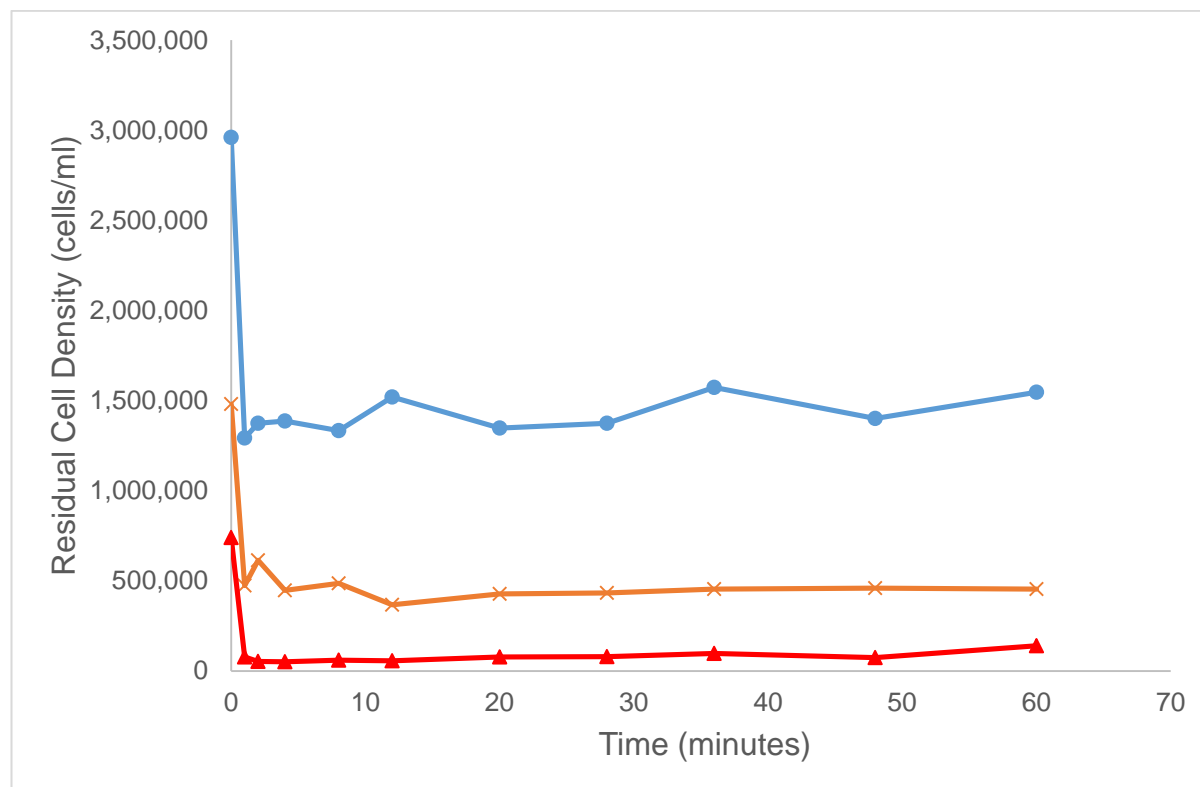


Figure 4:1 The residual cell density after adsorption of microalgae cells from suspension onto Nyex™. Initial microalgae suspension concentration of approximately 3,000,000 cells/ml (●) 1,500,000 cells/ml (■) and 750,000 cells/ml (▲).

However as evident from the graph (figures 4.1 and 4.2), continuous agitation of the mixture revealed some inconsistencies with respect to the amount of microalgae cells recovered. For instance at an initial concentration of 1,500,000 cells/ml, the percentage recovery decreased after the first minute but then increased at 4 minutes unlike at an initial concentration of 750,000 cells/ml where the percentage recovery kept increasing before slightly decreasing at 8 minutes. A number of reasons could be proposed for these observations; first, an initial rapid adsorption of microalgae cells may be followed by some desorption before "equilibrium" is attained; second, Nyex™ particles are known for attrition such that continuous agitation could lead to some adsorbent degradation; which would in effect cause some microalgae cells already attached to be desorbed (Nkrumah-Amoako *et al.*, 2014); third, some weakly attached microalgae cells can also be eluted from the surface of the adsorbent by hydrodynamic shear if mixing continues (Bitton and Marshall, 1980; Rivera-Utrilla *et al.*, 2001). Nevertheless, figures 4.1 and 4.2 seem to show that after

20 minutes, some “stability” was achieved in the system and this time was considered as the equilibrium time.

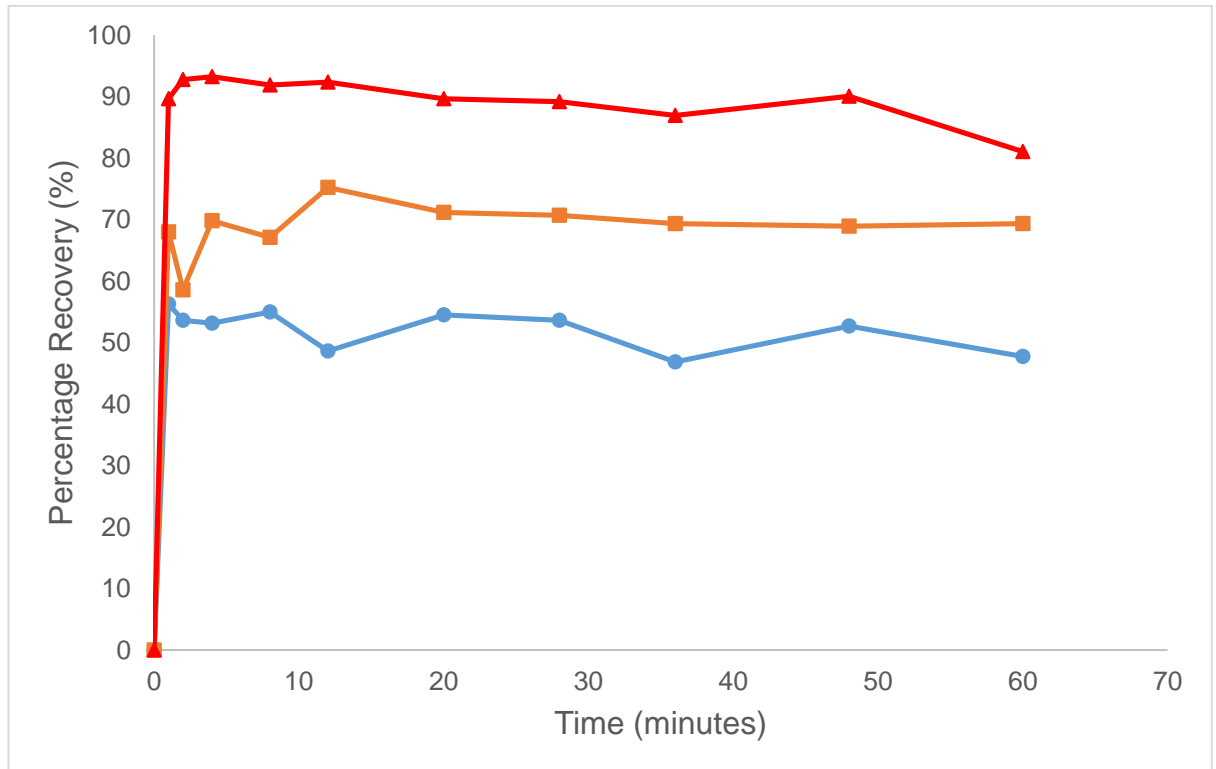


Figure 4:2: The percentage recovery of microalgae cells from suspension onto Nyex™. Initial microalgae suspension concentration of approximately 3,000,000 cells/ml (●), 1,500,000 cells/ml (■) and 750,000 cells/ml (▲).

4.1.3 Influence of Initial Concentration of Microalgae Suspension

The adsorption efficiency of an adsorbent to recover solute from solution is not independent of the initial concentration of the solute (Walker and Weatherley, 1997; Chern and Chien, 2002; Namasivayam and Kavitha, 2002). Hence, the need to investigate how the initial cell density of microalgae suspension might affect the amount of cells that can be recovered onto the Nyex™ particles. At a low initial concentration (circa 4×10^5 cells/ml), as depicted in figure 4.3, a percentage recovery of nearly 70% was attained and this efficiency reduces as the initial concentration increases. At a high initial concentration (circa 4.4×10^6 cells/ml), the percentage recovery was reduced to 43%.

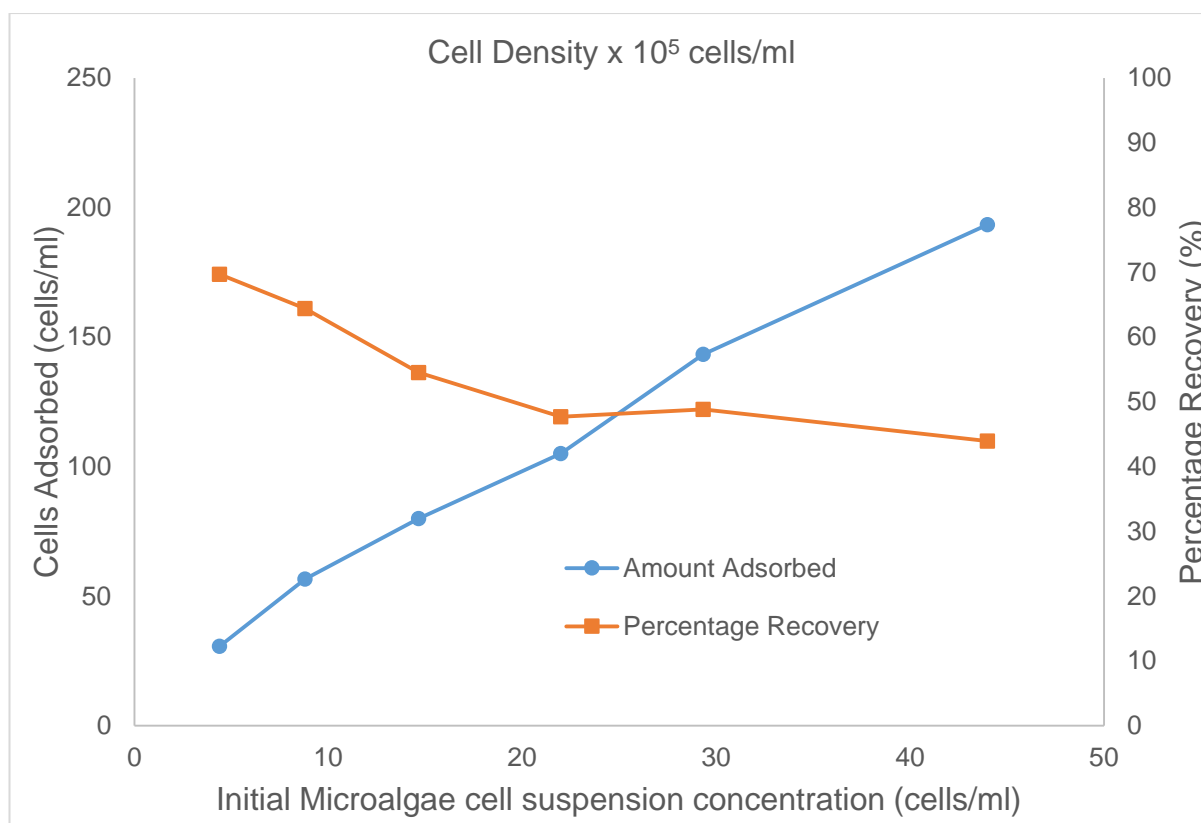


Figure 4.3; The amount of microalgae cells adsorbed ($\times 10^4$ cells/ml) and percentage recovery of cells from suspensions after mixing a measured mass NyexTM with varying initial concentration of microalgae suspension.

It is also evident, in figure 4.3, that beyond a certain initial concentration, the percentage recovery appears to tail off. Nonetheless, this decrease does not suggest that fewer microalgae cells were being recovered onto the NyexTM particles. On the contrary, more cells were recovered with an increase in the initial amount of cells in suspension.

As shown in figure 4.3, there is a linear relationship between the number of cells adsorbed and the initial cell density; which suggests that the NyexTM surface was not saturated despite the increase in the initial cell density. As a consequence, an attempt was made to achieve saturation of the adsorbent. Figure 4.4 depicts the outcome of reusing a measured amount of NyexTM with fresh microalgae suspension until the NyexTM surface was considered to be saturated.

The accumulated cell density is the sum total of microalgae cells recovered onto the NyexTM surface after each cycle of adsorption where the NyexTM is re-mixed (reuse) with a fresh batch of microalgae suspension. The equilibrium cell density on the horizontal axis is the residual cell density after each cycle of adsorption procedure.

As can be observed in figure 4.4 with respect to the percentage recovery, each time the Nyex™ is reused, the amount of microalgae cells recovered from supernatant decreases until it appears that the Nyex™ has been saturated with the cells.

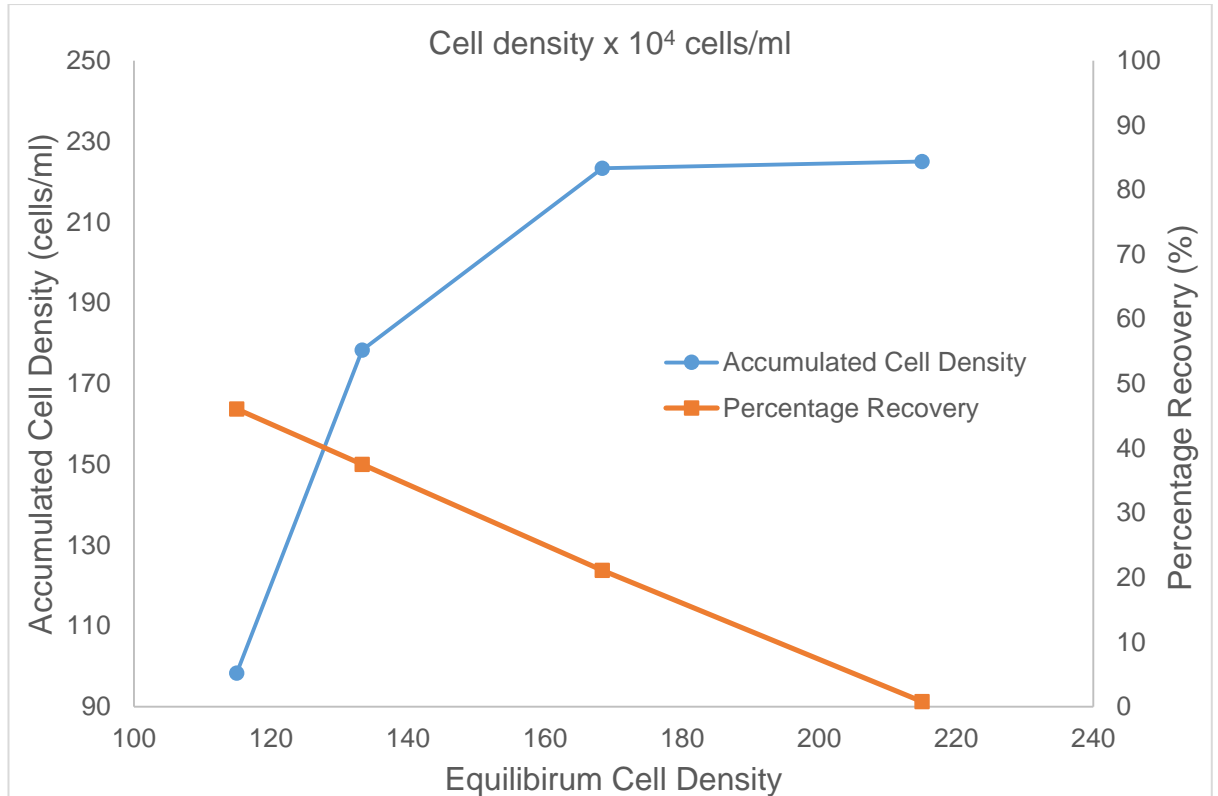


Figure 4:4; The accumulated cell density ($\times 10^4$ cells/ml) and percentage recovery of microalgae cells from suspension when a measured mass of Nyex™ is reused with fresh batch microalgae suspension until the Nyex™ surface is considered saturated.

From figure 4.4, it could be established that a fresh batch of Nyex™ particles can be reused and loaded with microalgae cells up to 3 adsorption cycles without the need for regenerating the adsorbent. However this depends on the initial concentration of the microalgae suspension; it is possible that fewer or more cycles will be achieved before the adsorbent surfaces are considered saturated.

4.1.4 Influence of the Intensity of Agitation

Figure 6.5 shows the residual cell density against the different intensities of agitation and the control experiment as previously described. As evident on the graph, the intensity of agitation initially had a positive effect on the quantity of microalgae cells recovered. The recovery efficiency for *Chlamydomonas reinhardtii* was significantly enhanced when the stirring speed was increased from 50 to 200 rpm.

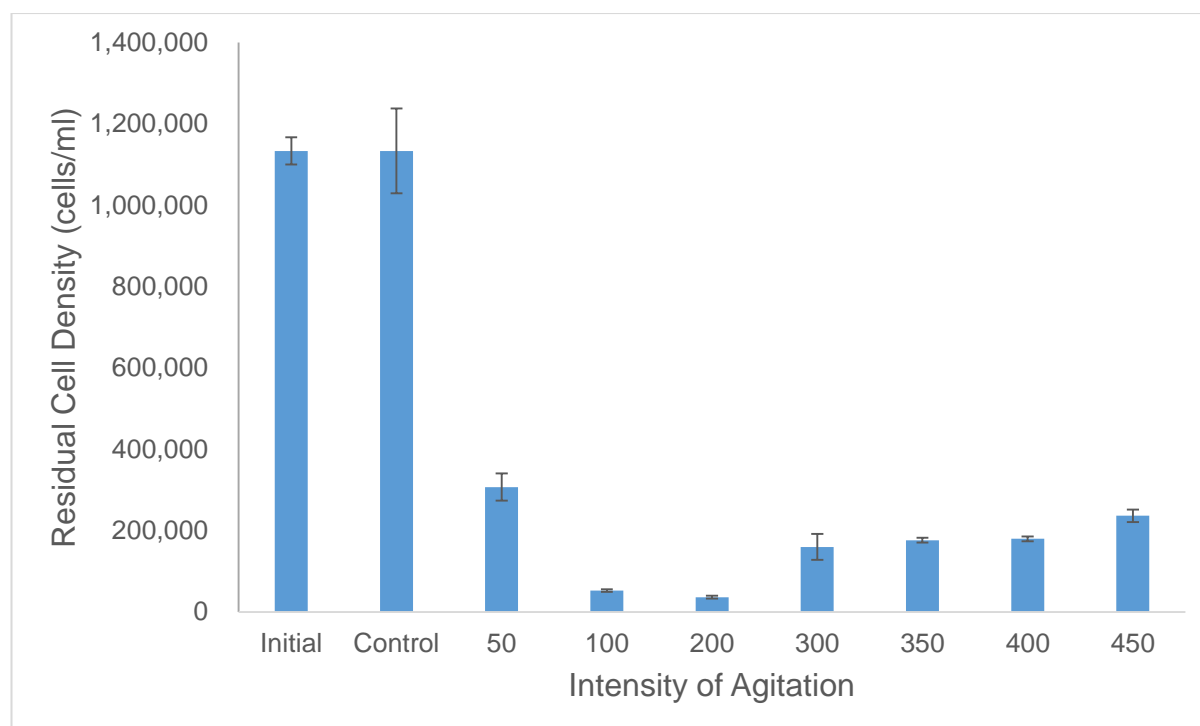


Figure 4:5; Residual cell density of microalgae suspensions after mixing with a measured mass of Nyex™ in a number of centrifuge tubes at various intensity of agitation.

Figure 4.6 depicts the percentage of microalgae cells recovered and shows that this increased by nearly 25% when the intensity of agitation was increased from 50 rpm to 100 rpm. A further increase in the intensity to 200 rpm, slightly improved the percentage recovery by just 2%.

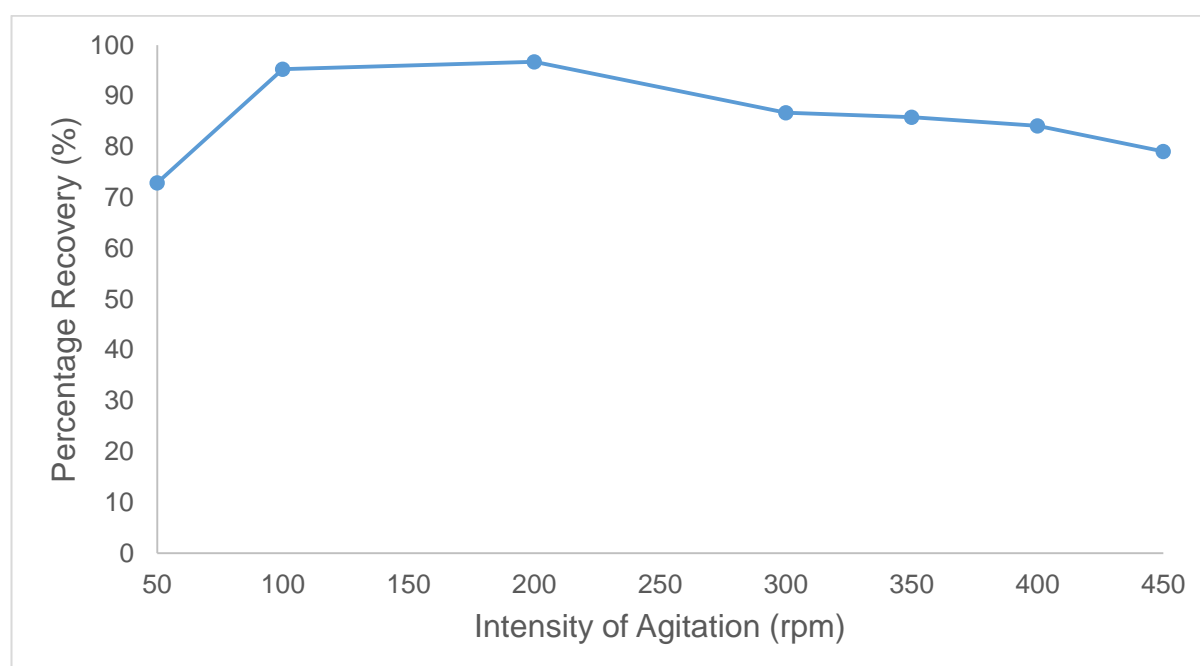


Figure 4:6; Percentage recovery of microalgae cells from suspensions after mixing with a measured mass of Nyex™ in a number of centrifuge tubes at various intensity of agitation.

This improved recovery with increasing intensity of agitation could be as a result of a better uniform distribution of the adsorbent particles within the suspension of the microalgae cells which improved their adsorption. However, an increase beyond 200 rpm did not enhance the recovery any further. In fact, it had a negative effect as fewer cells were recovered (20% fewer at 450 rpm in comparison at 200 rpm).

Two reasons can be put forward for the decrease in recovery efficiency at higher mixing speeds; first, increasing the agitation intensity can reduce the contact time required by the microalgae cells to form sufficient attachment to the adsorbent surface. Second, an increase in the intensity can cause disruption of the already formed adsorbent-cell aggregates. The implication is that the high-speed of stirring could cause some loosely attached microalgae cells to be eluted into the supernatant (Bitton and Marshall, 1980; Domínguez *et al.*, 2005; Li *et al.*, 2009; Xu *et al.*, 2011). Furthermore, as stated earlier, Nyex™ particles have a tendency to erode and these particles can be more susceptible at very high agitation. Based on this trend, it is very likely that a mixing speed of 200 rpm is just sufficient to attain a reasonable interaction between the Nyex™ particles and the microalgae cells that promotes adsorption with minimal desorption.

4.1.5 Influence of Microalgae Cell Size

Microalgae cells depending on the strain are of varying sizes and a number of studies have reported the inability of some harvesting techniques to recover small-celled microalgae strains (Shelef *et al.*, 1984; Molina Grima *et al.*, 2003; Uduman *et al.*, 2010; Brennan and Owende, 2010). The size distribution of *Chlamydomonas reinhardtii*, *Chlorella vulgaris*, and *Chlorella luteoviridis* are shown in figure 4.7.

The size distribution of *Chlamydomonas reinhardtii* was in the range 5.5 µm to 8.6 µm with an average size of 7.3 µm, while that of *Chlorella vulgaris* was in the range 3.2 µm to 4.6 µm with an average size of 4.1 µm, and *Chlorella luteoviridis* was in the range 2.7 µm to 4.3 µm with an average size of 3.5 µm. As evident in figure 4.8, it appears that a linear relationship exists between the average microalgae cell size and the amount of cells recoverable. *Chlorella luteoviridis* being the smallest microalgae strain also has the lowest percentage recovery of 30% whilst *Chlamydomonas reinhardtii* has the highest percentage recovery of 85%.

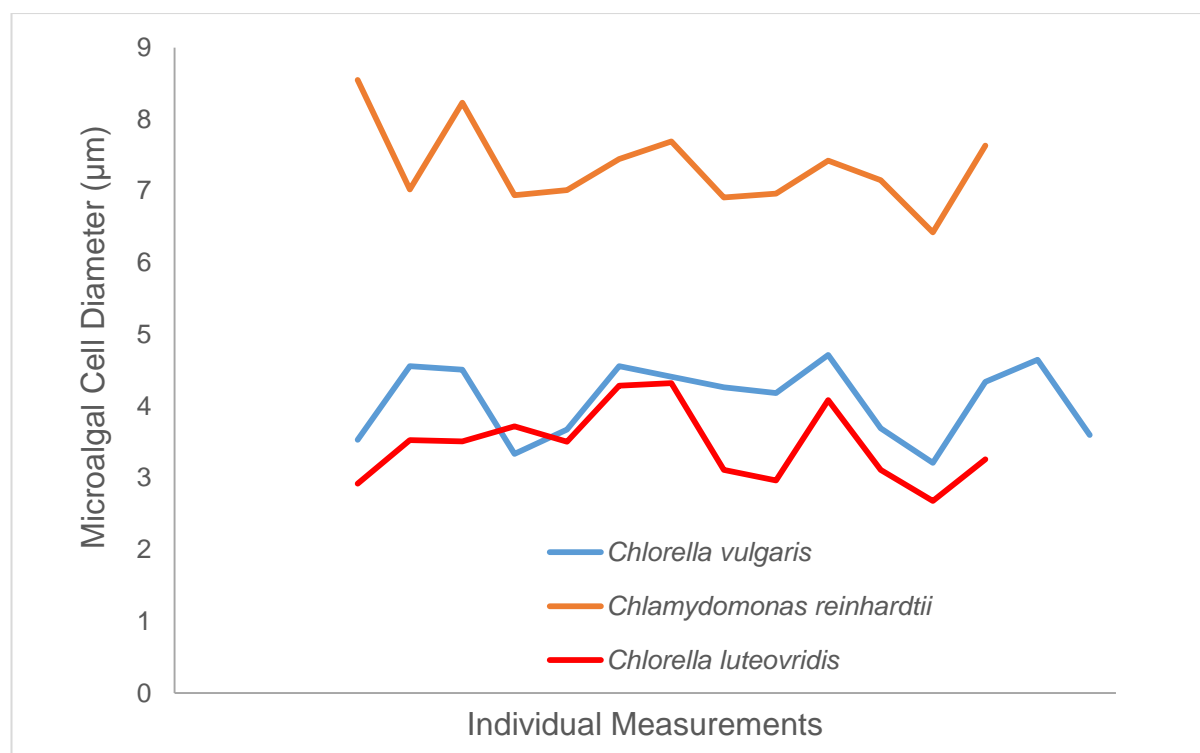


Figure 4:7; The size distribution of *Chlamydomonas reinhardtii*, *Chlorella vulgaris*, and *Chlorella luteoviridis* obtained from measuring the size of random microalgae cells with the aid of a microscopic graticule device and ImageJ software.

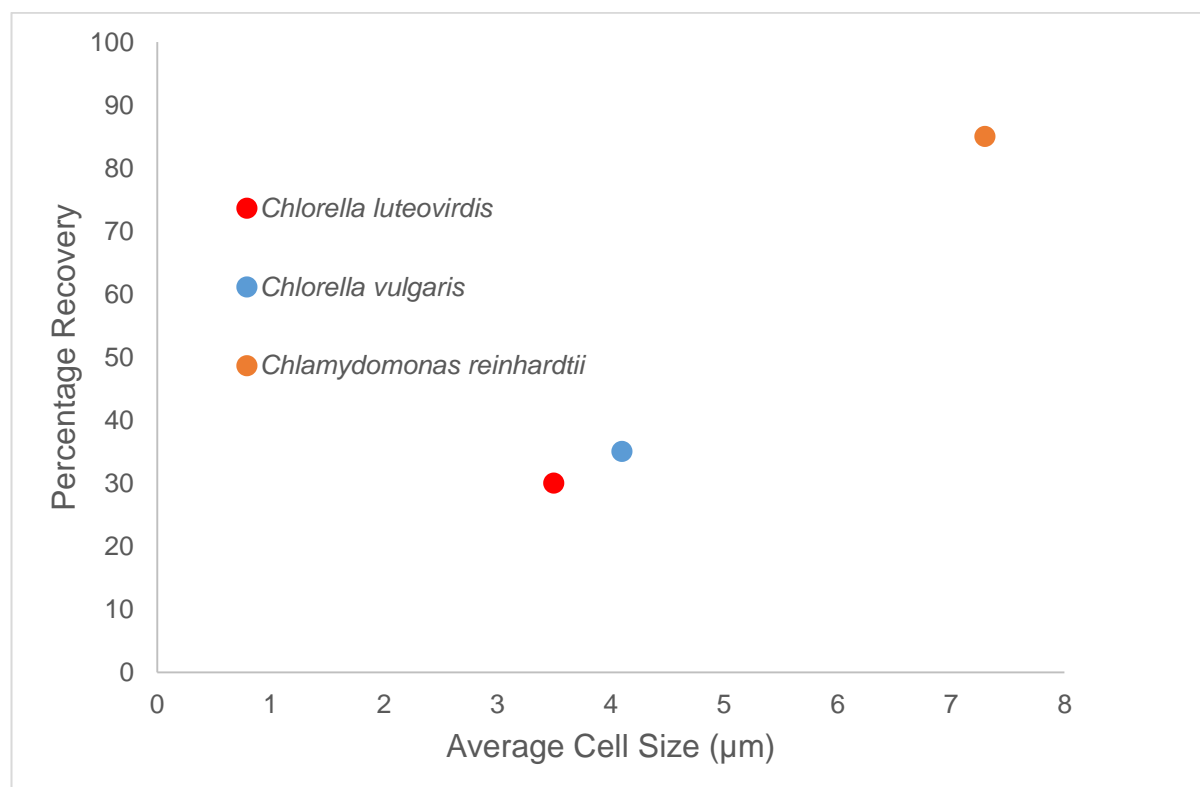


Figure 4:8; The percentage recovery and average cell size of *Chlamydomonas reinhardtii*, *Chlorella vulgaris*, and *Chlorella luteoviridis* when Nyex™ was brought in contact with the microalgae strains' suspensions.

In an experiment involving *Chlamydomonas reinhardtii* and *Chlorella vulgaris* cells at different agitation intensities, the percentage recovery of the (larger) *C. reinhardtii* from suspension was always higher than those of the (smaller) *C. vulgaris* irrespective of the intensity of agitation. This outcome underscores the influence of microalgae cell size in the recovery efficiency of cells by Nyex™ particles.

The reason for this observation might be a consequence of the fact that the probability of cells with larger sizes interacting and colliding with Nyex™ particles is higher than for small-celled algae. Hence, this might explain the higher percentage recovery observed for *Chlamydomonas reinhardtii* than for *Chlorella vulgaris* and *Chlorella luteoviridis*. Harvesting by an adsorption method may thus be more suitable for microalgae cells with relatively larger dimensions. Nonetheless, it is noteworthy to mention that despite the lower percentage recovery for the smaller microalgae cells; some harvesting techniques were reported as being not suitable to recover such small-celled microalgae. For instance, Molina Grima *et al.* (2003) reported that filter presses operated as a pressure or vacuum filter were unsuccessful in recovering microalgae cells such as *Chlorella vulgaris* from suspension as a result of their small sizes.

4.1.6 Influence of Media Change on Cell Viability and Recovery

The effect of suspension media on the recovery of microalgae cells was investigated by centrifuging the microalgae suspension and re-suspending in deionised water as previously described. Before the adsorption procedure, a possible impact of changing the media on the microalgae cells was considered by viewing the cells under the microscope. Figures 4.9a and 4.9b show that there was no “noticeable” effect of centrifuging and resuspending the resulting microalgae paste in deionised water as the microalgae cells remained intact and still retained their mobility.

The outcome of mixing the microalgae cells in 2 different suspension media is shown in figure 4.10. The resulting graph revealed that the residual cell density of microalgae cells in deionised water were less, which suggests that more of the cells have been recovered onto the adsorbent. While the percentage recovery in TAP media (original suspension media) was about 66%, there was an enhanced recovery in deionised water by a further recovery efficiency of 15% as depicted in figure 4.10.

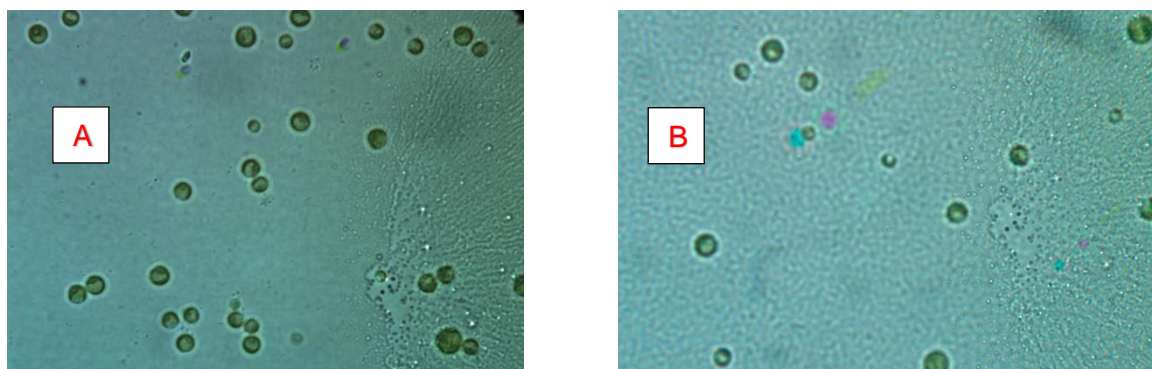


Figure 4:9; Microscopic images of microalgae cells (A) in their original TAP media and (B) suspended in deionised water.

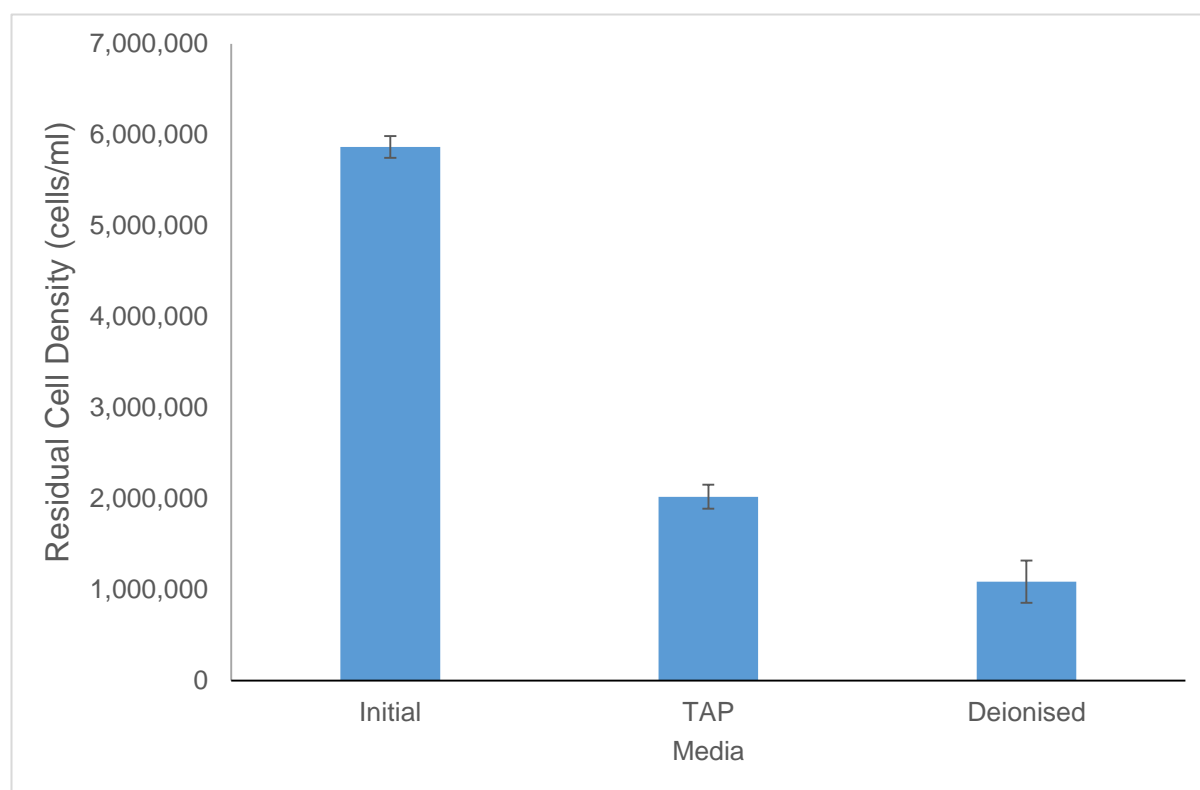


Figure 4:10; The residual cell density of microalgae cells in TAP and Deionised Water media after mixing the suspensions with 10 g of Nyex™ particles.

To shed light on the reason(s) for this observation, the initial and final pH of the suspension media was measured. It was discovered that changing the suspension media from TAP media to deionised water affected the media pH. The initial pH in the TAP media, was 8.05 as evident in figure 4.11. Interestingly, when the microalgae cells were washed and resuspended in deionised water, the initial pH dropped to 5.27. After the adsorption procedure, the final pH of the supernatant further decreased in both media to 7.61 and 3.65, respectively. The decrease in the pH for both suspension media was thought to be as a result of the acidic properties

of the adsorbent, Nyex™ particles. Though the reduction of TAP media pH was only slight, the marked decrease in the pH of the deionised water media may be responsible for enhanced recovery of microalgae cells from deionised water suspension as revealed by figure 4.10.

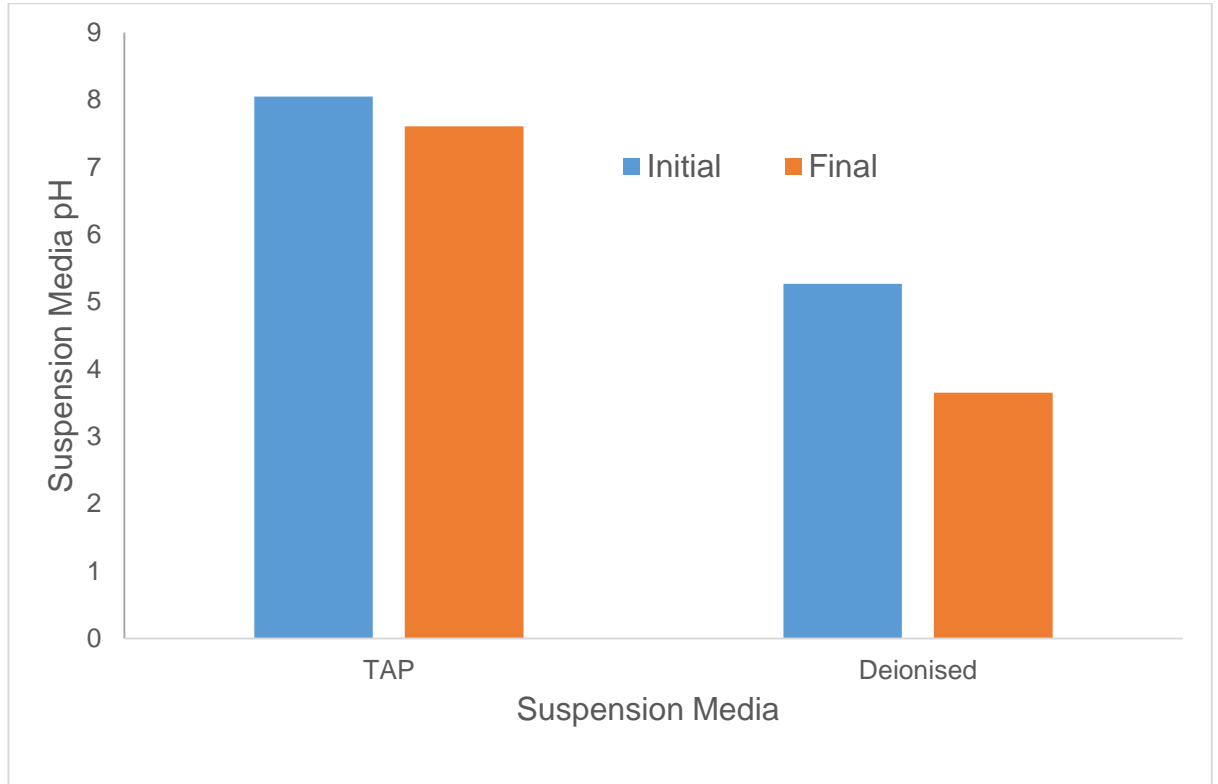


Figure 4:11; The Initial and Final pH of the suspension media of microalgae cells in TAP and Deionised Water media.

Also, figure 4.12 shows a pictorial evidence of the better recovery of microalgae cells from deionised water media. As seen from the image, the supernatant of the deionised water after adsorption is clearer than the supernatant of the TAP media. This could be due to more microalgae cells being recovered as well as a better settling of the Nyex™ fines responsible for the colouration of the suspension media. It has been reported that the interactions between microbial cells and adsorbent particles can be influenced by the media pH and its ionic strength. It was reported that adsorption of microbial cells was enhanced, as a result of the influence of a better interaction between adsorbent particles and microbial cells, in the presence of electrolytes and by the addition of multivalent cations to the suspension medium. This is due to the ability of multivalent cations such as aluminium, iron and calcium

ions, to reverse the negative surface charges of the microalgae cells leading to coagulation and enhanced recovery (Bitton and Marshall, 1980).

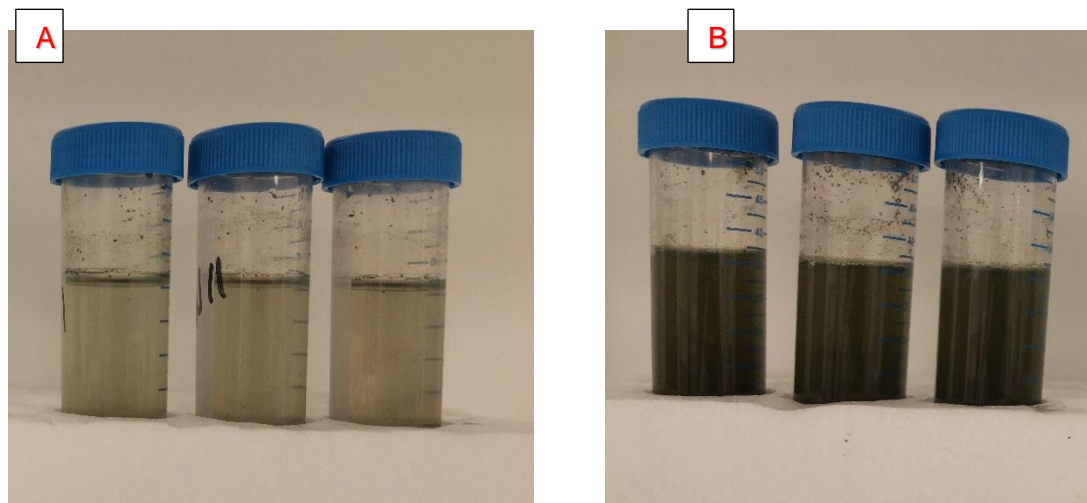


Figure 4.12; Pictorial image of the supernatant of (A) the deionised water media and (B) the TAP media after adsorption.

Furthermore, another study reported the influence of the presence of dissolved organic matter (DOM) in the recovery of microalgae cells. DOMs are mainly from polysaccharide exuded from the cells decaying. The study showed that suspensions made up in DOM free media required less alum than suspensions made up in its original media which is not DOM free. The study concluded that presence of DOMs interfered with the functional groups of the microalgae cell surface, thus reducing recovery efficiency (Zhang *et al.*, 2012). This could also be a reason for the enhanced adsorption of cells after washing the cells because of the presence of DOMs in the TAP media. The influence of suspension media pH and the acidic properties of Nyex™ are further discussed in the section 4.2.

4.1.7 Adsorption Isotherms and Capacities

The experimental data collected in the present work were fitted to Langmuir and Freundlich isotherms. These isotherms enable the analysis and design of the adsorption process for scale up purposes and gives information on the type of adsorption taking place. Figures 4.13 and 4.14 show the plots for the linearised isotherms based on the equations derived in Chapter 2 (section 2.3). The slopes and intercepts of the regression lines were used to estimate the parameters of the isotherms. Figure 4.13 shows the predicted linear plots of the Langmuir isotherm for

experimental data at low cell concentration and when the entire experimental data set is considered.

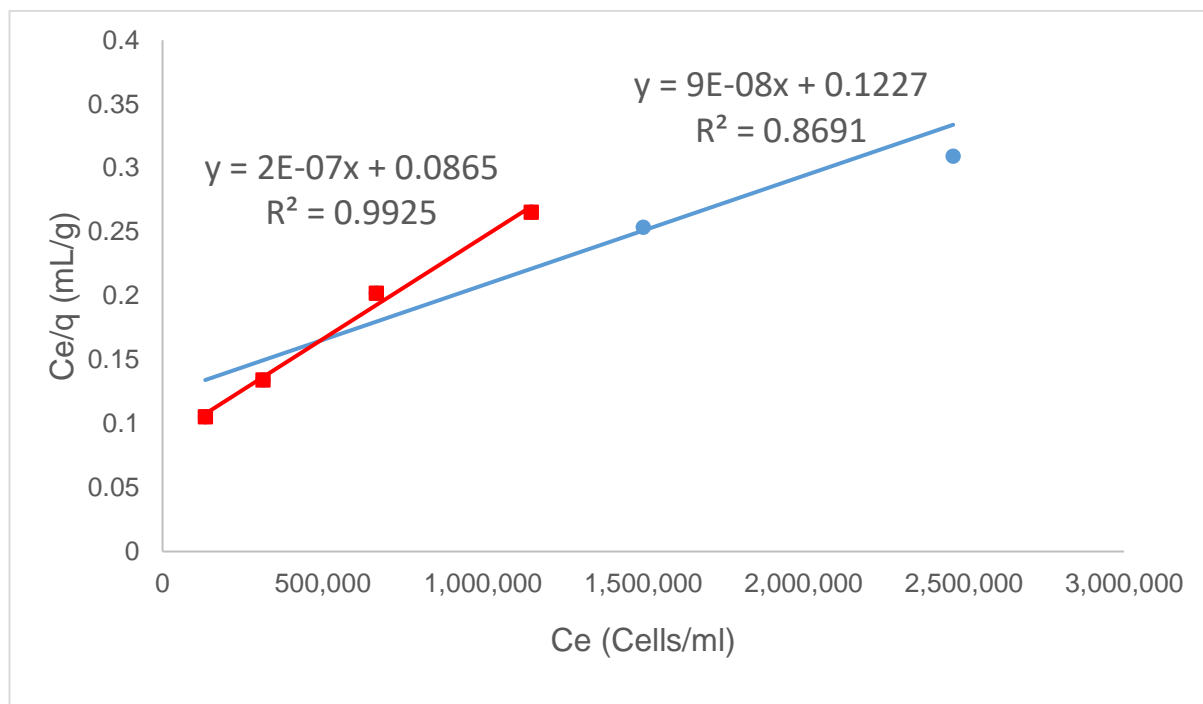


Figure 4:13; Linearised Langmuir adsorption isotherms (at low and high cell concentrations) for the microalgae cells recovered onto the surface of the adsorbent. Red and Blue lines are Langmuir model at low and high concentrations respectively.

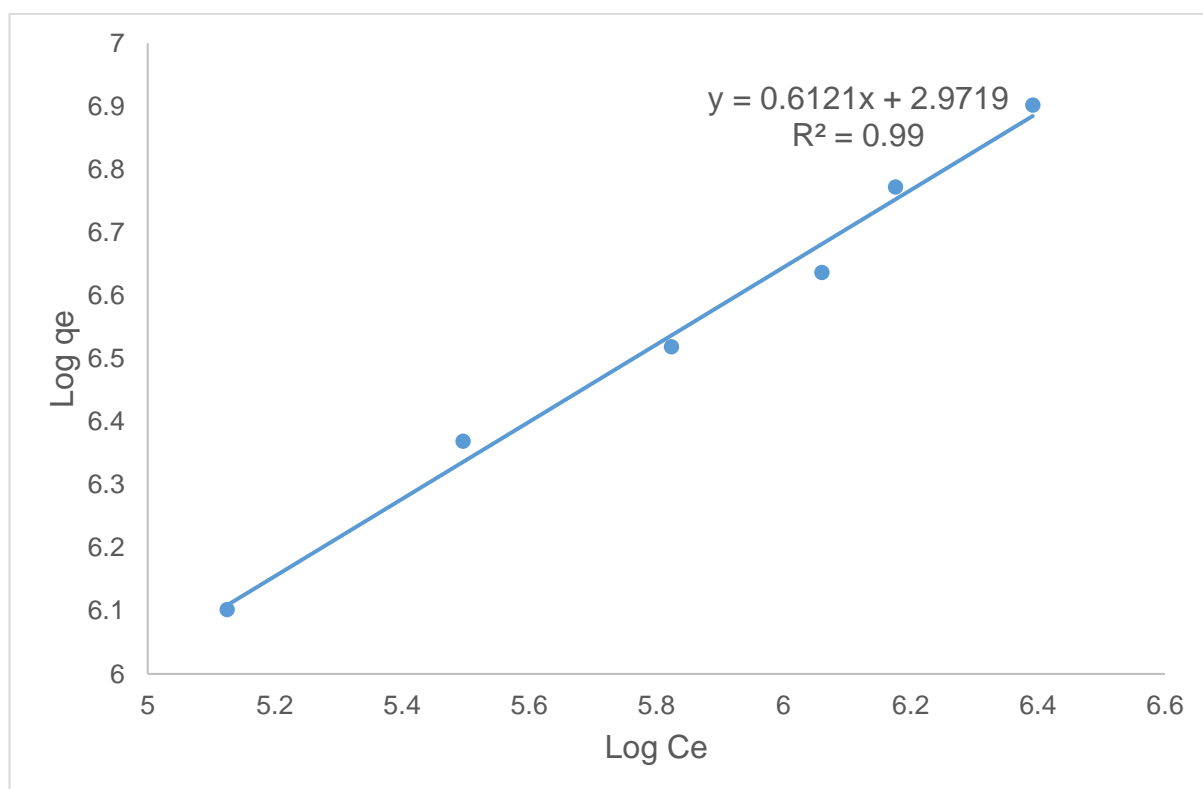


Figure 4:14; Linearised Freundlich adsorption isotherm for the microalgae cells recovered from suspension onto the surface of the adsorbent.

The reason for these 2 linear plots is obvious in the graph, where the correlation coefficient values of 0.8691 and 0.9925 was estimated for predicted Langmuir at high and low cell concentrations respectively. From this observation, the Langmuir isotherm seems to better represent the data at lower concentration. On the contrary, figure 4.14 shows that the Freundlich isotherm gives a better fit with a correlation factor $R^2 = 0.99$ despite taking into account the higher concentration of the microalgae suspension.

Table 4.4.1: Isotherm parameters for microalgae cells-Nyex™ system at 21°C.

	Langmuir Isotherm			Freundlich Isotherm
	Diluted Suspension	Concentrated Suspension		
K_L	2.31×10^{-6}	7.33×10^{-7}	K_f	937
q_z (cells/g)	5.0×10^6	1.1×10^7	n	1.63
q_z (mg/g)	0.25	0.55		
R²	0.9925	0.8961	R^2	0.99

Figure 4.15 shows the amount of microalgae cells adsorbed (q_e , cells/g) against the concentration of the cells at equilibrium (C_e , cells/ml) using the predicted Langmuir (for at low and high cell suspension concentrations) and Freundlich isotherm equations as shown below respectively;

$$q_e = \frac{11.55C_e}{1 + 2.31 \times 10^{-6}C_e} \quad (4.1)$$

$$q_e = \frac{8.15C_e}{1 + 7.33 \times 10^{-7}C_e} \quad (4.2)$$

$$q_e = 937 C_e^{0.61} \quad (4.3)$$

It is evident that despite the better fit of Langmuir at low cell suspension concentration (see figure 4.14), figure 4.15 shows the acute inadequacy of “Langmuir Low C” to predict the experimental data. However, “Langmuir High C” shows a good fit for the equilibrium data despite having a lower correlation

coefficient value. Fascinatingly, the equilibrium data were better represented by the Freundlich equation, suggesting that the coverage of the cells onto the Nyex™ particles may not be a simple monolayer. A reason for this might be a consequence of one of the assumptions of Langmuir, which proffers that only monolayer adsorption is possible.

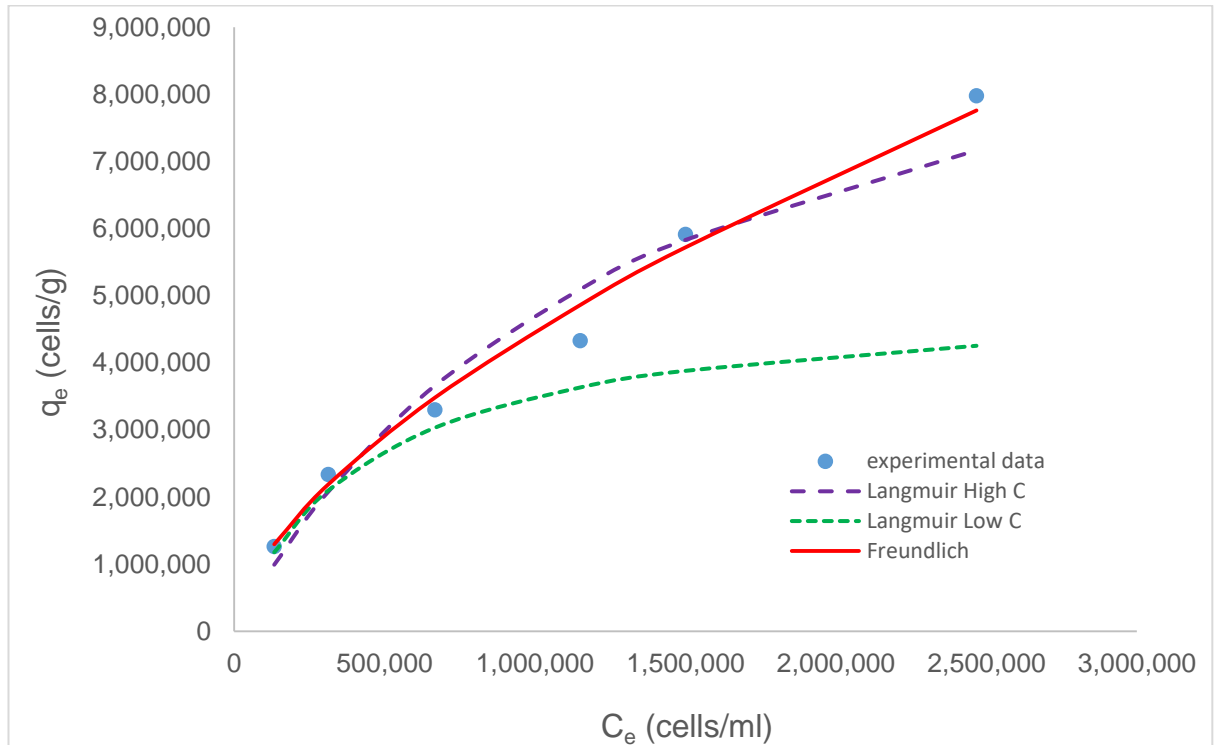


Figure 4:15; Comparison of the predicted Langmuir and Freundlich curves with the experimental curve for the adsorption of microalgae cells onto Nyex™ particles.

Langmuir theory describes an equilibrium saturation state such that once an adsorbate occupies a site, no further adsorption is possible (Hall *et al.*, 1966; Han *et al.*, 2008). On the contrary, at a higher suspension concentration, it is possible that microalgae cells form multiple layers on the adsorbent surface. The superiority of the Freundlich isotherm to better fit experimental data at higher concentrations have been reported elsewhere (Brown *et al.*, 2013). In contrast, other studies have reported the suitability and superiority of the Langmuir adsorption isotherm to describe the adsorption of *E. coli* onto activated charcoal cloth (ACC) as well as the adsorption behaviour of microalgal cells onto the magnetic nanoparticles (George and Davies, 1988; Xu *et al.*, 2011; Hu *et al.*, 2013).

The adsorptive capacity of Nyex™ for microalgae cells, *Chlamydomonas reinhardtii*, was estimated as 1.1×10^7 cells/g ; an equivalent of 0.55 mg/g (estimated from

figure 4.16). George and Davis (1988) reported a capacity of 3.78×10^{10} cells/g for *Escherichia coli* when activated carbon cloth (surface area $1,300 \text{ m}^2\text{g}^{-1}$) was used as the adsorbent. A number of other studies have also reported a better capacity when magnetic nanoparticles are used as adsorbent (Xu *et al.*, 2011; Cerff *et al.*, 2012; Hu *et al.*, 2013; Prochazkova *et al.*, 2013; Lin *et al.*, 2015). Nanoparticles have high surface area per unit volume of suspension as a result of their nano-sizes. However, nanoparticles are sometimes considered to behave more as flocculants than adsorbents. Given that the surface area of Nyex™ (circa $1 \text{ m}^2\text{g}^{-1}$) is significantly lower than most reported adsorbents, a low capacity for microalgae cells is not unexpected.

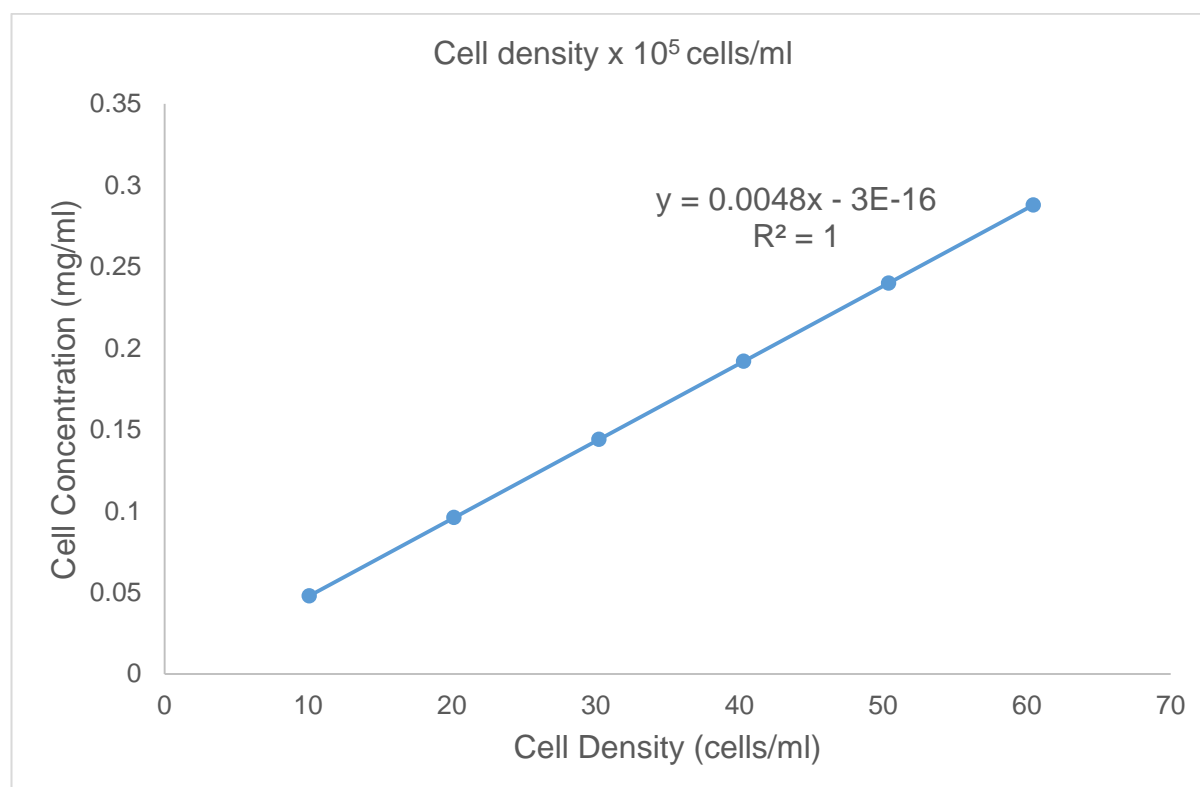


Figure 4.16; Calibration curve relating the concentration of microalgae suspension in mg/ml against the microalgae suspension density in cells/ml.

However, the value of $1/n$, a freundlich isotherm parameter, calculated as 0.61 falls between the range of 0 and 1, which suggests favourable adsorption behaviour of Nyex™ particles towards microalgae cells (Vadivelan and Kumar, 2005). In the same vein, Hall *et al.* (1966) reported an essential feature of an adsorption isotherm, a dimensionless equilibrium parameter, R_L , which defines the characteristics of the equilibrium curve of an adsorbent/adsorbate system. R_L can be calculated at

different initial concentrations of microalgae suspension to determine whether the adsorption of the cells by Nyex™ is favourable as stated in equation 4.4;

$$R_L = \frac{1}{1+KC_o} \quad (4.4)$$

Where K , the equilibrium parameter, is estimated from the linear regression in figure 4.14 and C_o is the initial microalgae suspension concentration. As shown in figure 4.17, it was evident that the value of R_L was in the range of 0 to 1 at all initial concentrations, which suggests the favourable recovery of microalgae cells onto Nyex™ particles.

Table 4.4.2: indicates the classification of isotherm curves generated from the calculated R_L values:

Value of R_L	Classification of isotherm
$R_L > 1$	Unfavourable
$R_L = 1$	Linear
$0 < R_L < 1$	Favourable
$R_L = 0$	Irreversible

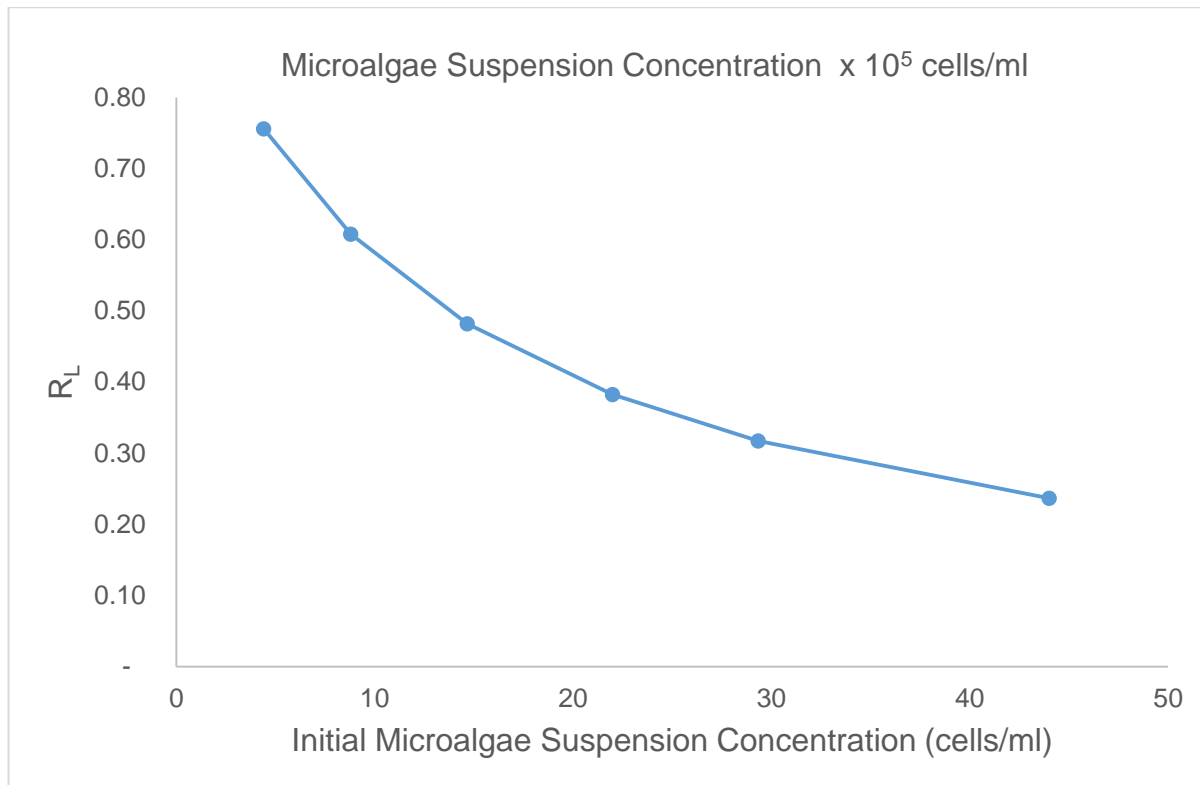


Figure 4:17; Separation factors for microalgae cells onto Nyex™ particles at a range of initial concentrations and a temperature of 21°C.

The significance of these findings demonstrate that the low capacity estimated has nothing to do with whether or not Nyex™ is a good adsorbent for microalgae cells. In fact, the shape of the predicted curves of Langmuir and Freundlich in figure 4.15 are similar to those plotted elsewhere to describe the favourable adsorption of solute particles (Weber and Chakravorti, 1974). As previously stated, the values $1/n$ and R_L confirm that the low BET surface area of Nyex™ particles (approximately $1 \text{ m}^2 \text{ g}^{-1}$) limits the extent to which more microalgae cells can be recovered.

The equilibrium parameters derived from the isotherms can be used to design the batch adsorption of microalgae cells. The performance and size of adsorber can be predicted assuming that the microalgae suspension of volume V is to be reduced from an initial concentration C_o to an equilibrium concentration C_e (cells/ml). Since the Freundlich isotherm better describes the equilibrium data for microalgae cells onto Nyex™ particles, a batch adsorption design equation can be derived as;

$$\frac{M}{V} = \frac{C_o - C_e}{q_e} = \frac{C_o - C_e}{937 C_e^{0.61}} \quad (4.5)$$

Figure 4.18 depicts the predicted amount of Nyex™ particles required to recover 50, 60, 70, 80 and 90% of microalgae cells from an initial concentration of 2.0×10^6 cells/ml at suspension volumes between 200 and 1000 ml. This graph was considered in the recovery of microalgae cells in the Arvia Y-cell.

4.1.8 Microalgae Recovery in the Arvia Y-cell

The Arvia Y-cell is a sequential batch reactor optimised to handle an adsorption-electrochemical process in a single throughput. The recovery of microalgae cells was achieved as described in Chapter 3. As depicted in figure 4.19, it seems that after 10 minutes, there was a complete recovery of microalgae cells. In fact as discussed previously in figure 4.2, recovery rate was so fast that within 1 minute, nearly 85% percentage recovery was attained in the first adsorption cycle. Curiously, despite adding “a measured mass” of Nyex™ particles into the system based on the design graph of figure 4.18, a percentage recovery of 100% was still being attained after the third cycle as evident in figure 4.19. Furthermore, during the adsorption cycles, it was observed that froth being formed was lifting the Nyex™ particles as shown in figure 4.20.

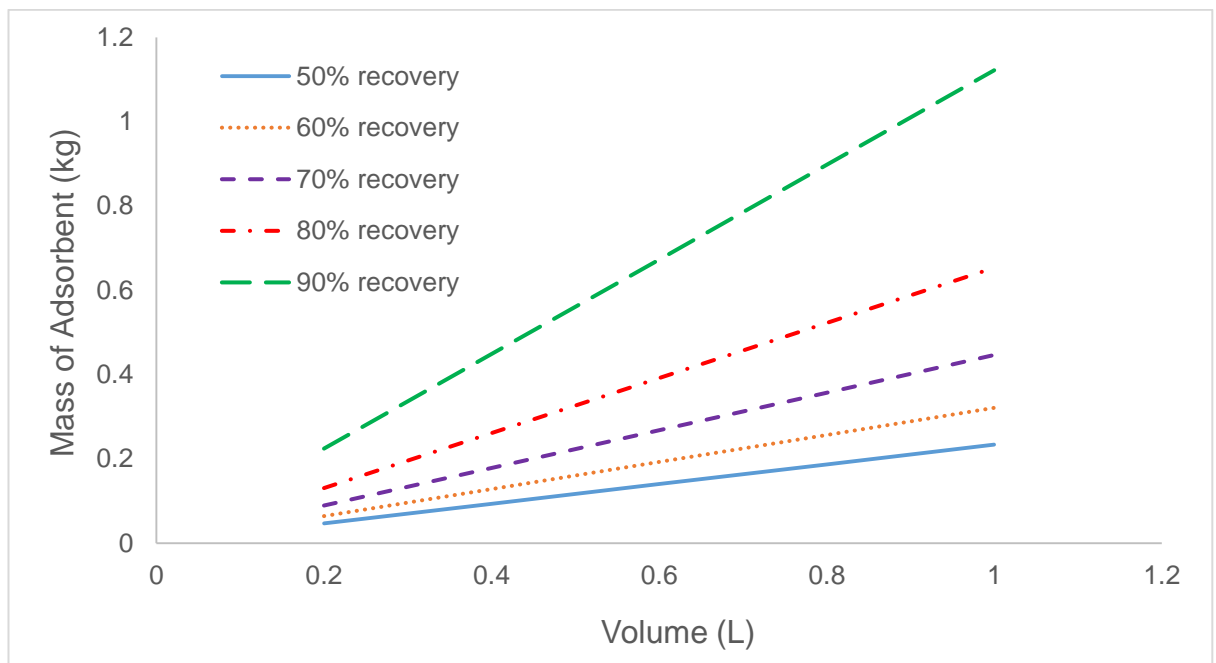


Figure 4.18; Design graph for the mass of adsorbent required to recover a given percentage of microalgae cells at initial concentration 2.0×10^6 cells/ml, for different volumes of suspension.

Accordingly, a control experiment in the absence of Nyex™ particles was carried and the result is also shown in figure 4.19. Similar to the adsorption cycles, ‘percentage recovery’ of microalgae cells was rapid and a value of 98% was “attained” despite the absence of Nyex™ particles. As a consequence, the reason for this ‘high recovery’ was therefore attributed to the formation of froth as clearly evident in figure 4.21.

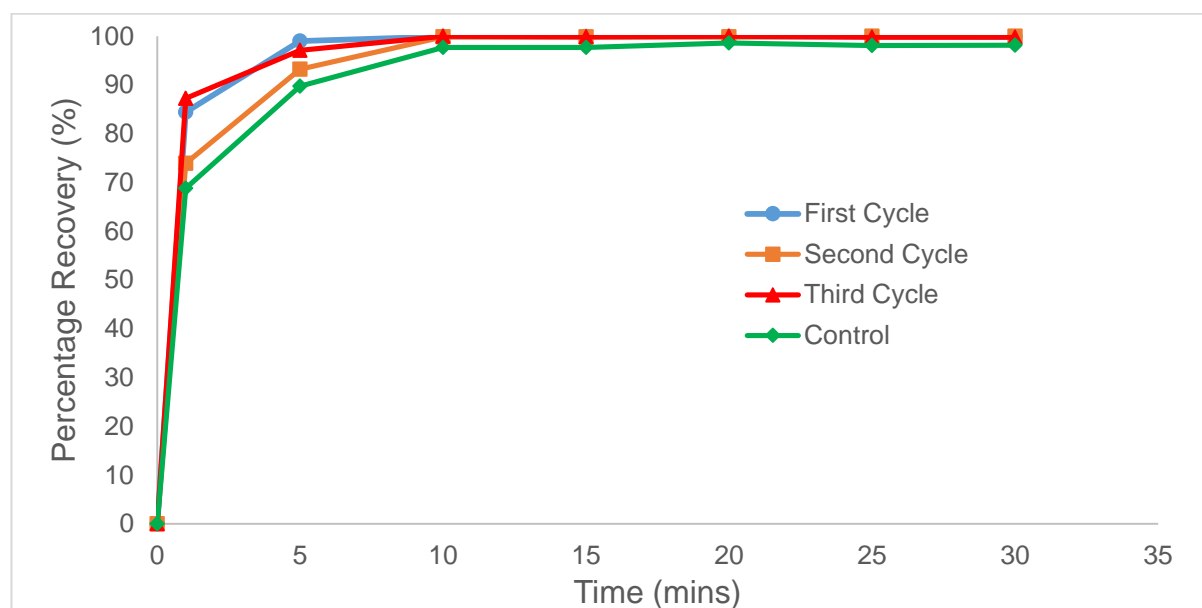


Figure 4.19; The percentage recovery of microalgae cells in the Arvia Y-cell over 3 adsorption cycles and a control experiment in the absence of Nyex™ particles.



Figure 4.20; Images of froth lifting Nyex™ particles from the adsorption zone of the Arvia Y-cell.

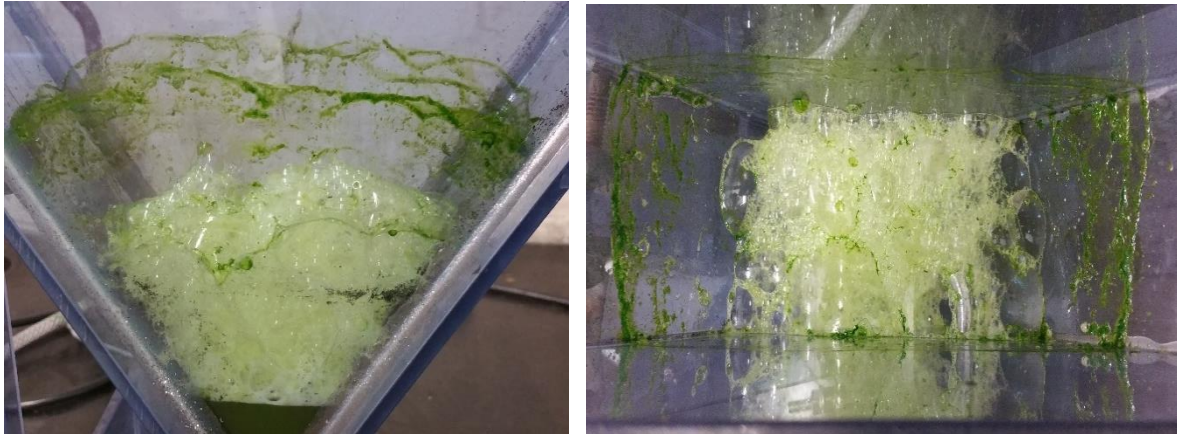


Figure 4:21; Images of froth lifting microalgae cells from the adsorption zone.

As a result, it was difficult to quantify the recovery of microalgae cells onto Nyex™ particles. To manage this problem, 2 strategies were considered. First, to add an antifoam to the suspension and/or to wash the microalgae cells from the original suspension. With the addition of antifoam, as evident in figure 4.22, no cells were noticeable on the wall of the reactor. Figure 4.23 also shows that antifoam needs to be added “throughout” the experiment to retain the microalgae cells in suspension, otherwise, adding the antifoam at the start of the experiment was not effective.

The washing of the cell suspension before adsorption further shed light on the effect of either washing or addition of antifoam. Figure 4.24 portrays a suspension that retained most of the cells. As shown in figure 4.25, measuring the optical density of the control experiment seems to suggest that the washing improved retention of microalgae cells in suspension; although it was not as effective as adding antifoam.



Figure 4:22; Images of the effect of the addition of antifoam to microalgae suspension to prevent the formation of froth.

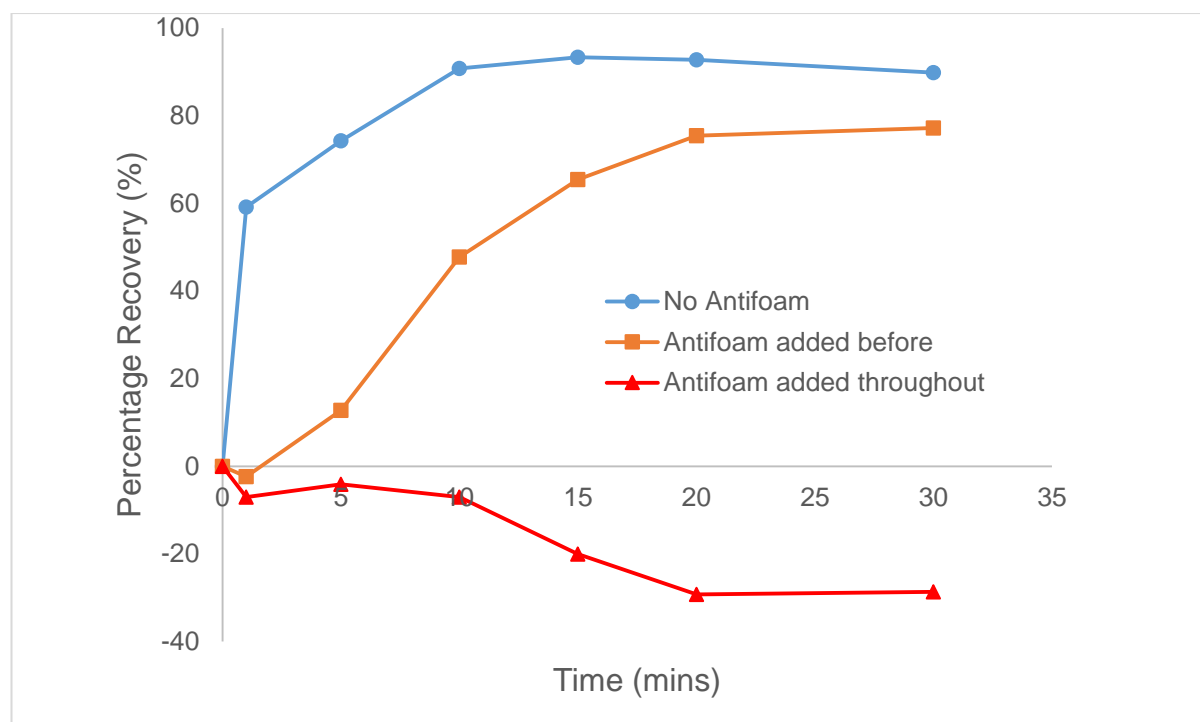


Figure 4:23; The percentage recovery (estimated on the basis of optical density measurements) of a number of control experiments in the Arvia reactor in the absence of Nyex™ particles with/without the addition of antifoam.

However, on counting the cells of the control suspension as also shown in figure 4.25, its “percentage recovery” was nearly as good as the adsorption experiment. What was observed under the microscope for the control samples was even more shocking. It was detected that the microalgae cells were being broken when the cells were retained in suspension (either through the use of antifoam or washing the cells). As revealed in figure 4.26, broken microalgae cells were obvious on the haemocytometer slide; in comparison, initial microalgae cells were unbroken



Figure 4:24; Images of the effect of the washing the suspension and resuspending the cells in deionised water.

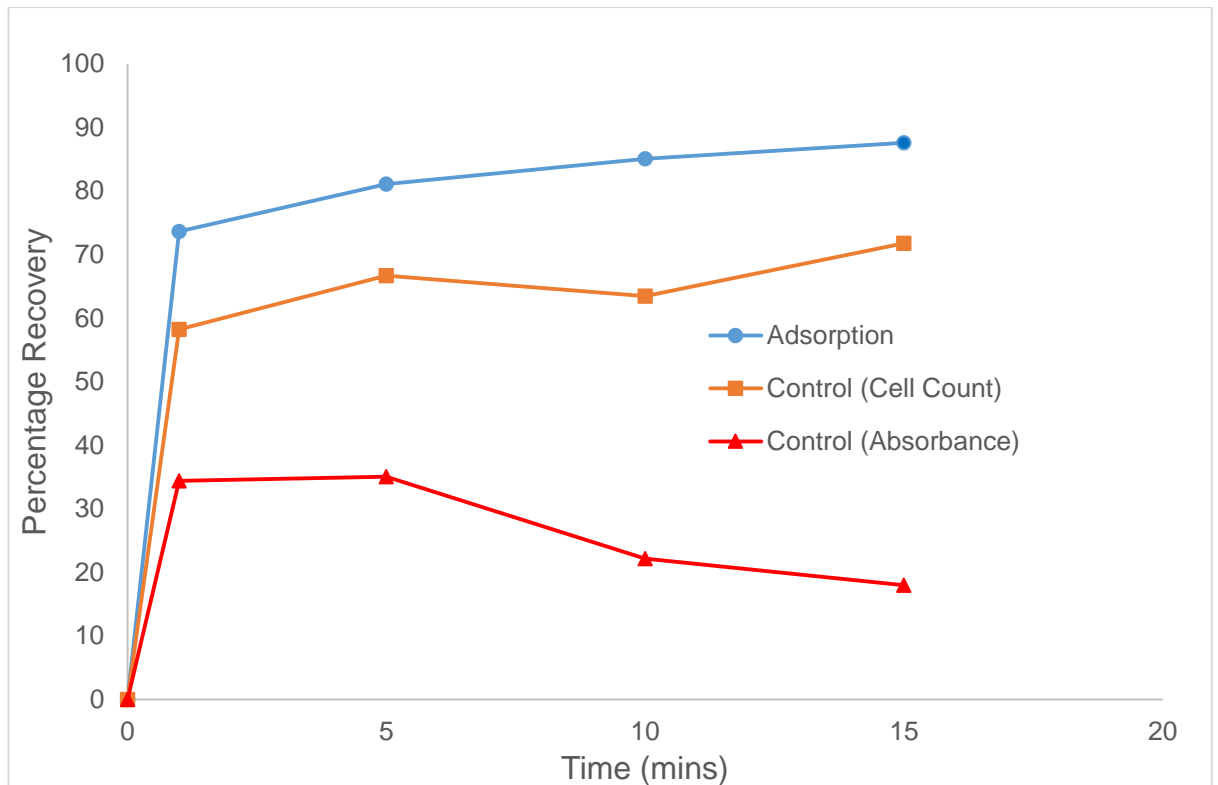


Figure 4:25; The percentage recovery of washed microalgae suspension and a number of control experiments in the Arvia Y-cell in the absence of Nyex™ particles with/without washing.

The reasons for these observations is connected to the mode of operation of the Arvia Y-cell. As described previously, air is blown through nozzles to fluidise the Nyex™ particles. It is worthy of note that flotation through the use of air or gas bubbles is one of the well-known conventional methods of recovering microalgae cells (Alfafara *et al.*, 2002; Cheng *et al.*, 2011; Jeong *et al.*, 2015). The bubbles can attach to the microalgae cells leading to a gravity separation such that they are accumulated as froth for easy removal. These froths were obvious as portrayed in the figures above and are the reasons for the lifting of the cells and some Nyex™ particles from suspension. Attempts to minimise the effect of froth formation were unsuccessful. The inability of the air bubbles to 'lift' the cells results in cell breakage. Hence, it appears that the recovery of microalgae cells in the Arvia Y-cell will prove to be very difficult if not impossible. This difficulty experienced is unique to the recovery of microalgae cells, as the equipment has found applications in the removal of wide varieties of adsorbates (Brown and Roberts, 2007; Mohammed *et al.*, 2011; Conti-Ramsden *et al.*, 2012; Brown *et al.*, 2013).

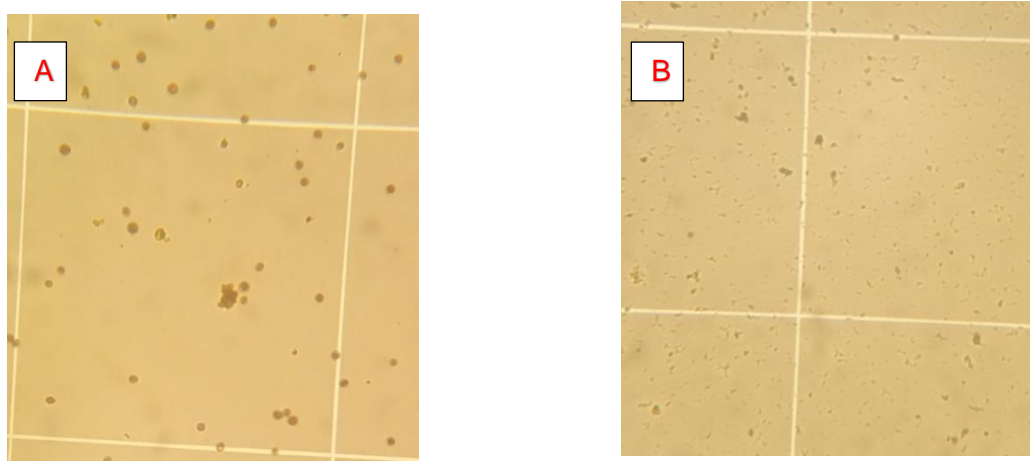


Figure 4:26; (A) unbroken microalgae cells before being placed into the Arvia Y-cell. (B) broken microalgae cells after air was passed to the suspension in the Arvia Y-cell.

4.1.9 Summary

The recovery of microalgae cells from suspension in a batch system was evaluated in this section. Studies previously reported in the literature regarding the adsorption of microbial cells all involved porous adsorbents. In contrast, the research reported in this thesis evaluated the recovery of microalgae cells onto a non-porous adsorbent. The lack of pores implies that adsorbates are recovered only to the external surface of Nyex™, hence, adsorption is not driven by intra-particle diffusion. The effect of this was evident in the rapid uptake of the microalgae cells by the adsorbent particles. Such that within one minute, up to 89% percentage recovery of the microalgae cells was attained.

Expectedly, the recovery of microalgae cells through adsorption was found to be influenced by the initial cell concentration of the adsorption, intensity of agitation, the composition of the suspension media. It was also discovered that Nyex™ particles can be reused for up to three adsorption cycles to recover cells from suspension without the need to regenerate the adsorbent. The suitability of the adsorption to recover a variety of microalgae cells, regardless of their cell size, underscores the robustness of the procedure as a recovery technique. Albeit a lower cell recovery was achieved for small-celled microalgae strains.

The Freundlich isotherm was discovered to better describe the adsorption of microalgae cells; which suggests the cell coverage onto the Nyex™ particles may not be a simple monolayer adsorption. The capacity of the adsorbent for *C.*

reinhardtii was estimated as 0.55 mg/g; a relatively low value. However, equilibrium parameters (the Freundlich isotherm parameter ($1/n$) and a dimensionless equilibrium parameter (R_L)) calculated were within the range of 0 and 1, which suggests that the adsorption of microalgae cells using Nyex™ particles is favourable. A design graph was obtained to predict the performance of the batch system as well as its size. However, the recovery of cells in a sequential batch system, the Arvia Y-cell was unsuccessful. This was attributed to the generation of bubbles which either lift the cells or cause cell breakage.

Nevertheless, the potential of adsorption as a recovery technique for microalgae cells has been demonstrated and proven. Despite a low adsorptive capacity, adsorption was discovered to be favourable which further underscores the inherent tendency of microalgae cells to attach to surfaces.

4.2 Understanding the mechanisms of adsorption; Zeta Potential and pH effects

4.2.1 Introduction

The effects of the highly negative microalgae cell surface cannot be underestimated in an adsorption process. Similar but quite different to what is obtainable in flocculation, it is likely that the mechanism of adsorption of microalgae cells may be governed by electrostatic attraction between the opposite charges of the adsorbent and those of the microalgae cells. In other words, undertaking the adsorption process at a pH that reduces the negative ZP of the cells and increases the positive ZP of the adsorbent might improve recovery efficiency. Hence, it is significant to investigate the effect of media pH as well as the ZP that influences the recovery efficiency. This knowledge may also offer clues as to the mechanism(s) governing the adsorption of microalgae cells by Nyex™ particles. Hence, it is also relevant to investigate how these growth phase characteristics might influence adsorption.

4.2.2 Effect of Growth Characteristics on the Adsorption of Microalgae Cells

The influence of the growth characteristics of microalgae cells was studied to investigate their effect(s) on adsorption recovery. The exponential and stationary growth phases were taken to correspond to days 4 and 7 on the growth curve shown in figure 4.27.

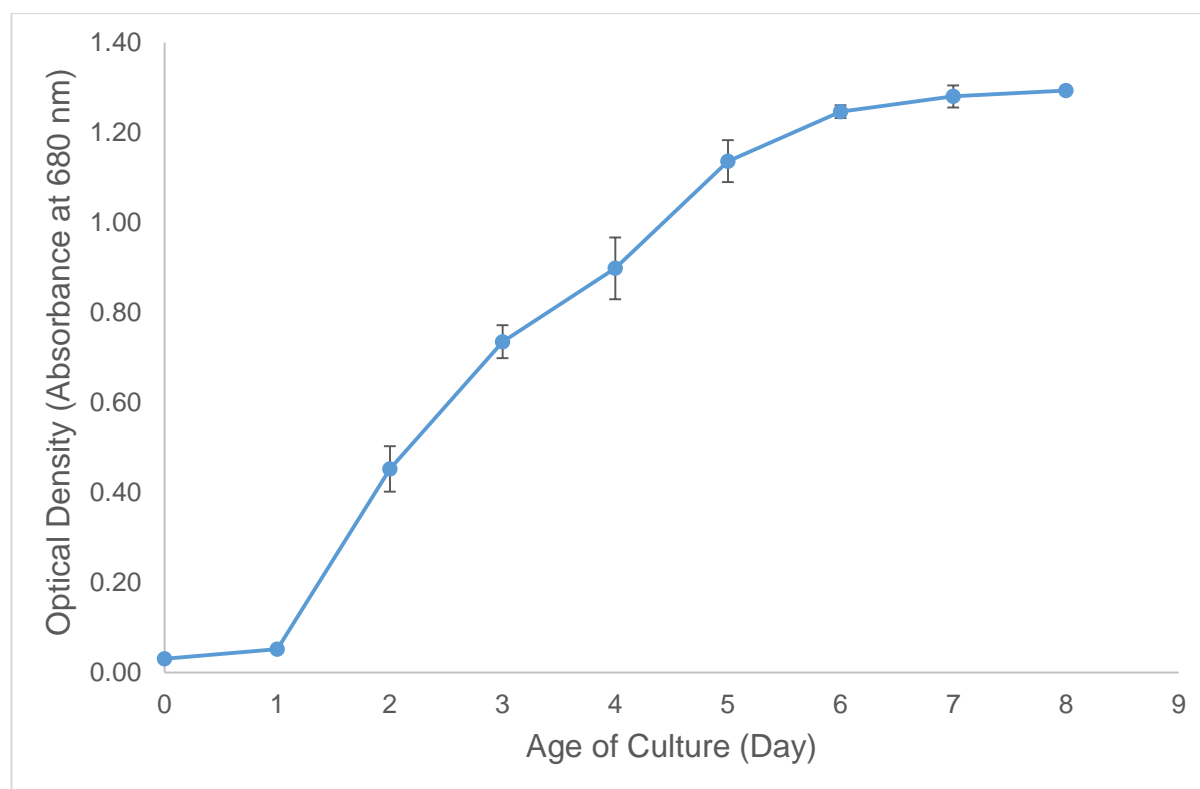


Figure 4:27: Growth curve for *Chlamydomonas reinhardtii*.

As shown in figure 4.28, the residual cell density of the cells varied depending on the growth phase. Specifically, about 1.5×10^6 cells/ml of microalgae remained in suspension for the exponential phase; at an initial cell density 2.7×10^6 cells/ml, this is equivalent to 43% microalgae cells being recovered. On the other hand, when microalgae cells were recovered in the stationary phase, nearly 1.08×10^6 cells/ml of microalgae remained in suspension after adsorption. This indicates that about 60% of microalgae cells were recovered. This observation is in agreement to what has been reported in the literature. Previous studies showed that the recovery efficiencies of a tangential flow filtration, autoflocculation, sedimentation and dissolved air flotation were enhanced for cells in their stationary growth phase (Lee *et al.* 1998; Danquah *et al.*, 2009; Zhang *et al.*, 2012; Salim *et al.*, 2013; Hu *et al.* 2013).

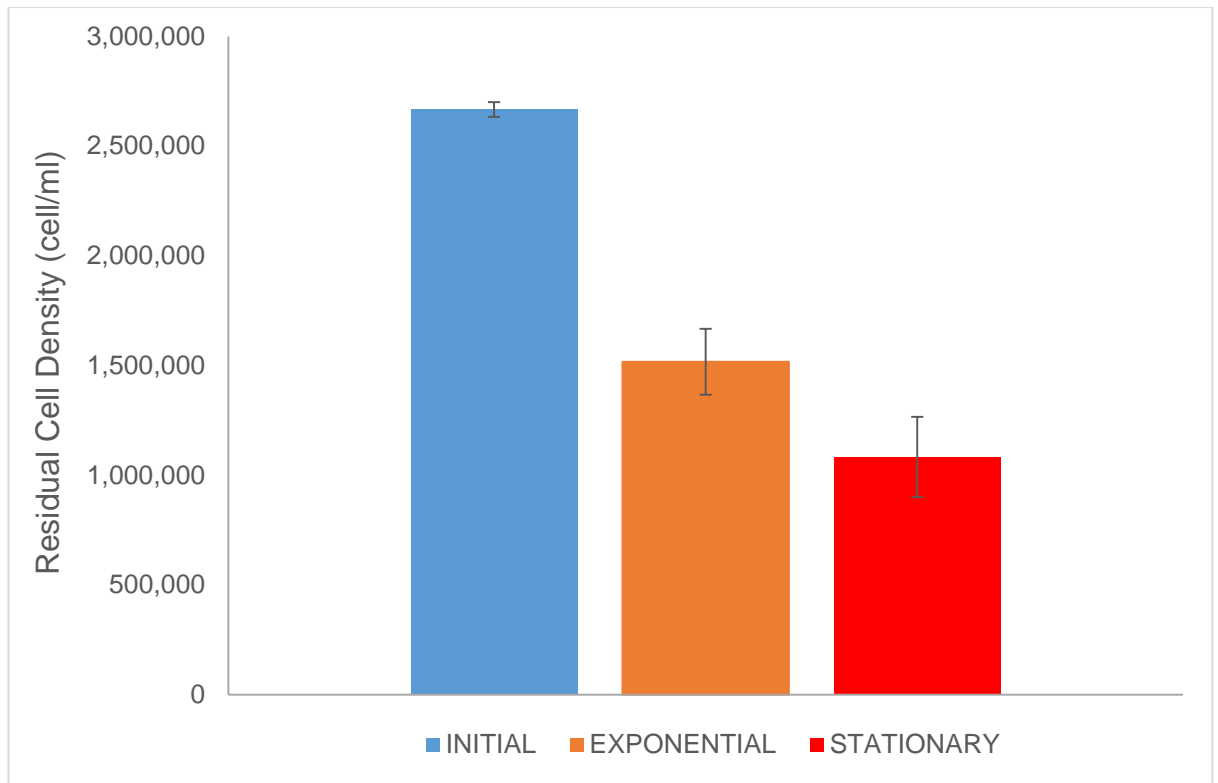


Figure 4:28: The residual cell density in the supernatant of a microalgae suspension at different growth stages after mixing with Nyex™ particles.

A reason for this observation might be related to what has been previously discussed in chapter 2 where cells in their exponential phase are more stable in suspension. This stability causes a shielding effect around the cells with the implication that their adsorption might be difficult. This is because cells with high electronegative ZP induce a net electronegative shield around one another, thus leading to huge repulsion between the cells on one hand, and between the cells and the adsorbent on the other hand. Meanwhile, for cells adsorbed in the stationary phase, such cells are less stable due to lower ZP, thus favouring the adsorption of cells.

In the same vein, cell sizes in the exponential phase are smaller in comparison to those in stationary phase. Danquah *et al.* (2009) revealed that during the exponential phase, the average particle size of mixed culture of *Tetraselmis suecica/Chlorococum sp.* cell was 4.1µm while during the stationary phase, the average particle size increased to 5.5 µm. In agreement with Danquah *et al.* (2009), a study reported a similar increase in the cell sizes of *Ettlia texensis*. The authors attributed the size increase to attractive van der Waals forces, which causes the cells to form larger flocs at a lower electronegative ZP (Salim *et al.* 2013).

For an adsorption process, larger particle cells indicate a higher probability of collision and/or interaction between the microalgae cells and Nyex™ particles. On the contrary, the smaller cell size in the exponential phase may not be favourable to cell adsorption due to less likelihood of contact between the cells and the adsorbent particles during agitation. Moreover, the reduced repulsive electrostatic forces, in the stationary phase, between the cells and the adsorbent particles can enhance a better interaction. These findings suggest the significance of monitoring the growth of cells, to ensure that cells are harvested during their stationary phase. For biofuel applications, it is an additional advantage as more lipids are accumulated during this phase which makes it a more favourable period to recover microalgae cells from suspension (Pragya *et al.*, 2013).

4.2.3 Effect of pH on the recovery of microalgae cells using Adsorption

The pH of the media has been reported to influence the flocculation and/or adsorption of colloids and/or microalgae cells from suspension (Yahi *et al.* 1994; Uduman *et al.* 2010; Wu *et al.* 2012; Olu-Owolabi *et al.* 2012; Barros *et al.* 2015). Figure 4.29 shows the variation in the percentage recovery of cells recovered when the pH of the media was altered. The behaviour of adsorption of cells onto the adsorbent, as evident in the graph, shows that at a very acidic pH of 3, about 99% of the cells were recovered onto the adsorbent. A further increase of the pH within the acidic range, at pH 4 and 5, led to nearly a 13% and 18% decrease in the amount of cells recovered respectively. As the suspension becomes neutral (pH 7), a further reduction in recovery to 74% was estimated, which remained constant as the suspension tended towards becoming alkaline (pH 7.7). Surprisingly, further increases in the pH showed a marked improvement in the amount of cells recovered. The percentage recovery at pH 9 - 11 was of the same magnitude to what was estimated for cell recovery in the acidic media (pH 4 - 5). Even though, the recovery appears to tend towards remaining constant after pH 9 as evident in figure 4.29.

Previous studies that have investigated the influence of suspension pH on the recovery of microalgae cells using adsorption do not report consistent outcomes. For instance, Xu *et al.* (2011) reported that an increase in pH (from acidic to alkaline) resulted in a “consistent” decrease in the recovery of cells (*Botryococcus brauni*); a similar trend was reported by another study for cyanobacterial *Microcystis*

aeruginosa (Li *et al.*, 2009; Xu *et al.*, 2011). On the contrary, Hu *et al.* (2013) reported, for *Nannochloropsis maritima*, an initial decrease in the percentage recovery when pH increased in the acidic range but recovery was enhanced when the pH increased in the alkaline range; similar to figure 4.4 below. Curiously, in the same study reported by Xu *et al.* (2011), for cell strain *Chlorella ellipsoidea*, recovery was enhanced when the pH increased in the acidic environment peaking at pH 7. An increase in pH in the alkaline range decreased the percentage recovery of the cells. Regrettably, these studies failed to provide reason(s) for this behavioural trend in the results they reported.

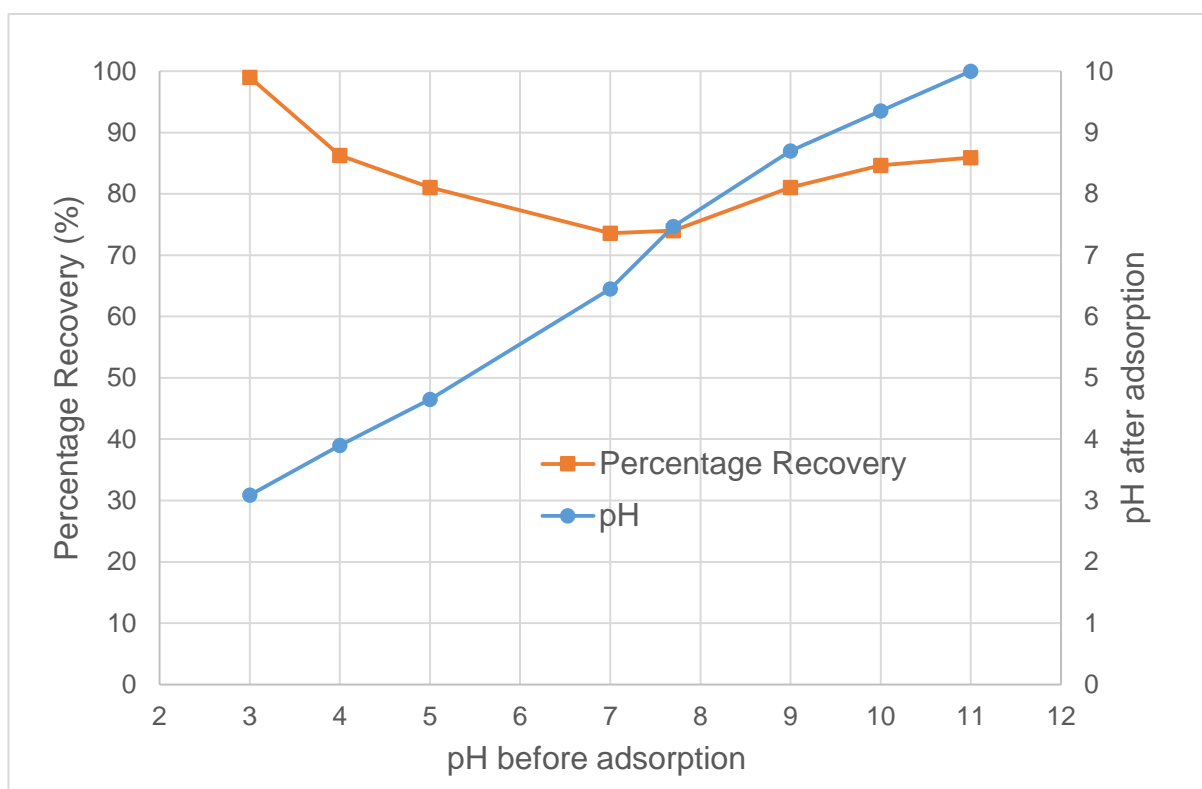


Figure 4:29: The percentage recovery and pH of suspension after mixing with Nyex™ at various suspension pH.

Another observation evident in figure 4.29, which has not been previously reported was that the suspension pH before and after the adsorption procedure differs. Except at pH 3, where the pH slightly increased to 3.09, the pH decreased after adsorption for others. As the initial suspension pH increased, the reduction in suspension pH after adsorption becomes more evident. This was more remarkable at pH 11, where the pH reduced to 10 after adsorption.

In addition, figure 4.30 shows the tubes after the adsorption procedure. As perceived from the image, the supernatant of the suspension at pH 3 after adsorption was

clearer than for the others. As the suspension pH increases, the turbidity of the suspension increases. The following reasons may be put forward for this observation; firstly, it could be that fewer cells were being recovered from suspension as the pH increases. This would negate the results presented in figure 4.29. Alternatively, Nyex™ particles/fines may have a better settling characteristics at lower pH such that the unsettled fines are responsible for the increased turbidity of the suspension at elevated pH.

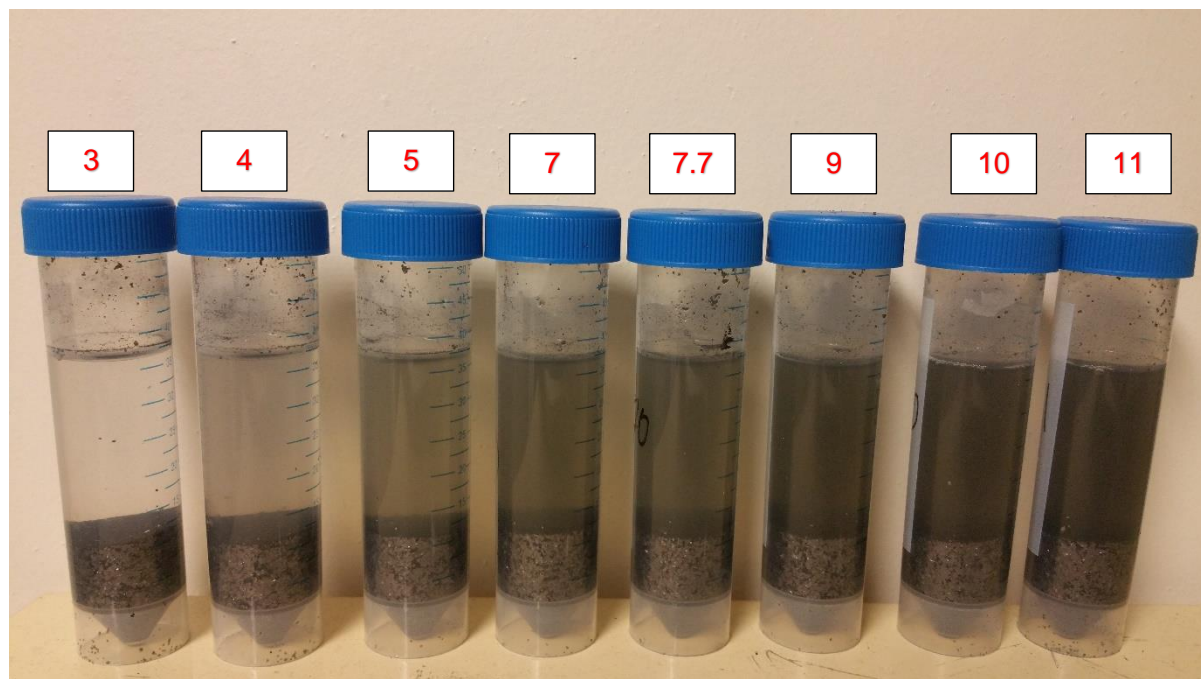
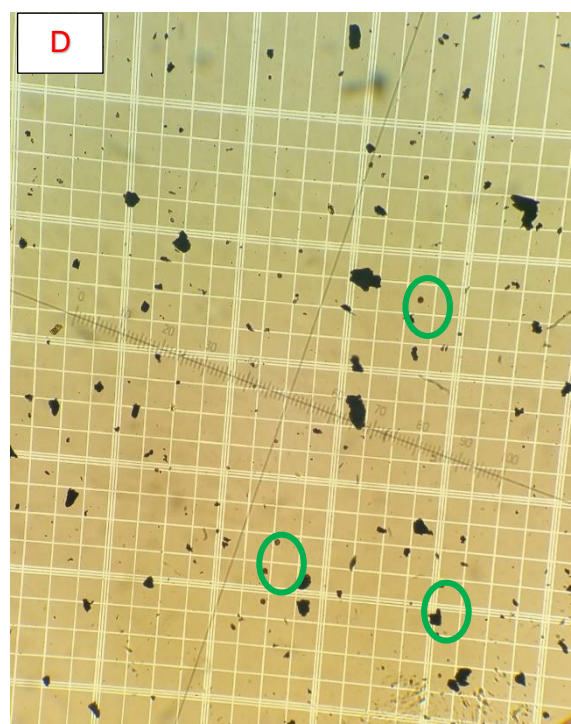
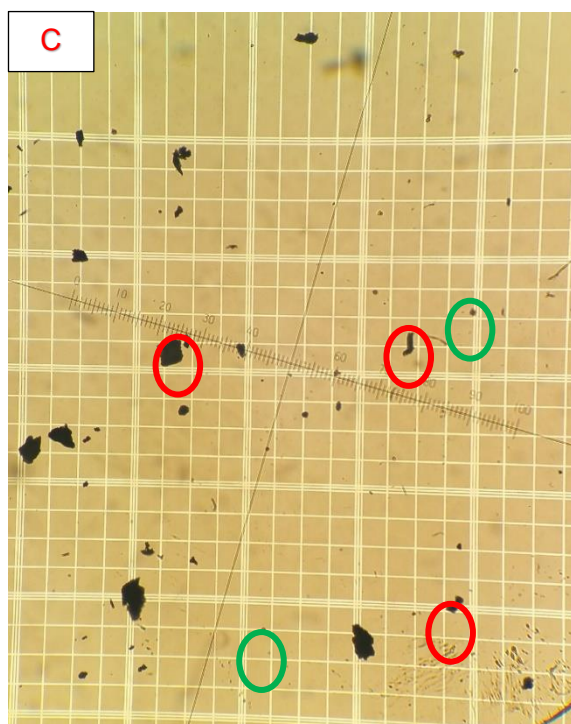
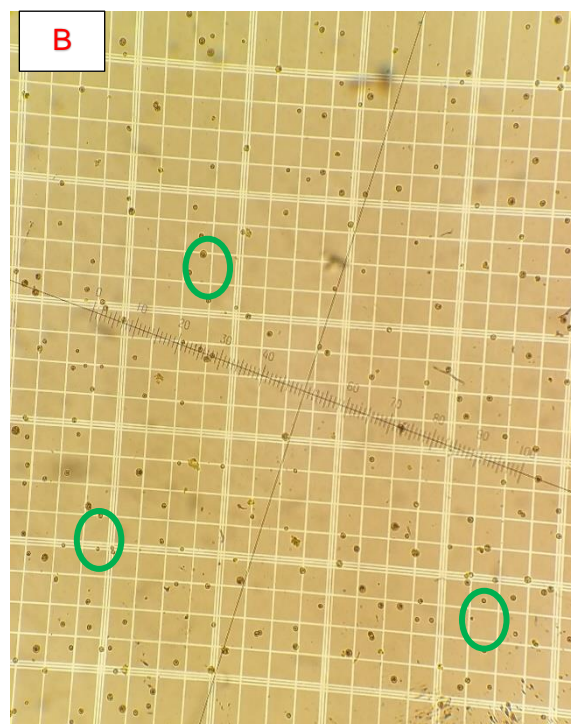
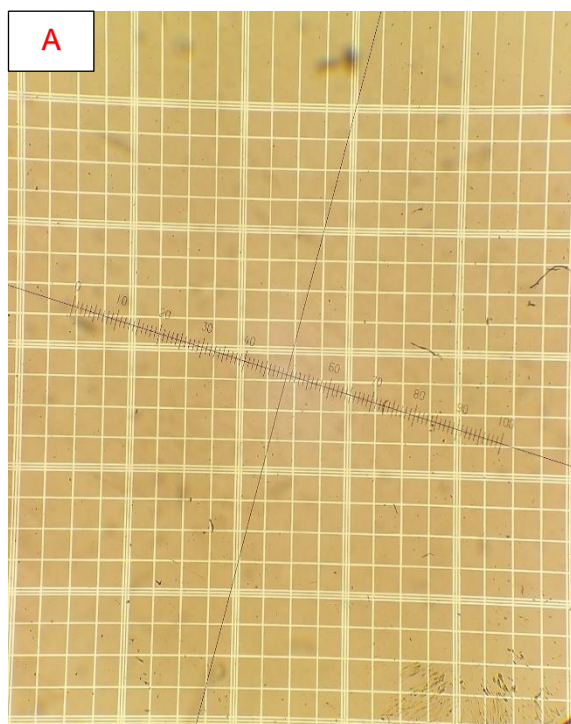
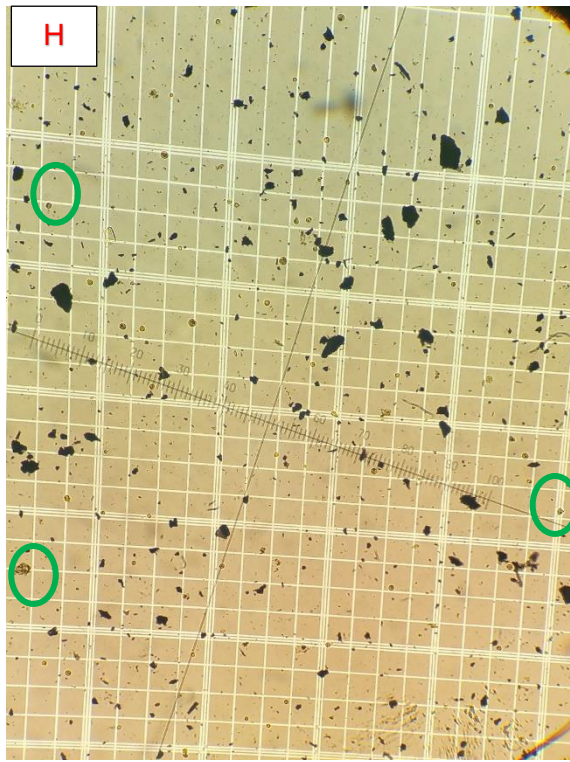
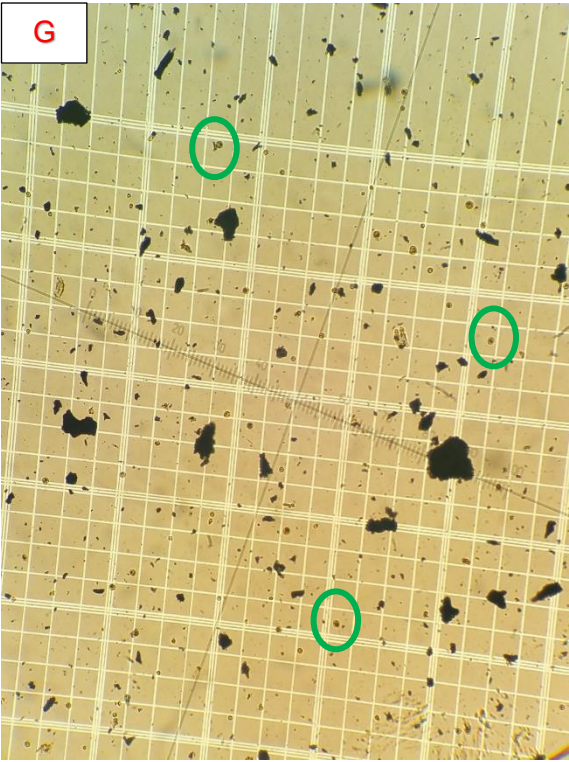
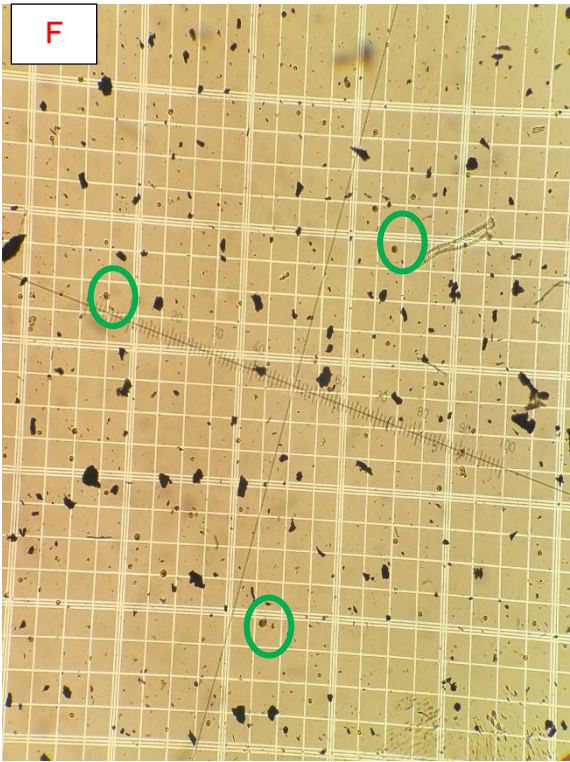


Figure 4:30: The mixture of microalgae cells suspension and Nyex™ after adsorption at different suspension pH is left to settle for 60 minutes. From left to right, suspension pH varies from 3 – 11.

To verify/disprove these two claims, samples of the mixtures from figure 4.30, were taken and pipetted on a haemocytometer. The latter was observed under a light inverted microscope at a 100x magnification. As evident in figures 4.6 (A – J), the increasing turbidity observed in figure 4.30, was very likely linked to the presence of Nyex™ particles. The latter covered more of the haemocytometer as the suspension pH increased. Expectedly, as manifest in figures 4.31 (C - J), some microalgae cells were present in all the suspensions, but their quantity could not significantly have affected the turbidity of the resulting supernatant. Hence, it seems the settling rate of the Nyex™ particles was considerably affected as the suspension pH increased.





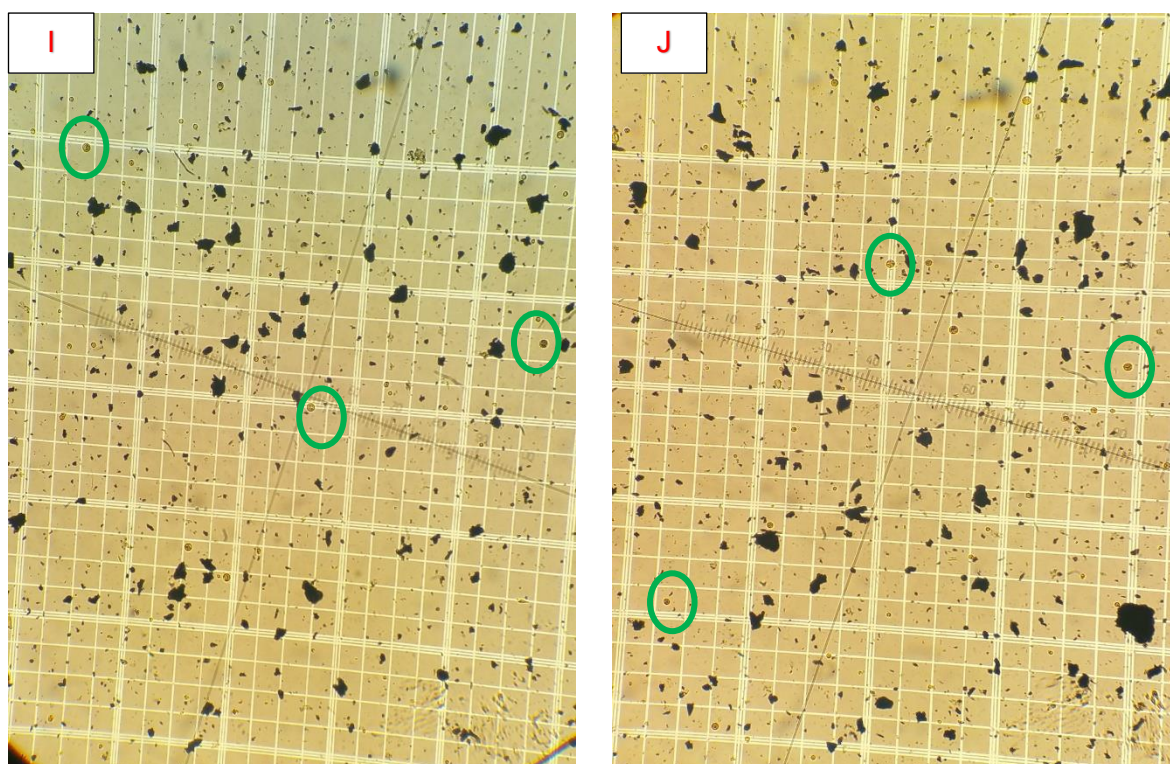




Figure 4:31: microscopic images of a mixture of microalgae cells  and NyexTM particles  after adsorption and a settlement time of 30 minutes for (A) blank haemocytometer, and cell suspension (B) without NyexTM (C) at pH 3 (D) at pH 4 (E) at pH 5 (F) at pH 7 (G) at pH 7.7 (H) at pH 9 (I) at pH 10 and (J) at pH 11.

As a consequence of these observations, the adsorbent pH was investigated. Figure 4.32 reveals that on introducing the adsorbent into deionised water, the pH of the mixture reduced instantly. The acidity characteristics of NyexTM became apparent such that regardless of the intensity of agitation, the pH of the mixture remained at about 3.8. The latter justifies the reason for the slight increase in the suspension media from pH 3 to 3.09 and the decreases observed for other suspension pH after adsorption as portrayed in figure 4.29. This finding appears to lend credence to the deduction that NyexTM is inherently acidic. Nkrumah-Amaoko *et al.* (2014) reported the presence of acidic oxygen containing functional groups such as carboxylics, lactones and quinones on the surface of fresh NyexTM. These functional groups seem to dominate the adsorbent surface and are considered to be responsible for the acidic nature of NyexTM particles. At elevated pH, the likelihood of the surface charge of the NyexTM particles being reversed is greatly increased. Therefore, enhancing the stability of NyexTM particles in suspension as evident in figures 4.31 (C - J).

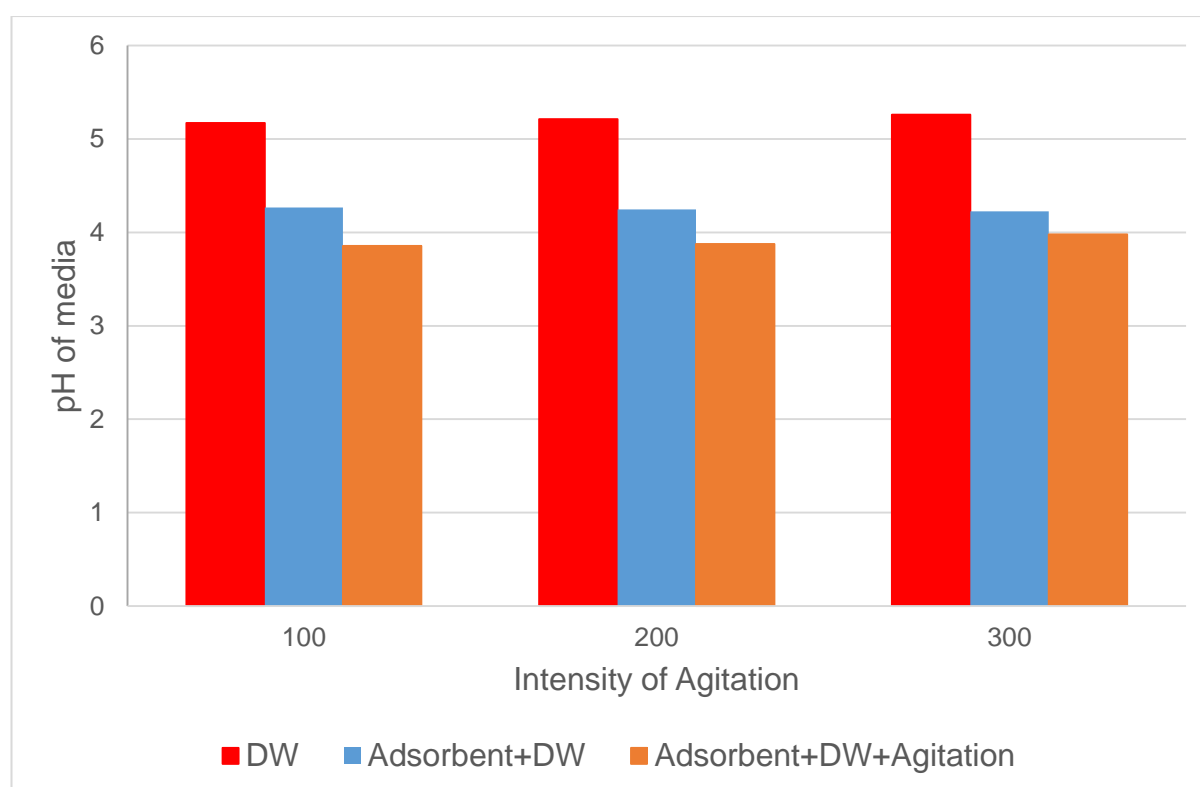


Figure 4:32: Acidic properties of Nyex™ particles in deionised Water (DW) showing variation in media pH when the adsorbent is added to deionised water (DW), before (■) and after (■) mixing at different intensities of agitation.

4.2.4 Proposed Mechanisms for Cell Recovery from Suspension

4.2.4.1 Influence of Nyex™ particles acidity

As shown in Figure 4.33, cells agitated in the absence of Nyex™ particles, expectedly, were not recovered from the suspension. However, cells that were left in the tubes in a vertical position in the absence of Nyex™ and without any form of agitation, were “recovered” from suspension. Those cells appear to have settled after 30 minutes and account for about 20% of total cells in suspension. When the adsorbent particles were added to the suspension, at least 45% of the cells were recovered despite the absence of any form mixing. This observation suggests two possible scenarios;

- (i) that the adsorption of the cells was so rapid that attachment took place at the point of contact and/or
- (ii) the acidic properties of Nyex™ particles introduces hydrogen ions into suspension thereby destabilising the cells to form larger cells as flocs,

which then settle (Tenney *et al.*, 1969; Shelef *et al.*, 1984; Sukenik *et al.*, 1988; Borowitzka, 1992; Vandamme *et al.*, 2013; Wan *et al.*, 2015).

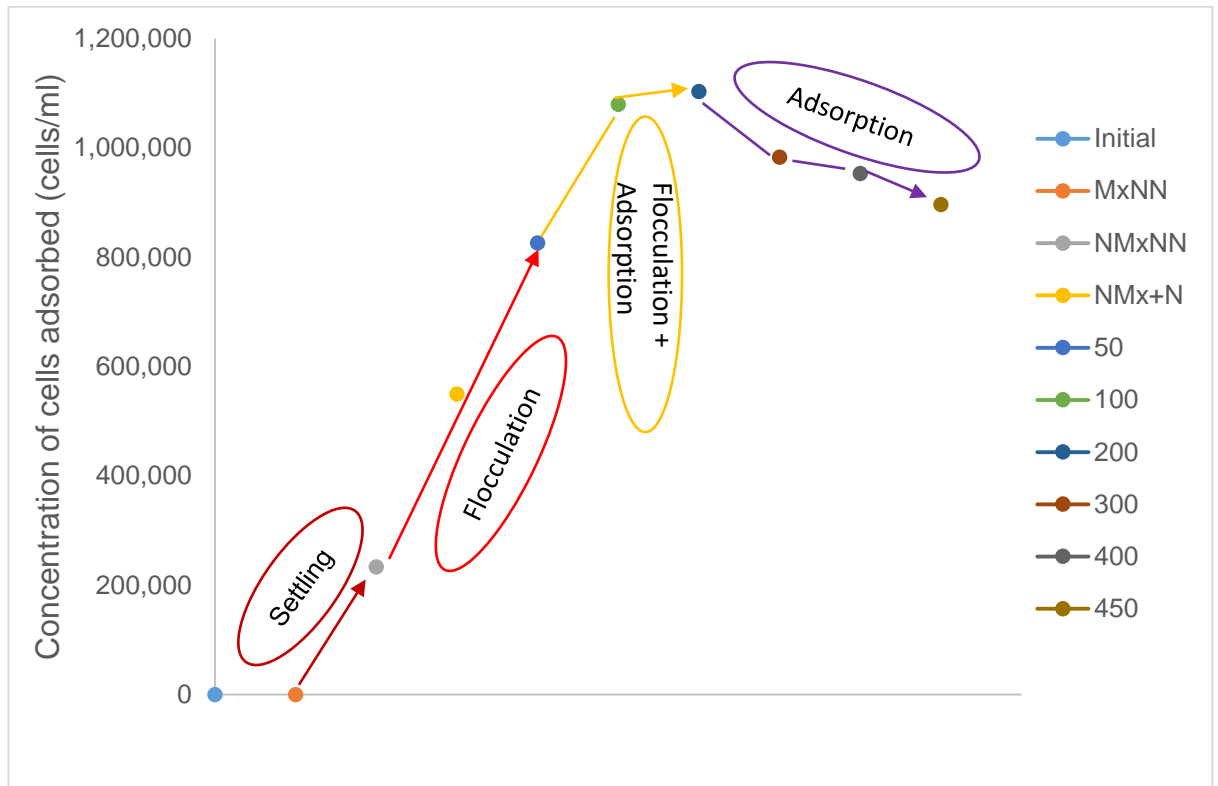


Figure 4:33: The concentration of cells adsorbed after a measured mass of Nyex™ was mixed with microalgae cells suspension at different intensities of agitation. Controls include: MxNN - Mixing, No Adsorbent; NMxNN - No Mixing, No Adsorbent; NMx+N-No Mixing, Adsorbent present.

Similarly, at an intensity of 50 rpm, most the adsorbent particles were observed, lying at the bottom of the cylindrical tube, rather than fluidised with the cells in suspension. Yet, recovery efficiency of the cells was 73%. A possible reason for this may be as discussed in (ii) above; where the presence of hydrogen ions (from Nyex™ particles) leads to reduction in the net negative charges of the cells enabling floc formation. The increase noticed in cell adsorption at 50 rpm, in comparison to when the mixture was not agitated (NMx+N), could be due to the gentle intensity of agitation. The latter can encourage cells to form larger flocs which then “settle” onto the adsorbent akin to jar test studies (Asrafuzzaman *et al.*, 2011).

At intensities from 100 – 200rpm, when the agitation improved the uniform distribution of Nyex™ particles in suspension, both adsorption and flocculation could be taking place. This is because the adsorbent particles were completely fluidised,

so that any flocs formed would easily come in contact with the adsorbent, which enhanced the recovery of cells to peak at 97%. However, at higher intensities, 300 – 400 rpm, the amount of cells adsorbed reduced by nearly 20% in comparison with the peak at 200 rpm. One reason for this observation was discussed in section 4.1, which has to do with elution of cells. In addition, the flocs being formed could be broken up in such a high mixing regime, thus, recovery of cells would mainly occur because of cells adsorption. This might explain the reason for the recovery of fewer cells at these elevated mixing intensities.

4.2.4.2 Influence of Media pH and Isoelectric point

To shed more light on the mechanisms governing cell adsorption, the zeta potential (ZP) of *Chlamydomonas reinhardtii* against various pH was measured and is shown in figure 4.34. The isoelectric point (IEP) of a particle is the pH at which the ZP is zero; an indication that the net surface charge on the particles is zero. When the $\text{pH}_{\text{media}} < \text{IEP}$, the particles in the media are positively charged but when the $\text{pH}_{\text{media}} > \text{IEP}$, the particles in the media are negatively charged as evident in Figure 4.34. This is because, in the case of microalgae cells, when they are in media with a low pH, their functional groups (see section 2.3.2) are protonated and the net surface charge is positive. In contrast, if the cells are in media with high pH, the functional groups are deprotonated, which result to a net negative surface charge. At the IEP, some groups are either protonated or deprotonated, thus resulting in a neutral surface charge (Dai, 1994; Newcombe and Drikas, 1997; Namasivayam and Kavitha, 2002; Al-Degs *et al.*, 2008; Hadjoudja *et al.*, 2010; Gonçalves *et al.*, 2015).

From figure 4.34, the IEP of the *Chlamydomonas reinhardtii* was estimated to be *circa* pH 2.8, which correlates within the pH range that has been reported for the IEP of microalgae cells (Henderson *et al.*, 2008b; Hadjoudja *et al.*, 2010; Gonçalves *et al.*, 2015). Furthermore, a previous study has reported the IEP of NyexTM particles to be at pH 5 (Asghar *et al.*, 2012). If adsorption is largely due to electrostatic forces of attraction between opposite charges, then the high recovery efficiency observed for the suspension medium at pH 3 in figure 4.29 is explicable. At pH 3, as shown in figure 4.34, *C. reinhardtii* is less electronegative and the NyexTM particles will be electropositive ($\text{pH}_{\text{media}} < \text{IEP of Nyex}^{\text{TM}}$), so that the electrostatic forces of attraction overcome the electrostatics forces of repulsion to enhance cell adsorption. As the

pH increases, so does the electronegativity, as evident in figure 4.34, which therefore explains the reasons for fewer cells being adsorbed (see figure 4.29).

However, beyond a suspension pH of 7.7, cell adsorption recovery was enhanced despite continued electronegativity increases in the ZP for both cells and Nyex™ particles. As previously discussed and “validated” in figure 4.29, cell recovery at suspension pH 9 – 11 should be negatively impacted. It is evident that in addition to the electrostatic forces of attraction, other mechanisms are responsible for cell adsorption onto the Nyex™ particles. This then begs the question, what could be responsible for the adsorption of microalgae cells in the elevated pH range?

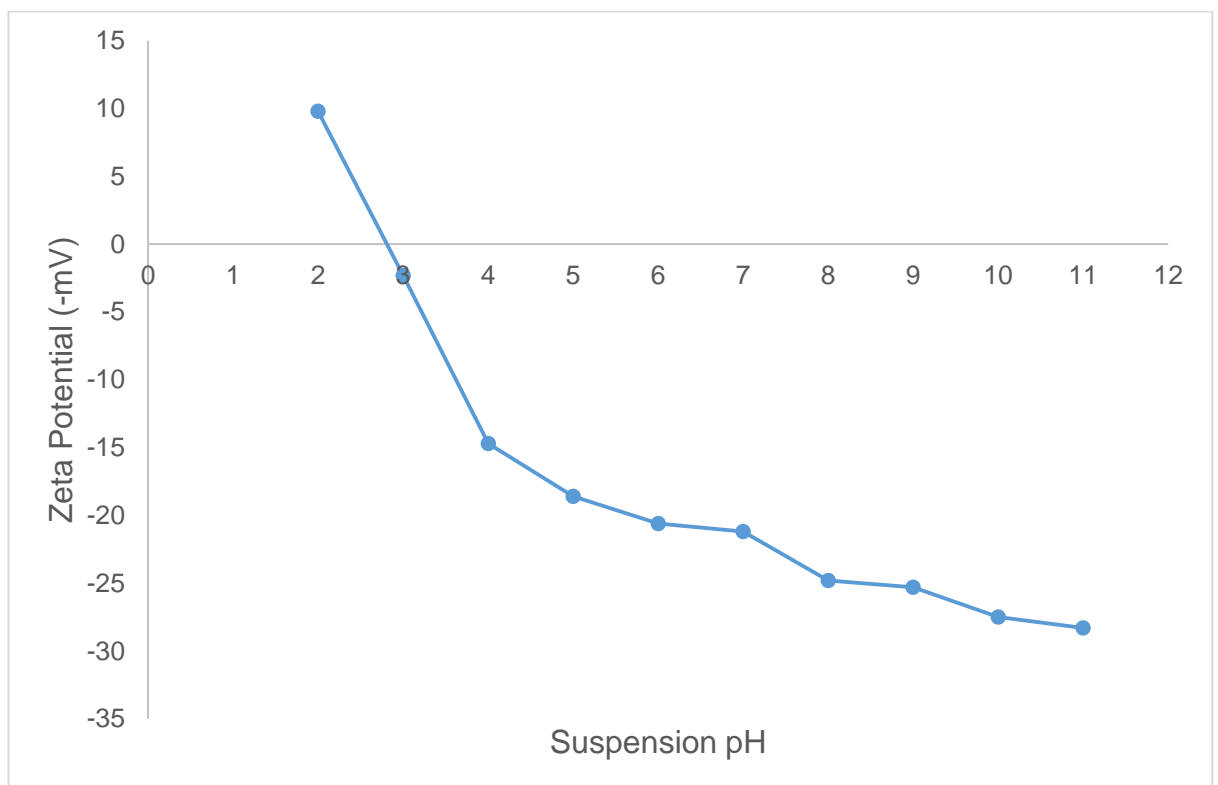


Figure 4:34: Zeta potential of *C. reinhardtii* at various suspension pH.

4.2.4.3 Hydrophobicity of Microalgae cells and Nyex™ particles

Henderson *et al.* (2008a) reported that the proteins present in the membrane of microalgae cells induce some hydrophobicity on the surface of the cells. Likewise, Nyex™ particles are flakes known to comprise graphite basal planes and broken edges. The latter are considered to be hydrophilic due to the dense presence of acidic functional groups at their surface. Conversely, the graphite basal plane is thought to be hydrophobic largely due to sparse availability of those functionalised acidic groups. The flake structure of Nyex™ particles implies an aspect ratio with a

small surface area of hydrophilic broken edges and a large surface area of hydrophobic graphite basal plane. In view of this, the NyexTM is predominantly considered to be hydrophobic (Conti-Ramsden *et al.*, 2013).

Hence, at elevated pH, when the functional groups are deprotonated, the hydrophobic interaction between the hydrophobic parts of the NyexTM particles and those of the microalgae cells is believed to be predominant. As a consequence, this governs the recovery of cells from suspension onto the NyexTM particles. The preferential adsorption by NyexTM particles for hydrophobic organic compounds in the presence of hydrophilic compounds has been previously reported (Conti-Ramsden *et al.*, 2013; Brown *et al.*, 2013). Furthermore, the hydrophobic characteristics of the membrane/walls of microbial cells has been cited as a reason for the attachment of microorganisms to wettable solid surfaces (Rosenberg *et al.*, 1980; Rosenberg and Kjelleberg, 1986; Van Loosdrecht *et al.*, 1987).

The hydrophobic characteristics of microalgae cells and NyexTM particles may also offer reasons why the Freundlich isotherm was a better fit for the experimental data. At high concentrations of the cells, hydrophobic – hydrophobic interactions between the cells is also highly favoured (Ozkan and Berberoglu, 2013). This explains the reason behind the aggregation of cells sometimes noticed at high cell concentrations. As a consequence, multi-layer adsorption of the cells onto the adsorbent is encouraged, so that the Langmuir isotherm is inadequate to predict equilibrium data at high concentrations of the microalgae cells.

4.2.4.4 Other possible mechanisms

Likewise, hydrogen bonding can occur between the carbonyl groups of the NyexTM particles and the amino groups on the surface of the microalgae cells. A number of studies have also reported that interaction between the π electrons of the graphitic surface of the adsorbent and the aromatic carbon of the adsorbate can aid adsorption (Tenney *et al.*, 1969; Newcombe and Drikas, 1997).

In addition, Hu *et al* (2013) suggested that at elevated alkaline pH conditions, the hydraulic diameter of microalgae cell aggregates increased significantly. As a result, better cell recovery efficiency could be attained. Co-incidentally, a similar observation was noted in the research reported in this thesis. As shown in figure 4.35, cells in a suspension medium at pH 11 sediment easily (red oval). This may

be due to the increased hydraulic diameter of the cells which aids the settling of the cell aggregates. Although, sufficient time was not allowed to observe the settling pattern of other suspension pH, this is a further evidence that a number of mechanisms govern the adsorption of cells. Depending on the suspension conditions, it is possible that a combination of these mechanisms or one specific mechanism dominates the cell adsorption process.

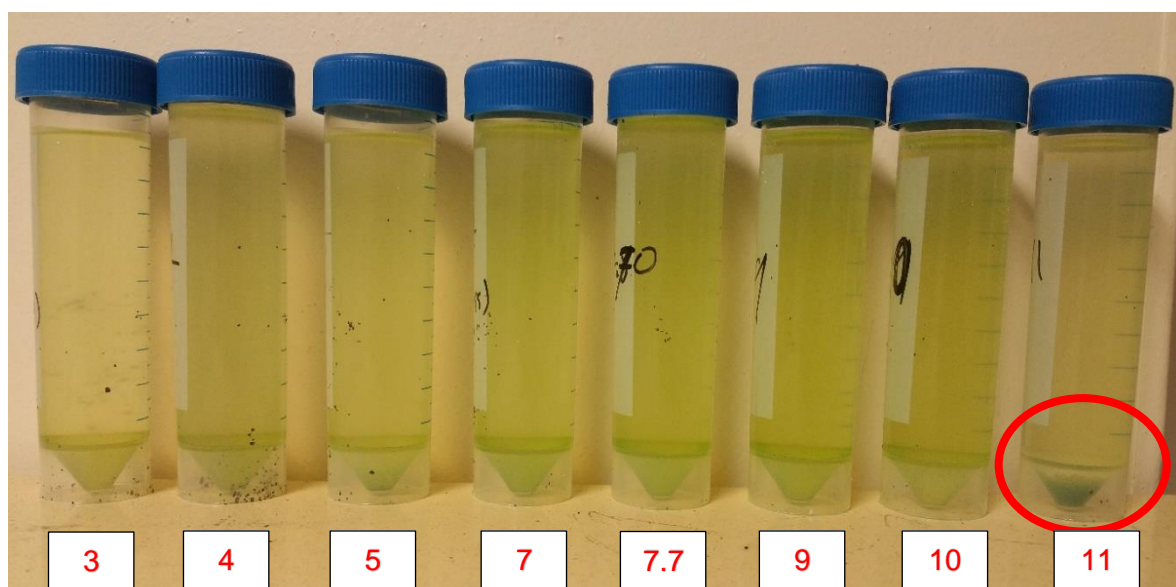


Figure 4:35: Changes in the suspension of microalgae cells at various pH where suspension medium at pH 11 had more cells sediment. The red oval shows cell flocculation and sedimentation.

4.2.5 Summary

This section provides an insight into a number of mechanisms driving the recovery of microalgae cells from suspension onto Nyex™ particles. The behaviour of cells as colloidal particles when in suspension suggests that conditions such media pH and zeta potential can influence cell recovery using adsorption. What is also interesting is how the zeta potential is affected by the growth characteristics of the cells on one hand, while the zeta potential affects cell aggregation and size on the other hand.

For the first time, the acidic characteristics of the Nyex™ particles, in addition to the growth characteristics of cells, was found to influence adsorption. The mechanisms governing adsorption were discovered to vary from flocculation of cells to the hydrophobic nature of the cells and the Nyex™ particles. Such that it is possible to have one and/or a combination of those mechanisms simultaneously driving the

recovery of cells from suspension. This phenomenon is believed to depend on a number of factors such as media and adsorbent pH, the isoelectric point of cells and Nyex™ particles and the intensity of agitation. Remarkably, the recovery of cells was found to be relatively high (at least 73%) regardless of the medium pH. The significance of such good recovery demonstrates the robustness of adsorption as a recovery technique for microalgae cells.

4.3 Adsorption Column Studies of Microalgae Cells Recovery

4.3.1 Introduction

Adsorption studies in a fixed bed column are essential to predict column breakthrough and exhaustion, which helps in understanding the operational duration of the bed. Fixed bed columns can function singly either in a parallel or series mode of operation. The suspension to be treated can be applied from the bottom and withdrawn from the top in upward flow and vice versa for downward flow (Goel *et al.*, 2005; Karunarathne and Amarasinghe, 2013).

A number of factors that can influence the performance of a column includes but are not limited to (McKay, 1995; Hammer, 2008; Pastrana-Martínez *et al.*, 2010; Canteli *et al.*, 2014);

- Effect of flow rate
- Effect of bed height
- Upward or Downward mode of operation
- Effect of submerged bed

While adsorption studies in a batch process are important, column studies give information which can be useful for scale up to a continuous industrial system. Besides, the challenges faced in the research reported in this thesis (see section 4.1), requires that the recovery of microalgae cells in a fixed-bed column be examined. This section aims to demonstrate the effectiveness or otherwise of a fixed bed column to recover microalgae cells from suspension.

4.3.2 Effect of Flow Rate

The fixed bed column was operated at different feed flowrates of 5, 10 and 40 mL/min to investigate the effect on cell recovery. As manifest in figure 4.36, the bed performed best at the lowest flowrate of 5 mL/min; at higher flowrates, the breakthrough curve was steeper. As expected, the breakthrough and exhaustion times were attained faster, as the flowrate increased from 5 to 40 mL/min. For instance, the exhaustion time was reduced from 250 min to 40 min when the flow rate was increased from 5 to 10 mL/min. In the same vein, the exhaustion time decreased to 8 min when the flowrate was increased to 40 mL/min. Similar decreases in the breakthrough times were observed when the feed flowrate was increased from 5 to 40 mL/min. In fact, the breakthrough for flowrates at 40 mL/min was at 2 min; almost at the instant of the first drops of the effluent. This suggests that an inverse relationship exists between the initial feed flowrate and the breakthrough and exhaustion times.

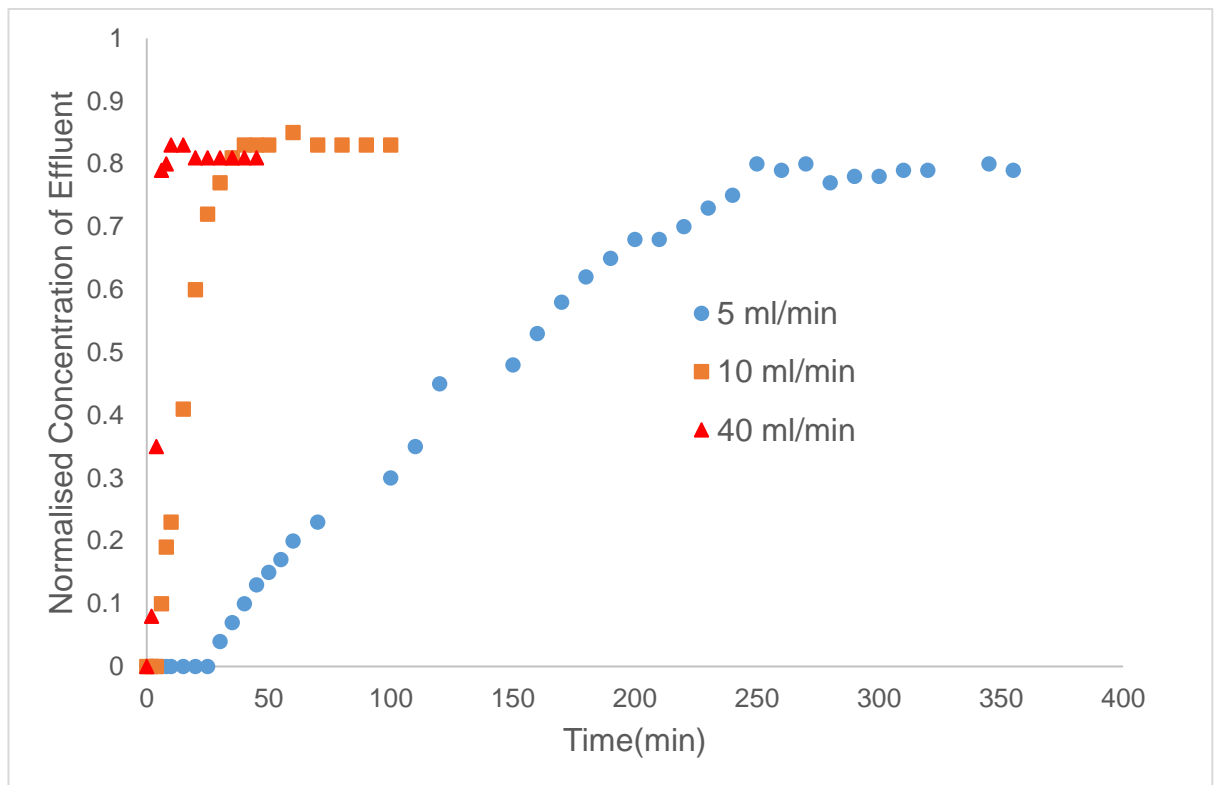


Figure 4.36: Breakthrough curves for the recovery of cells using Nyex™ particles at various flowrates with conditions ($Q = 5, 10, 40$ mL/min, $h = 20$ cm, $C_o = 0.2$ OD).

These observations can be attributed to the decrease in the residence time, thereby limiting the contact of cells with the Nyex™ particles due to an increase in the

flowrates. As the cells transfer from bulk solution to the film surface surrounding the Nyex™ particles, a concentration gradient develops at the interface, thereby allowing the cells to penetrate through the film, and reach the Nyex™ surface. At high flow velocities, the film surrounding the adsorbent particles breaks, thus decreasing the adhesive capacity of the cells to the Nyex™ surface. These observations are consistent with studies reported on the removal of adsorbable particles within a fixed-bed column (Vadivelan and Kumar, 2005; Kundu and Gupta, 2007; Canteli *et al.*, 2014)

4.3.3 Effect of Bed Depth

Three bed heights of 5, 10, 20 cm were used for the purpose of examining the effect on cell recovery. As shown in figure 4.37, the breakthrough times varied with bed height. Steeper breakthrough curves were observed as bed depth decreased, although this was more evident when bed height decreased from 20 cm to 10 or 5 cm. Moreover, the breakthrough times decreased with a decrease in bed depth from 20cm to 10cm, from 30min to 6min respectively.

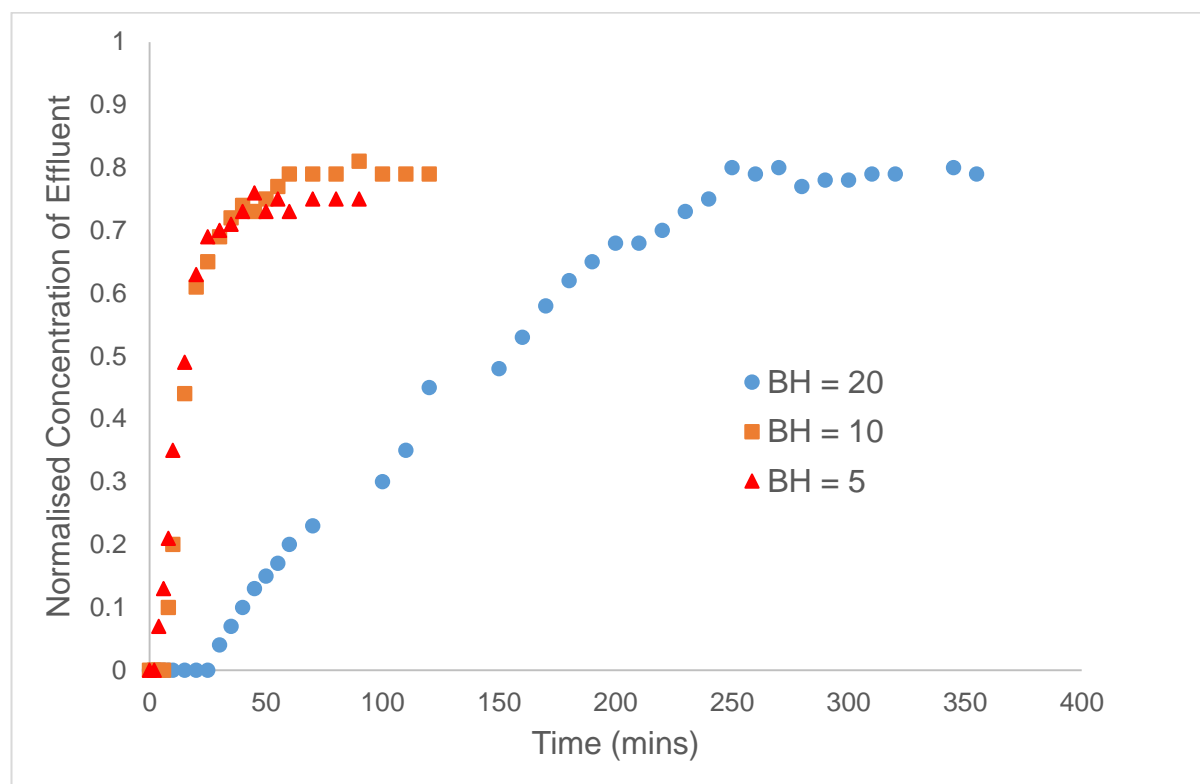


Figure 4:37: Breakthrough curves for the recovery of cells using Nyex™ particles for different bed heights at conditions ($h = 5, 10, 20$ cm, $C_0 = 0.2$ OD, $Q = 5$ mL/min).

At lower bed heights, the adsorbent particles get saturated quite quickly. This can be linked to restriction of the adsorption sites available as a result of lower bed depths. At low bed depth, the microalgae cells have less surface area to come in contact with, thereby leading to a reduction in breakthrough and exhaustion times. Conversely, an increase in bed height comes with an increase in the residence time of the cells as well as more surface area available for adsorption (Lehmann *et al.*, 2001; Yoshida *et al.*, 2004; Karunaratne and Amarasinghe, 2013).

4.3.4 Effect of the Initial Feed Concentration

The breakthrough curves of the column obtained by varying the initial suspension concentration are shown in Figure 4.38. The bed height was kept constant at 20 cm as was as the flow rate at 10 mL/min while the initial suspension concentration was varied between 0.1 and 0.4 OD.

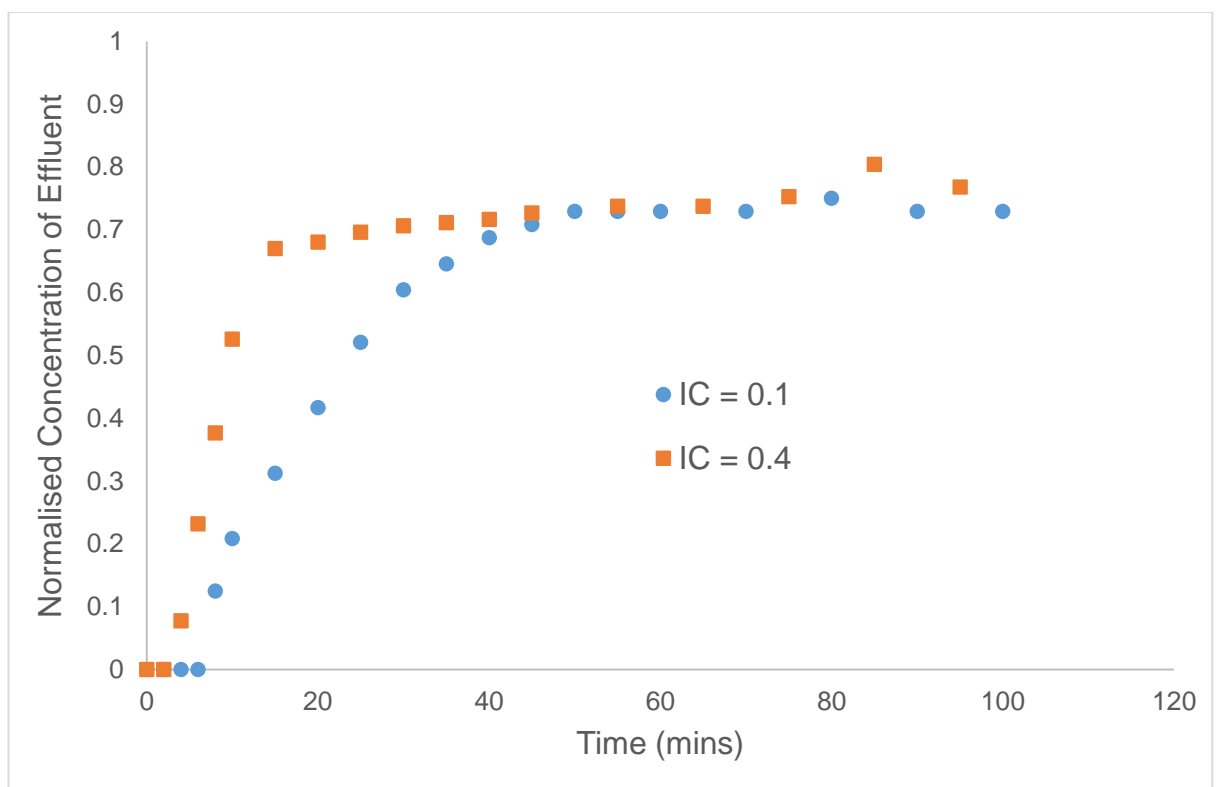


Figure 4:38: Breakthrough curves for cell recovery using Nyex™ particles at varying initial concentration (IC) with conditions ($C_0 = 0.1, 0.4$ OD, $Q = 10$ mL/min, $h = 20$ cm).

A decrease in the concentration resulted in an increase in the time required for breakthrough to occur. The volume of suspension treated was least for the highest concentration. This is due to an increase in the mass transfer coefficient. For

instance, at an initial concentration of 0.1 OD, the breakthrough and exhaustion times were at 8 min and 50 min respectively, while an increase to an initial suspension concentration of 0.4 OD decreased the breakthrough and exhaustion times to 4 min and 15 min respectively.

At a high initial concentration, the cells rapidly attach to the available adsorption sites, thus the bed becomes saturated quickly. As a consequence, the time required to attain breakthrough decreases. On the contrary, at a low initial concentration, the mass transfer coefficient is smaller, thereby leading to slower transport of microalgae cells to the available adsorption sites. Similar to other effects, an inverse relationship exists between the initial feed concentration to the column and the breakthrough and exhaustion times of the bed (Singh and Pant, 2006; Goel *et al.*, 2005; Kundu and Gupta, 2007; Crini and Badot, 2010).

4.3.5 Fixed-Bed Scenarios and Performance Comparison.

Column studies can hardly be carried out without understanding the effects of the flow rate, bed height and initial feed concentration. Whilst most studies rely on the breakthrough (and sometimes on exhaustion) times to evaluate the performance of the column for each effect, other parameters are often ignored which could shed further light on the bed performance. These parameters include but are not limited to the total amount of solute adsorbed, the capacity of the bed and the recovery efficiency of the bed. In addition, these parameters can also provide the opportunity to compare performance between different conditional 'effects'. For instance, performance comparison between an increased height and a decreased flow rate.

As shown in Table 4.3, for scenarios 'A' and 'B' where flow rates and initial cell concentration were equal but have different bed heights of 5 cm and 10 cm, the total cells adsorbed were 4.2 mg and 7.2 mg respectively. On the face of it, this seems to agree with what was discussed in section 4.3.2. However, the bed capacity was estimated to be 0.45 mg/g and 0.52 mg/g mg for the bed heights of 10 cm and 5 cm respectively. This shows that a lower bed height better utilises the adsorbent bed, though not as efficiently as a bed height of 20 cm (for scenario 'C') as shown in Table 4.3. However, in terms of efficiency to recover cells, bed heights of 5 cm and 20 cm performed equally well at a percentage recovery of 58% when compared to a bed height of 10 cm with 42% recovery. Yet again, the lower bed height was more

efficient in terms of percentage recovery and was as effective as a bed height of 20 cm. Even though the breakthrough times seem to suggest that the performance at bed height of 5 cm was the poorest, the amount of adsorption per gram of adsorbent was better at this height than at 10 cm.

Table 4.3: Comparison between column performances based on breakthrough times and other parameters such as percentage recovery and bed capacity.

	Flow Rate	Initial Cell Concentration	Bed Height	Break-through time	Percentage Recovery	Total Cells Adsorbed	Bed Capacity
	(mL/min)	(Absorbance at 680 nm)	(cm)	(min)	(%)	(mg)	(mg/g)
A	5	0.2	5	4	58	4.2	0.52
B	5	0.2	10	8	42	7.2	0.45
C	5	0.2	20	35	58	41.7	1.3
D	10	0.1	20	8	50	6.9	0.22
E	10	0.2	20	6	46	10.5	0.33
F	10	0.4	20	4	35	10.8	0.34
G	40	0.2	20	2	43	9.9	0.31

Similarly, for scenarios 'D' and 'F' where flow rates and bed height were equal but have different initial cell concentrations of 0.1 OD and 0.4 OD, the total cells adsorbed were 6.9 mg and 10.8 mg respectively. This is contrary to the conclusion derived from just considering the breakthrough times. However, in terms of cells recovered by percentage of the feed concentration, 50% and 35% recovery were attained for the initial cell concentrations of 0.1 OD and 0.4 OD respectively. In the same vein, when scenarios 'C', 'D', 'E', and 'F' are considered, they all have the same bed height, but different flow rates and initial cell concentrations. Table 4.3 shows the effects of doubling the flow rates (scenarios C and E), which reduces both the breakthrough time and total cells recovered.

These observations as discussed above signify how the flow rates, bed height and cell concentrations interact and influence the performance of the column system. This is because a high bed height with a low flow rate implies that the algae suspension has a high residence time. Thereby allowing more time for the algae suspension to be exposed to the adsorbent particles; thus leading to a better adsorption of the cells as evident in scenarios C, E and G. Also, the significance of considering total cells adsorbed and not just the breakthrough time is that, unlike most studies, there is still an interest to continuously adsorb more cells, even after breakthrough. The objective here is to recover as many cells as possible, hence, whilst breakthrough time is a necessary parameter, it does not seem to be sufficient to fully understand the bed performance with respect to cell recovery.

4.3.6 Performance Comparison of Upward and Downward Flows

Downward flow is commonly used to minimize the possibility of accumulating materials at the bottom of the bed. Furthermore, in upward mode, there is a tendency to fluidise and/or lift the bed even though the aim is to operate a fixed bed (Tchobanoglous *et al.*, 2003). However, one of the disadvantages of a downward flow bed is that channelling can occur. Air pockets within the bed and/or exposing the bed to the atmosphere could lead to channelling, thereby lowering the bed utilisation (Ko *et al.*, 2000). To minimise channelling, a film layer of water can be allowed at the top of the bed to prevent air from causing channels in the bed as previously described. Sometimes, the choice of which mode to use seems to depend on what a study “considers” to be better between the two flow modes. These two types of flow systems for microalgae cell recovery in a fixed bed have not been reported in the literature. Even for some other adsorbates, a number of studies held that both the flow modes would give the similar results (Crini and Badot, 2010). Hence, the two modes were investigated in this research with an objective to identifying which is either more suitable and/or effective in the recovery of cells. Figure 4.39 shows the resulting breakthrough curves for the upward and downward flow modes. The results revealed an interesting observation; the curve of the upward flow was atypical of the characteristic S-shape of a breakthrough curve as observed for the downward flow. As evident in the figure, the “breakthrough time” of the upward flow was at time 0 min. The breakthrough curve of the upward flow can be sub-divided into 3 main parts, viz;

- I. Breakthrough at time zero and an initial increase in the cells leaving the column up to 4/6 minutes,
- II. Hold up of cells in the bed up to about 40 minutes, and
- III. Rapid rise in the amount of cells leaving the column after 50 minutes.

Although based on some sampled studies reviewed in this thesis, the downward flow mode appears to be more common. Other studies that have reported the upward flow mode have not reported similar occurrences (Maji *et al.*, 2007; Basha and Culligan, 2010; Saadi *et al.*, 2013).

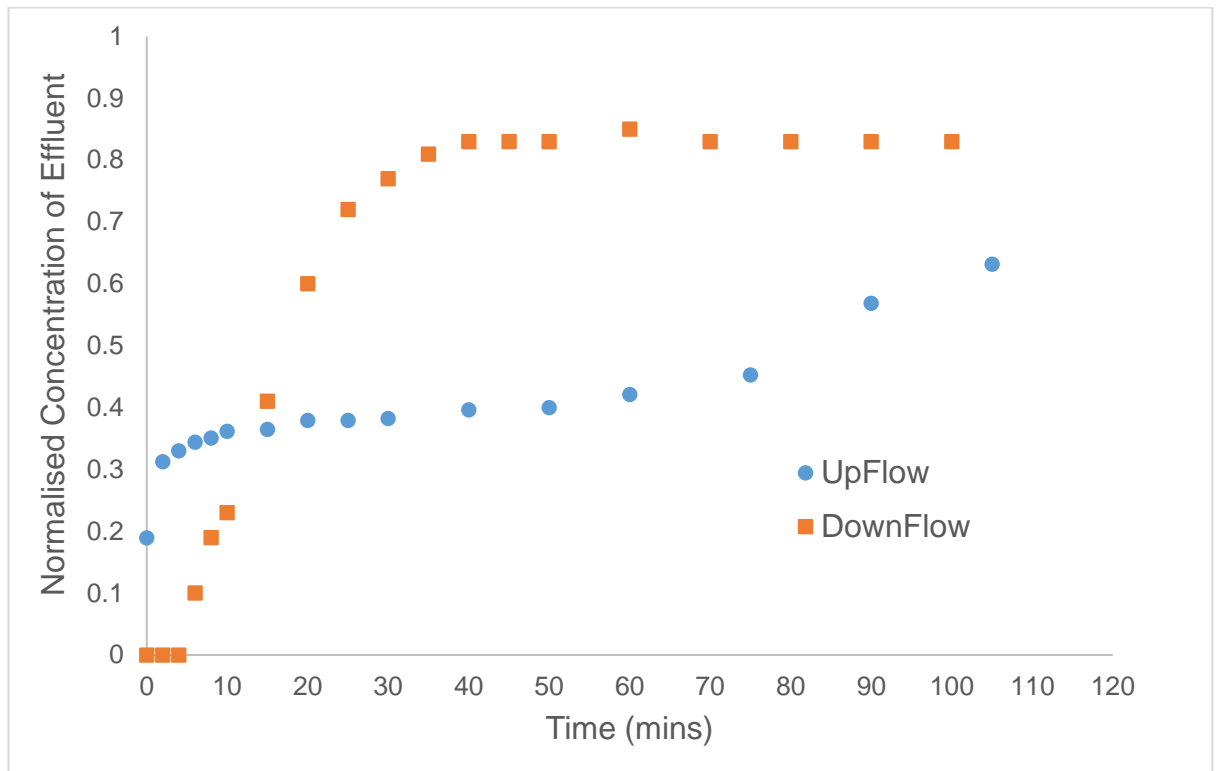


Figure 4:39: Breakthrough curve for cell recovery cells using Nyex™ at flow conditions ($h = 20$ cm, $C_0 = 0.3$ OD, $Q = 10$ mL/min) for upward and downward flow modes.

In fact, the upward flow mode seems to have “an inverse” characteristic S-shape of a breakthrough curve – imagine the normalised concentration of the effluent was the x-axis. The breakthrough curve observed for the upward flow above can be attributed to a number of reasons but may not be limited to;

- a. the presence of non-adsorbable compounds in the suspension, and
- b. the leakage of the microalgae cells due to the length of the mass transfer zone, L_{MTZ} , being greater than the bed height.

If either of the two reasons stated above were true, the same should have been observed for the downward flow as well; as those factors do not seem to be

influenced by the mode of flow. In addition, if it was due to (b) above, the shape of the BTC should have been exponential after the first few minutes up until the bed was exhausted. Rather what was observed as evident in figure 4.39 was that after 4 minutes, the breakthrough curve shows a bed that is tending towards exhaustion. For 20 minutes, the breakthrough curve was almost 'depressed', which appears to suggest that the bed column retains most of the cells. However, after 50 mins a rapid breakthrough of the cells was evident. However, a scrutiny of the bed column, for upward flow mode, showed that cells were either settling in the bed or forming "flocs" which then settle in the bed, as shown in figure 4.40.

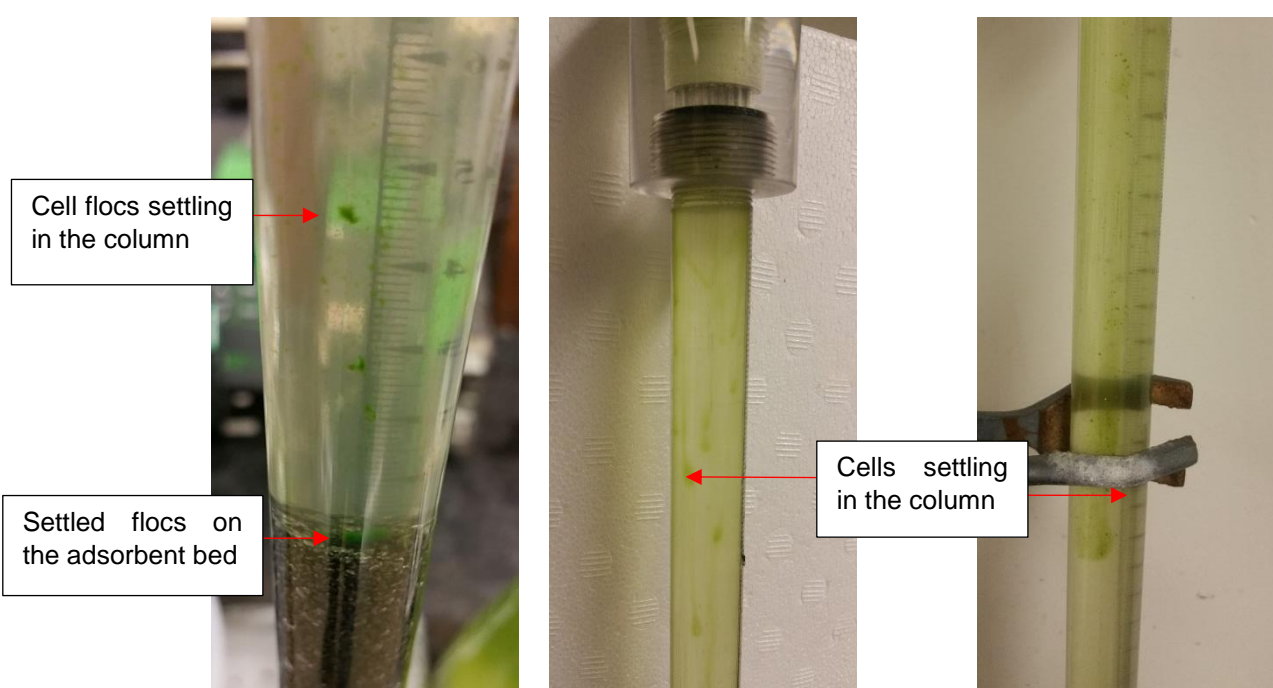


Figure 4:40: Pictorial image of floc formation, including cells and flocs settling in a bed for upward flow mode.

The exponential rise in the number of cells leaving the column, after 50 minutes, could be as a result of these flocs escaping the bed. In addition, it could also be due to one of the problems reported for upward flow mode; the accumulation of microalgae cells at the bottom of the bed which then seep through the bed at some point as more suspension flows through. While the latter might offer an explanation for the observations of the (II) and (III) aspect of the breakthrough curve, the reason for (I) remains unclear. Furthermore, as noted in some studies, operating a bed column could result in the fixed bed being lifted. In some instances, the Nyex™ bed was lifted when operated in upward flow as depicted in figure 4.41.

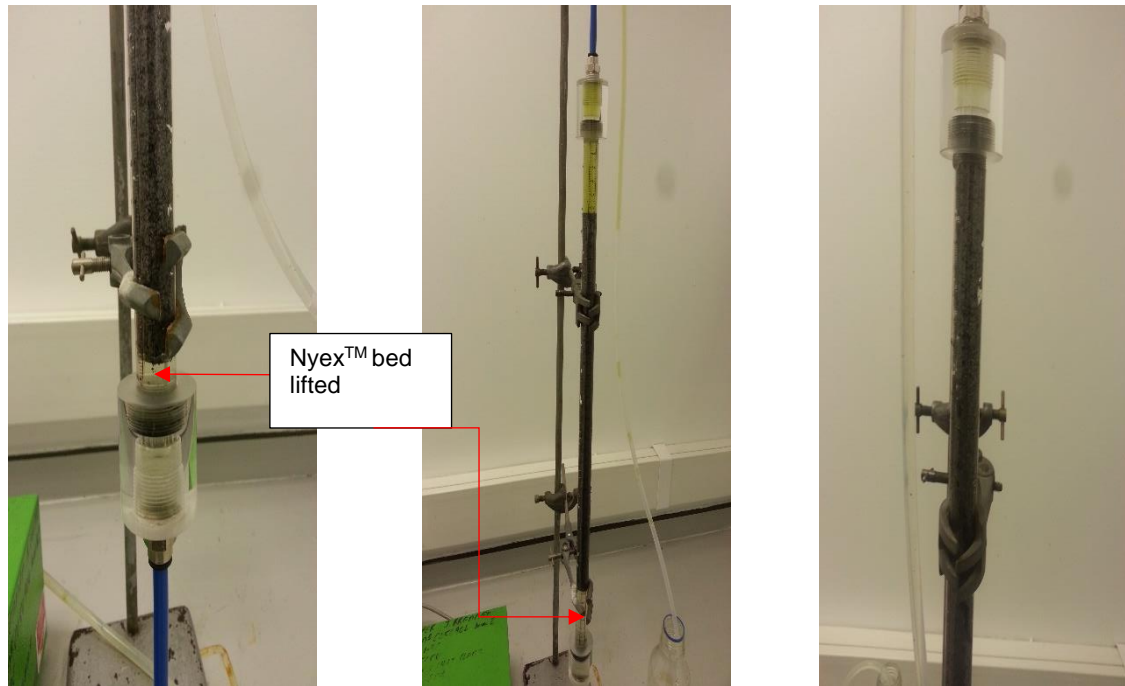


Figure 4.41: Pictorial images of a Nyex™ bed being lifted for upward flow mode. The third picture clearly shows the bed height had expanded considerably beyond its initial level.

4.3.7 Performance Comparison of Submerged and Conventional Fixed Bed

The breakthrough time and the equilibrium capacity are vital parameters in order to design a fixed bed adsorption column. These parameters are determined by the surface utilization of the adsorbent particles in the bed. Interestingly, flow patterns can have an influence on the surface utilization of the bed. The main difference between submerged (SB) and conventional fixed (CF) beds is in their flow patterns. The latter has a flow through pattern whilst the former has the bed continuously immersed in the suspension to be treated (Kawai *et al.*, 2000; Khan *et al.*, 2016). Figure 4.42 shows the breakthrough curves for the 2 flow patterns in terms of the optical density of the effluent suspension. As is clear from the figure, breakthrough occurs very early for both SB and CF (around 8 and 4 minutes respectively). Apart from the difference in breakthrough times, the breakthrough curves look similar as do the total adsorbed cells (TAC) and percentage recovery. The total adsorbed cells for the SB and CF beds were estimated to be 9.1 mg and 8.7 mg whilst their percentage recoveries was 63% and 60% respectively.

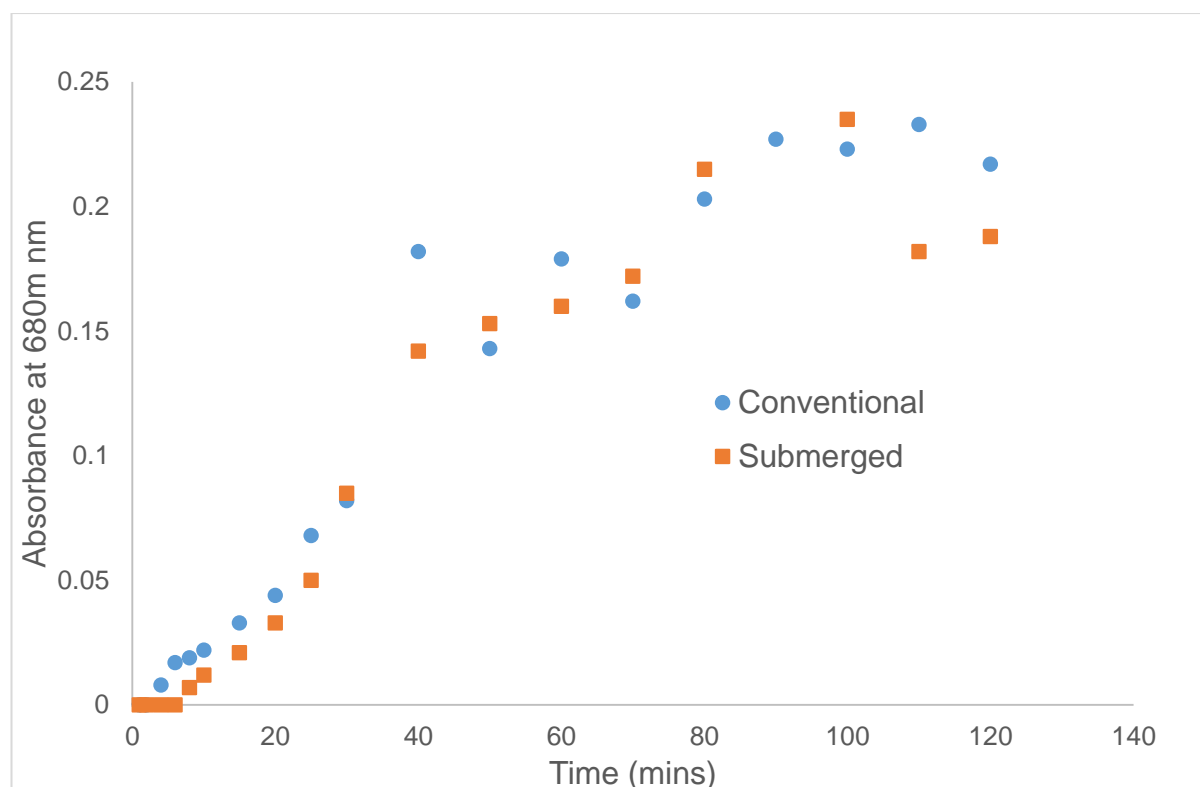


Figure 4:42: Breakthrough curves for the recovery of microalgae cells using Nyex™ particles at flow conditions ($h = 20\text{cm}$, $C_o = 0.3\text{ OD}$, $Q = 10\text{ mL/min}$) for submerged and conventional bed configurations.

A number of studies have reported the use of fixed bed submerged in the solution/suspension to be treated, but comparison between an SB and a CF seems quite limited (Wilson and Danner, 1983; Othman *et al.*, 2001; Goel *et al.*, 2005; Khan *et al.*, 2016). However, Khan *et al.* (2016) compared both configurations for the treatment of methylene blue using a fixed bed of jackfruit (*Artocarpus heterophyllus*) leaf powder. The study reported that the total adsorbed cells of an SB in comparison to a CF increased by 22.7% and the breakthrough time increased by up to 86%.

However, the enhanced improvement reported for a submerged bed by Khan *et al.* (2016) was not achieved in the present research. Also, an extra pump was needed to flow the suspension in the SB and to maintain a constant static head in the column. The implication is that it may not be a simple, cost-effective and energy-saving process to embark upon when it comes to microalgae cell recovery especially with less than a 5% improved recovery. In consequence, it appears the recovery of cells using Nyex™ particles in a submerged fixed bed column may not be an attractive option.

4.3.8 Anomalous behaviour of Microalgae Cell Recovery in the Fixed Bed

4.3.8.1 Depressed Breakthrough Curves

An observation evident in all instances was that the ratio of the effluent concentrations to the feed concentration of the suspension never attained a value of 1.0. Theoretically, exhaustion of the bed is assumed to have been attained when $C_e/C_o = 1.0$. Although some reports have it that $0.9 \leq C_e/C_o \leq 1.0$ is sufficient to assume bed exhaustion. Throughout the experiments undertaken in the research reported in this thesis, the maximum C_e/C_o was 0.85 while much lower values of C_e/C_o were also observed. As depicted in Figures 4.43 and 4.44, the initial microalgae suspension was monitored and measured at different time intervals with a view to understanding if this was lower than the value measured before the start of the experiments. Figure 4.43 shows some settling of the cells, this was not significant though, and was less than 2.5% of the initial value on average for both concentrations.

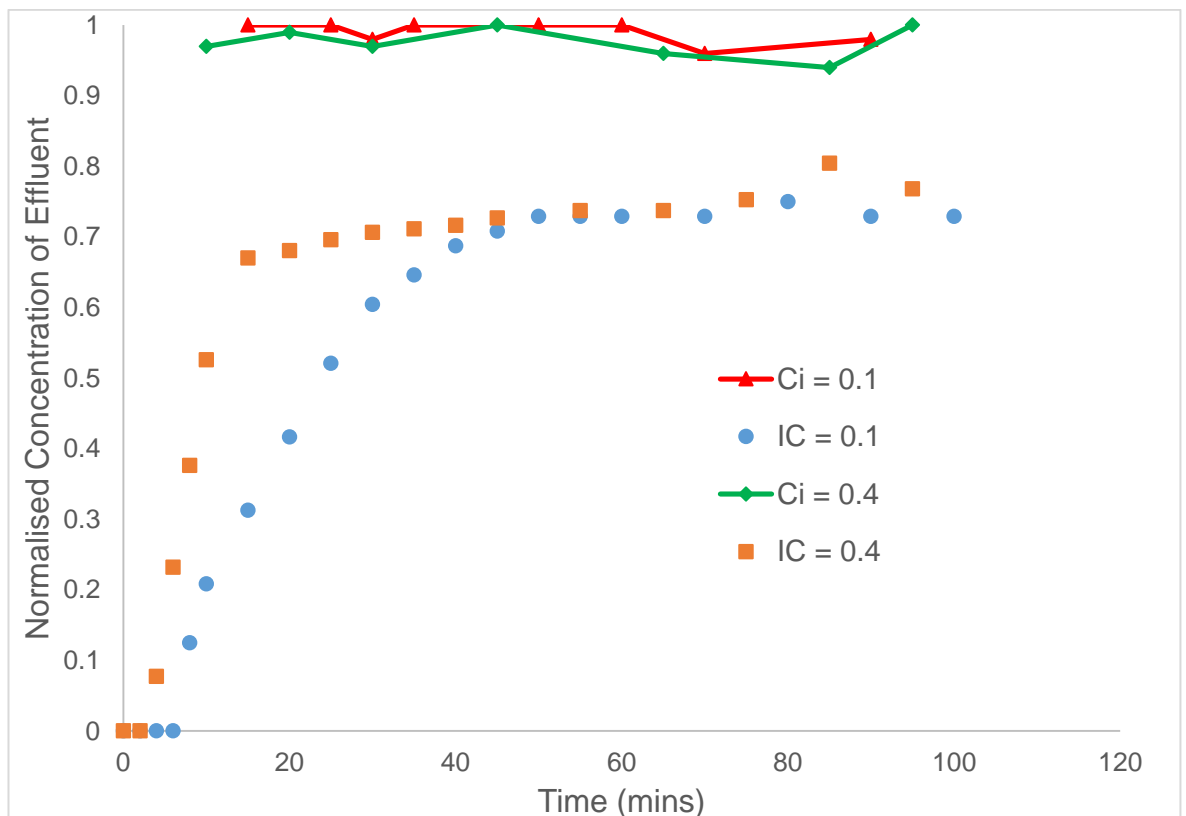


Figure 4.43: Breakthrough curves for the recovery of microalgae cells using Nyex™ particles at two suspension concentrations ($IC = 0.1$ and 0.4 OD) with the feed concentrations re-measured (C_i) throughout the experiment.

Figure 4.43 indicates the breakthrough when normalised against the re-measured initial suspension concentration. From the graph, it could be concluded that the minimal cell settling of the suspension does not offer sufficient explanation as to why the C_e/C_o ratio was never equal to 1.0. Though it is worthy of mention that cell settling was minimised by agitating the suspension at fixed time intervals.

The implication of such an anomaly is depicted in figure 4.45, where the ‘observed breakthrough curve’ (observed BTC), as revealed in the research reported in this, appeared to suggest that the adsorbent bed had an “infinite” capacity to recover cells whilst the “typical BTC” suggests otherwise.

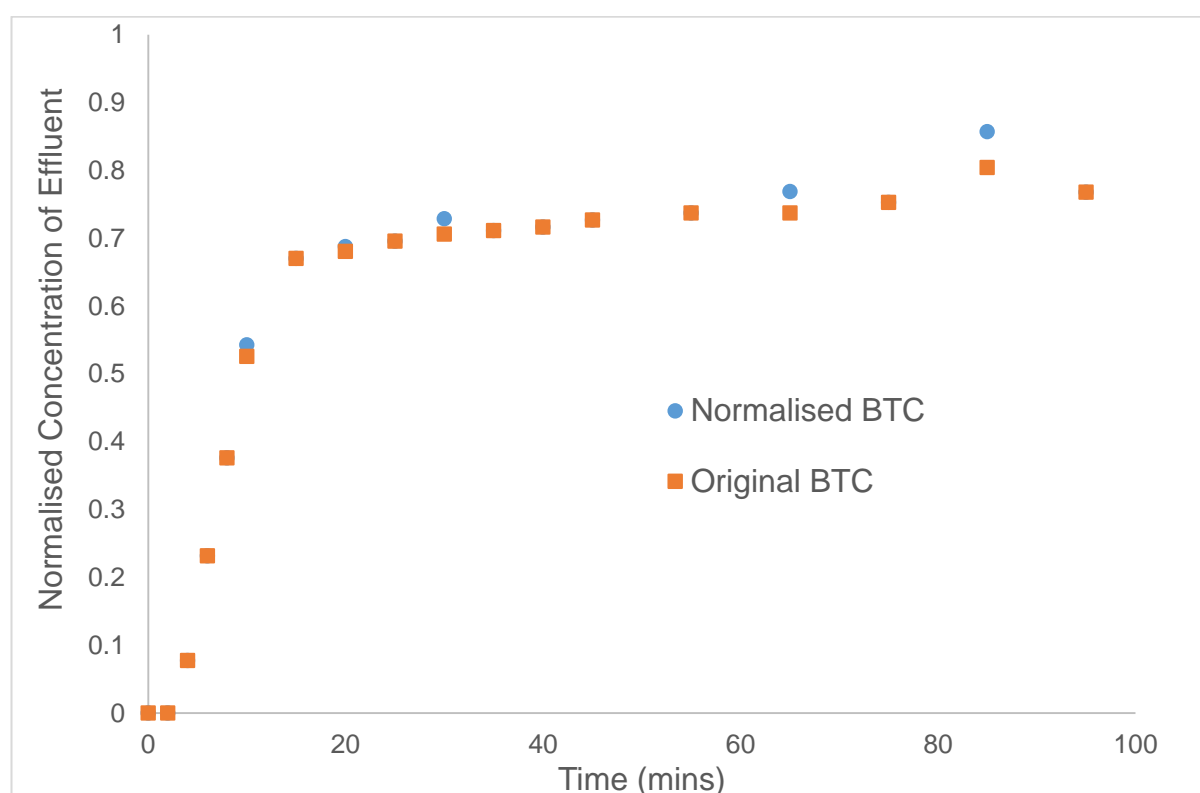


Figure 4:44: Normalised breakthrough curve for the recovery of microalgae cells using Nyex™ particles. Concentration data are presented as measured OD/re-measured suspension OD.

Snoeyink (1990) reported a strong effect that the presence of biodegradable constituents/compounds had on the breakthrough curve. The author suggested that removal of biodegradable constituents/compounds by microbial degradation in a fixed bed column could result in a depressed breakthrough curve whose C_e/C_o never attained 1.0. This suggestion for the depressed breakthrough curve was supported

elsewhere (Tchobanoglous *et al.*, 2003). The microalgae cells were ‘harvested’ after the stationary growth phase of the suspension medium was attained.

Despite this, it was still very possible that some cells continued to grow through chemical dissolution of the available nutrients. Whether this was sufficient to observe the level of depression experienced with the breakthrough curves reported in this thesis is open to debate.

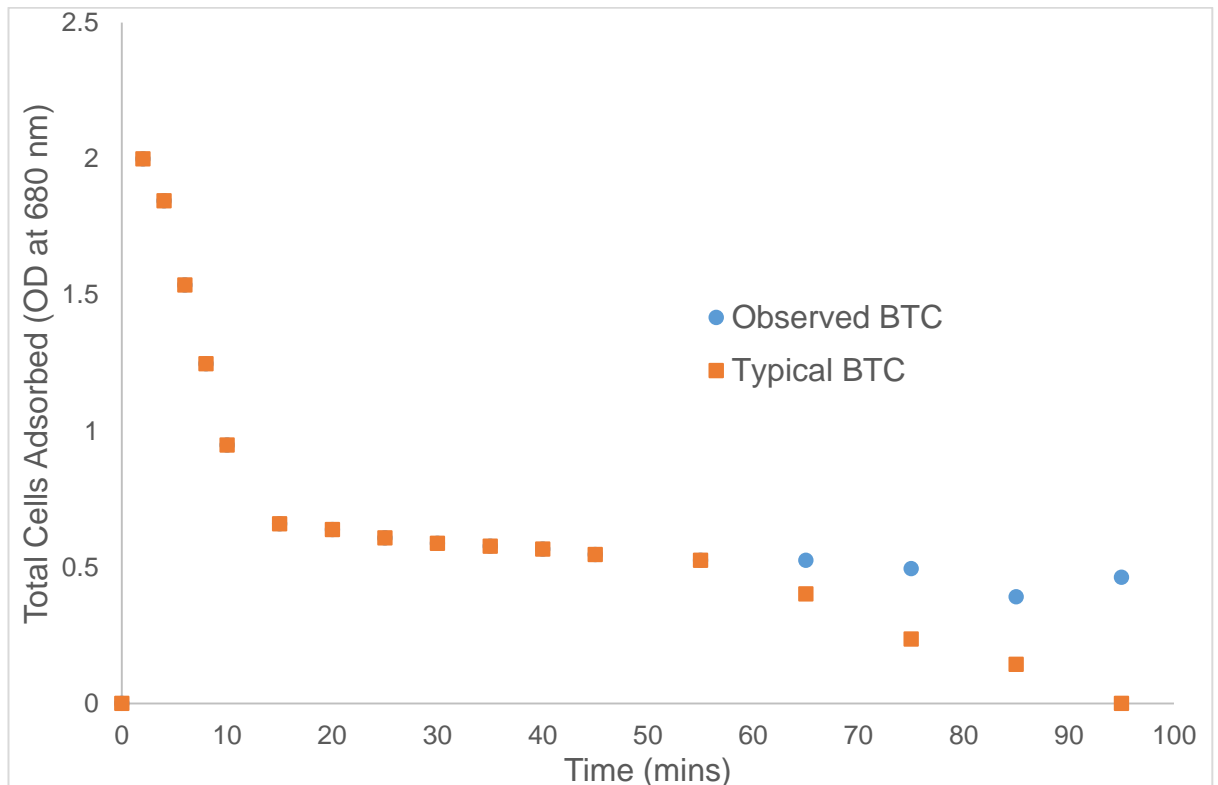


Figure 4:45: Total cells adsorbed for the experimental and “typical” breakthrough curves.

Interestingly, a one-off control experiment carried out where the “effluent concentration” was measured as it entered the bed revealed that an average of 10% of the feed concentration did not reach the adsorbent bed. This still leaves another 10 – 15% of cells unaccounted for. However, it was also observed that microalgae cells stuck to some parts of the column as depicted in figure 4.46. Furthermore, in some instances, cells could have been “lost” along the tubing and column wall as well as there being some form of agglomeration inside the column as shown in figure 4.46. But again, these observations were not consistent in all the experiments carried out. Consequently, it would be difficult to assume the “lost cells” were due to the aforementioned reasons. It could as well be a rare occurrence where Nyex™

bed exhaustion is at about 80% of the inlet concentration. Another possible explanation would be if the Nyex™ bed behaves as a filter medium at some point during cell recovery.

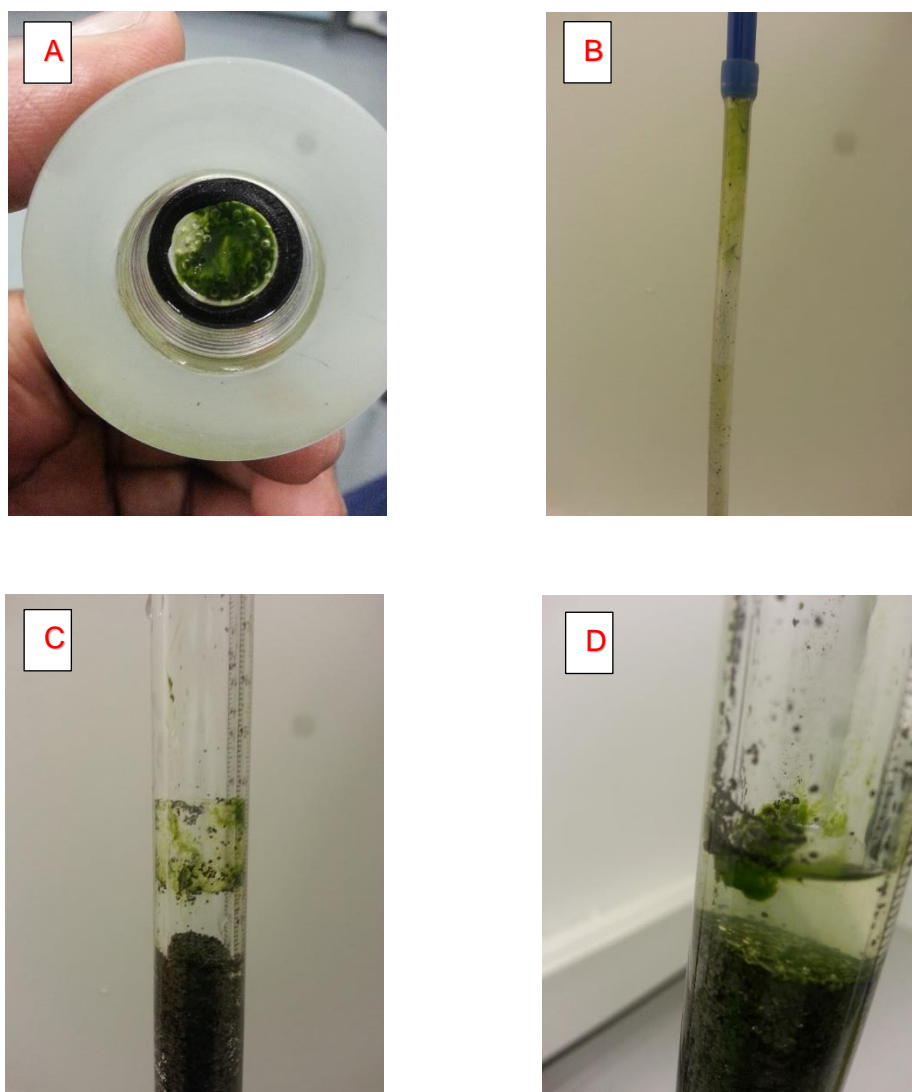


Figure 4:46: Pictorial images of cell accumulation on (A) top aspect of the column, (B) along the tubing, (C) on the column wall, and (D) cell aggregation.

4.3.8.2 Biofouling of the Bed Column?

An attempt was undertaken to investigate whether continuously running the column would eventually lead to a breakthrough curve where the C_e/C_o ratio could attain 1.0. Hence, a flow rate of 20 mL/min, bed height of 5 cm and initial feed concentration of 0.43 OD were considered in a downward mode of flow. The flow conditions were selected with the aim of “forcing” the cells through the bed such that it could be possible for C_e/C_o to attain a ratio of 1.0. As shown in figure 4.47, as anticipated the breakthrough occurred at the first minute of effluent sample. Within

5 minutes, the bed could be considered as exhausted. However, the bed was still being fed with suspension. As evident from the graph, a “consistent” pattern of increase and decrease could be observed and at one instance a C_e/C_o of 0.87 was attained; the highest recorded. Unfortunately, at 60 minutes the bed became blocked.

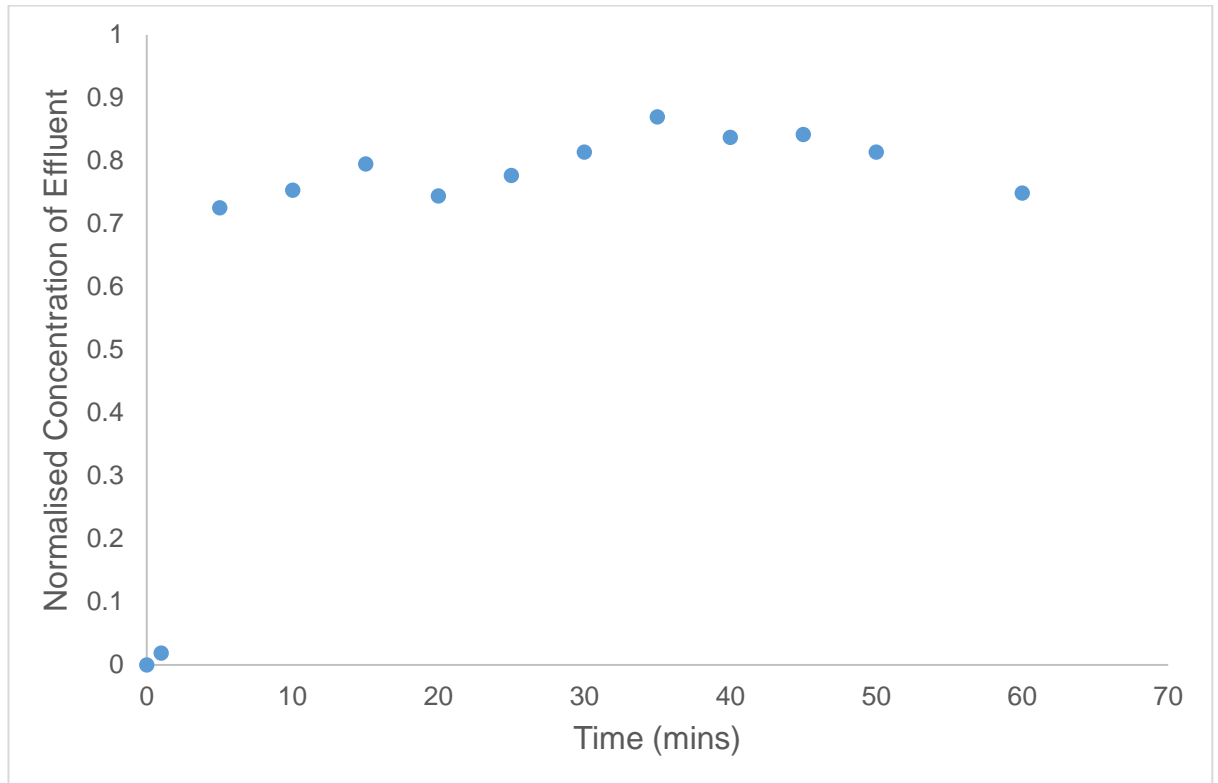


Figure 4:47: Breakthrough curve for the recovery microalgae cells using Nyex™ particles at the flow conditions ($h = 5$ cm, $C_o = 0.43$ OD, $Q = 20$ mL/min) in the downward flow mode.

A similar experiment was also carried out but with a flow rate of 40 mL/min, bed height of 30 cm and initial feed concentration of 0.4 OD as flow conditions in a downward mode of flow. As illustrated in figure 4.48, the bed could be considered to be exhausted within 15 minutes. Nonetheless, the bed was still being fed with suspension, even though there was little or no effect on the effluent concentration. After 45 minutes, similar to what was experienced in figure 4.47, the bed became blocked. In each case, as shown in Table 4.4, the total adsorbed cells and the bed capacity were quite high in comparison to the earlier data reported in Table 4.3.

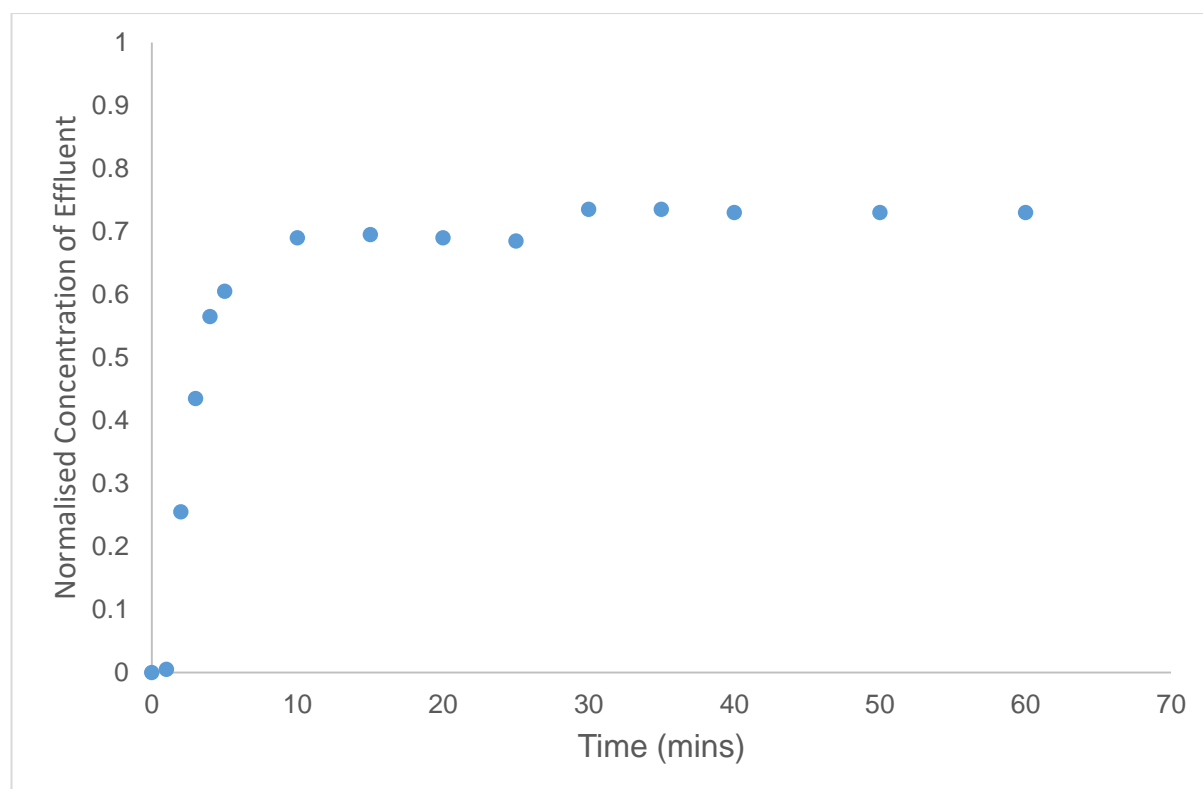


Figure 4:48: Breakthrough curve for the recovery of microalgae cells using Nyex™ particles at the flow conditions ($h = 30$ cm, $C_o = 0.4$ OD, $Q = 40$ mL/min) in the downward flow mode.

Table 4.4: The total adsorbed cells and bed capacity for figures 8.14 and 8.15

Scenarios	Flow Rate	Initial Cell Concentration	Bed Height	Breakthrough time	Percentage Recovery	Total Cells Adsorbed	Bed Capacity
	(mL/min)	(Absorbance at 680 nm)	(cm)	(min)	(%)	(mg)	(mg/g)
A	20	0.43	5	1	22	33.1	4.13
B	40	0.4	30	2	31	86.4	1.8

Bed blockage implies that the suspension could not pass through the bed such that effluent could not be collected as illustrated in figures 4.49 and 4.50. Another implication is that the suspension built up in the bed and almost resulted in an overflow of the column. In all the cases where this was experienced, blockage time was around 60 min. This observation further underscores the difficulty of the ratio C_e/C_o to attaining 1.0 for a bed column in the recovery of microalgae cells.



Figure 4:49: Pictorial image of bed blockage, showing that liquid above the bed is not able to pass downward through the column.

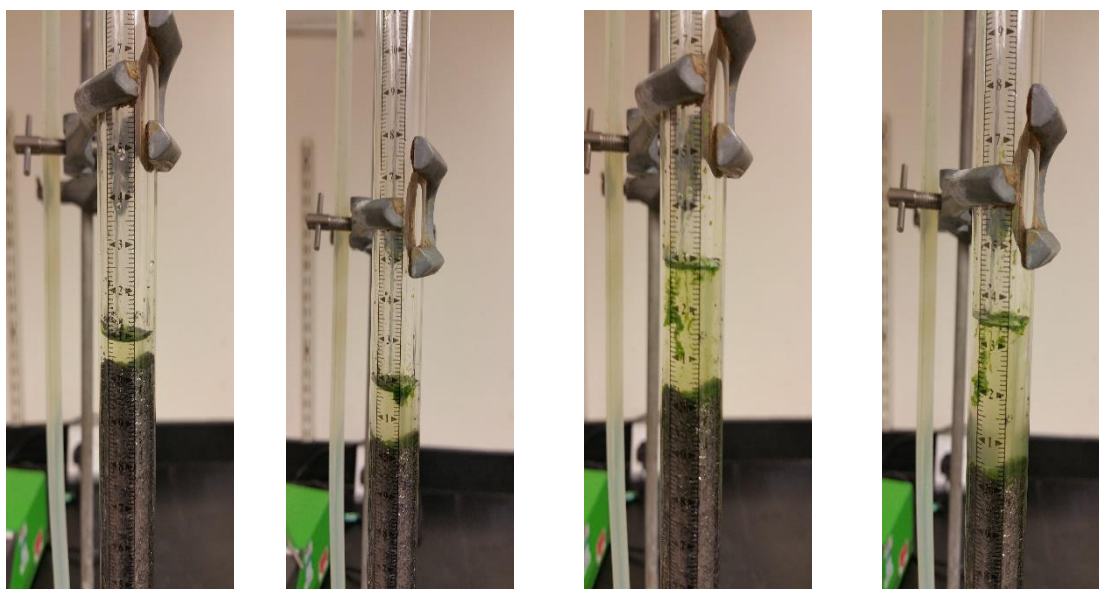


Figure 4:50: Pictorial image showing build-up of suspension (from left to right) in the column as a result of a potential bed blockage.

This observation seems to be linked to the phenomenon known as biofouling. Biofouling is the gradual accumulation of microbial organisms on surfaces such as vessel walls (Bitton and Marshall, 1980; Ozkan and Berberoglu, 2013). In the bed column employed in this research, it is possible that as the bed became ‘exhausted’, the cells then began to fill in “spaces” between the adsorbent flakes, thereby making it tightly packed and impermeable. An evidence of this explanation is manifest in the high total adsorbed cells as shown in Table 4.4.

4.3.9 Control Studies

4.3.9.1 Adsorption of Acid Violet (AV) 17 Dye

A dye was chosen because the literature is replete with “successful” investigations of dye removal in a bed column regardless of whether the mode of flow is either upward or downward (Walker and Weatherley, 1997; Namasivayam and Kavitha, 2002; Rozada *et al.*, 2003; Al-Degs *et al.*, 2008). The (AV) 17 dye was considered due to a number of previous batch studies involving the use of Nyex™ particles as the adsorbent (Brown *et al.*, 2004; Mohammed *et al.*, 2011; Asghar *et al.*, 2012). However, its adsorption in a bed of column of Nyex™ has not been investigated. This study could be used to facilitate a comparison between the adsorption characteristics of microalgae cells in a bed and those of the dye. Figure 4.51 revealed the resulting outcome and a distinct difference from when the adsorbates in the column were microalgae cells.

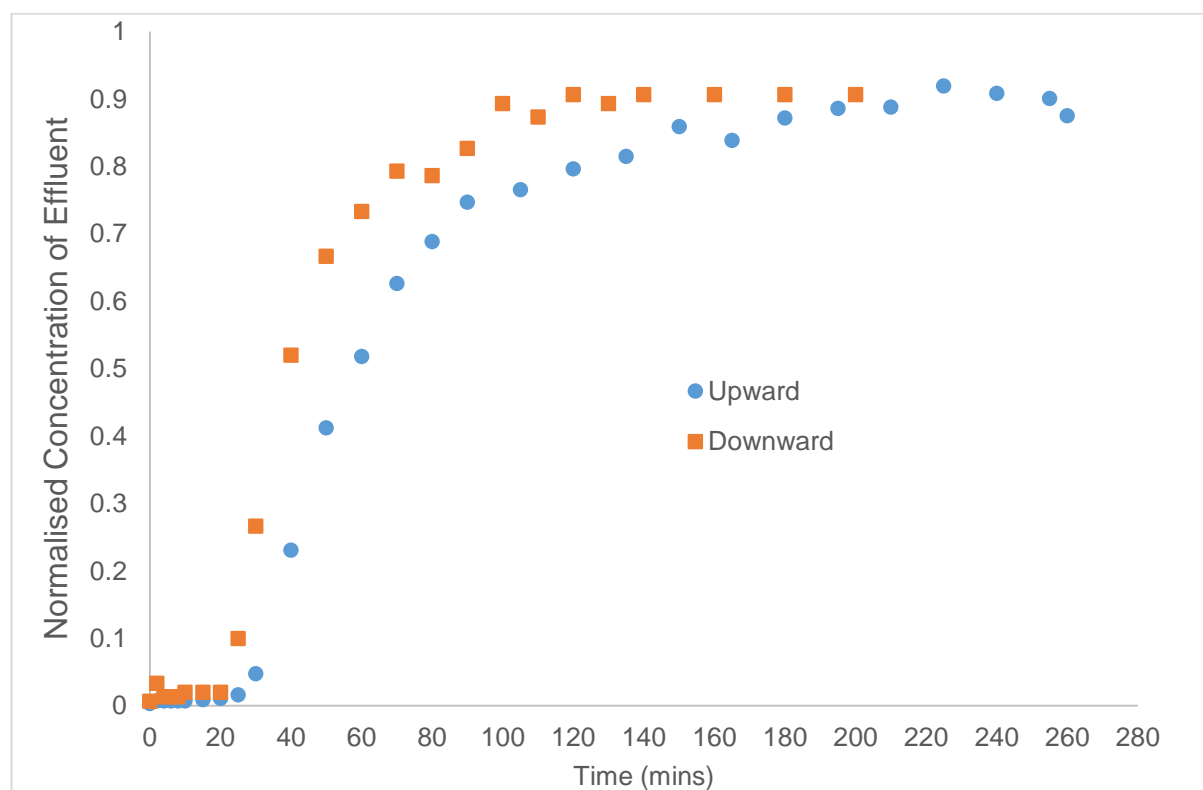


Figure 4:51: Breakthrough curves for the recovery AV 17 dye using Nyex™ particles at the flow conditions ($h = 20$ cm, $C_o = 0.3$ OD, $Q = 10$ mL/min) in the upward and downward modes of flow.

As is evident, the upward and downward flows look quite similar. More importantly, both show the characteristic S-curve expected of a breakthrough curve (BTC). Unlike, the BTCs of microalgae cells, the BTCs of the dye attain C_e/C_o ratio much

closer to 1.0 for both downward and upward flows. In fact, based on the BTCs, it was easy to suggest that the upward mode was slightly better than the downward mode in terms of the breakthrough and exhaustion times as well as the bed capacity. This control outcome exposes the challenges in the recovery of microalgae cells in a fixed bed column and clarifies that adsorption features reported earlier are unique to microalgae cells being the adsorbate.

4.3.9.2 Recovery of Microalgae Cells with Glass Beads and Sands

The control experiments that were also conducted include “adsorbing” cells onto other types of materials, such as glass beads and coarse sand as described in previously described in Chapter 3. This was to provide insight in to whether adsorption or filtration or a combination of both were responsible for the recovery of cells in the column. Figure 4.52 showed the resulting breakthrough curve for each of the materials in comparison to Nyex™ particles under similar flow conditions. From the figure, it becomes apparent that there are differences between the recovery properties of Nyex™ particles and those of other materials.

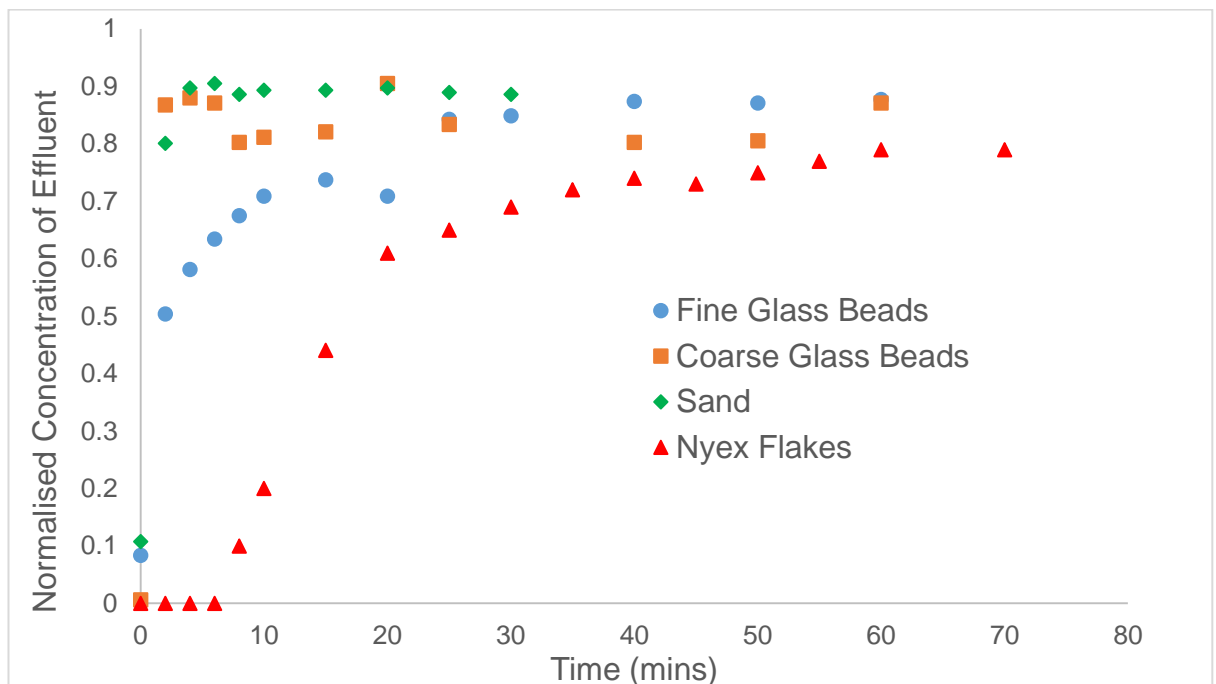


Figure 4.52: Breakthrough curves for the recovery of microalgae cells using Nyex™ particles at the flow conditions ($h = 20$ cm, $C_0 = 0.3$ OD, $Q = 10$ mL/min) in the downward flow mode for a variety of materials.

The industrial sand and the coarse glass beads behaved reasonably alike as both materials could not “retain” any cells in their beds. Fairly swiftly, both materials

leaked cells into the effluent and easily attained C_e/C_o ratio values exceeding 0.9. Their non-adsorbing and their non-filtrating properties became immediately manifest.

As for the fine glass beads, although they also easily allowed the breakthrough of cells along the bed, the trend was better. In fact, its “BTC” performed similar to when a high flow rate, high initial feed concentration and a low bed height of NyexTM was used. Conversely, if the BTC was compared to that of NyexTM particles under similar conditions, the performance of the adsorbent was clearly superior.

Laboratory observations revealed that most, perhaps all, of the cells retained on the fine glass beads were due to the filtering properties of the fine glass beads. This is because when the glass beads were ‘rinsed’ after the experiment, all the cells effortlessly came off the beads. Although, it would be difficult to assign what percentage of the cells retained by NyexTM particles was due to filtration or adsorption, it does appear that some form of filtration was also taking place. It is also worthy of mention that depending on the size ratio of the cells to the adsorbent particles, straining can also be a removal mechanism in the column. Straining is the trapping of the cells when the channel of transport is too small to allow for cell passage (Foppen *et al.*, 2007). Nonetheless, these control experiments coupled with earlier batch studies further lend credence to the adsorption properties of NyexTM particles in a fixed bed column. However, the flaky structure of the adsorbent used in the research reported in this thesis suggests that the packing of NyexTM particles in a column has a high likelihood of behaving as a filter medium. This might explain the difficulty in attaining C_e/C_o ratio to equal 1.0 as well as the bed blockage experienced at high initial concentrations of the microalgae suspension.

4.3.10 Summary

Similar to other fixed bed systems, effects of flow rate, bed height and initial suspension concentration were observed to affect the recovery of microalgae cells. However, an obvious difference between other applications is that the aim of the research reported in this thesis is to recover as many cells as possible. Hence, parameters such as breakthrough and exhaustion times do not give a true picture when the scenarios are compared. The bed capacity was found to be a more useful parameter for the purpose of this research.

Furthermore, the use of an upward flow mode to recover cells has been demonstrated as being inappropriate to recover cells as a result of cell settling. In addition, operating the bed as a submerged system was shown to not be an attractive option when other constraints such as requirement of an extra pump were considered. The consistent depression of the breakthrough curves coupled with the occasional biofouling appear to be challenges encountered with the fixed bed system to recover cells.

Through control experiments with an acid violet dye, this chapter has shown that problems with an upward flow mode and a depressed breakthrough curve appear to be limited to when microalgae cells are being recovered. In addition, a comparison with other types of materials, revealed that a combination of adsorption and filtration could be the basis of cell recovery in the fixed bed system. However, further work would be required to assess which of the processes largely dominates cell recovery. It would also be useful, for future work, to consider construction materials that limits the attachment of cells to the column.

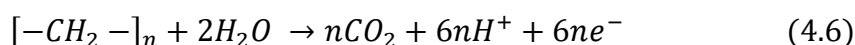
In the bed column, the adsorbent particles near the column entrance are continuously contacted by the fresh suspension of the initial concentration. Therefore, the concentration of the suspension in contact with a given layer of adsorbent in a column basically remains the same. This results in maximum loading of the adsorbent at constant concentration of the solute, which ensure an efficient utilization of the adsorbents in the fixed bed system. In contrast, in the batch mode, there is a continuous decline in the solute concentration, thus decreasing the adsorbent effectiveness. However, in the batch system, there is sufficient time for equilibrium to be attained between the cells and the adsorbent particles; a situation rarely attained in the fixed bed column.

The advantages of operating a fixed bed as a continuous system and the difficulties experienced in the Arvia Y-cell as highlighted in section 4.1 are evident. For the purpose of the research reported in this thesis, it does appear that cell recovery in the fixed bed system has distinctive advantages over the batch system.

4.4 Adsorbent Regeneration, Reuse and Lipids Recovery

4.4.1 Introduction

The recovery of microalgae cells onto Nyex™ particles both in batch and fixed bed continuous systems has been established. The factors affecting cell recovery, and mechanisms of adsorption, as well as the models governing those adsorption systems were also discussed in the previous chapters. What happens after adsorption to the microalgae cells and the Nyex™ particles is a fundamental question the research reported in this thesis attempts to answer in this Chapter. The conductive characteristic of the Nyex™ particles offers the prospect of using electrochemical methods to regenerate the spent adsorbent particles, which is well documented in the literature (see Chapter 2). The destruction of adsorbed pollutants (mainly organics), during the adsorbent regeneration, as a result of their oxidation in the anodic compartment of the electrochemical cell is a unique feature of the Arvia® process. Typically, the oxidation of the organics can be generally represented by the following expression;



This suggests that organics oxidation gives off carbon dioxide, hence, resulting in a complete removal of the organics from the adsorbent surface. The balanced equation also provides the required information needed to estimate the theoretical moles of electron and the theoretical charge to achieve complete oxidation. As a result, the regeneration efficiency with regards to the amount of current passed can be evaluated.

On the other hand, the application of electrochemical methods as a recovery technique for microalgae biomass or to disinfect wastewater (containing microbial organisms) was highlighted in Chapter 2. However, the application of electrochemical methods on microalgae cells adsorbed onto an adsorbent has not been previously reported. The effects and implications of subjecting the adsorbed microalgae cells and the 'host' adsorbent material to an electrochemical treatment is unknown. Is it possible to regenerate such an adsorbent? Can the regenerated adsorbent particles be reused? Can the microalgae cells be destroyed in a similar way to organics? Will the impact of such electrochemical treatment of the cells lead

to their wall rupture? Answers to these questions is what this Chapter endeavours to proffer based on experimental studies.

However, the first challenge, unlike in organics destruction as stated in equation 4.6, is that an expression to represent the effect(s) of electrochemical treatment of adsorbed microalgae cells seems implausible. This also implies that it would be difficult to evaluate the regeneration efficiency of such a system. Therefore, a more tedious route of using different current densities has to be considered.

To paraphrase, this section endeavours to shed light on the;

- (i) regeneration of NyexTM particles after an adsorption procedure,
- (ii) reuse of regenerated adsorbent within batch and fixed bed systems,
- (iii) effects on the adsorbed cells during regeneration of the adsorbents,
- (iv) potential of lipid release and recovery.

4.4.2 Reuse of Regenerated Adsorbent at Varied Current Densities in Batch

The regenerated adsorbents were used to recover microalgae cells as described in section 3.4. The total adsorbed cells as well as the equivalent percentage recovery for each batch of adsorbent subjected to the various current densities are depicted in figure 4.53. As is evident from the graph, the total adsorbed cells and the percentage recovery increase as the current densities increase. A significant increase in the total cells adsorbed was observed at a current density of 32 mA.cm⁻², which represents about 40% increase compared to the total cells adsorbed at a current density of 24 mA.cm⁻². Interestingly, beyond 32 mA.cm⁻², no further increase was observed. In fact in comparison to when a maximum total adsorbed cells was observed at a current density of 32 mA.cm⁻², about 10% decrease was evident at a current density of 80 mA.cm⁻². This seems to suggest that a current density of 32 mA.cm⁻² was sufficient to regenerate the adsorbent and ensure that the maximum quantity of microalgae cells can be recovered from suspension when the regenerated adsorbent is reused.

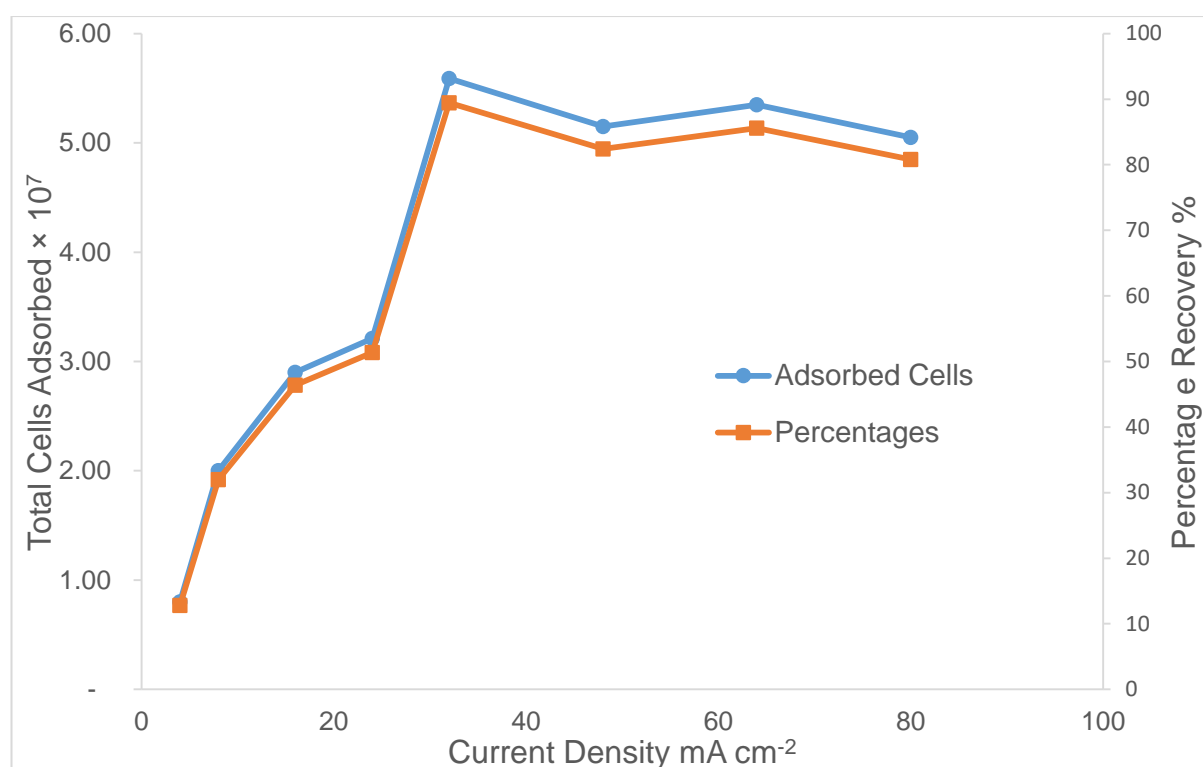


Figure 4:53: The total adsorbed cells and percentage recovery, on adsorbent reuse, after batches of adsorbent were subjected to various regeneration current densities.

4.4.3 Evaluation of Adsorption Recovery Performance of Nyex™ ‘Variants’

The variants of Nyex™ particles used to recover microalgae cells were as previously described. The resulting observations were plotted as depicted in figure 4.54. The ‘initial’ indicates the cell density of the suspension before any adsorption took place. As portrayed in the figure and as expected, using ‘Spent Nyex’ resulted in more cells remaining in suspension in comparison to ‘Fresh Nyex’. Figure 4.55 shows the percentage recovery and the fraction of the adsorbent variants normalised against the ‘Fresh Nyex’. As revealed in the figure, the normalised fraction of ‘Regenerated’ and ‘ETC treatment’ Nyex™ particles were more than 1.0, which suggests that those variants adsorb more cells from suspension than ‘Fresh Nyex’. Furthermore, ‘Spent’ and ‘Regenerated’ Nyex™ particles were utilised to recover more cells in a number of adsorption cycles as depicted in figures 4.56 and 4.57.

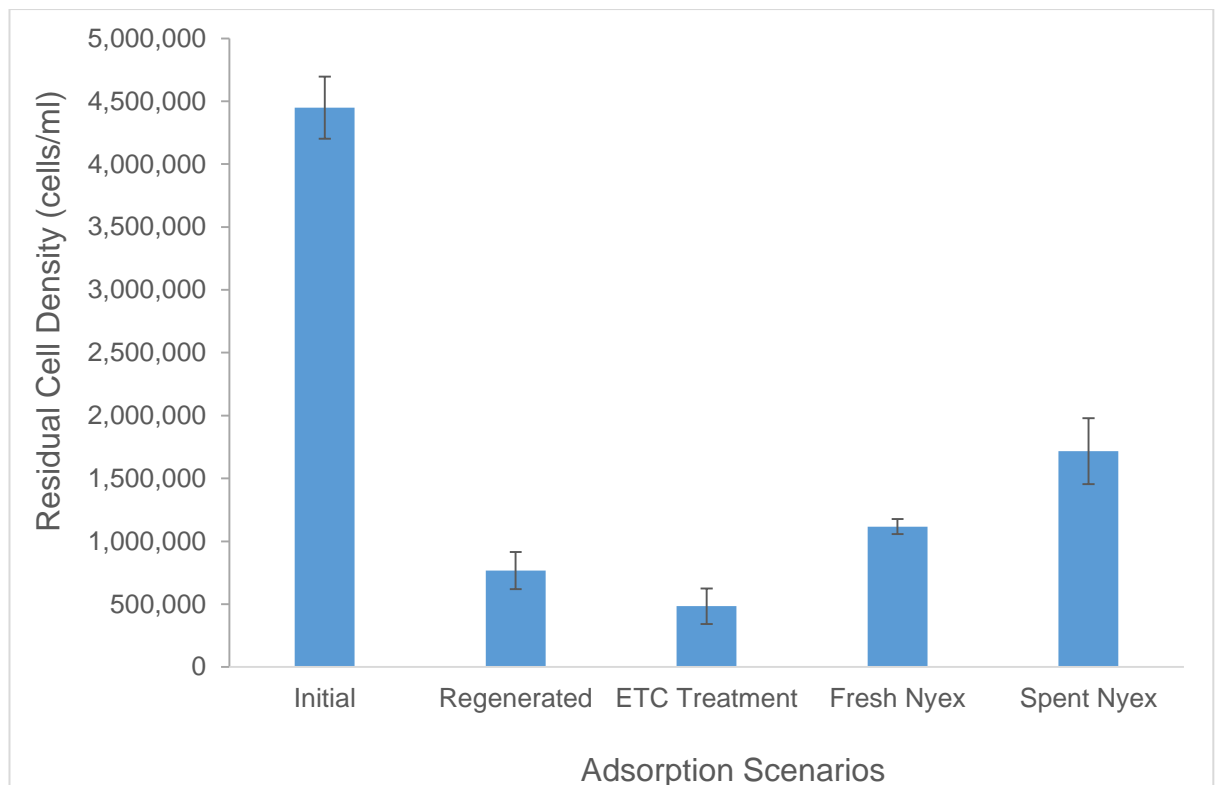


Figure 4:54: The residual cell density of microalgae suspensions after using variants of Nyex™ particles to recover microalgae cells.

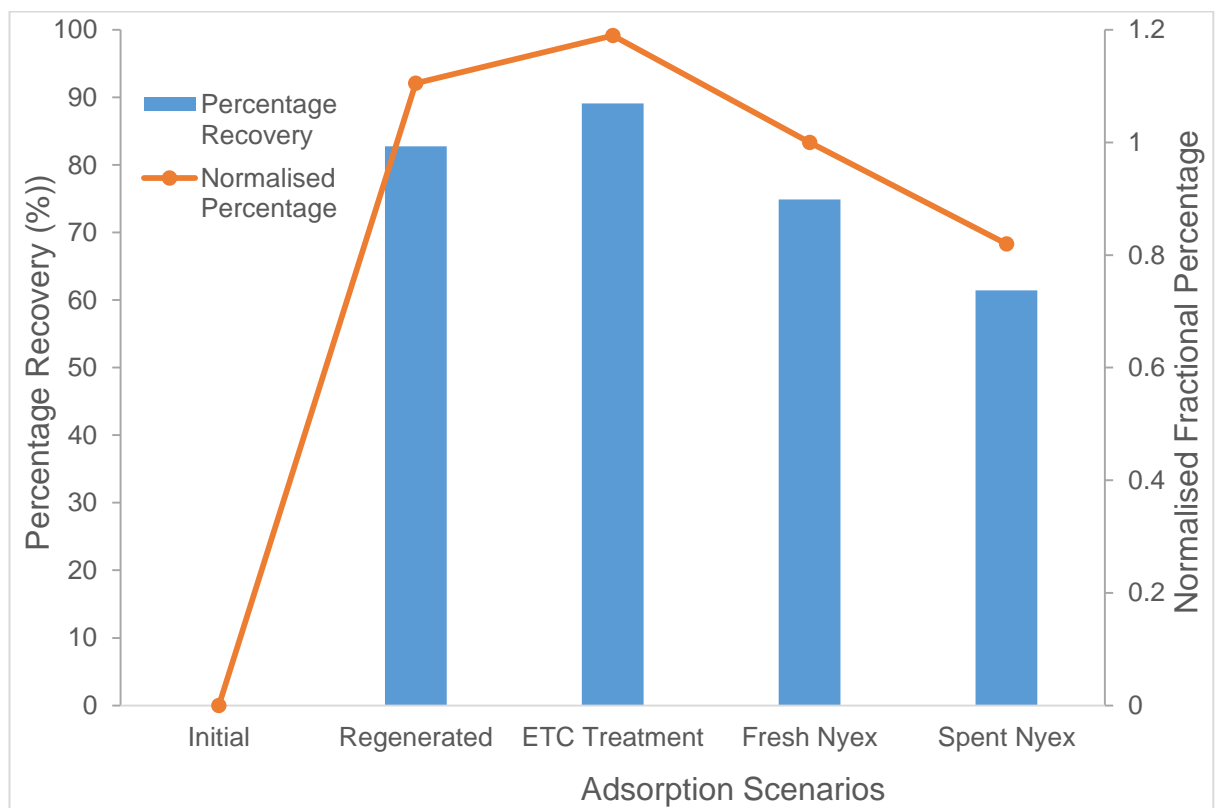


Figure 4:55: The percentage recovery and normalised fraction of variants of Nyex™ particles after being used to recovery microalgae cells suspension.

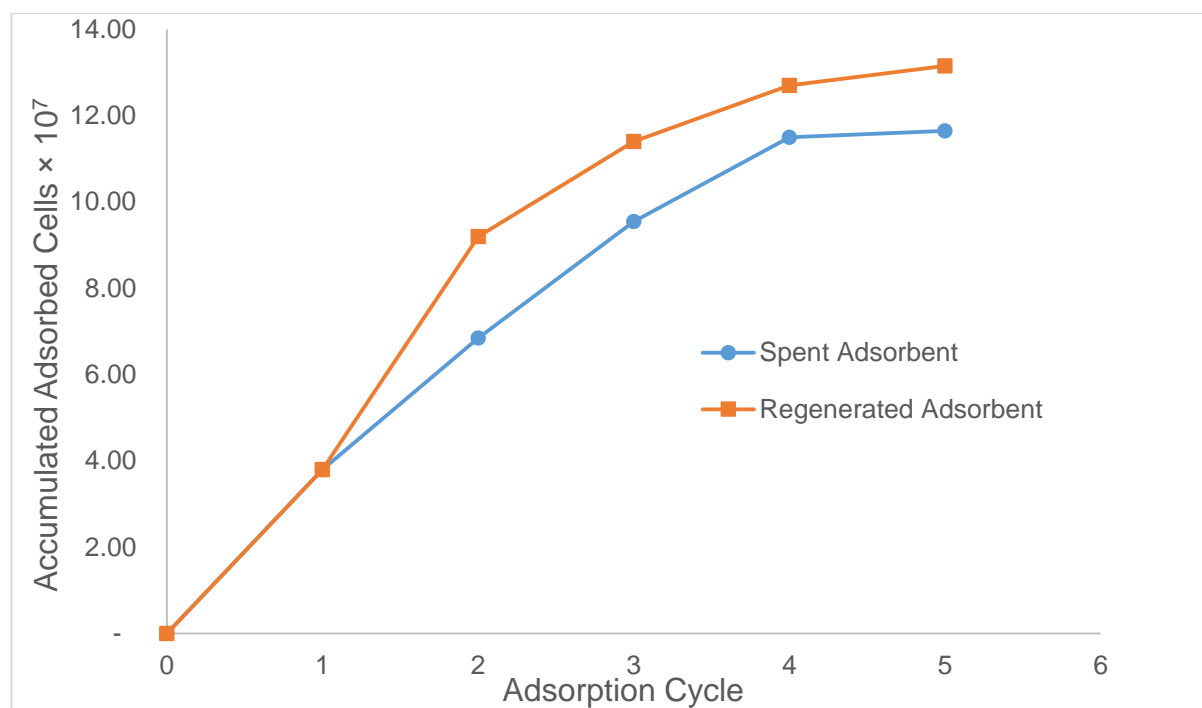


Figure 4:56: The accumulated adsorbed cells over each adsorption cycle after using 'Spent' and 'Regenerated' Nyex™ particles to recover microalgae cells.

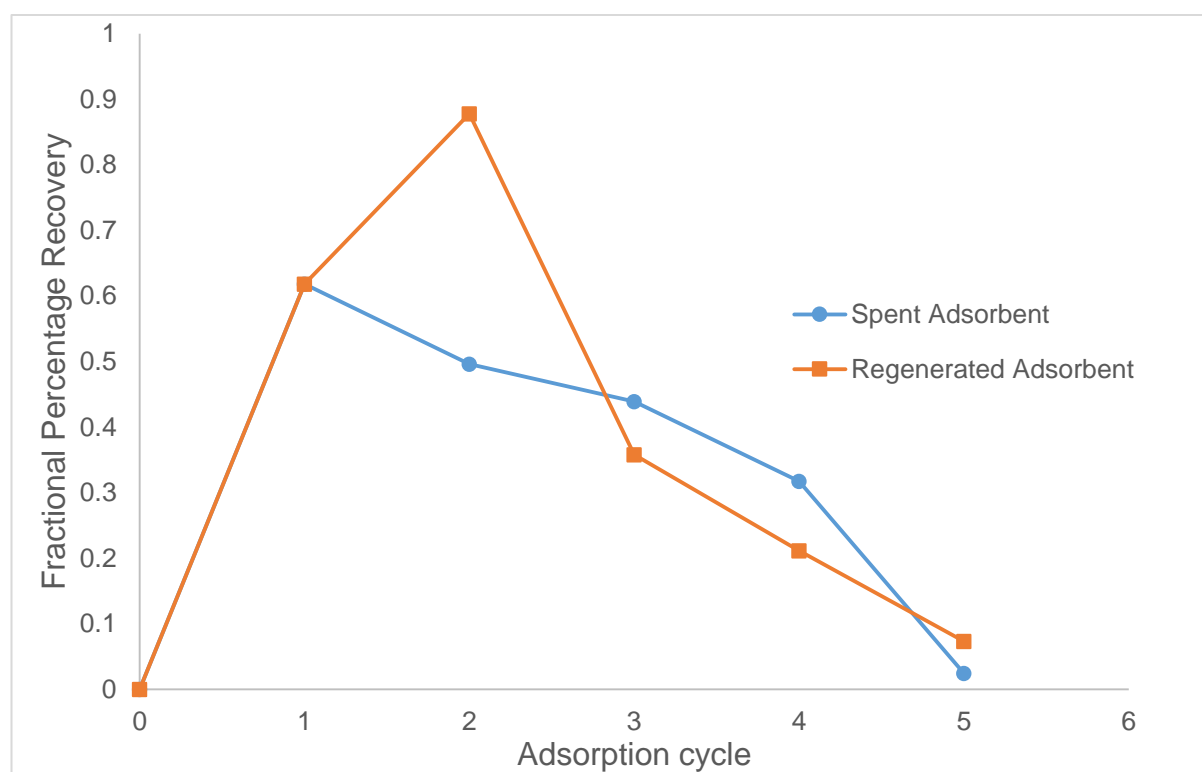


Figure 4:57: The fractional percentage recovery for each adsorption cycle after using 'Spent' and 'Regenerated' Nyex™ particles to recover microalgae cells.

As evident in figures 4.56 and 4.57, regenerated Nyex™ particles accumulated more cells over the entire adsorption cycle than 'Spent' Nyex™ particles. This indicates that 'Regenerated' and 'ETC treatment' Nyex™ particles have more capacity to

adsorb more cells than the Unused and 'Spent' NyexTM. It is as if subjecting NyexTM particles to some form of electrochemical treatment creates more adsorption capacity on the adsorbent. The enhanced adsorption capacity of NyexTM particles after electrochemical regeneration has been previously reported (Brown *et al.*, 2004; Brown and Roberts, 2007; Mohammed *et al.*, 2011; Asghar *et al.*, 2012; Conti-Ramsden *et al.*, 2012; Brown *et al.*, 2013).

In detail, Brown *et al.* (2004) showed that during the removal of atrazine, the adsorptive capacity of regenerated NyexTM particles was in excess of the original capacity. In the same vein, while comparing the adsorptive capacity of different NyexTM materials, Asghar *et al.* (2012) revealed that the regenerated particles had a better adsorption capacity than the fresh NyexTM particles. One of the reasons for this observation has been linked to the 'roughening' of the adsorbent surface as a result of the electrochemical treatment. Possible changes to surface functionality has also been put forward as a reason for the increase in adsorption capacity (Nkrumah-Amoako *et al.*, 2014).

Nkrumah-Amoako *et al.* (2014) showed that the acidity on the surface of NyexTM particles increased with electrochemical treatment with more formation of carboxylics. This could be due to the formation of more active sites as a result of the decomposition of acidic oxygen containing functional groups such as carboxylics. As previously established in section 4.2, one of the mechanisms of adsorption is due to the interaction between the functional groups on the surfaces of the adsorbent and the microalgae cells. This therefore explains the fact that the electrochemical treatment of the NyexTM particles, which increases the surface functional groups, results in greater interaction between the adsorbent and the cells, thus, increasing cell recovery.

In addition, through Boehm titration, Nkrumah-Amoako *et al.* (2014) showed that the total acidity, measured as the acidity due to acidic functional groups and lactones, increased significantly when NyexTM particles are electrochemically treated. Again, increased acidity of the suspension media was shown in section 4.2 to enhance the recovery of microalgae cells onto the adsorbent surface. As previously argued that a number of mechanisms could drive the recovery of microalgae cells onto the NyexTM particles. These observations further reinforce that posit.

4.4.4 Effects of Electrical Charge and Energy on Regeneration and Reuse

Amongst the operating conditions studied were the effects of electrical charge passed and the energy consumed per gram of the adsorbent. This was relevant in order to understand how these key parameters affect the electrochemical regeneration of the adsorbent. From the results described in the previous sections, both the electrical charge and energy consumed increased. Hence, studies were undertaken to see the effects, if any, of keeping either one constant whilst the other was allowed to vary. The adsorbent particles were regenerated by subjecting them to each of the constant conditions and were reused to recover microalgae cells from suspension. Figure 4.58 revealed the observations recorded when the adsorbent regenerated under constant electrical charges were reused to recover microalgae cells.

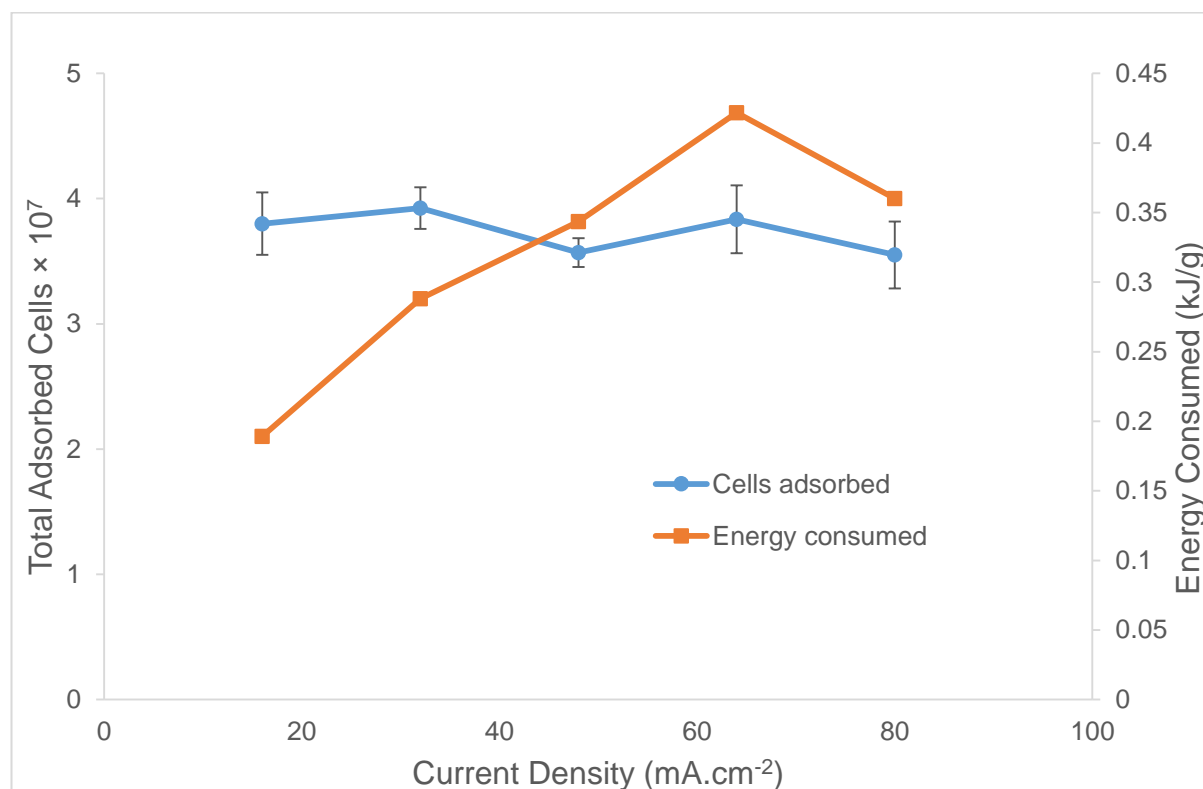


Figure 4:58: The total adsorbed cells onto the regenerated Nyex™ particles after mixing with microalgae suspension. Regenerated adsorbent is based on constant electrical charges but variable energy consumption, as shown on the secondary axis.

As is evident from figure 4.58, energy consumption during the regeneration of the adsorbent consistently increased substantially as the current density increased, despite keeping the electrical charge passed constant. The increase in energy consumed peaked at about 0.42 kJ/g at a current density of 60 mA.cm⁻².

On the other hand, the total adsorbed cells recovered from the suspension onto the regenerated adsorbent does not seem to be affected by the condition of constant electrical charge and variable electrical energy under which those adsorbents were regenerated. As revealed in figure 4.58, considering the statistical analysis, it can be considered that a constant electrical charge effectively means the adsorbents were subjected to similar regeneration conditions despite considerable changes in the energy consumption.

On the contrary for adsorbents regenerated under constant electrical energy, whilst the charges passed were varied, the total adsorbed cells increased as the charges passed increased.

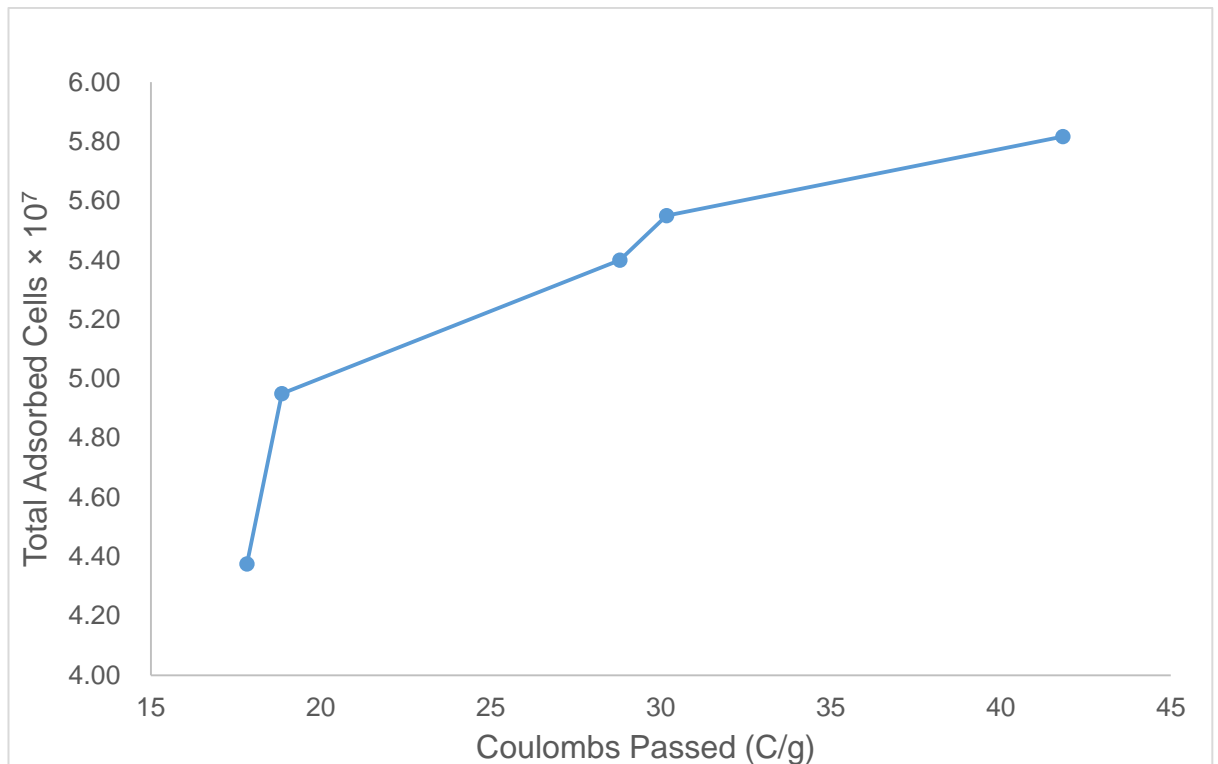


Figure 4:59: The total adsorbed cells onto the regenerated Nyex™ particles after mixing with microalgae suspension. Regenerated adsorbent is based on constant electrical energy but variable electrical charges.

As is clear from figure 4.59, there was a consistent increase in the total adsorbed cells onto the adsorbent regenerated under the condition of variable electrical charges but constant energy consumption. Figure 4.60 further illustrates the effects of variable charge passed. The current densities during the adsorbent regeneration and their corresponding charges passed, underscore the fact that increasing current density does not have a positive effect on the total adsorbed cells recovered onto

the regenerated adsorbents. On the contrary, as apparent from figure 4.60, increasing the current density, coupled with an increase in the electrical charge led to an increase in the total adsorbed cells onto the regenerated adsorbents. An increase in the current density from 20 mA.cm⁻² to 80 mA.cm⁻² resulted in a decrease in the total cells adsorbed by nearly 25%. This is as a consequence of the decrease in the charge passed within the current densities by more than 50%. Hence, this evidently strengthens the role electrical charge plays in the regeneration of adsorbents, which appears to override the significance of the amount of energy consumed. It further suggests that a 'process strategy' of regenerating adsorbents through electrochemical means can be achieved without incurring the costs of high energy consumption.

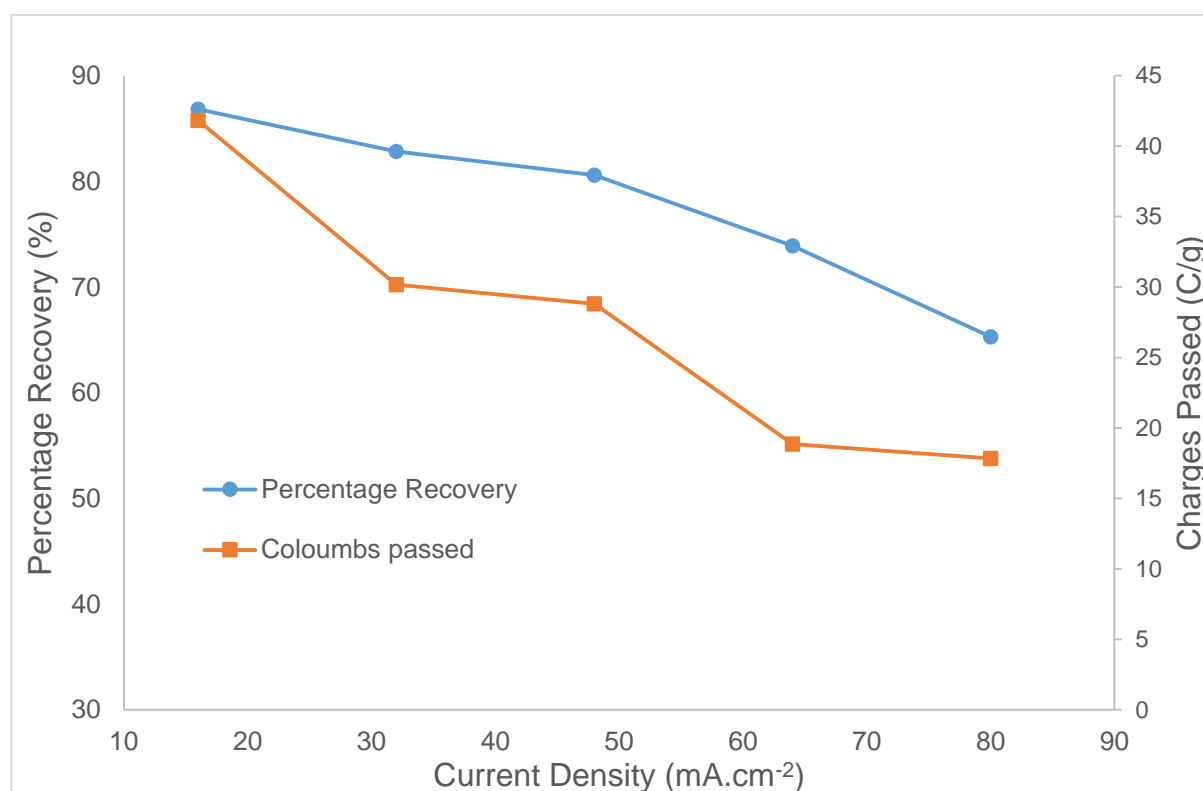


Figure 4:60: The percentage recovery of cells onto the regenerated NyexTM particles after mixing with microalgae suspension. Regenerated adsorbent is based on constant charges passed but variable energy consumption.

4.4.5 Reuse of Regenerated Adsorbent in a Fixed Bed Column

The adsorbent regenerated as well as fresh NyexTM particles were used to recover microalgae cells in a fixed bed column. As depicted in figure 4.61, for the breakthrough curve of the regenerated NyexTM, the initial part of the breakthrough

curves appear as though some cells/cell debris or some 'degraded' adsorbent particles were coming off the bed column at the onset of the effluents.

Unlike the regenerated Nyex™ particles and as expected, the fresh adsorbents curve has a breakthrough curve more closely to a sigmoidal shape. Nonetheless as depicted in figure 4.61, it appeared that after the initial coming of 'the particles' through the column for the regenerated adsorbent (after six minutes), the breakthrough curve was quite similar to the fresh adsorbent.

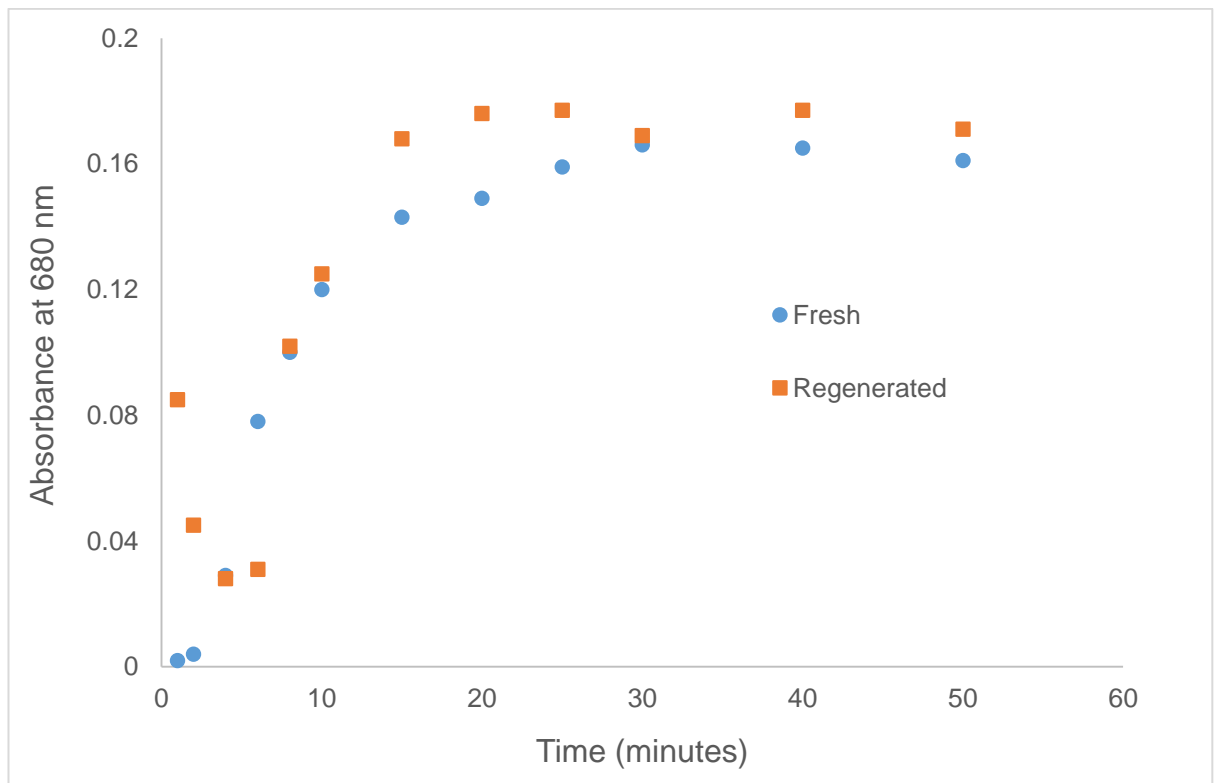


Figure 4:61: Breakthrough curves for the recovery of microalgae cells using fresh and regenerated Nyex™ particles at flow conditions ($h=20\text{cm}$, $C_o=0.3\text{ OD}$, $Q=10\text{ mL/min}$).

As a result, the regenerated adsorbents were rinsed before being used as a bed. As a control, similar to the batch system, fresh adsorbents were electrochemically treated, to recover cells from suspension in the column. As shown in figure 4.62, the behaviour of the curves at the onset of the effluents, for all the adsorbent variants, was quite similar. However, as the experiment proceeded, there was an apparent breakthrough of a higher concentration of cells through the beds of the regenerated adsorbents. This continued until the bed appeared to be exhausted. However, the breakthrough of microalgae cells through the beds of ETC treated and the fresh Nyex™ particles behaved similarly, almost to the degree of having exactly the same

breakthrough characteristics. One point of note is that the rinsing of the regenerated adsorbent seems to improve its breakthrough characteristics, contrary to that in figure 4.61.

However, more noteworthy, is that unlike the batch systems, the electrochemical treatment of either the loaded or fresh Nyex™ particles, confer no significant enhancement to the adsorptive capacity of the adsorbent particles. In fact, the fresh Nyex™ appears to have a higher bed capacity than the regenerated, which is contrary to the batch system where the capacity of the latter was a lot higher than that of the former.

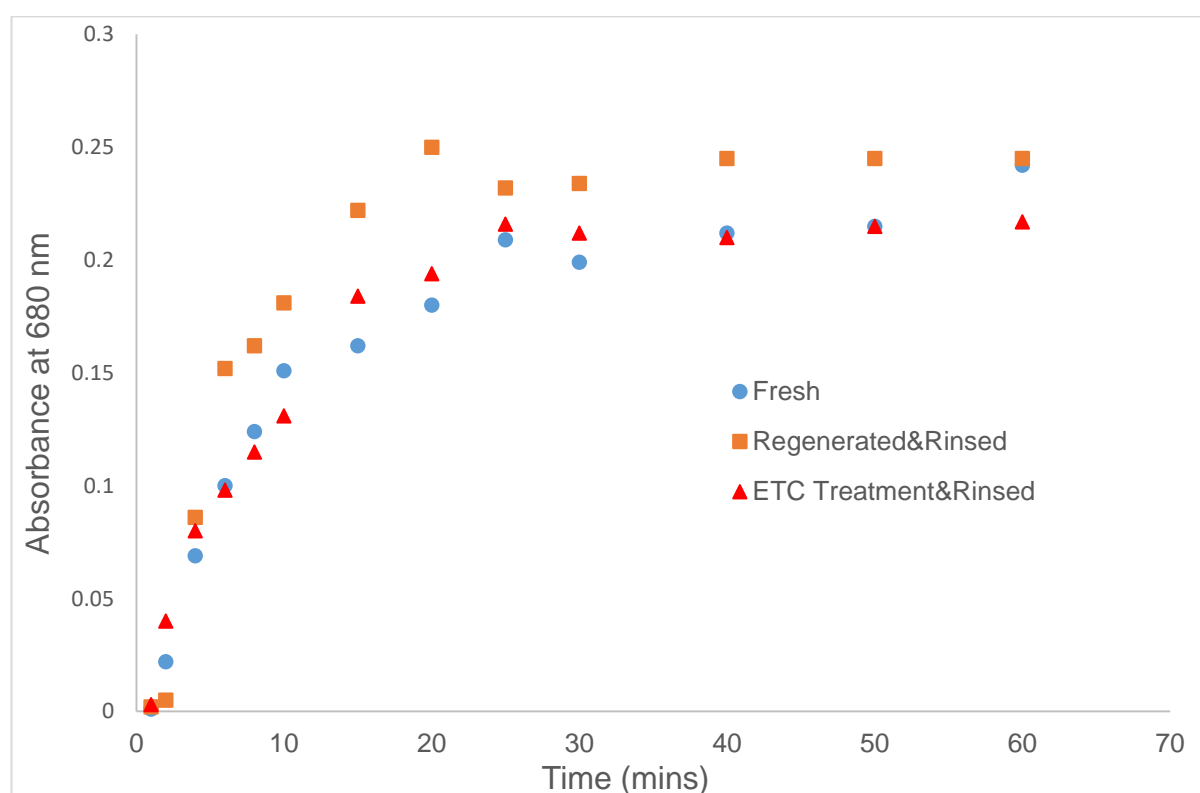


Figure 4.62: Breakthrough curves for the recovery of microalgae cells using fresh, electrochemical treated fresh and regenerated Nyex™ particles at flow conditions ($h = 20\text{cm}$, $C_o = 0.3\text{ OD}$, $Q = 10\text{ mL/min}$).

A control investigation carried out with adsorption of AV 17 dye with fresh and regenerated adsorbents (initially loaded with the dye) revealed an interesting observation, contrary to observations with microalgae cells. As illustrated in figure 4.63, the breakthrough curves of fresh and regenerated adsorbents behaved similarly, showing nearly identical breakthrough characteristics. To further emphasize the effects on electrochemical regeneration, a loaded (spent & rinsed)

Nyex™ bed used to adsorb the dye solution show breakthrough characteristics that were extremely steep; which demonstrates the presence of the initially adsorbed dye still retained on the Nyex™ particles.

The differences in the characteristics of breakthrough curves for regenerated adsorbents with microalgae cells and dye could be as a result of the differences in the electrochemical effects on the adsorbates. For instance, the electrochemical oxidation reaction of AV 17 dye can be represented thus;

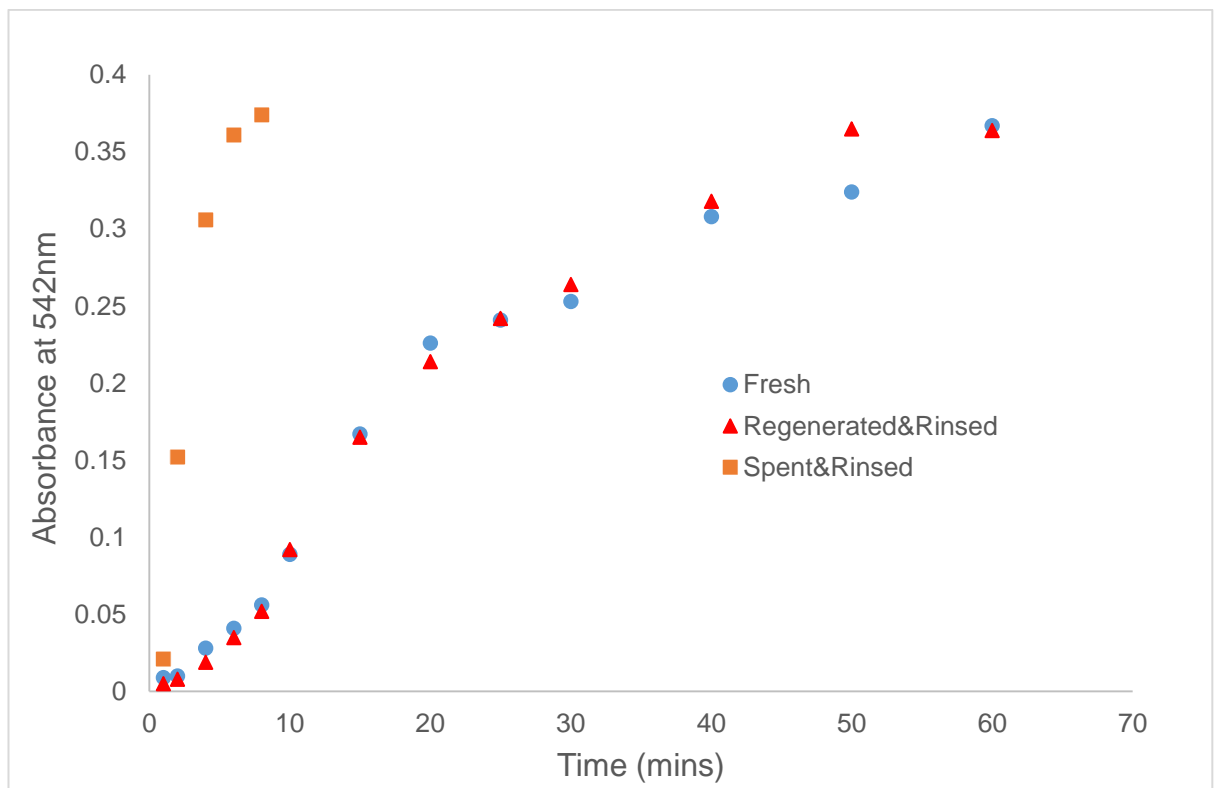
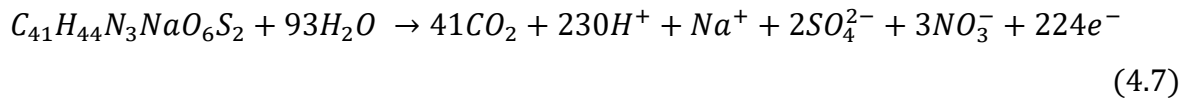


Figure 4:63: Breakthrough curves for dye adsorption using fresh, regenerated, loaded (Spent&Rinsed) Nyex™ particles at conditions ($h = 5$ cm, $C_o = 0.3$ OD, $Q = 10$ mL/min).

Equation 4.7 describes an electrochemical regeneration of Nyex™ particles, loaded with dye, but results in the destruction of the dye thereby giving off CO_2 , similar to the general expression stated in equation 4.6. Therefore, resulting in a complete reactivation of the adsorbent such that when used again, it behaves similarly to a fresh batch of adsorbent. In contrast, the regeneration of Nyex™ particles, loaded with microalgae cells, may result to broken cells and/or released intracellular materials such as lipids still occupying the active adsorption sites of the Nyex™

particles. Hence, a ‘true’ reactivation of the adsorbent may not be achieved in this case. Unlike the batch system, it appears that the bed column does not benefit significantly from the changes in the surface chemistry of the Nyex™ particles after an electrochemical treatment. Curiously, it begs the question of whether alteration(s) to the surface chemistry of the Nyex™ particles is only responsible for the higher capacity experienced with batch systems.

As a consequence, the effects of material degradation, caused by electrochemical treatment of the adsorbent, was investigated. This was simulated using different size variations of the Nyex™ particles.

4.4.6 Effects of Nyex™ particles size variation on cells recovery

Figures 10.64 and 10.65 depict the total cells adsorbed and the percentage recovery when the size fraction variants of Nyex™ particles were used to adsorb microalgae cells within a batch system. Different size fractions of Nyex™ particles, obtained as described in section 3.5.8, were used to simulate the degradation effects of Nyex™ particles after regeneration. The aim was to understand the effect of such degraded particles on the recovery of microalgae cells from suspension when they are reused.

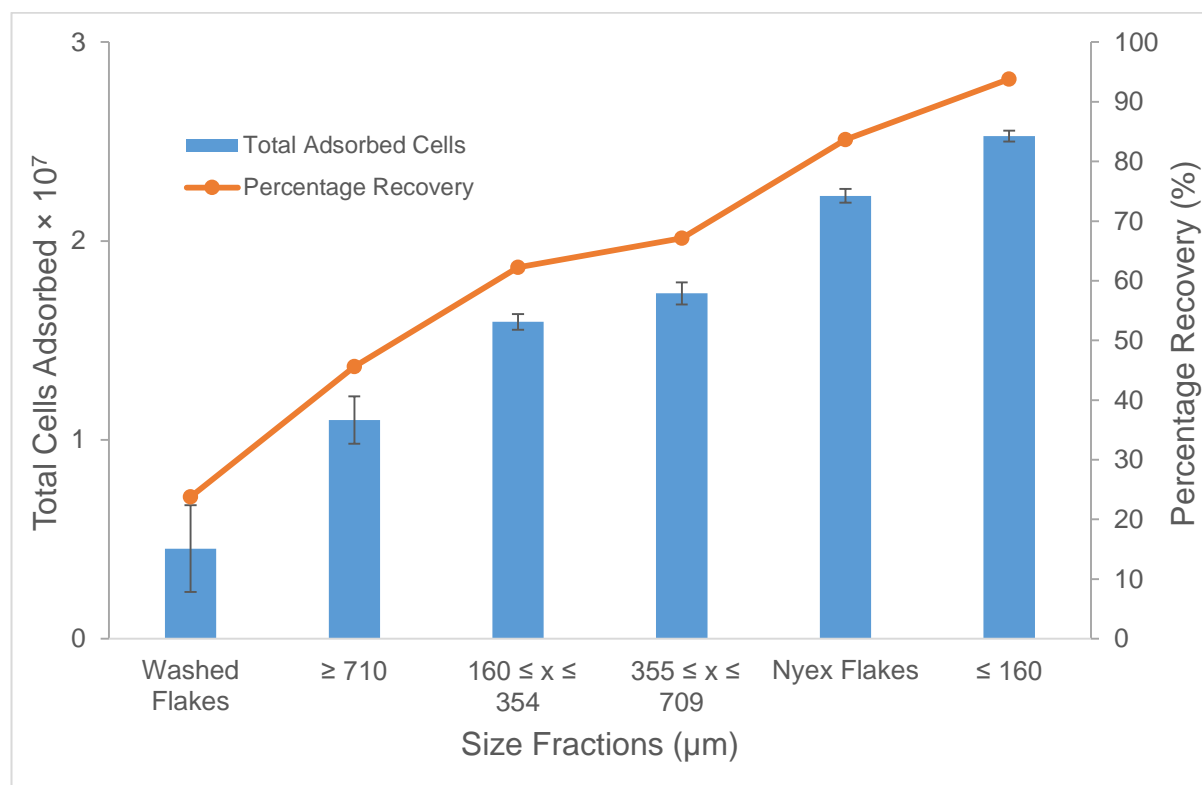


Figure 4:64: The total cells adsorbed and percentage recovery when cells were recovered from suspension using different size fractions of the Nyex™ particles.

As evidently illustrated in figures 4.64 and 4.65, the total adsorbed cells and the percentage recovery of cells from suspension was highest for the size fraction less than 160 μm . Even though in each of the figures shown (difference was in the concentration of cells in suspension and number of Nyex™ variants), the order of variants performance was inconsistent.

Nonetheless, the percentage recovery for size fraction less than 160 μm were 93.8% and 99.3% as shown in figures 4.64 and 4.65 respectively. In addition, the percentage recovery for size fractions greater than 710 μm consistently was much lower, being about 46% in each case study. Interestingly, the unwashed Nyex™ particles also performed significantly well, attaining a percentage recovery of more than 80% in each scenario. The reason for this high recovery may have to do with the presence of smaller size fractions that aided the adsorption of microalgae cells.

Surprisingly, the washed Nyex™ particles had the least percentage recovery, being 23.7% and 31.8% respectively for the case studies investigated. Without a shadow of doubt, this appears to be largely linked to the removal of the smaller size fractions that were rinsed off during the washing of Nyex™ particles. It could as well be that the washing reduces the acidity effects of the Nyex™ particles, which have been shown to enhance cell recovery from suspension (see section 4.2).

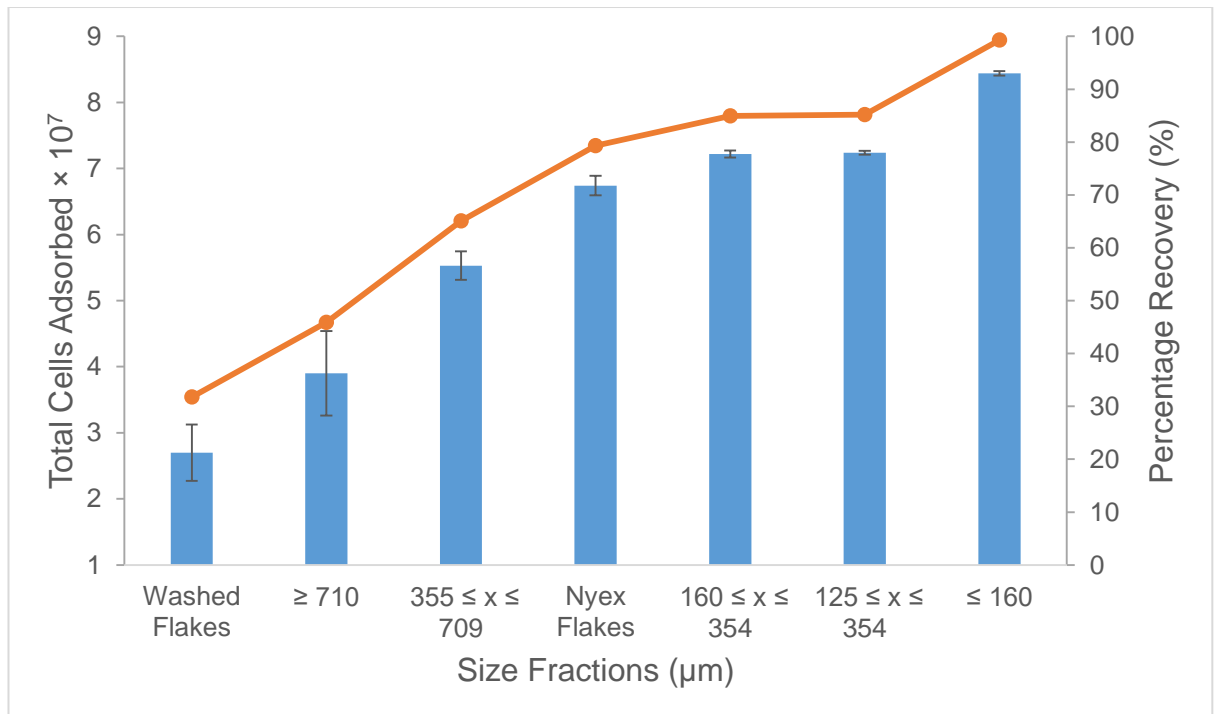


Figure 4:65: The total cells adsorbed and percentage recovery when cells were recovered from suspension using different size fractions of the Nyex™ particles.

Interestingly, microscopic images as presented in figures 4.66 (A) – (D) revealed that not only do the smaller size fractions settle quicker, they also have a less intense colour effect on the microalgae suspension. In other words, the settling of the smaller size fractions of the Nyex™ particles as well as their decolouration of the supernatant differ completely from the perception that the presence of fines or smaller size fractions of Nyex™ particles is undesirable for adsorption studies.



Figure 4:66: Microscopic images of microalgae suspension samples on haemocytometer before adsorption (A) and after adsorption procedure with Nyex™ particles with size less than 160 μm (B), unwashed (C) and washed (D) variants. Green and red oval shapes show some microalgae cells and Nyex™ particles on the haemocytometer slides respectively.

The clear microscopic images (see figure 4.66B) of the haemocytometer for Nyex™ particles with a size less than 160 μm attest to the 99% cell recovery measured as well as their better settling characteristics. Curiously, as apparent in figure 4.66(D),

the so called washed Nyex™ particles left more of the adsorbent particles in suspension, which further confirms their poor settling characteristics. In contrast, unwashed Nyex™ particles were better adsorbents as well as settling quicker, as shown in figure 4.66(C).

This observation does not seem to agree with what is widely accepted; which is the need to wash Nyex™ particles in order to limit colouration (intense greyish colour) of the supernatant and improve settling features of the adsorbents.

It is worthy of mention that the washed Nyex™ particles had been used throughout the research reported in this thesis. As it had always been the norm to wash off the fines and/or smaller size fractions before being employed for adsorption studies. Similar to other peculiarities, it may be that these results and observations are only typical to the use of microalgae cells as the adsorbates of interest. Nevertheless, these findings could be deployed to better optimise the use of Nyex™ particles as adsorbents in the recovery of microalgae cells.

To put it in context, the total cells adsorbed with unwashed Nyex™ particles is more than double the total cells adsorbed by the washed Nyex™ particles. So also, in comparison with Nyex™ particles with size less than 160 µm, the latter adsorbed more than three times the total adsorbed cells by washed Nyex™ particles. Coupled with their better settling characteristics, it raises the question, going forward, whether there is a need to continue to wash Nyex™ particles before being used to recover microalgae cells from suspension.

This also substantiates the fact that the improved microalgae cell recovery experienced with electrochemically treated Nyex™ particles, whether used or fresh, is prominently influenced by the adsorbents' degradation. This is because of the higher levels of Nyex™ fines created after such electrochemical treatment. With more Nyex™ fines present in the system, it implies that the surface area available for adsorption per mass of the adsorbent is greatly enhanced. Nyex™ particles with smaller size fractions have a better recover more algae cells due to more surface area available for adsorption. As evident in figures 4.65, as the size fractions of the Nyex™ particles become increase, the recovery of algae cells reduces due to their lower surface area. Also, electrochemical treatment changes the surface chemistry of the adsorbents to become more acidic; such acidic enhancement has been

demonstrated to improve cell recovery (see section 4.2). Undoubtedly, it now seems that both the alterations in the surface chemistry and the fines formation (which allows for more surface area) are predominantly responsible for the better adsorption characteristics. What remains unknown is by what degree one of the two changes contributes to the better recovery of cells.

4.4.7 Effects of Electrochemical Regeneration on Adsorbed Microalgae Cells

4.4.7.1 Physical Observation of Eluted Adsorbed Cells

As shown in figure 4.67, the effects on adsorbed microalgae cells during the regeneration of beds of Nyex™ show a distinctive difference between loaded adsorbents that were regenerated and those that were not regenerated.

After an initial adsorption with the Nyex™ bed in a column, the bed was placed in the electrochemical cell and regenerated as previously described. The regenerated bed was then re-suspended in deionised water within the column (figure 4.67B) while a control ‘used’ bed that was not regenerated was similarly suspended (figure 4.67A). The green colourisation of the deionised water is as a result of the elution of adsorbed microalgae cells (figure 4.67A). In contrast, figure 4.67B show the deionised water colour becoming grey largely as a result of the Nyex™ particles as well as the degraded adsorbent particles.

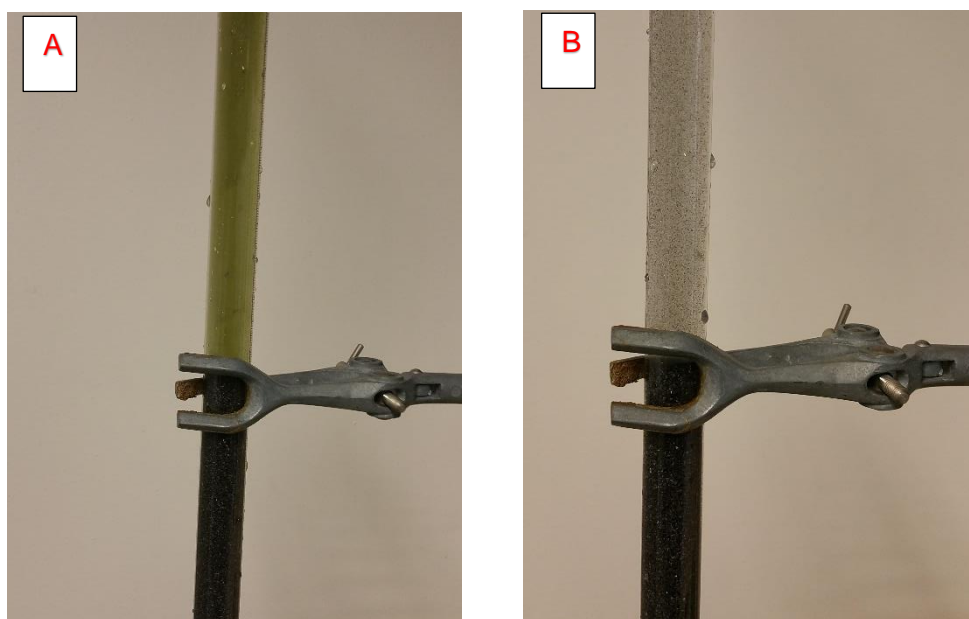


Figure 4:67: Elution of adsorbed microalgae cells from a bed of Nyex™ that (A) was not regenerated and (B) a regenerated Nyex™ bed.

4.4.7.2 Microscopic Observation of Eluted Adsorbed Cells

Furthermore, as described in section 4.4.3, eluted cells from regenerated and unregenerated Nyex™ particles were stained with Trypan blue and viewed under the microscope. As evident from the images in figure 4.68, the stained cells eluted after adsorption but before regeneration of Nyex™ were not coloured (blue/black). In contrary, the trypan blue appears to have traversed the membrane of stained cells eluted from adsorbents that were electrochemically regenerated. This lends credence to the inactivation/death of adsorbed microalgae cells that were electrochemically treated during Nyex™ regeneration.

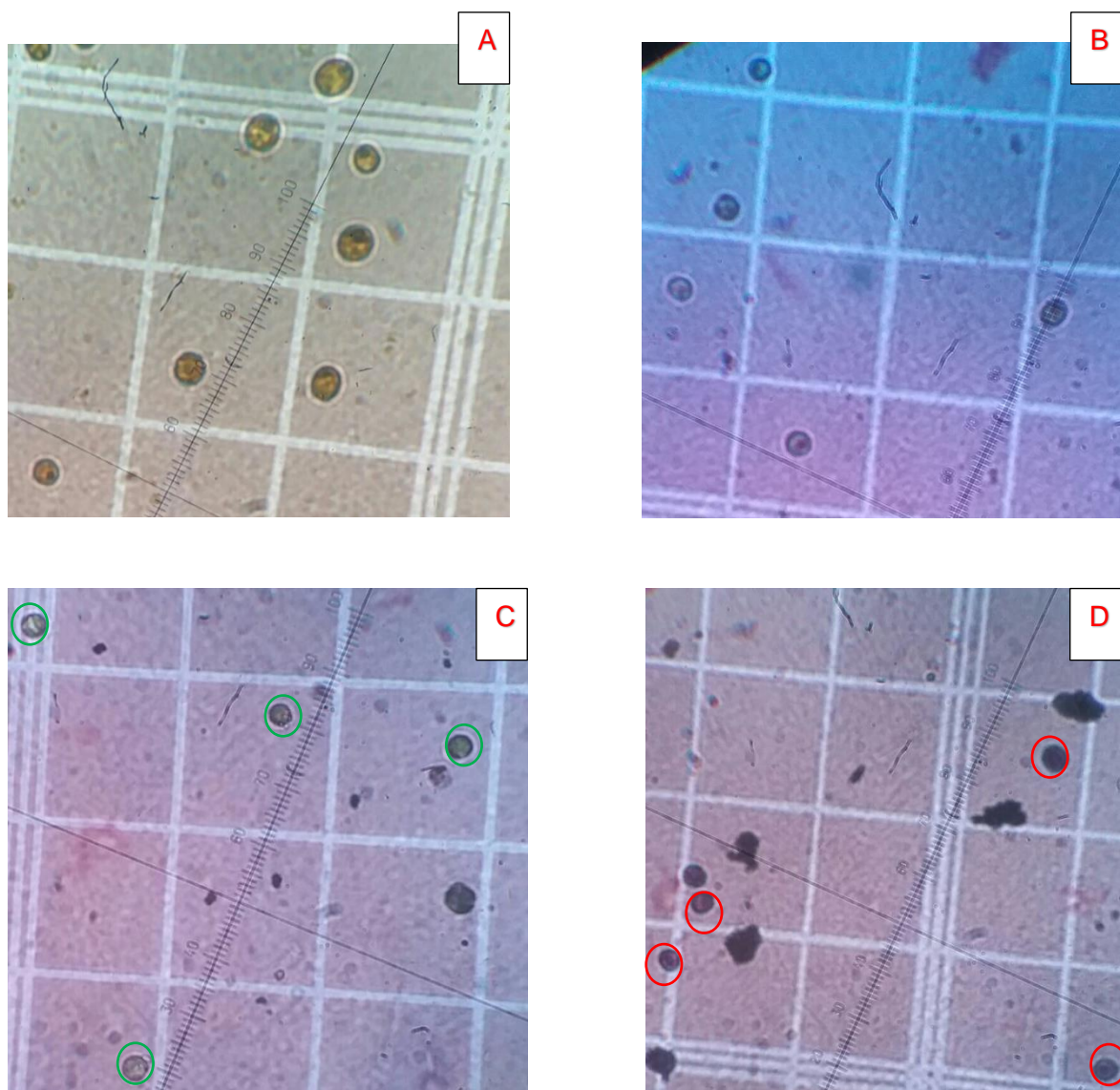


Figure 4:68: Microscopic images of microalgae cells (A) in their original suspension, stained (B) before adsorption (C), eluted and stained after adsorption (D) after electrochemical treatment. Green and Red oval shapes show living and inactivated (dead) microalgae cells respectively.

4.4.7.3 SEM Observation of Adsorbed Microalgae Cells on the Adsorbent

Scanning electron micrograph (SEM) of adsorbent samples were obtained as described in previously in Chapter 3. The scanning electron micrographs of fresh Nyex™ particles before and after adsorption show the presence of recovered microalgae cells on the adsorbent, see figures 4.69 and 4.70 respectively. While, figures 4.70 – 4.73 depict scanning electron micrographs showing cell disruption at different stages, which is thought to be due to the electrochemical treatment of the adsorbed cells during the adsorbent regeneration. Earlier works have shown that electrochemical treatment of water polluted with microbial cells can cause cell disruption (Stoner *et al.*, 1982; Paternarakis and Fountoukidis, 1990; Matsunaga *et al.*, 1992, 1994; Feng *et al.*, 2004; Diao *et al.*, 2004; Kraft, 2008; Martínez-Huitle and Brillas, 2008). No previous work has reported that cells recovered onto a non-porous adsorbent material can be ruptured during the electrochemical regeneration of the latter.

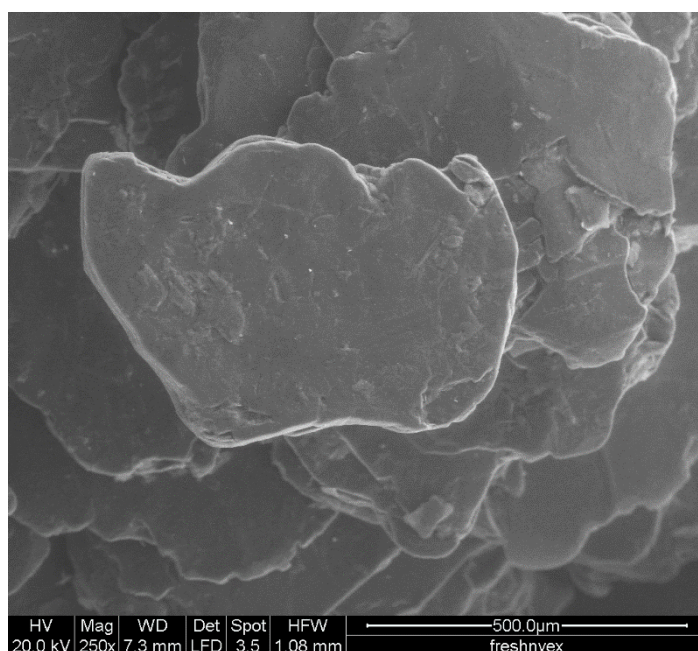


Figure 4:69: Scanning Electron Micrograph of fresh Nyex™ particles before adsorption.

For the first time, the research reported in this thesis has revealed this possibility. Although, there is no clear evidence that all the adsorbed cells were ruptured, figure 4.68D indicates that all the adsorbed cells were inactivated; a prerequisite phase before cell disruption. This is a significant finding that demonstrates the recovery of microalgae cells onto non-porous adsorbent particles and release of intracellular materials due to rupturing of the adsorbed cells. The latter was achieved during the

regeneration of the adsorbent, which shows the dual effects of electrochemical methods to reactivate adsorbents for reuse as well as causing cell wall/membrane disruption for release of intracellular materials.

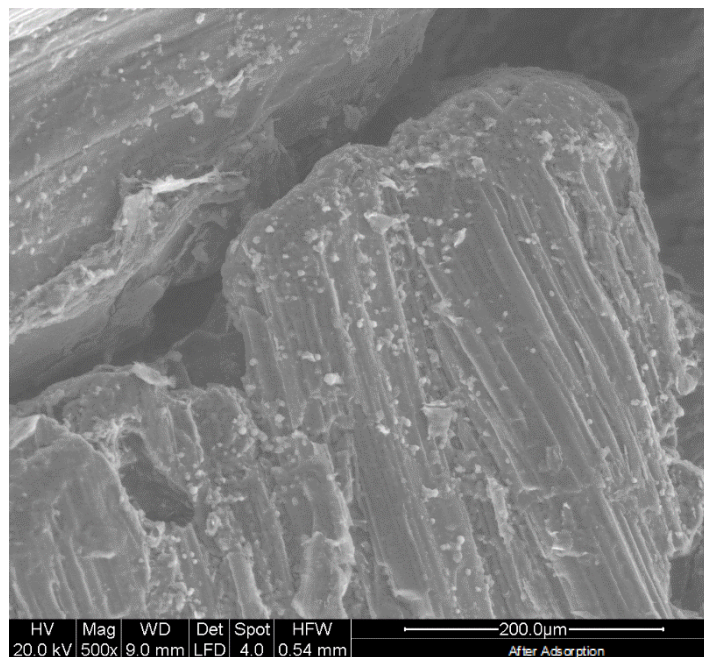
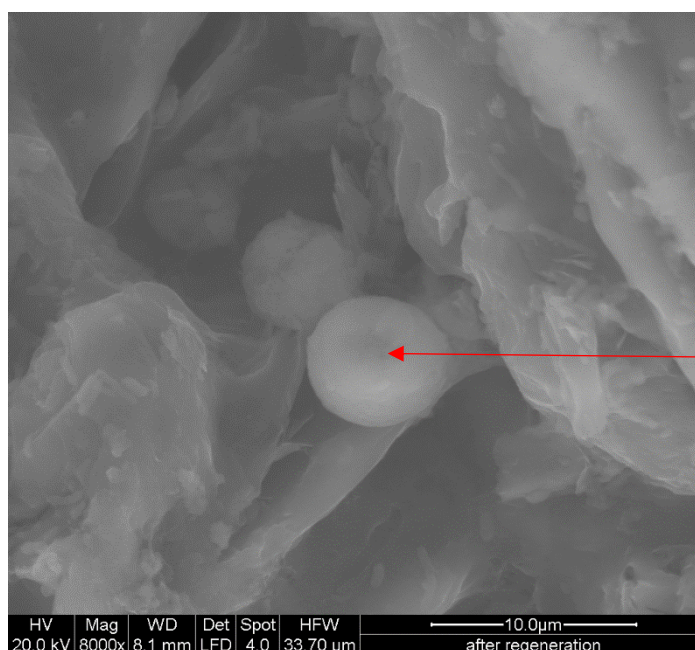


Figure 4:70: Scanning Electron Micrograph of adsorbed microalgae cells on the Nyex™ particles after adsorption.



Dimple appearance at the point of contact of cells with the adsorbent, thought to be as a result of electrochemical treatment

Figure 4:71: SEM of microalgae cells on the Nyex™ surface after regeneration shows dimple at point of contact with the adsorbent which could be due to movement of electrons.

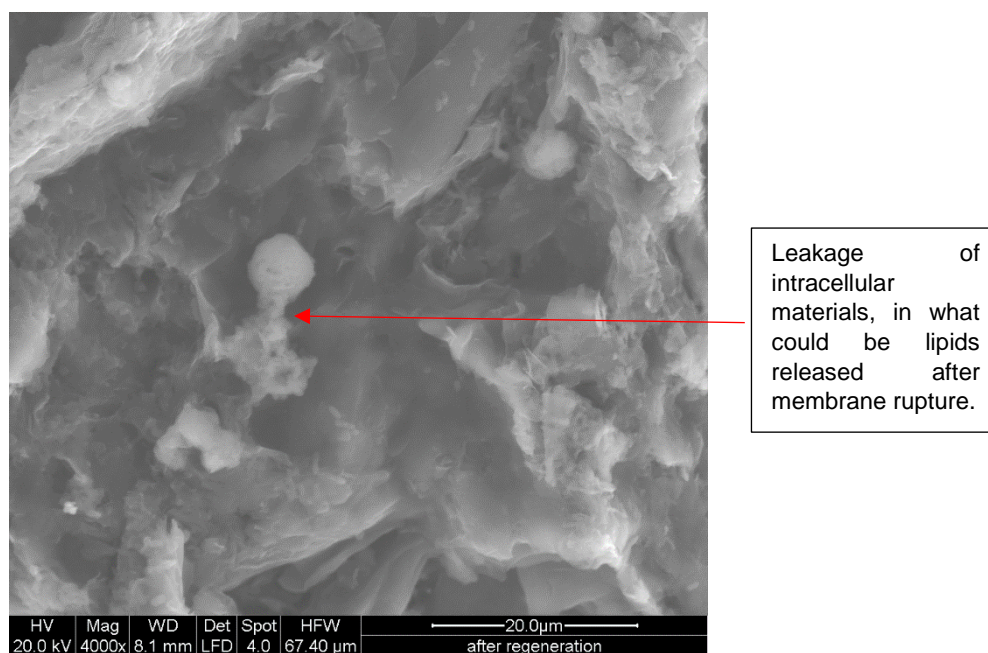


Figure 4:72: SEM of microalgae cells on the Nyex™ surface after regeneration shows what appears to be release of intracellular material due to cell lysis.

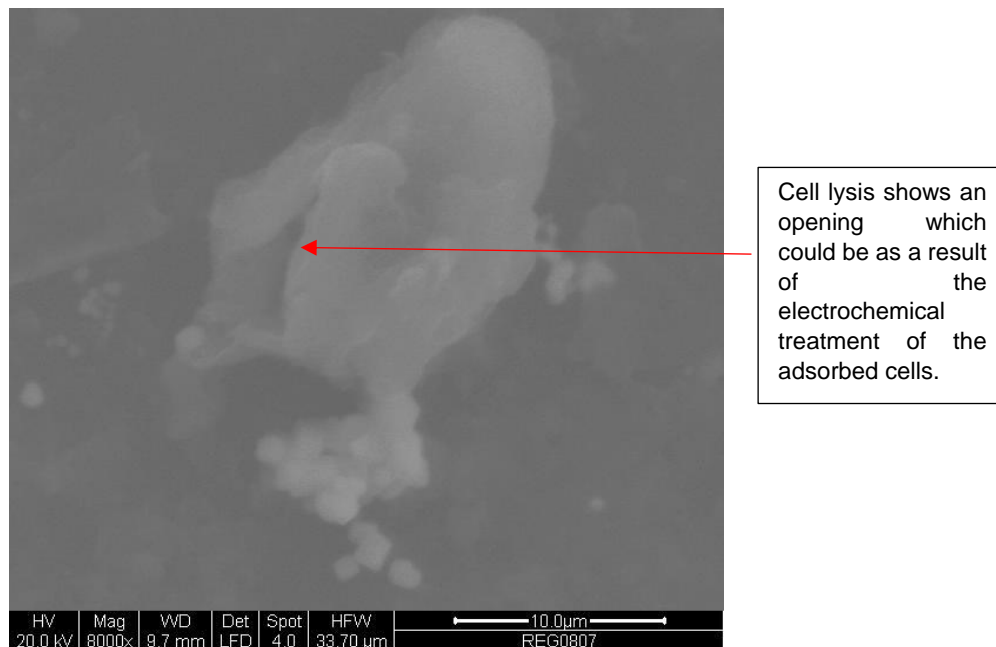


Figure 4:73: SEM of a microalgae cell on the Nyex™ surface after regeneration of the adsorbent shows what appears to be the result of cell lysis.

4.4.8 Lipid Recovery Analysis

This was undertaken as described in Chapter 3 to demonstrate whether the inactivation and/or disruption of cells resulted in release of intracellular materials such as lipids.

Figure 4.74 revealed the significance of using the appropriate solvent to wash off any lipids on the adsorbent material. As evident from figure 4.74, the use of deionised water and ethanol was unsuccessful in quantifying any lipids present regardless of the process stage; this might suggest the limitation of using water and ethanol to ‘wash off’ any lipids present.

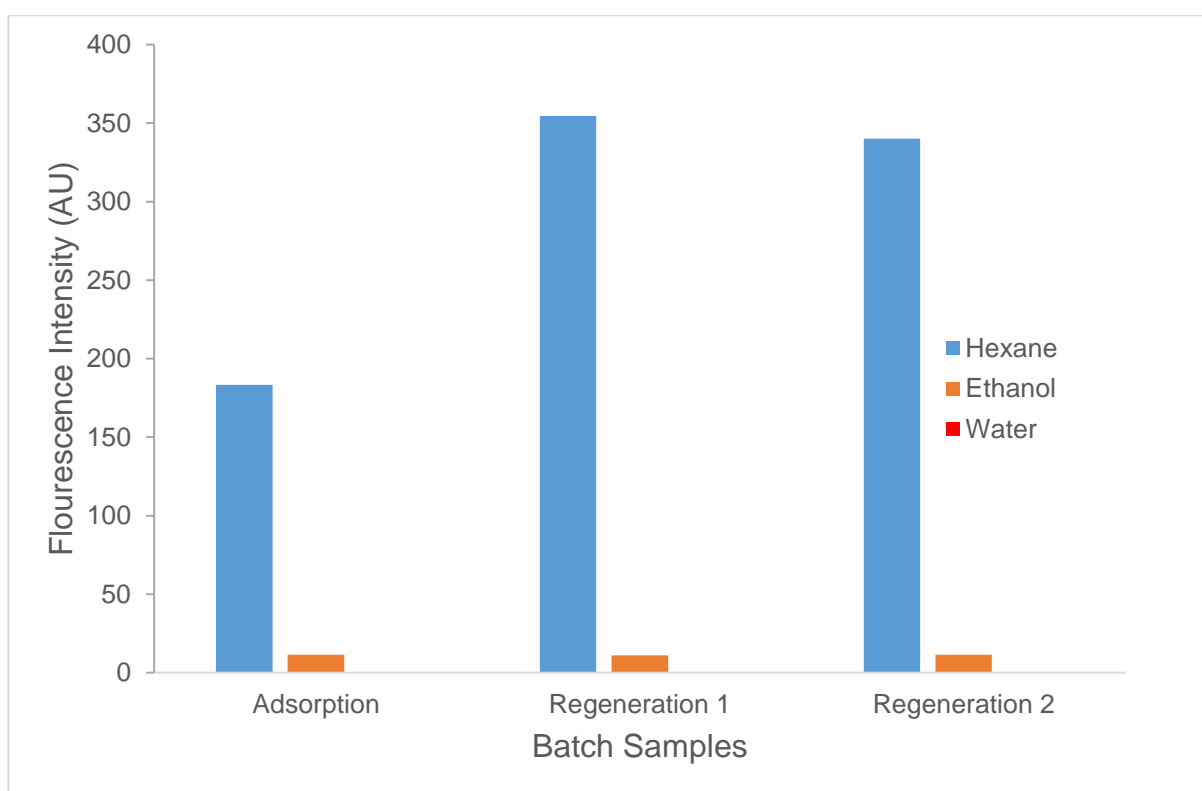


Figure 4:74: Fluorescence intensity of batch samples of Nyex™ particles loaded with microalgae cells after being in contact with a variety of solvents.

Conversely, the use of hexane shows the presence of lipids on the Nyex™ surface. More important is the amount of lipids present after adsorption and after electrochemical treatment of the adsorbed cells during adsorbent regeneration. After the latter, the quantity of lipids present was almost twice the lipids before the adsorbent particles were regenerated. This further lends credence to the disruption of the membrane of the adsorbed cells during the electrochemical regeneration of the Nyex™ particles. In the same vein, figure 4.75 demonstrates that electrochemical treatment of the adsorbed cells was required to improve lipid

recovery. However, the figure also revealed that the optimum current density sufficient to regenerate the adsorbent as well as inactivating/ disrupting the cells resulted in the least amount of lipids recovered.

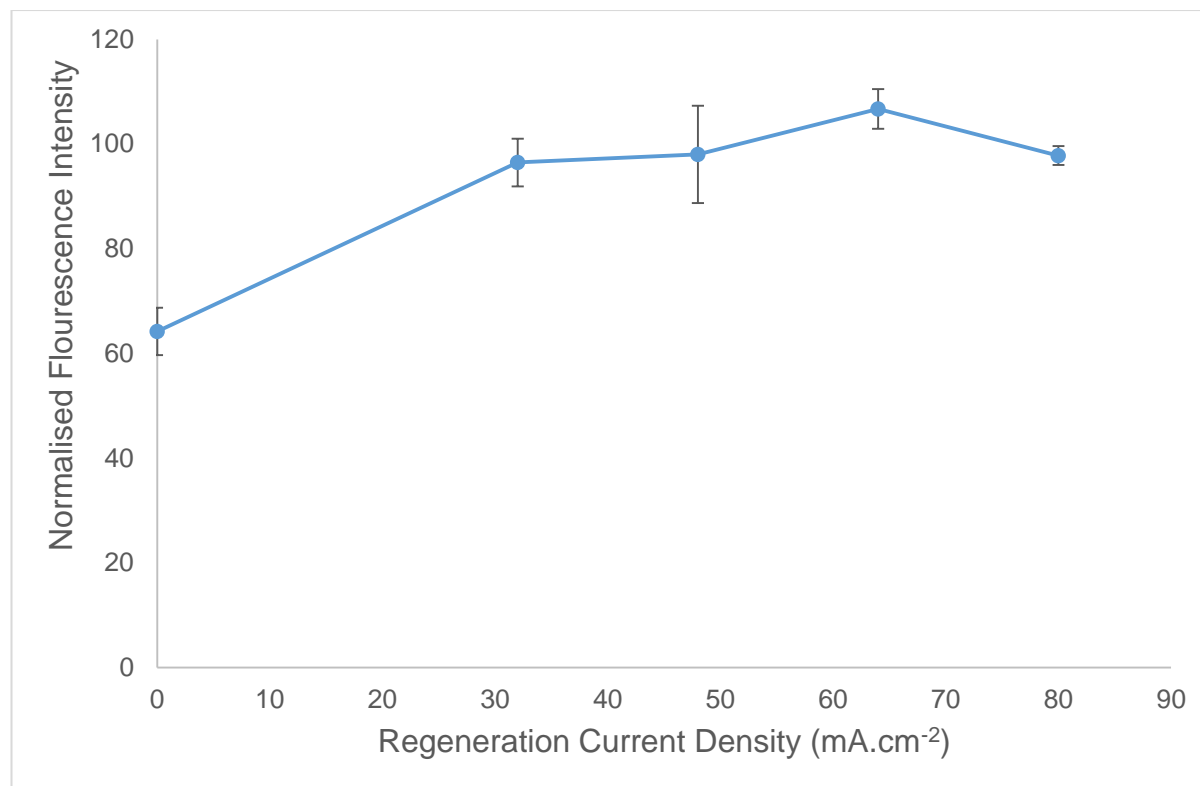


Figure 4:75: Normalised Fluorescent intensity of batch samples of Nyex™ particles loaded with microalgae cells after being regenerated at different current densities and in contact with hexane.

The amount of lipids recoverable continued to increase with increasing current density until 64 mA.cm⁻², beyond which the amount of lipids recovered decreased. This could be due to a possible ‘oxidation/burning’ of the released lipids when the current density is relatively high.

At a current density of 64 mA.cm⁻², concentration of lipids quantified was about 30 µg/mL in hexane. Compared to lipid extractions reported in the literature, this represents a very low recovery (Halim *et al.*, 2011; Mercer and Armenta, 2011; Prabakaran and Ravindran, 2011; Lee *et al.*, 2010; Cooney *et al.*, 2009; Halim *et al.*, 2012; Rawat *et al.*, 2013; Gerardo *et al.*, 2015). This shows that more research is needed to further explore this aspect of the process in order to recover reasonable level of lipids for biofuels applications.

4.4.9 Summary

Typically, after an adsorption procedure, preference is given to regeneration of the adsorbent for reuse; this is a more economical and environmentally friendly option. While such regeneration has been established in the literature for organic pollutants, the same is not the case when microalgae cells are the adsorbate.

The electrochemical regeneration of the adsorbent often leads to the destruction of the adsorbed organics (through anodic oxidation), in contrast, such a 'destruction' is not feasible with microalgae cells. This also makes it difficult to represent and estimate the theoretical number of electrons required to regenerate adsorbents used to recover cells. Through a more tedious route, it was established in the research reported in this thesis that a current density of 32 mA.cm^{-2} was sufficient to regenerate the adsorbent particles and reuse them to achieve a maximum cell recovery. It was also discovered that the electrochemical treatment of fresh adsorbent enhanced cell recovery in comparison to fresh adsorbent that was not electrochemically treated. Unlike in a batch system, the reuse of the regenerated adsorbent in a fixed bed column does not enhance the recovery of cells. In fact, it appears that fewer cells were recovered in a column with regenerated adsorbent; an observation believed to be peculiar to the adsorbates being microalgae cells.

A process strategy where it was possible to regenerate the adsorbent at a lower energy consumption was also suggested. This was discovered through a comparison between keeping the electrical charge constant and varying the electrical energy and vice versa. The investigation revealed that electrical charge passed was the driving force to regenerate the adsorbent particles. Furthermore, variants of NyexTM size fractions were used to demonstrate the beneficial effects of NyexTM regeneration plus the need to halt washing adsorbent before it was used to recover microalgae cells.

For the first time, the research revealed the potential of rupturing the membrane of microalgae cells during the NyexTM particles regeneration. Other than by using SEM micrograph to validate the cell wall/membrane rupture, a hexane extraction was also used to 'wash off' lipids released onto the surface of the NyexTM particles. The highest recovery (*circa* $30 \text{ }\mu\text{g/mL}$) was at 64 mA.cm^{-2} , above which there was no increase in lipids released.

5 Modelling the Recovery of Microalgae Cells in a Fixed Bed Column

5.1 Introduction

The experimentation involved in the recovery of microalgae cells within a fixed bed column was outlined in the previous chapter. It was necessary to obtain breakthrough curves that provide the principal information required to design an adsorption column system for industrial applications. Breakthrough curves can be obtained via two main approaches; laboratory investigations and mathematical modelling. The former can be time-consuming as well as being economically undesirable, whilst the latter is more straightforward. However, models must be validated, for which extensive experimentation is required. Hence, the preference for mathematical modelling as a powerful and robust tool over laboratory studies must always be tempered by the need for such models to be realistic.

Validation of the model is implemented on the basis of the data collected from the laboratory trials. A number of mathematical models have been employed to represent and predict the dynamics of a fixed bed column in the liquid or gaseous phase. These models have been successfully applied to describe the adsorption processes that entailed the removal of a solute (either in the gaseous or liquid phase), usually with a porous material being the adsorbent. The application of these models to characterise and predict the dynamics of the removal of microalgae cells by non-porous adsorbent particles has not been reported in the literature. As a consequence, this chapter presents an interesting opportunity to investigate the suitability of these models for such an adsorption system.

The models used to describe the experimental investigations carried out in this research include the Bohart-Adams, the bed depth service time (BDST), the Thomas, the Clark and the modified dose response (MDR) models. The literature is replete with other models, but as will be shown in the research reported in this thesis, some of these models should not be considered as separate and independent models. Quite a number of articles have been published where researchers report parameters from these variant models and compare their capabilities; even though their parameters can easily be calculated from one another. Hence, this chapter will also attempt to show this misconception using the microalgae/NyexTM adsorption system.

To achieve the aforementioned, different approaches were considered, which involved conventional linear and non-linear regression analysis of the models considered in this research. A comparison between the solutions obtained from linear and non-linear regression analysis of the models is also discussed in this chapter. Furthermore, due to the depression of the breakthrough curves experienced in this research study (as discussed in section 4.3), an alternative approach to 'fitting' a model such as Bohart-Adams to the experimental data is considered.

Ultimately, the aim was to find a suitable model that sufficiently describes the dynamics involved in the recovery of the microalgae cells using a non-porous adsorbent in a column. The identification of such a model would ensure that the breakthrough curves of the microalgae/NyexTM adsorption system could be successfully predicted for industrial applications without the need for experimentation.

5.2 Fixed bed process models

The adsorption mechanisms in a column are typically divided into four phases, namely;

- I. Bulk solution transport; mass transfer of adsorbates from the liquid phase to the boundary layer surrounding the adsorbent particle through convective mass transfer and/or molecular diffusion.
- II. Film diffusion transport; transport of the adsorbates through interface diffusion between the exterior surface of the adsorbent and the liquid phase.
- III. Pore transport; intrapellet mass transfer of the adsorbates through the adsorbent pores to available adsorption sites through either pore diffusion or surface diffusion.
- IV. Adsorption; attachment of the adsorbate to the adsorbent occurs along with the possibility of some desorption (Faust and Aly, 1998; Hammer, 2008; Crini and Badot, 2010; Goshadrou and Moheb, 2011).

The transport processes in a fixed bed column are governed by the equations derived from the material balances between the solid and the fluid.

The differential mass balance equation is often written in the form;

$$u \frac{\partial C}{\partial z} + \varepsilon \frac{\partial C}{\partial t} + (1 - \varepsilon) \rho_p \frac{\partial q}{\partial t} = D_L \frac{\partial^2 C}{\partial z^2} \quad (5.1)$$

Where the initial and boundary conditions are given by

$$t = 0, C = q = 0; \quad z = 0, \frac{D_L}{u} \frac{\partial C}{\partial z} = C - C_o; \quad z = Z, \frac{\partial C}{\partial z} = 0$$

In equation 5.1, u is the superficial velocity, C is the adsorbate concentration in the liquid phase, ε is the void fraction of the bed, z is the axial coordinate, D_L is the axial dispersion effect, Z is the bed height, ρ_p is the adsorbent density and q is the adsorbate concentration on the adsorbent.

The first term of equation 5.1 depicts the convective flow within the bed, while the second term represents adsorbate accumulation in the fluid phase, and the third term symbolises the rate of adsorption, which depends largely on the adsorption mechanism(s). The last term in on the right hand side of equation 5.1 represents the axial dispersion within the fixed bed. If plug flow is assumed, the effect of the axial dispersion can be neglected, hence equation 5.1 becomes,

$$u \frac{\partial C}{\partial z} + \varepsilon \frac{\partial C}{\partial t} + (1 - \varepsilon) \rho_p \frac{\partial q}{\partial t} = 0 \quad (5.2)$$

Together with equation 5.2, an adsorption isotherm equation as well as a suitable adsorption rate equation that relates $\frac{\partial q}{\partial t}$, C and q are required for the modelling of a fixed bed column. As a result, a number of mathematical models have been developed to enable the prediction of the dynamic behaviour of a fixed bed column and this allows estimation of some kinetic coefficients to be achieved (Hand *et al.*, 1984; Crittenden and Thomas, 1998; Crini and Badot, 2010; Xu *et al.*, 2013). The various key models considered in this research are discussed below;

5.2.1 The Bohart-Adams Model

The equations representing a breakthrough curve were established by Adams and Bohart in 1920. The model postulates that the rate of adsorption is proportional to the concentration of the adsorbate in the bulk fluid and the residual capacity of the adsorbent (Bohart and Adams, 1920). Their original work investigated the

adsorption of chlorine gas with charcoal, nevertheless, the approach developed has been successfully applied to a number of other adsorption systems, which include dyes (Walker and Weatherley, 1997; Namasivayam and Kavitha, 2002) phenols (Wolborska, 1989; Aksu and Gönen, 2004) heavy metals (Yan *et al.*, 2001; Goel *et al.*, 2005; Maji *et al.*, 2007) and protein purification (Hashim and Chu, 2007). The two mass transfer rate equations obtained were;

$$\frac{\partial q}{\partial t} = -K_{BA}q_r C \quad (5.3)$$

$$\frac{\partial C}{\partial z} = -\frac{K_{BA}qC}{u} \quad (5.4)$$

Where K_{BA} is the kinetic constant ($l/mg/min$) and q_r is the residual adsorptive capacity.

The analytical solution to equation 5.2 when combined with equations 5.3 and 5.4 as derived by Bohart and Adams is given by;

$$\frac{C_t}{C_o} = \frac{\exp(K_{BA}C_o t)}{\exp(K_{BA}C_o t) + \exp\left(\frac{K_{BA}N_o Z}{U}\right) - 1} \quad (5.5)$$

The two exponential terms in the denominator are considered to be generally much greater than 1, hence the term “1” in the denominator can be ignored. Also, by dividing the right-hand side of equation 5.5 with $\exp(K_{BA}C_o t)$, the equation can be simplified to;

$$\frac{C_t}{C_o} = \frac{1}{\exp\left(\frac{K_{BA}N_o Z}{U} - K_{BA}C_o t\right) + 1} \quad (5.6)$$

In addition, the equation can also be rearranged, and by taking the natural logarithm of both sides gives a linearised expression as;

$$\ln\left(\frac{C_o}{C_t} - 1\right) = \frac{K_{BA}N_o Z}{U} - K_{BA}C_o t \quad (5.7)$$

The parameters of the Bohart-Adams model can be determined from equation 5.7 by relating the equation to that of a straight line given as;

$$y = mx + C \quad (5.8)$$

So that when $\ln(\frac{C_o}{C_t} - 1)$ is plotted against t , the slope equals $-K_{BA}C_o$, and K_{BA} can be estimated with C_o known. Likewise, the intercept equals $\frac{K_{BA}N_oZ}{U}$, so that N_o can also be estimated.

5.2.2 The Bed Depth Service Time (BDST) Model

Hutchins (1973) reportedly simplified equation (5.7) by proposing a linear relationship between the service time, t and the bed height, Z given as (Hutchins, 1973);

$$t = \frac{N_o}{C_o U} Z - \frac{1}{K_{BA} C_o} \ln\left(\frac{C_o}{C_t} - 1\right) \quad (5.9)$$

Equation 5.9 is referred to as the bed depth service time (BDST) model (Walker and Weatherley, 1997). For the research reported in this thesis, t has been taken as the time for the adsorbent bed to attain a predetermined saturation percentage.

The critical bed depth, Z_o is the theoretical minimum height of the adsorbent particles to ensure that the effluent concentration does not exceed a predetermined value.

To determine the breakthrough concentration at time $t = 0$, equation 5.9 can be rearranged to give the critical bed depth, Z_o as

$$Z_o = \frac{U}{K N_o} \ln\left(\frac{C_o}{C_b} - 1\right) \quad (5.10)$$

The BDST as stated by equation 5.9 can be simplified to

$$t = AZ - B \quad (5.11)$$

Where $A = \frac{N_o}{C_o U}$ and $B = \frac{1}{K_{BA} C_o} \ln\left(\frac{C_o}{C_t} - 1\right)$

From equation 5.11, the amount of adsorbent particles (measured by the bed height) for a predetermined service time can be estimated and vice versa, if parameters ' A ' and ' B ' are known for different adsorption systems.

The slope in equation 5.11 can be used to predict the bed performance for other initial concentrations C'_o , given as

$$A' = A \frac{C_o}{C'_o} \quad (5.12)$$

Where A' is the slope for the new initial concentration C'_o , a new equation similar to equation 5.11 can be derived by also estimating its corresponding B' given as

$$B' = B \frac{C_o \ln(\frac{C'_o}{C_B} - 1)}{C'_o \ln(\frac{C_o}{C_B} - 1)} \quad (5.13)$$

Where C'_B is the 'new' breakthrough concentration of the new initial concentration C'_o . So that the new equation becomes

$$t' = A'Z' - B' \quad (5.14)$$

Where t' and Z' are the new service time and bed height required to predict the breakthrough curve for the new adsorption system.

Similarly, if different flowrates are applied, the slope can be estimated from equation 5.12. Changes in the flow rate have been reported not to have an effect on the intercept, b , hence it remains unchanged (Ko *et al.*, 2000; Kundu and Gupta, 2007; Han *et al.*, 2009).

5.2.3 The Thomas Model

The Thomas model (Thomas, 1944) assumes that adsorption can be defined by a pseudo second-order reaction rate equation given as

$$\frac{\partial q}{\partial t} = k_1 C(q_m - q) - k_2 q \quad (5.15)$$

Where q_m is the adsorbent capacity, k_1 is the second-order forward rate constant and k_2 is the first-order reverse rate constant. At equilibrium ($\frac{\partial q}{\partial t} = 0$), equation 5.15 reduces to the Langmuir isotherm model.

$$q = \frac{q_m b C_e}{1 + b C_e} \quad (5.16)$$

Where $b = \frac{k_1}{k_2}$, hence, equation 5.15 can be expressed as

$$\frac{\partial q}{\partial t} = k_1 [C(q_m - q) - \frac{q}{b}] \quad (5.17)$$

Thomas (1944) neglected the axial dispersion and also assumed that external resistance and intra-particle diffusion during the mass transfer processes were negligible to derive the analytical solution of equation 5.17 when combined with equation 5.2 (Thomas, 1948). The solution derived for the Thomas model has been given by elsewhere (Chu, 2010).

If b in equation 5.17, is sufficiently large, q/b can be neglected and such simplification reduces the equation to equation 5.3. Where $(q_m - q)$ is the same as the residual capacity q_r . Likewise, if the adsorption isotherm is considered to be highly favourable, equation 5.16 reduces to the rectangular isotherm. As a result, the Bohart-Adams and Thomas models give very similar solutions (Chu, 2004; Hashim and Chu, 2007). The Bohart-Adams model can therefore be regarded as a limiting form of the Thomas model. Hashim and Chu (2007) reported that these two models gave identical breakthrough curves for protein adsorption because of the highly favourable equilibrium behaviour of such an adsorption system.

The Thomas model is widely used and reported as being of the following equation

$$\frac{C_t}{C_o} = \frac{1}{\exp\left(\frac{K_T q_o M}{Q} - K_T C_o t\right) + 1} \quad (5.18)$$

The linearised form is given as

$$\ln\left(\frac{C_o}{C_t} - 1\right) = \frac{K_T q_o M}{Q} - K_T C_o t \quad (5.19)$$

But as shown in the research reported in this thesis, equations 5.18 and 5.6 are mathematically indistinguishable and have parameters that are interchangeable. In fact from equations 5.7 and 5.19, it is evident that the linearised form would fit the same graph. Yet, a number of studies have reportedly compared the solutions and parameters of both Bohart-Adams and Thomas models (Aksu and Gönen, 2004; Han *et al.*, 2007; Kundu and Gupta, 2007; Borba *et al.*, 2008; Zhang *et al.*, 2011).

5.2.4 The Clark Model

Clark (1987) developed a model to predict a granular activated carbon adsorption system based on a mass transfer concept and the Freundlich isotherm (Clark, 1987). The mass transfer coefficient concept along a differential height of the column, dZ gives

$$U \frac{dC}{dZ} = K(C - C_e) \quad (5.20)$$

Where K , is a mass transfer coefficient (min^{-1}) and U is the flow rate of the suspension to be treated per unit cross-sectional area ($\text{m}^3 \text{min}^{-1} \text{m}^{-2}$). Equation 5.20 indicates the rate of adsorbate transfer over a differential height of the fixed bed.

Clark (1987) reported an ideal mass balance over the column, assuming that all the treated suspension is removed at the bottom of the column, as

$$UC = Lq_e \quad (5.21)$$

Where L ($\text{g}/\text{m}^2/\text{min}$) is the mass velocity of adsorbent to keep the mass-transfer zone stationary and q_e is the amount of the adsorbed solute per unit mass of the adsorbent.

The Freundlich isotherm between the suspension/solution and the adsorbent is given as

$$q_e = K_f C_e^{1/n} \quad (5.22)$$

Where K_f and $1/n$ are as previously defined in Chapter 6.

As reported by Clark (1987), substituting equations 5.22 and 5.21 into equation 5.20, yields an equation, which can be further simplified to;

$$\frac{dC}{C - KC^n} = R dt \quad (5.23)$$

$K = (1/K_f)^n (U/L)^n$, $R = (K/U)V$ and $V = dZ/dt$ is the adsorption zone velocity.

Integrating equation 5.23 between the breakthrough concentration, C_b and C , and between breakthrough time, t_b and t gives the following solution;

$$C = \left(\frac{C_o^{n-1}}{1 + \left[\left(\frac{C_o^{n-1}}{C_b^{n-1}} - 1 \right) \exp(rt_b) \right] \exp(-rt)} \right)^{\frac{1}{n-1}} \quad (5.24)$$

Equation 5.24 can be further simplified to

$$\frac{C}{C_o} = \left(\frac{1}{1 + I \exp -rt} \right)^{\frac{1}{n-1}} \quad (5.25)$$

Where $I = \left(\frac{C_o^{n-1}}{C_b^{n-1}} - 1 \right) \exp(rt_b)$, $r = R(n-1)$

Equation 5.25 is the generalised function of the Clark model. For a specific adsorption system in a fixed bed, values of ' r ' and ' I ' can be estimated using equation 5.25 by non-linear regression analysis, which enables the prediction of the breakthrough curve (Lee *et al.*, 2014). Alternatively, equation 5.25 can be linearised as shown below, and its parameters can be estimated as previously described.

$$\ln\left[\left(\frac{C_o}{C_t}\right)^{n-1} - 1\right] = -rt + \ln I \quad (5.26)$$

Two plots of empty bed contact times against the values ' I ' and ' r ' (determined from regression analysis) can be used to simulate pilot or full scale adsorption systems through interpolation or extrapolation depending on the column design requirements. The model is suitable for predicting the breakthrough times of adsorption systems (Aksu and Gönen, 2004; Crini and Badot, 2010; Xu *et al.*, 2013).

5.2.5 The Modified Dose Response (MDR) Model

The empirical MDR model was developed to minimise the errors that result from the use of the conventional Bohart-Adams and Thomas models, which depend on the adsorption system being studied (Yan *et al.*, 2001). Using statistical analysis of experimental data, Yan *et al.* (2001) discovered that the data fitted well to a non-linear regression model given as;

$$Y = 1 - \frac{1}{1 + \left(\frac{X}{\beta}\right)^\alpha} + \varepsilon \quad (5.27)$$

Where Y and X depict the response and dose respectively with respect to the fraction of maximum possible response. In terms of an adsorption system, Y symbolises the adsorbate removal (C/C_0), and X corresponds to V , the throughput volume from the column and ε represents a random error. Yan *et al.* (2001) reported that the parameter ' β ' indicates the throughput volume that produces half of the maximum response and ' α ' gives the slope of the regression function. The authors used a non-linear least squared method to estimate the parameters in equation 5.27, which they denoted as α_N and β_N . The Thomas model was then employed to

build a relationship between the parameters of equation 5.27 and the experimental data.

They discovered that at 50% removal, the Thomas model reduces to

$$V'_{50\%} = \frac{q_0 M}{C_o} \quad (5.28)$$

Yan et al (2001) also reported that using the Thomas model to fit data predicted by equation 5.27 revealed that the two curves intersect when $Y = 50\%$. To paraphrase, equation 5.27 and the Thomas model produce the same $V_{50\%}$ value. As a result, equation 5.27 can be re-written as

$$50\% = 1 - \frac{1}{1 + \left(\frac{V''_{50\%}}{\beta_N} \right)^{\alpha_N}} + \varepsilon \quad (5.29)$$

If the random error is ignored, equation 5.29 also reduces to,

$$\left(\frac{V''_{50\%}}{\beta_N} \right)^{\alpha_N} = 1 \quad (5.30)$$

From equation 5.30, $\beta_N \neq 0$ and $V'_{50\%} = V''_{50\%}$, $\frac{V''_{50\%}}{\beta_N} = 1$ then $\beta_N = V''_{50\%} = V'_{50\%} = q_0 M / C_o$. Substituting for β_N in equation 5.27 gives the following equation

$$Y = 1 - \frac{1}{1 + \left(\frac{C_o V}{q_0 M} \right)^{\alpha_N}} \quad (5.31)$$

Yan et al (2001) referred to equation 9.31 as the modified dose response (MDR) curve. They claimed that a good fit of the experimental data was obtained when the linearised form of the equation was also used, which was given as

$$\ln\left(\frac{C_t}{C_o - C_t}\right) = \alpha \ln(V) - \alpha \ln(\beta) \quad (5.32)$$

Similar to other expressions above, the parameters of the linearised equation can be estimated from the equation of a straight line. A number of studies have reportedly found the suitability of the MDR model to predict breakthrough curves particularly at lower or upper time periods of the curves (Yan and Viraraghavan, 2001; Senthilkumar *et al.*, 2006; Mungasavalli *et al.*, 2007; Calero *et al.*, 2009).

5.3 Data and Error Analysis

Non-linear regression analysis was undertaken using the model equations stated above to simulate breakthrough curves. With the aid of Microsoft Excel 2013, the parameters of the non-linear equations were estimated using the solver add-in function of the Microsoft office software. Linear regression analysis was also carried out and the parameters from the analysis were compared to those from non-linear analysis. Breakthrough curves from experimental observations (plotted as scattered data points) were plotted with the theoretical calculated points (plotted as smooth lines) for both linear and non-linear analysis. Regression coefficients (R^2) and the sum of the squared errors (SSE) were used to show the fit between the theoretical and experimental data. The smaller the SSE, the better the data fit, while for R^2 , the closer the value is to unity the better the fit. Data points from experimental conditions were compared for each model as discussed below. The deviation, ϵ , measured as a percentage difference between the experimental and predicted bed capacity was also used to assess the model accuracy as described in Chapter 4 (Section 4.3).

5.4 Results and Discussions

5.4.1 Non Linear Analysis

All the models described above were applied, employing the non-linear approach, to the experimental data to study the breakthrough characteristics of cell recovery onto Nyex™ particles. The case studies considered are discussed below;

5.4.1.1 Scenario I: Experiment conditions ($h = 20$ cm, $C_0 = 0.2$ OD, $Q = 5$ mL/min)

Applying equations 5.6, 5.18, 5.25 and 5.31 as described in section 5.3 resulted in figure 5.1. For all the models considered, except for the Modified Dose Response (MDR), none could adequately describe the breakthrough curve below $C_t/C_0 < 0.1$. Beyond $C_t/C_0 > 0.1$, all the models appear to describe the experimental data to a reasonable extent. What is also evident in figure 5.1, is the superimposition of the Bohart-Adams and the Thomas models; which clearly demonstrates their mathematical similarity as expounded in section 5.2. However, the Modified Dose Response model sufficiently described the experimental data and was adequate to predict the time when the microalgae cells breakthrough the Nyex™ bed.

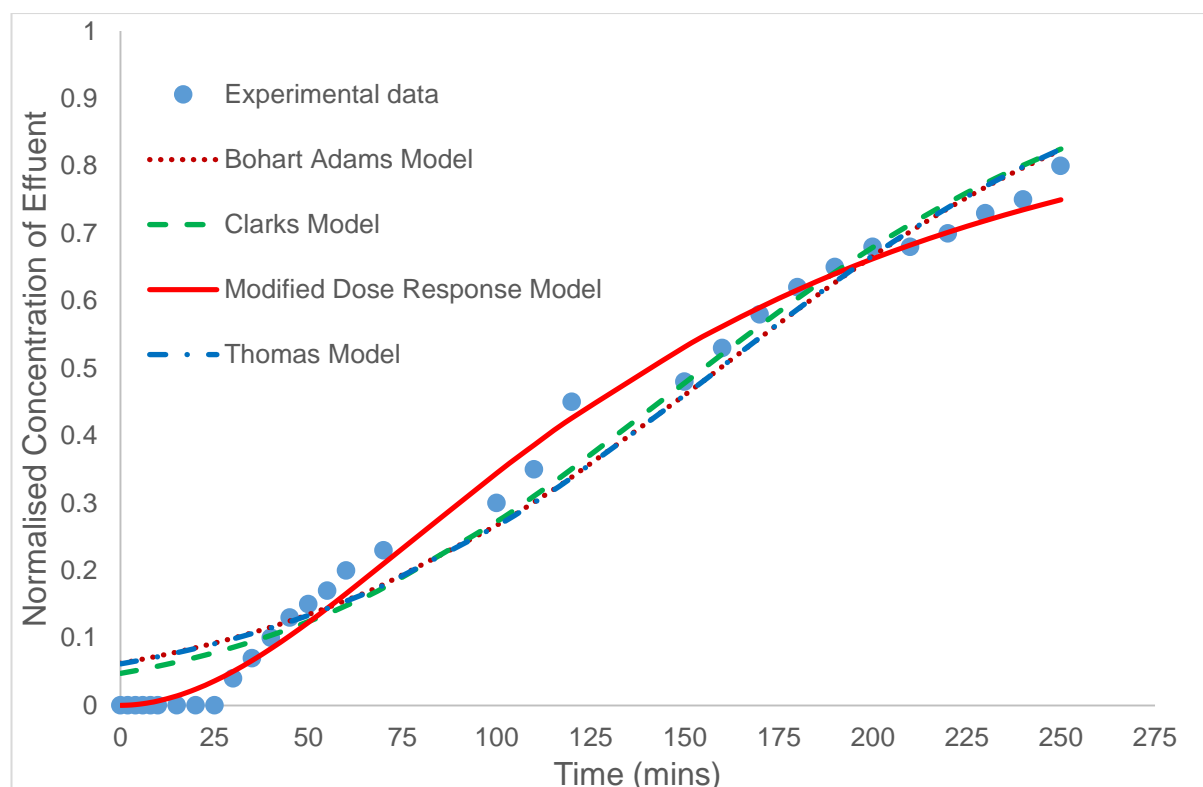


Figure 5.1; Experimental and modelled breakthrough characteristics of recovery of microalgae cells onto Nyex™ particles at ($h = 20$ cm, $C_o = 0.2$ OD, $Q = 5$ mL/min).

The values of SSE, R^2 and ϵ are given in Table 5.1. As evident in the Table, the modified dose response model (MDR) has the lowest SSE, and the highest correlation coefficient. More importantly the calculated bed capacity of the adsorbent was less than 3%, in comparison to the experimental bed capacity as shown below. This underscores the suitability of the MDR model to describe the dynamics involved in the recovery of microalgae cells onto Nyex™ particles in a bed column for the scenario considered.

Table 5.1: Experimental and model parameters for the recovery of microalgae cells onto Nyex™ particles at ($h = 20$ cm, $C_o = 0.2$ OD, $Q = 5$ mL/min).

	SSE	R^2	q_c (mg/g)	ϵ (%)
Bohart-Adams	0.084	0.97	1.44	10.4
Clark	0.064	0.98	N/A*	N/A*
Modified Dose Response	0.017	0.99	1.26	2.9
Thomas	0.086	0.97	1.44	10.4

N/A* - Not applicable as the model does not give q_c values, hence ϵ was not calculated.

5.4.1.2 Scenario II: Experiment conditions ($h = 10$ cm, $C_0 = 0.2$ OD, $Q = 5$ mL/min)

Figure 5.2 shows the experimental and modelled breakthrough characteristics of cells recovery onto Nyex™ particles for the scenario II. In contrast to scenario I, this condition has a lower bed height. But similar to what was previously observed, none of the models, including MDR, could adequately describe the experimental breakthrough curve below $C_t/C_0 < 0.1$. However, unlike the MDR, all the other models appear to predict the initial aspect between $0.1 \geq C_t/C_0 \geq 0.6$. Beyond which, all the models except MDR, predicted a theoretical breakthrough curve where $C_t/C_0 = 1.0$ was attained. This was expected, due to the depression of the experimental data as discussed in section 4.3. On the other hand, whilst the MDR was not adequate to predict the initial aspects of the experimental breakthrough curves, the model seems to describe the experimental data better towards the latter part of the breakthrough curve. Comparable to what was previously described, the Bohart-Adams and Thomas models were superimposed.

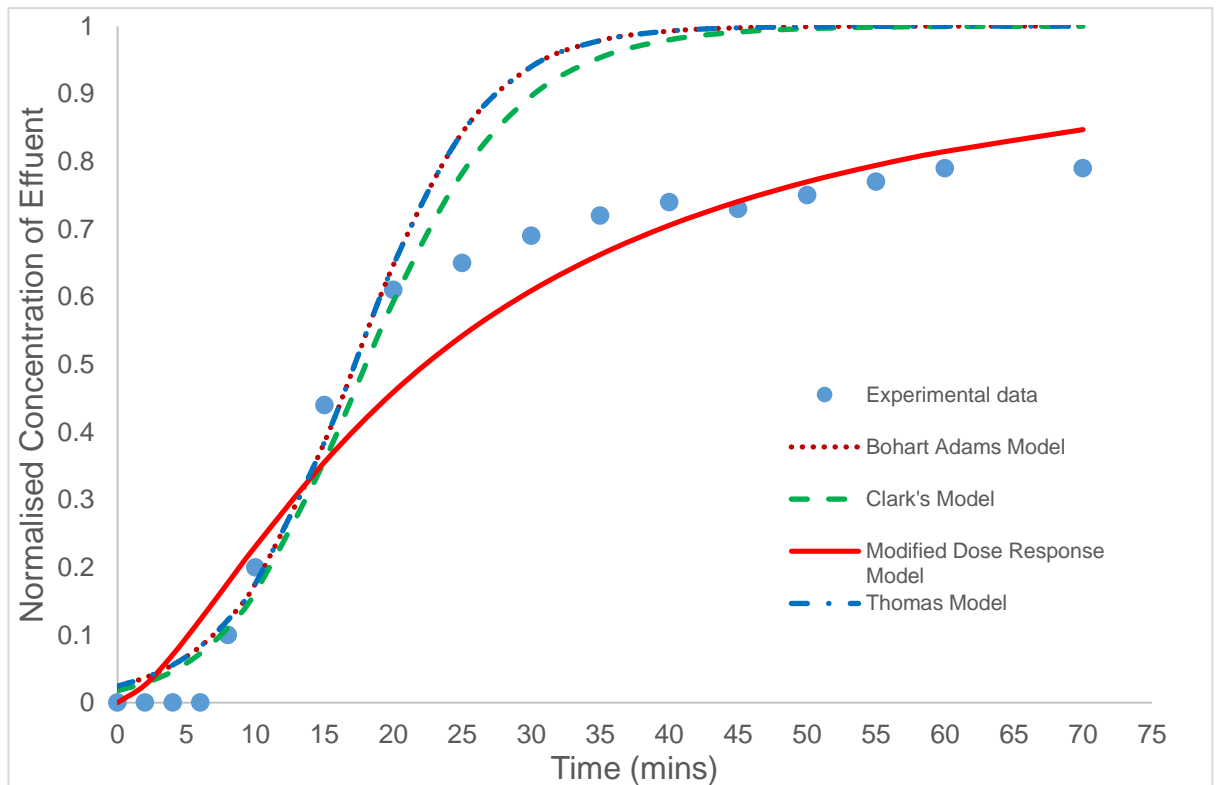


Figure 5.2: Experimental and modelled breakthrough characteristics of recovery of microalgae cells onto Nyex™ particles at ($h = 10$ cm, $C_0 = 0.2$ OD, $Q = 5$ mL/min).

The values of SSE, R^2 and ϵ for this case study are shown in Table 5.2. Despite what appears to be a less than satisfactory fitting of the experimental data by the MDR, the values of SSE, R^2 and ϵ suggest otherwise.

In terms of the correlation coefficient value, the MDR has the lowest, while the Bohart-Adams and Thomas models were the highest. However, the SSE of MDR was much lower, followed by the Clark's model. With respect to the theoretical bed capacity, the Bohart-Adams and Thomas models predicted values that suggest that the experimental value was about 30% underestimated. On the other hand, the MDR calculated value was more accurate; at an underestimation of about 10%.

Table 5.2: Experimental and model parameters for recovery of microalgae cells onto Nyex™ particles at ($h = 10$ cm, $C_o = 0.2$ OD, $Q = 5$ mL/min).

	SSE	R ²	$q_e = 0.45$ (mg/g)	q_c (mg/g)	ϵ (%)
Bohart-Adams	0.604	0.97	0.31	31.2	
Clark	0.458	0.965	N/A	N/A	
Modified Dose Response	0.084	0.96	0.40	10.6	
Thomas	0.522	0.97	0.31	31.2	

5.4.1.3 Scenario III: Experiment conditions ($h = 5$ cm, $C_o = 0.2$ OD, $Q = 5$ mL/min)

The Clark's model appears to fit the experimental data at the initial part of the curve up to when $C_t/C_o = 0.35$ as depicted in figure 5.3. Beyond that, the model deviated from the experimental data until $C_t/C_o = 1.0$ was attained. The superimposition of the Bohart-Adams and Thomas models was obvious as well as their inadequacy to fit the experimental data when $C_t/C_o < 0.1$. The two models also deviated from the experimental data, albeit lesser, but predicted breakthrough curves where $C_t/C_o = 1.0$ was attained. The Modified Dose Response model was a good fit and unlike the other models the maximum C_t/C_o was about 0.8; quite close to the maximum experimental value of 0.76.

The fitting of the MDR model was further established by the statistical values as given in Table 5.3. The MDR gave the lowest SSE and the calculated bed capacity of 0.65 mg/g was only about 10% less than the experimental value; compared to 0.51 mg/g predicted by the Bohart-Adams and Thomas models. This further emphasises the greater suitability of the MDR to predict the recovery of cells onto Nyex™ particles.

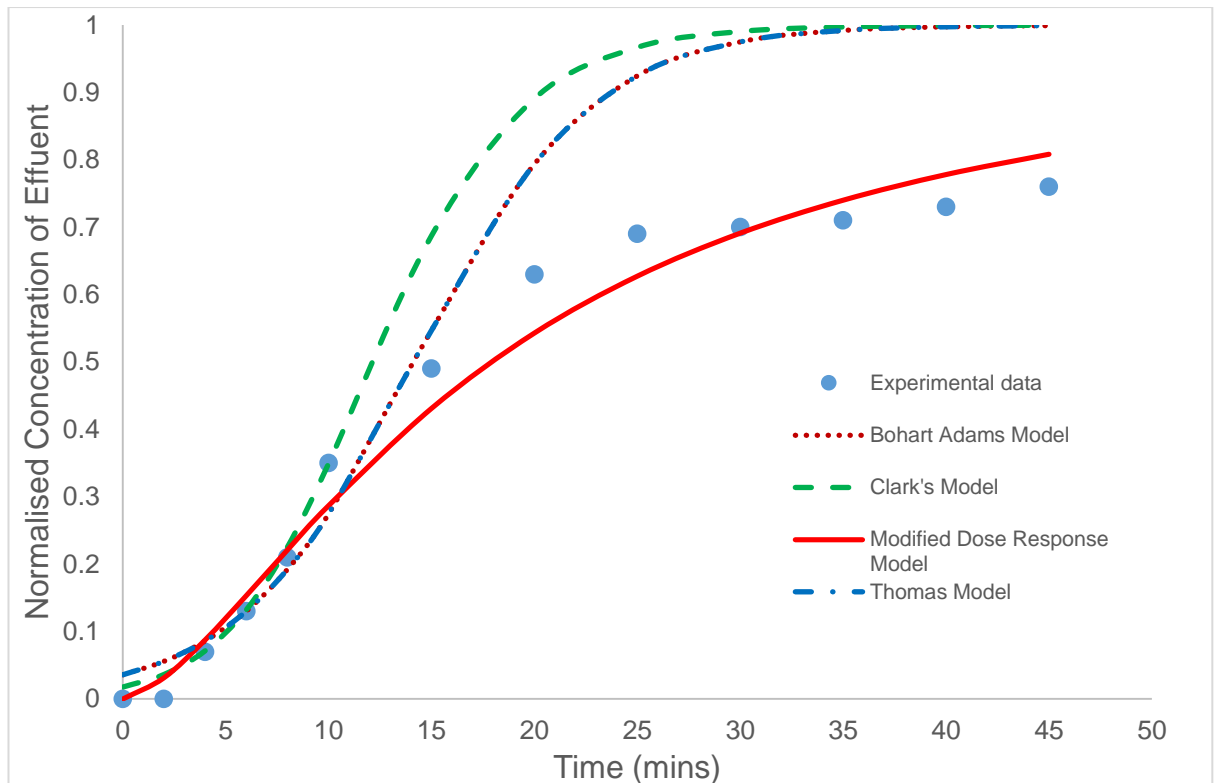


Figure 5:3: Experimental and modelled breakthrough characteristics of recovery of microalgae cells onto Nyex™ particles at ($h = 5$ cm, $C_o = 0.2$ OD, $Q = 5$ mL/min).

Table 5.5.3: Experimental and model parameters for recovery of microalgae cells onto Nyex™ particles at ($h = 5$ cm, $C_o = 0.2$ OD, $Q = 5$ mL/min).

	SSE	R^2	$q_e = 0.72$ (mg/g)	ϵ (%)
Bohart-Adams	0.380	0.97	0.51	29.0
Clark	0.483	0.988	N/A	N/A
Modified Dose Response	0.026	0.976	0.65	10.4
Thomas	0.380	0.97	0.51	29.0

5.4.1.4 Scenario IV: Experiment conditions ($h = 20$ cm, $C_o = 0.2$ OD, $Q = 10$ mL/min)

At a higher flow rate compared to scenario I, the experimental breakthrough curve was expected to be steeper due to the higher flow velocities as previously discussed. As a result, the predicted breakthrough curves by the models was expected to behave similarly. As shown in figure 5.4, all the models predicted a steeper breakthrough curve and a faster breakthrough time in comparison to figure 5.1.

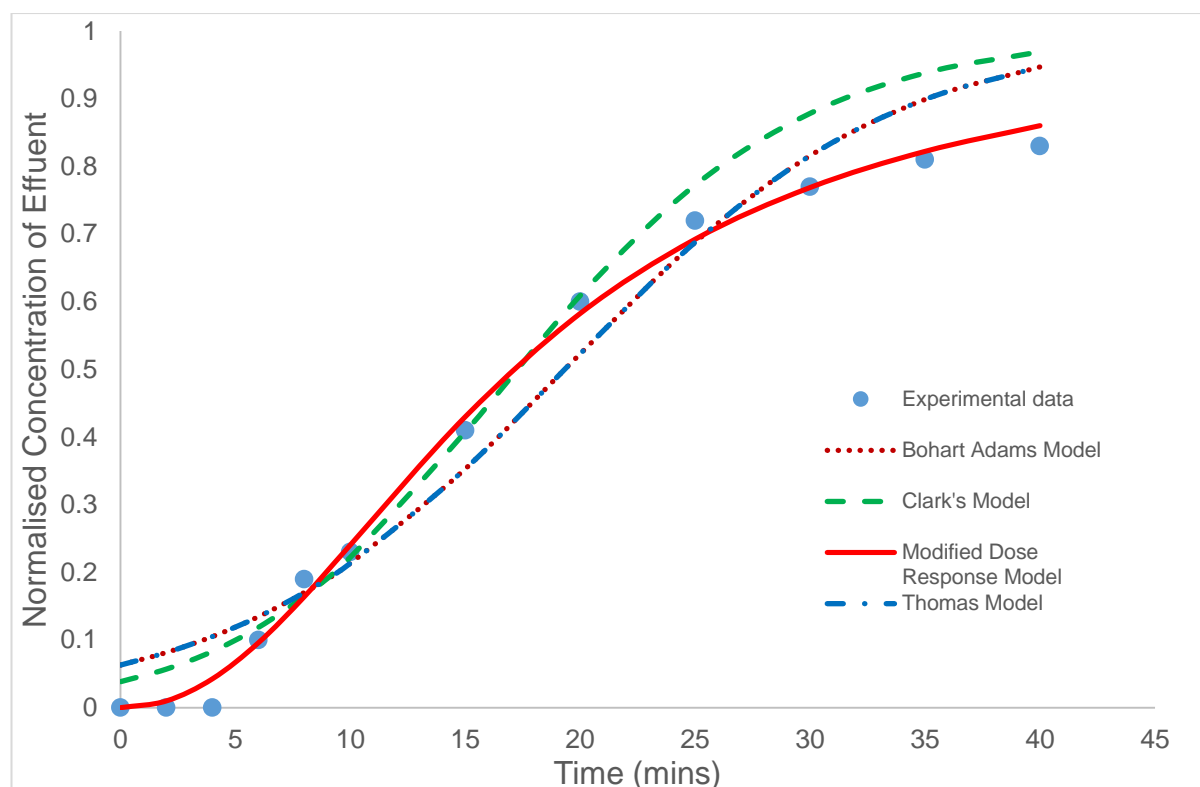


Figure 5.4: Experimental and modelled breakthrough characteristics of recovery of microalgae cells onto Nyex™ particles at ($h = 20$ cm, $C_0 = 0.2$ OD, $Q = 10$ mL/min).

All the models predicted the breakthrough times accurately to a reasonable extent, although the modified dose response model seems to fit the experimental data best, followed by the Clark's model. As with other case studies, all the models, except for the MDR, tend towards $C_t/C_0 = 1.0$.

The statistical analysis carried out, as shown in Table 5.4, lends further credence to the superiority of the MDR model. Even though the deviation of the calculated bed capacity from the experimental value was the same for all the models, the SSE and R^2 shows that the MDR was a better fit.

Table 5.4: Experimental and model parameters for recovery of microalgae cells onto Nyex™ particles at ($h = 20$ cm, $C_0 = 0.2$ OD, $Q = 10$ mL/min).

	SSE	R^2	$q_e = 0.33$ (mg/g)	q_c (mg/g)	ϵ (%)
Bohart-Adams	0.0575	0.963		0.35	6.1
Clark	0.0632	0.984		N/A	N/A
Modified Dose Response	0.0052	0.996		0.31	6.1
Thomas	0.0575	0.963		0.35	6.1

The similarity in the ϵ values could be explained by what is evident in figure 5.4 where the inability of the Bohart-Adams and Thomas models to predict the initial part of the experimental breakthrough curve was offset by the theoretical C_t/C_0 tending towards 1.0. As with all the case studies considered so far, the modified dose response model appears to better predict the recovery of cells onto Nyex™ particles at a relatively higher flow rate.

5.4.1.5 Scenario V: Experiment conditions ($h= 20$ cm, $C_0= 0.4$ OD, $Q= 10$ mL/min)

This was considered to investigate a higher initial concentration of the microalgae suspension. As previously highlighted, under these conditions, the mass transfer coefficient is high thereby leading to a rapid saturation of the adsorbent bed. In other words, the breakthrough time is attained faster and the curve is steeper. As predicted by the models, and evident in figure 5.5, the Clark's, Bohart-Adams and Thomas models, adequately describe the initial aspect of the breakthrough curves. Similar to previous case studies, large deviations were obvious when C_t/C_0 was greater than 0.5.

However, the Modified Dose Response model predicted a much steeper curve, such that microalgae cells would break through the bed at the instance of the first effluent sample. On the other hand, it adequately predicted the exhaustion aspect of the breakthrough curve. Despite the inability of the MDR to sufficiently predict the breakthrough aspect of the curve, the statistical analysis carried out, as stated in Table 5.5, underscore the overall fitness of the model.

The deviation of the calculated bed capacity from the experimental value was 6% for MDR, whilst, it was 41% for the Bohart-Adams and Thomas models. However, all the other models have a better correlation coefficient ranging from 0.966 for Clark's model to 0.97 for Bohart-Adams and Thomas models; the MDR model gave the lowest SSE value. Combining all these statistical variables and the objective of this research work seem to suggest a better prediction by the MDR model.

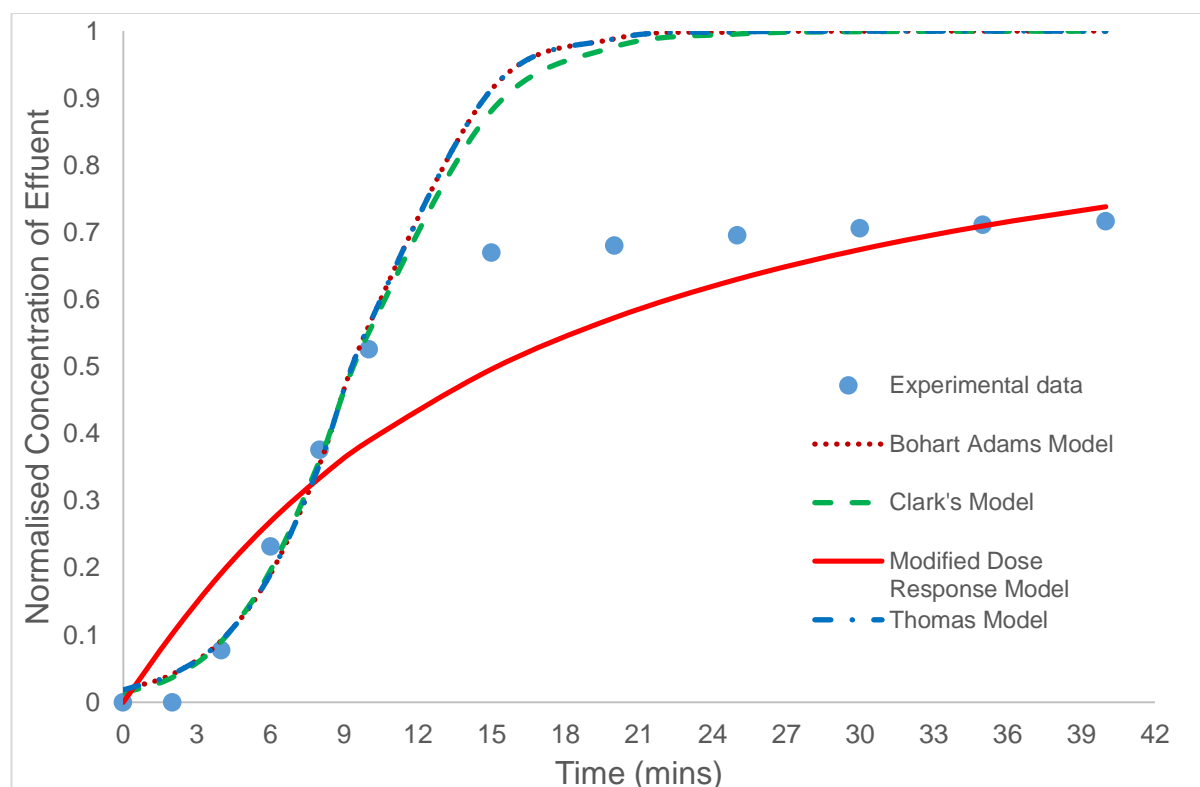


Figure 5.5: Experimental and modelled breakthrough characteristics of recovery of microalgae cells onto Nyex™ particles at ($h = 20$ cm, $C_o = 0.4$ OD, $Q = 10$ mL/min).

Table 5.5: Experimental and Model parameters for recovery of microalgae cells onto Nyex™ particles at ($h = 20$ cm, $C_o = 0.4$ OD, $Q = 10$ mL/min).

	SSE	R^2	$q_e = 0.58$ (mg/g)	ϵ (%)
Bohart-Adams	0.645	0.97	0.34	41
Clark	0.620	0.966	N/A	N/A
Modified Dose Response	0.093	0.93	0.55	6
Thomas	0.645	0.97	0.34	41

5.4.2 Linear Analysis

A number of studies have reported the linearization of the models to estimate their parameters (Hamdaoui, 2006; Kundu and Gupta, 2007; Gomathi Priya *et al.* 2011; Saadi *et al.*, 2013). This is more straightforward as it does not require the need for optimisation tools to fit the model with the experimental data. The case studies considered for the non-linear analysis were also applied to the linearised version of the models as symbolised by equations 5.7, 5.19, 5.26 and 5.32 of the Bohart-Adams, Thomas, Clark's and modified dose response models respectively. The literature is replete with linearised fits of the models without an attempt to

understand the implication when compared to non-linear analysis. For the research reported in this thesis, the parameters derived from the linearised models were compared with the non-linear ones in order to ascertain which is better, if any. The correlation coefficients (R^2) and the deviation (ε) between the linear and non-linear parameters were the statistical parameters to chosen to make the comparison.

5.4.2.1 Linearised Bohart-Adams and Thomas Models

The derived linear plots for Bohart-Adams and Thomas Models are depicted by figures 5.6 – 5.8. The reason for plotting the two models on the same graph is evident from equation 5.7 and 5.19, which are reproduced below;

$$\ln\left(\frac{C_o}{C_t} - 1\right) = \frac{K_{BA}N_oZ}{U} - K_{BA}C_o t \quad (5.7)$$

$$\ln\left(\frac{C_o}{C_t} - 1\right) = \frac{K_T q_o M}{Q} - K_T C_o t \quad (5.19)$$

From the equations, it is evident that the two models are mathematically identical. In fact as plotted below, the values of the Bohart-Adams and Thomas equilibrium constants, K_{BA} and K_T would be the same. Having said that, it is possible to equate the ‘intercept’ of equation 5.7 and 5.19 as given below;

$$\frac{K_{BA}N_oZ}{U} = \frac{K_T q_o M}{Q} \quad (5.33)$$

Equation 9.33 can be rearranged to give the equation below;

$$q_o = \frac{N_o Z S}{M} \quad (5.34)$$

Where S is the bed cross sectional area given as;

$$S = \frac{Q}{U} \quad (5.35)$$

ZS is the fixed bed column volume and $\frac{ZS}{M}$ indicates the reciprocal of the adsorbent bulk density. Estimating N_o and q_o from the plots below is possible if one of the parameters is estimated from the linear plot allowing the other to be calculated from the equation 5.34 can also be calculated. Hence, the reason for the superimposition of the two models as clearly seen from the non-linear plots.

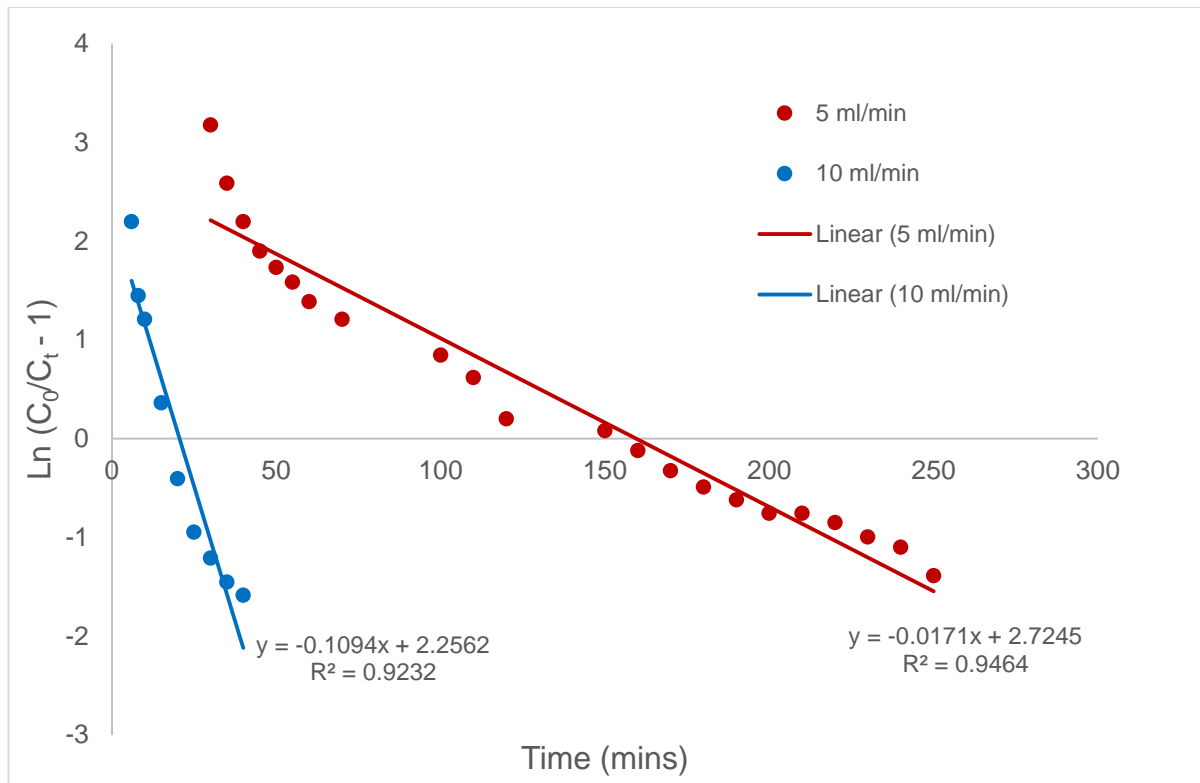


Figure 5:6: Linearised Bohart-Adams and Thomas models to predict breakthrough characteristics of recovery of microalgae cells onto Nyex™ particles at ($h = 20$ cm, $C_0 = 0.2$ OD, $Q = 5$ and 10 mL/min).

Tables 5.6 and 5.7 indicate the parameters of the linearised and non-linear models of the Bohart-Adams and Thomas models respectively. For the benefit of doubt, the parameters given in Tables 5.6 and 5.7 were estimated from the linear plots and compared with estimations based on equation 5.33. More importantly, as evident from the figures and tabulated parameters, there is a large deviation between the linear and non-linear plots. The limitation of the linear plots is evident from the correlation coefficient values which were quite low for most of the scenarios. This apparently shows the inability of the linearised Bohart-Adams and Thomas models to adequately describe the recovery of microalgae cells.

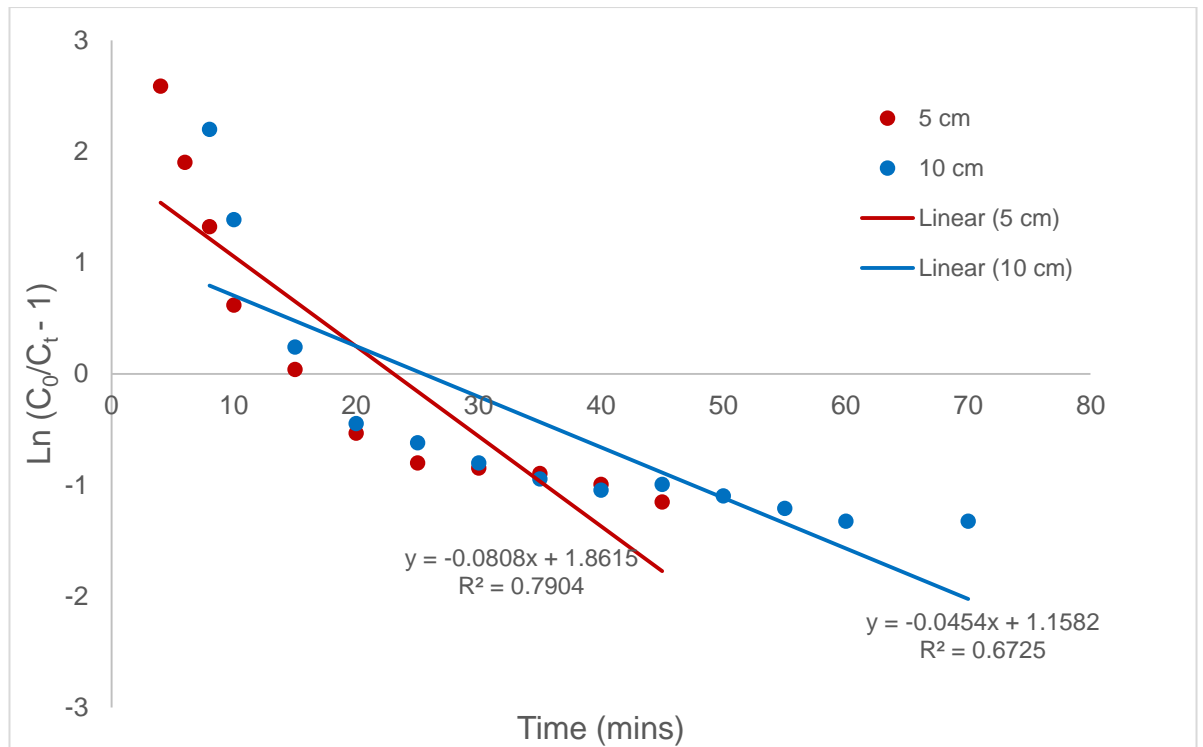


Figure 5:7: Linearised Bohart-Adams and Thomas models to predict breakthrough characteristics of recovery of microalgae cells onto Nyex™ particles at ($h = 5$ and 10 cm, $C_0 = 0.2$ OD, $Q = 5$ mL/min).

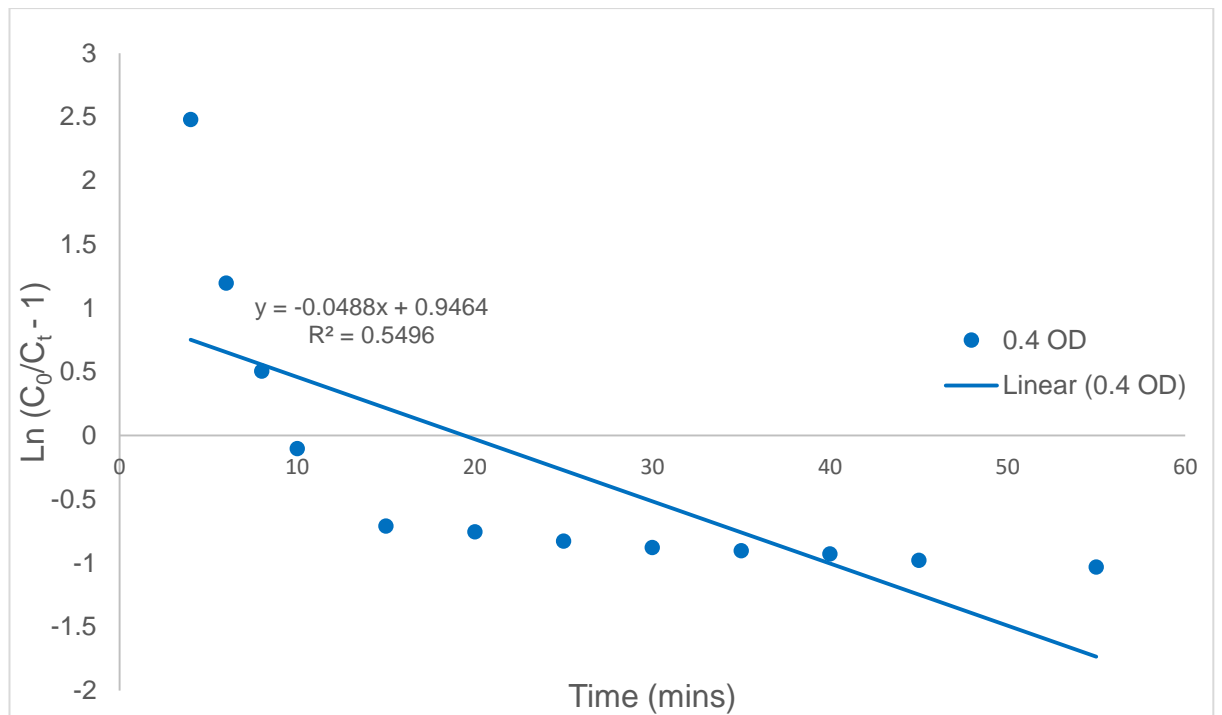


Figure 5:8: Linearised Bohart-Adams and Thomas models to predict breakthrough characteristics of cell recovery at ($h = 20$ cm, $C_0 = 0.4$ OD, $Q = 10$ mL/min).

Table 5.6: Parameter comparison of linear and non-linear Bohart-Adams to model the breakthrough characteristics of recovery of microalgae cells onto Nyex™ particles.

Scenario		K_{BA} (L/min/mg)	N_0 (mg/L)	R^2	ϵ (%)
1	Linear	0.085	1.172	0.9	
	Non Linear	0.085	1.172	0.971	0
2	Linear	0.227	0.375	0.6725	
	Non Linear	1.074	0.253	0.972	48.5
3	Linear	0.404	0.678	0.7904	
	Non Linear	1.159	0.417	0.97	62.4
4	Linear	0.547	0.303	0.9232	
	Non Linear	0.698	0.284	0.963	6.7
5	Linear	0.122	0.572	0.5496	
	Non Linear	1.055	0.277	0.97	106.3

Table 5.7: Parameter comparison of linear and non-linear Thomas to model the breakthrough characteristics of recovery of microalgae cells onto Nyex™ particles.

Scenario		K_T (L/min/mg)	q_0 (mg/g)	R^2	ϵ (%)
1	Linear	0.085	1.44	0.946	
	Non Linear	0.085	1.44	0.971	0
2	Linear	0.227	0.46	0.673	
	Non Linear	1.074	0.31	0.972	48.5
3	Linear	0.404	0.83	0.790	
	Non Linear	1.159	0.51	0.970	62.4
4	Linear	0.547	0.37	0.923	
	Non Linear	0.698	0.35	0.963	6.7
5	Linear	0.122	0.70	0.550	
	Non Linear	1.055	0.34	0.970	106.3

5.4.2.2 Linearised Clark Model

Figures 5.9 – 5.11 show the linearised predicted data using the Clark model.

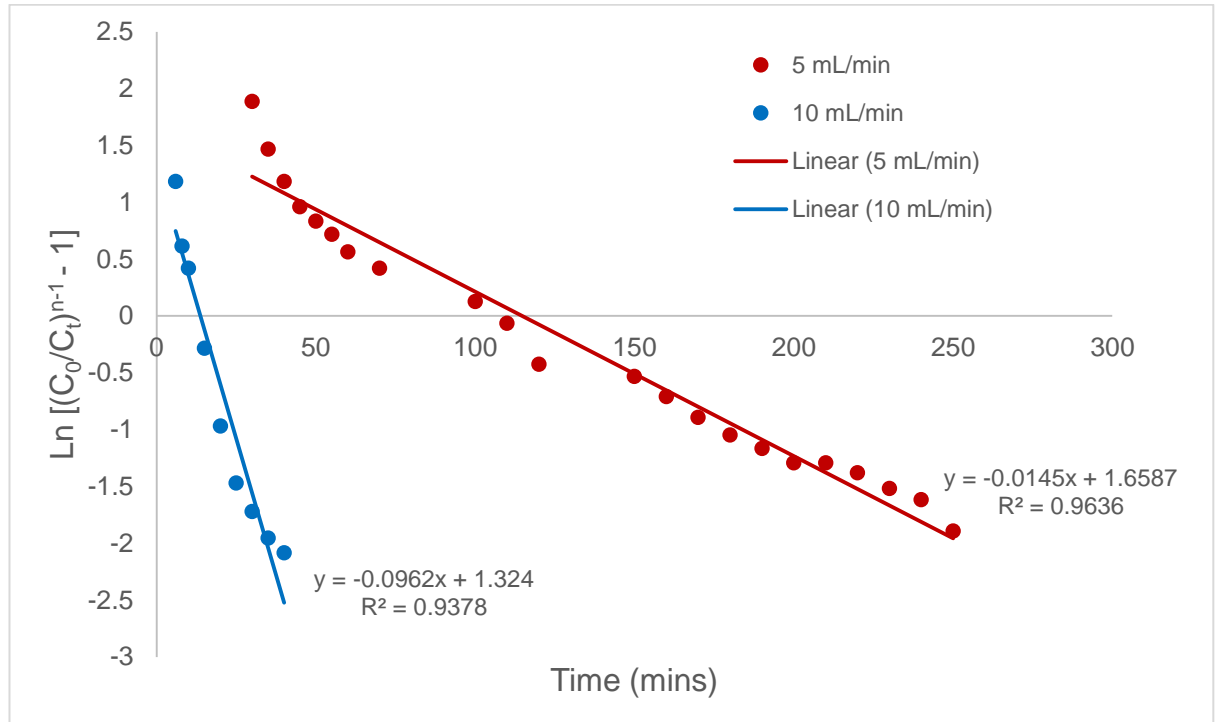


Figure 5.9: Linearised Clark to model breakthrough characteristics of recovery of cells onto Nyex™ particles at ($h = 20$ cm, $C_0 = 0.2$ OD, $Q = 5$ and 10 mL/min).

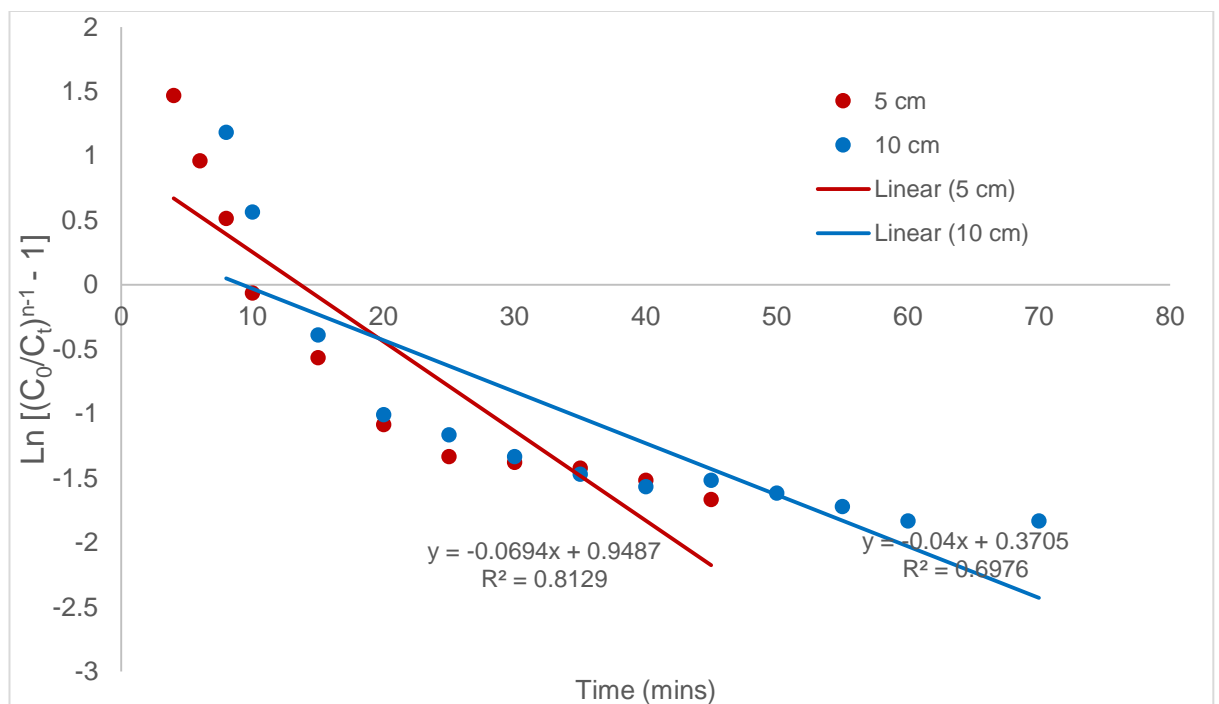


Figure 5.10: Linearised Clark to model breakthrough characteristics of recovery of cells onto Nyex™ particles at ($h = 5$ and 10 cm, $C_0 = 0.2$ OD, $Q = 5$ mL/min).

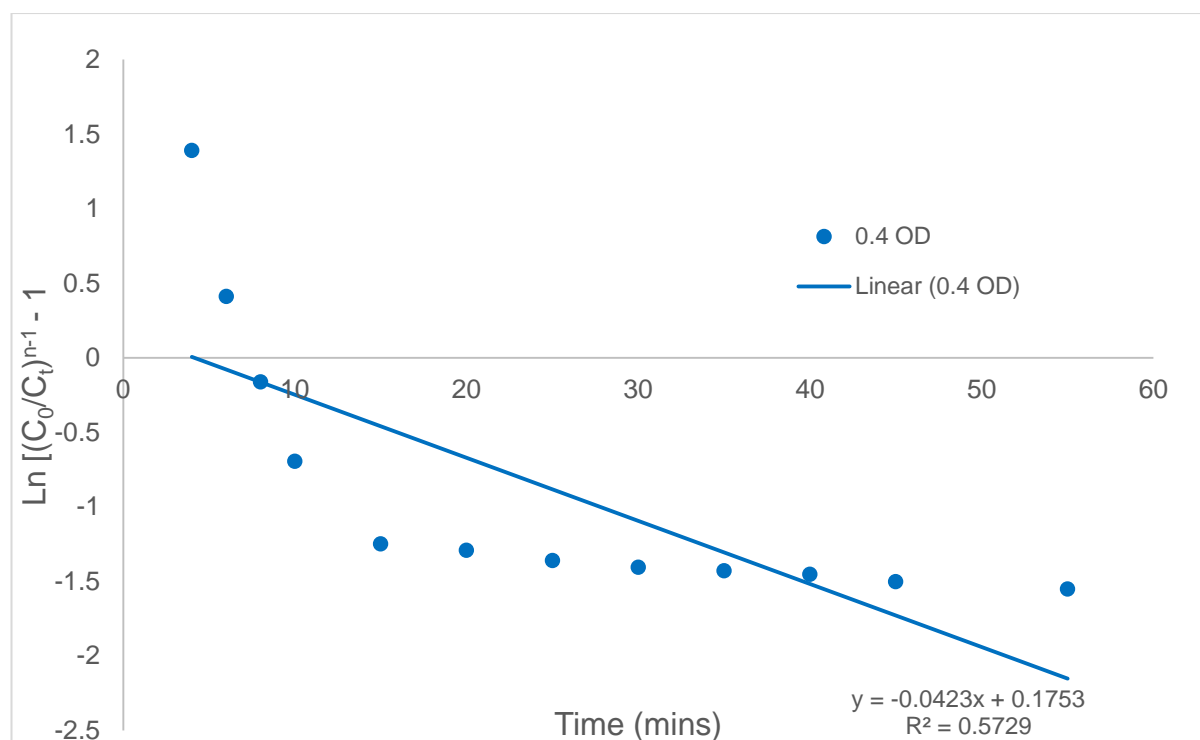


Figure 5.11: Linearised Clark to model breakthrough characteristics of recovery of cells onto Nyex™ particles at ($h = 20$ cm, $C_0 = 0.4$ OD, $Q = 10$ mL/min).

Table 5.8: Parameter comparison of linear and non-linear Clark to model the breakthrough characteristics of recovery of microalgae cells onto Nyex™ particles.

Scenario		r (1/min)	I	R^2	ϵ (%)
1	Linear	0.0145	5.252	0.9636	
	Non Linear	0.0152	5.824	0.977	9.8
2	Linear	0.04	1.449	0.6976	
	Non Linear	0.17	11.687	0.965	87.6
3	Linear	0.069	2.582	0.8129	
	Non Linear	0.252	11.688	0.988	77.9
4	Linear	0.096	3.827	0.9378	
	Non Linear	0.146	6.793	0.984	43.7
5	Linear	0.042	1.192	0.5729	
	Non Linear	0.341	13.828	0.966	91.4

The linear regression analysis was performed with Clark model using the 'n' parameter from the Freundlich isotherm as well as equation 5.26. The values of R^2 and the model parameters are listed in Table 5.8. Values of R^2 range from 0.5729

to 0.9636 for the linearised results unlike the non-linear ones where R^2 was between 0.966 and 0.988. The deviation of the parameters between the linear derived and non-linear derived values range between 9.8% and 91.4%.; which underscores the inadequacy of using both linear and non-linear regression analysis for breakthrough curve prediction without identifying which is more suitable for the adsorption system.

5.4.2.2 Linearised Modified Dose Response Model

Using equation 5.32, linear regression analysis was carried out to estimate the parameters of the modified dose response (MDR) model. Figures 5.12 – 5.14 show the linearised predicted data using the MDR model. The values of R^2 and the model parameters are listed in Table 5.9. Values of R^2 range from 0.8205 to 0.9936 for the linearised results whilst for the non-linear ones, R^2 was between 0.93 and 0.996. Notably, the breakthrough curves predicted by the linear and non-linear regression analysis of the MDR have relatively high correlation coefficients.

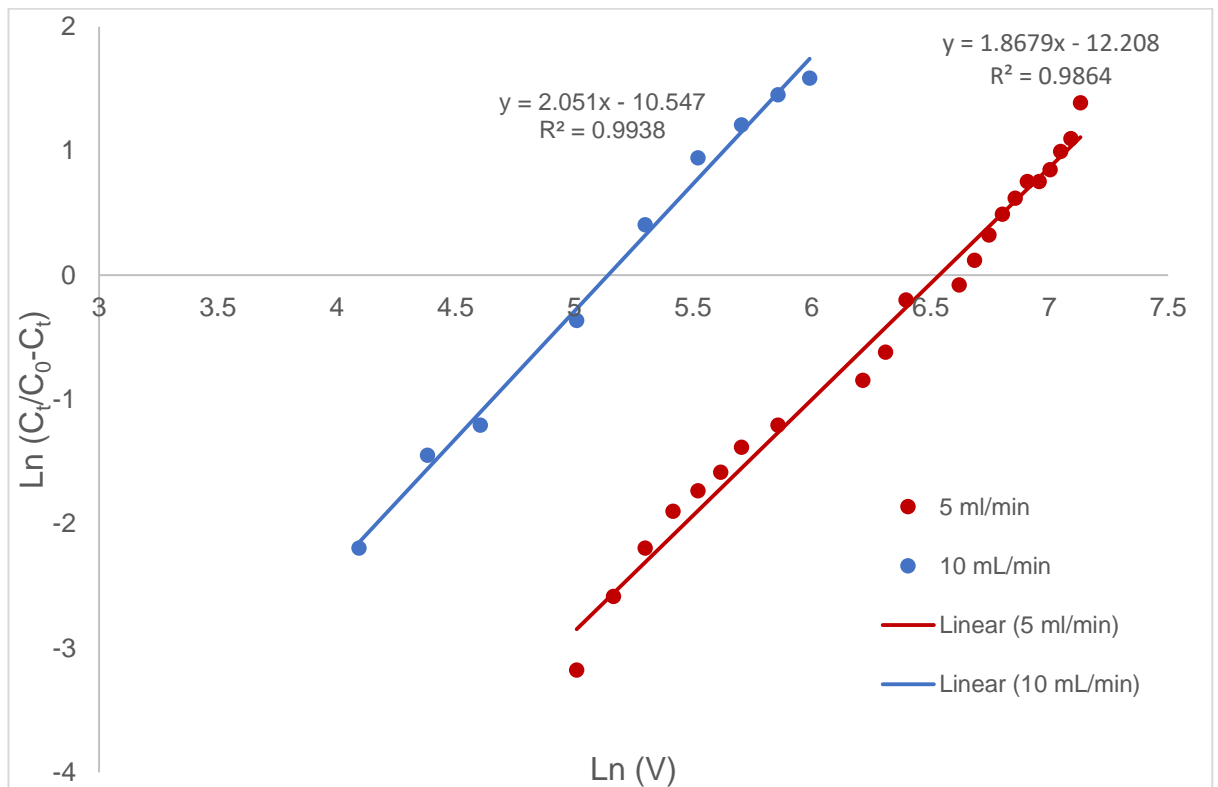


Figure 5.12: Linearised MDR to model breakthrough characteristics of recovery of cells onto Nyex™ particles at ($h = 20$ cm, $C_0 = 0.2$ OD, $Q = 5$ and 10 mL/min).

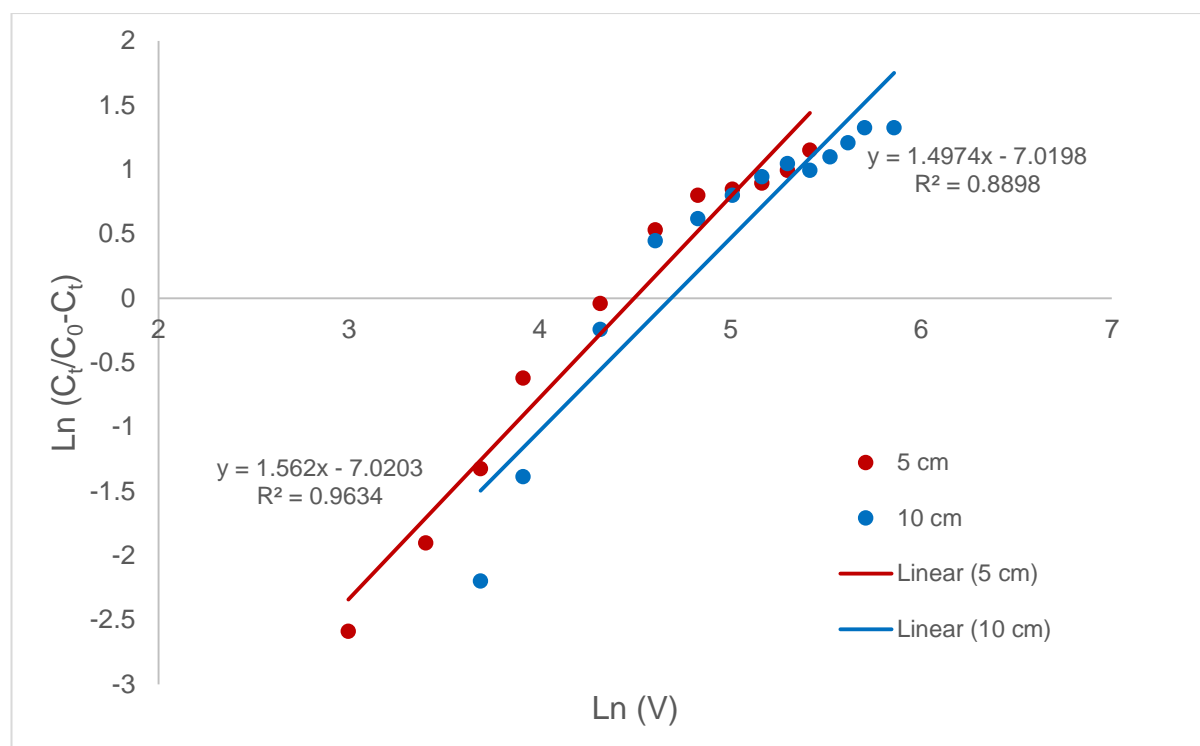


Figure 5:13: Linearised MDR to model breakthrough characteristics of recovery of cells onto Nyex™ particles at ($h = 5$ and 10 cm, $C_0 = 0.2$ OD, $Q = 5$ mL/min).

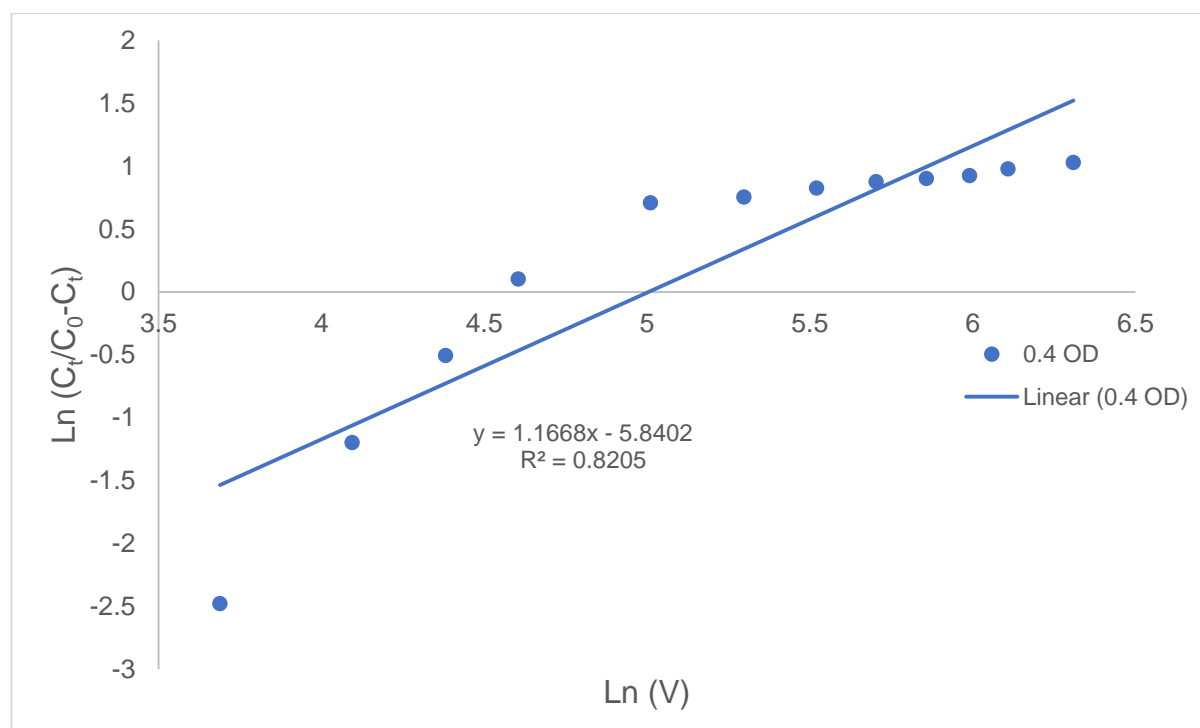


Figure 5:14: Linearised MDR to model breakthrough characteristics of recovery of cells onto Nyex™ particles at ($h = 20$ cm, $C_0 = 0.4$ OD, $Q = 10$ mL/min).

As shown in Table 5.9, the deviations of the parameters between the linearly derived and non-linear derived range between 0% and 2.7%; which emphasises the

exceptional ability to use both linear and non-linear regression analysis with the modified dose response model to predict the breakthrough curves.

Table 5.9: Parameter comparison of linear and non-linear MDR to model the breakthrough characteristics of recovery of microalgae cells onto Nyex™ particles.

Scenario		α	q_c (mg/g)	R^2	ε (%)
1	Linear	1.868	1.242	0.9636	
	Non Linear	1.901	1.264	0.977	1.8
2	Linear	1.497	0.391	0.6976	
	Non Linear	1.512	0.402	0.965	2.7
3	Linear	1.562	0.645	0.8129	
	Non Linear	1.562	0.645	0.988	0.0
4	Linear	2.051	0.308	0.9378	
	Non Linear	2.140	0.308	0.984	0.0
5	Linear	1.167	0.538	0.5729	
	Non Linear	1.072	0.548	0.966	1.9

5.4.2.3 Bed Depth Service Time (BDST) Model

The linear regression analysis of equation 5.9 was undertaken to estimate the model parameters as stated in equation 5.11. This was achieved by estimating the service times for a predetermined saturation percentage for different bed heights; for the purpose of the research reported in this thesis, these percentages are 40% and 70%. Figures 5.15 and 5.16 were the graph obtained when the service times were plotted against bed height for each saturation percentage. The correlation coefficients of the line of best fit for the saturation percentages was 0.9082 and 0.9067 for 40% and 70% respectively. Using the parameters of the model, the service times of the breakthrough curves for cell recovery onto Nyex™ particles could be predicted as listed in Table 5.10. Parameters for the experimental conditions that fall outside those of the bed height considered could be estimated as previously described and stated by equations 5.12 and 5.13. This estimate would help validate the suitability of the BDST model to adequately predict the service times for microalgae cell adsorption. The values of those parameters are all shown in Table 5.10 below.

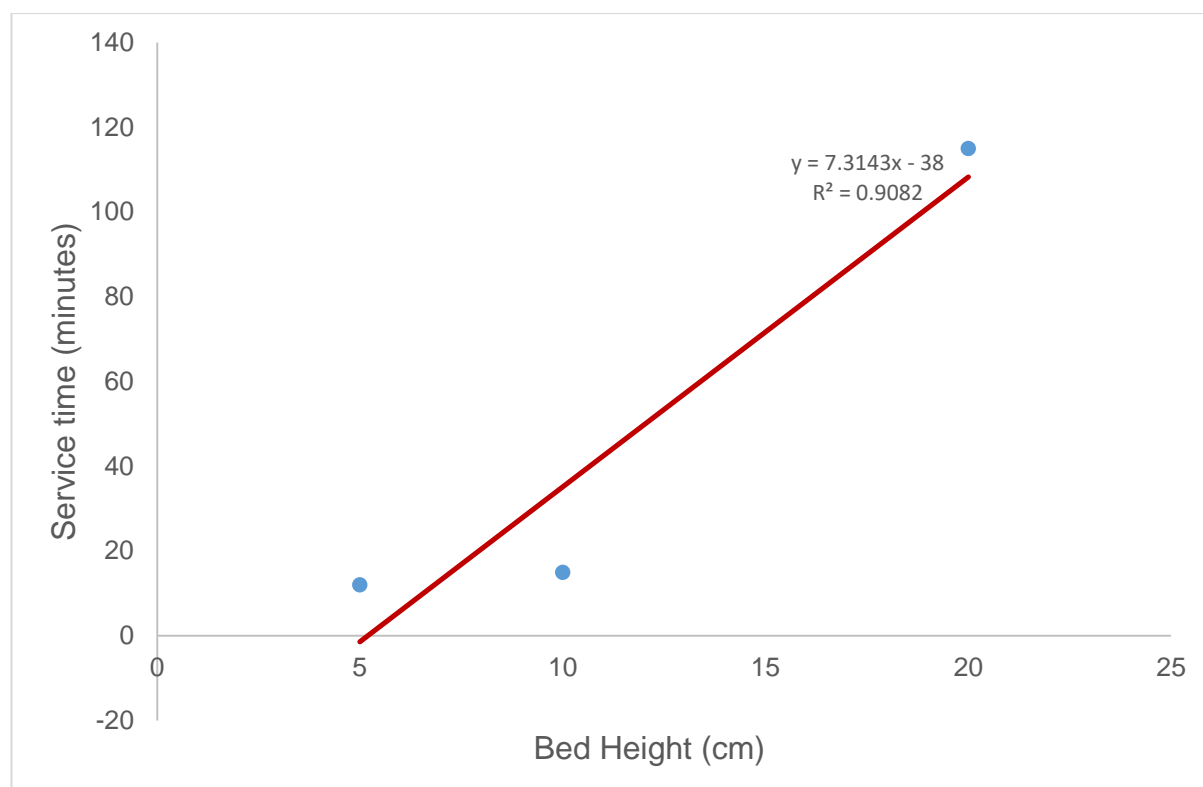


Figure 5:15: Service time against bed height at 40% saturation of the Nyex™ particles by the microalgae cells.

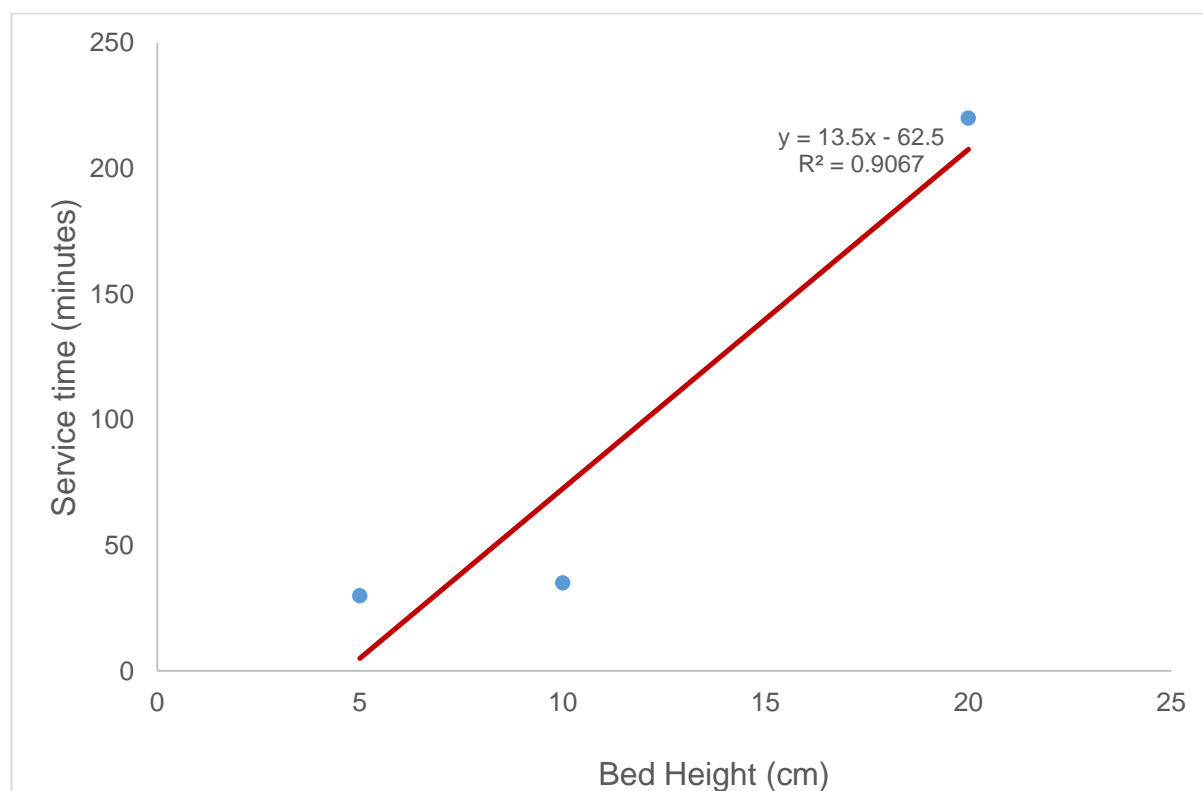


Figure 5:16: Service time against bed height at 70% saturation of the Nyex™ particles by the microalgae cells.

Table 5.10: BDST model parameters and the experimental and predicted service times to model the breakthrough characteristics of cell recovery at 40% bed saturation.

Scenario	A	B	Z (cm)	t _c (mins)	t _e (mins)
1	7.31	38	20	108	115
2	7.31	38	10	35	15
3	7.31	38	5	-1.5	12
4	3.66	38	20	35	15
5	3.66	19	20	54	8

As is apparent from Table 5.11, the BDST model failed to accurately predict all but one of the scenarios considered. In fact the predicted service time for scenario 3 ($h = 5$ cm, $C_o = 0.2$ OD, $Q = 5$ mL/min), was negative. For most of the scenarios, deviation between the experimental and the predicted service times exceeded 100%.

Table 5.11: BDST model parameters and the experimental and predicted service times to model the breakthrough characteristics of cell recovery at 70% bed saturation.

Scenario	A	B	Z (cm)	t _c (mins)	t _e (mins)
1	13.5	62.5	20	207.5	220
2	13.5	62.5	10	72.5	35
3	13.5	62.5	5	5	30
4	6.75	62.5	20	72.5	25
5	6.75	31.25	20	103.75	30

5.5 Adaptation of the Logistic Functionality of Bed Column Models

The models developed for the dynamic studies of fixed bed columns and prediction of their breakthrough characteristics are known to be logistic functions. The latter are mathematical expressions that combine two types of exponential growth functions; a pattern of increase at an exponential rate and a bounded exponential limit due to a fixed capacity. The fixed bed models being logistic functions give rise to breakthrough curves being sigmoidal in shape so that the model numerator is customarily fixed to a value of '1' (Oulman, 1980; Crini and Badot, 2010; Mueller, 2016). This implies that when the bed is exhausted, at maximum capacity, the initial influent concentration should always be equal to the final effluent concentration.

However, the research reported in this thesis shows that a breakthrough curve with a normalised maximum value of '1' is atypical. The consequence is that the predicted breakthrough curves from the Bohart-Adams/Thomas and the Clark models will always attain a value of '1' whereas the observed experimental data was never '1'. Hence, the models were adapted such that the predicted breakthrough curve maximum value will be closer to the experimental maximum. In practice, it was observed that the effluent concentration in experiments was rarely above about 80% of the inlet concentration. Hence, the maximum value was taken as '0.8' rather than '1'. This suggests that about 20% of the cells could not be accounted for. The likely reasons for such depressed breakthrough curves were outlined in section 4.3.

The adapted equations are given below;

Adapted Bohart-Adams model

$$\frac{C_t}{C_o} = \frac{0.8}{\exp\left(\frac{K_{BA}N_oZ}{U} - K_{BA}C_o t\right) + 1} \quad (5.35)$$

Adapted Clark model

$$\frac{C}{C_o} = \left(\frac{0.8}{1 + I \exp -rt}\right)^{\frac{1}{n-1}} \quad (5.36)$$

The Thomas model as is being currently reported in the literature and as shown in this thesis is mathematically identical to Bohart-Adams, hence, either would suffice. The MDR model consistently gave a relatively better prediction of the cell adsorption dynamics especially at the exhaustion part of the breakthrough curve, hence, its modification was not considered.

The non-linear regression analysis of equations 5.35 and 5.36 was applied to selected scenarios previously described and illustrated in figures 5.17 – 5.22.

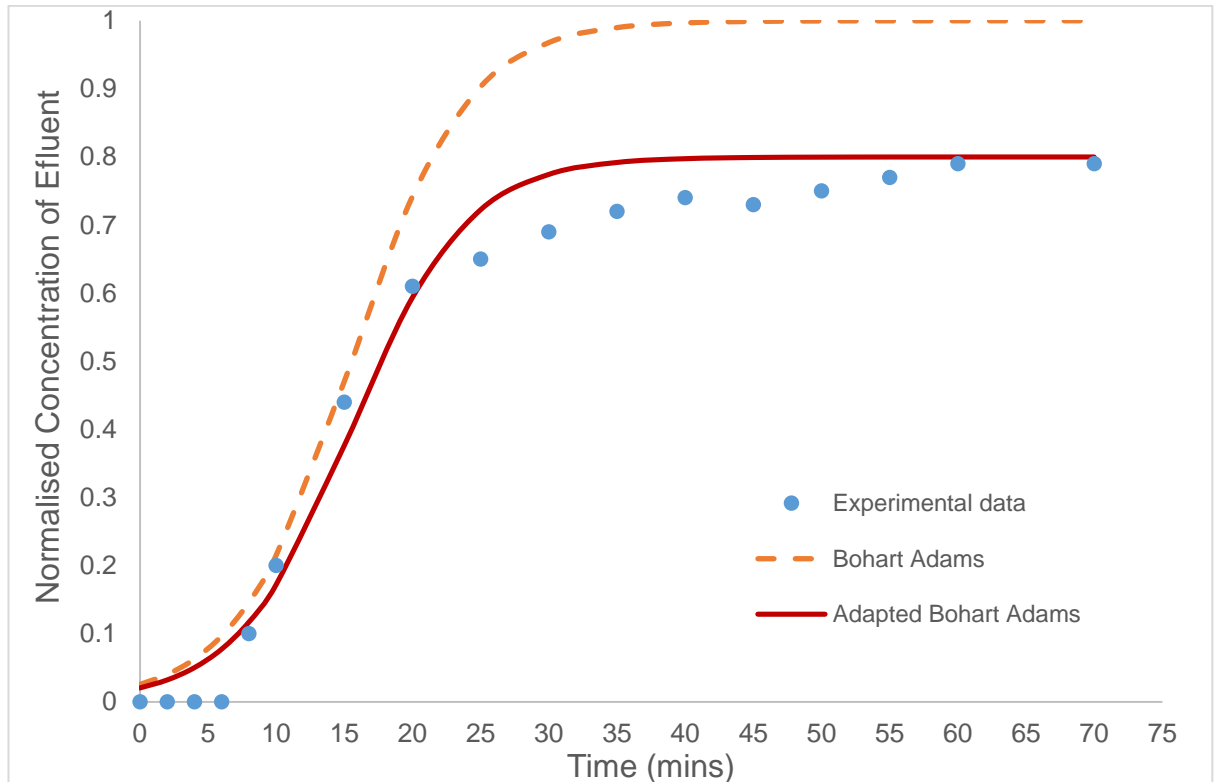


Figure 5:17: Breakthrough characteristics for recovery of microalgae cells onto Nyex™ particles at ($h = 10$ cm, $C_0 = 0.2$ OD, $Q = 5$ mL/min), predicted with the original and adapted Bohart-Adams models.

The resulting graph of the adapted Bohart-Adams (BA) equation are shown in figures 5.17 5.18 and 5.19. Interestingly, the adapted Bohart-Adams model predicted a breakthrough curve that accounted for the ‘depression’ reported in this thesis. The predicted breakthrough curves from the adapted model were a better fit of the experimental data for all the scenarios considered. Statistically, as listed in Table 5.12, the better fit of the predicted curves is manifest in a much lower SSE and higher correlation coefficients.

Remarkably, for all the scenarios considered, in comparison to the MDR model, the adapted BA model gave a better fit of the experimental data in terms of the SSE and the R^2 values. However, with respect to the predicted bed capacity, q_c , the MDR model was superior. In actual fact, the predicted bed capacity by the adapted BA model was less accurate, with higher deviation percentages from the experimental ones, when compared to the BA model. Likewise, the Bohart-Adams constant also changed; increasing for scenarios 2 and 4 whilst decreasing for scenario 5.

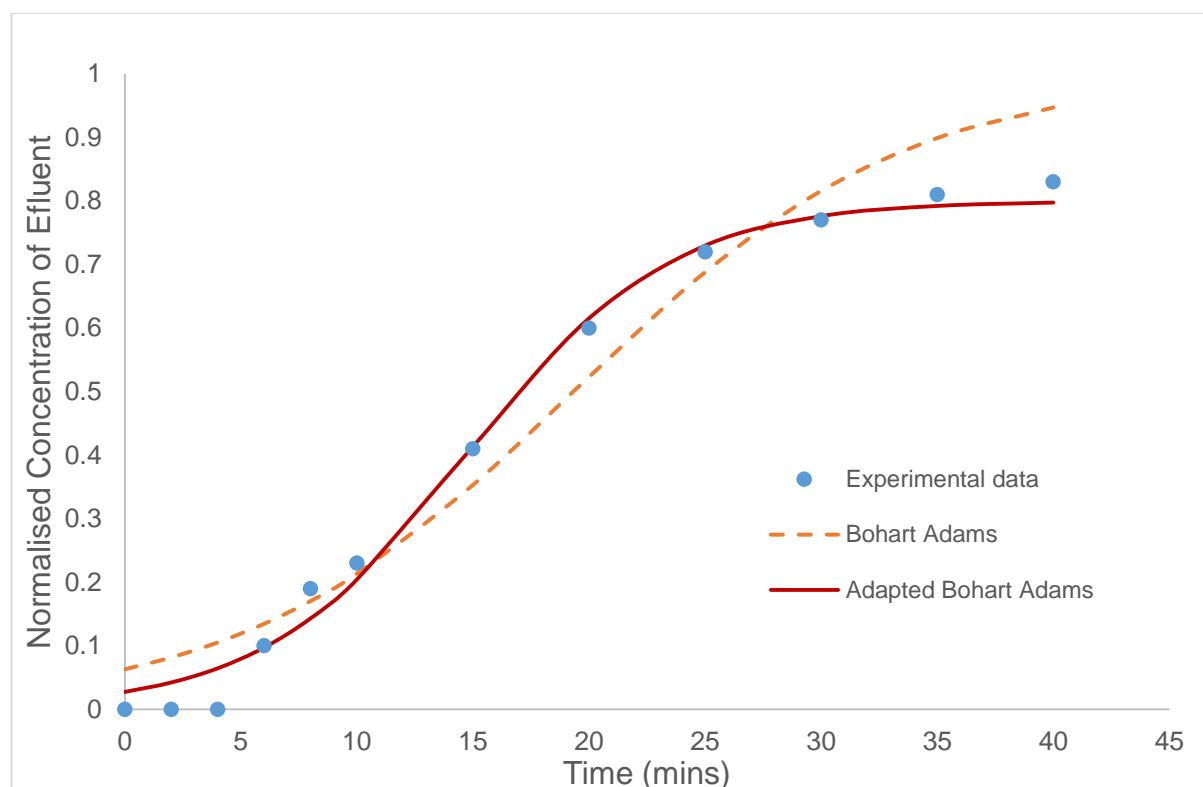


Figure 5:18: Breakthrough characteristics of recovery of microalgae cells onto Nyex™ particles at ($h = 20$ cm, $C_0 = 0.2$ OD, $Q = 10$ mL/min), predicted with the original and adapted Bohart-Adams models.

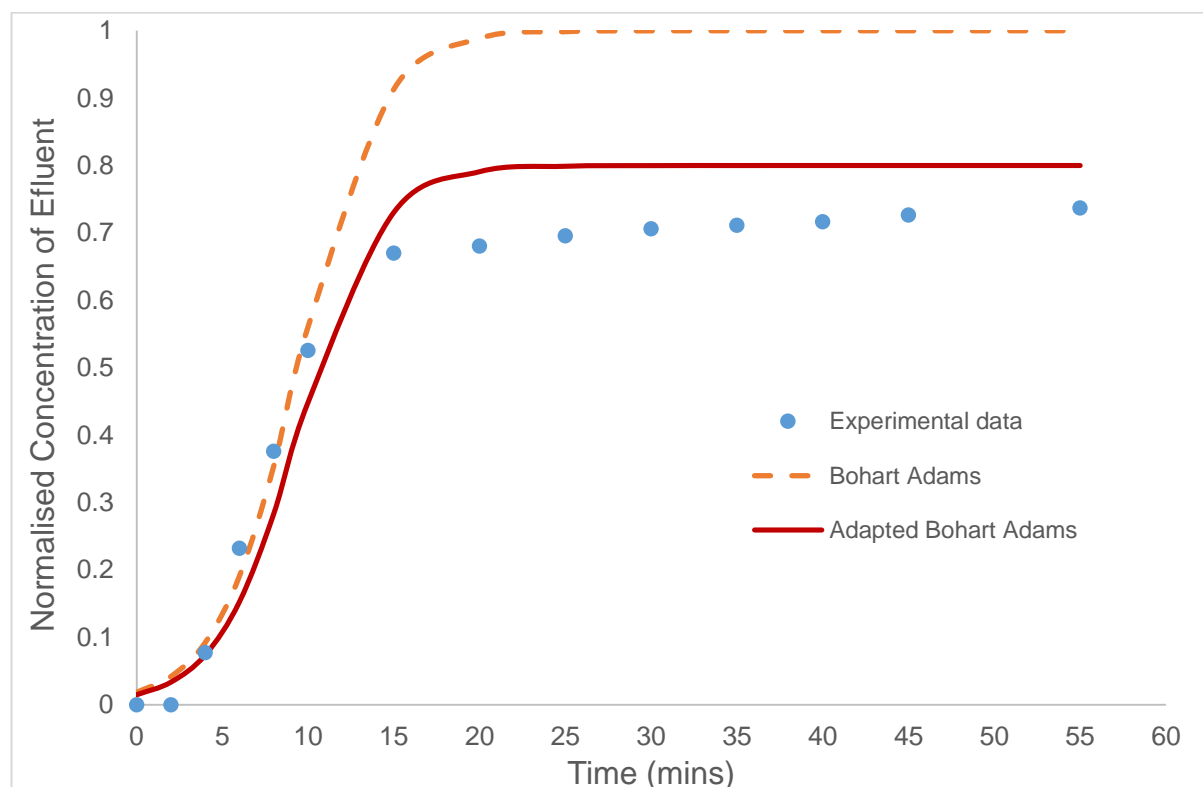


Figure 5:19: Breakthrough characteristics of recovery of microalgae cells onto Nyex™ particles at ($h = 20$ cm, $C_0 = 0.4$ OD, $Q = 10$ mL/min), predicted with the original and adapted Bohart-Adams models.

Table 5.12: Bohart-Adams parameters in the original, and adapted forms to predict breakthrough characteristics of cells recovery onto Nyex™ particles.

Scenario	K_{BA}	N_0	q_0	R^2	SSE
2	L/min/mg	mg/L	mg/g		
Original	1.074	0.253	0.310	0.972	0.522
Adapted	1.175	0.228	0.280	0.986	0.045
4					
Original	0.698	0.284	0.349	0.963	0.058
Adapted	1.137	0.216	0.265	0.99	0.011
5					
Original	1.055	0.277	0.340	0.97	0.645
Adapted	0.955	0.255	0.310	0.985	0.067

Similarly, the adapted Clark model was compared to the original Clark model, and the resulting graph are given in figures 5.20, 5.21 and 5.22. Unlike the adapted BA model, the adapted Clark model appears to better predict the lower times of the breakthrough curves.

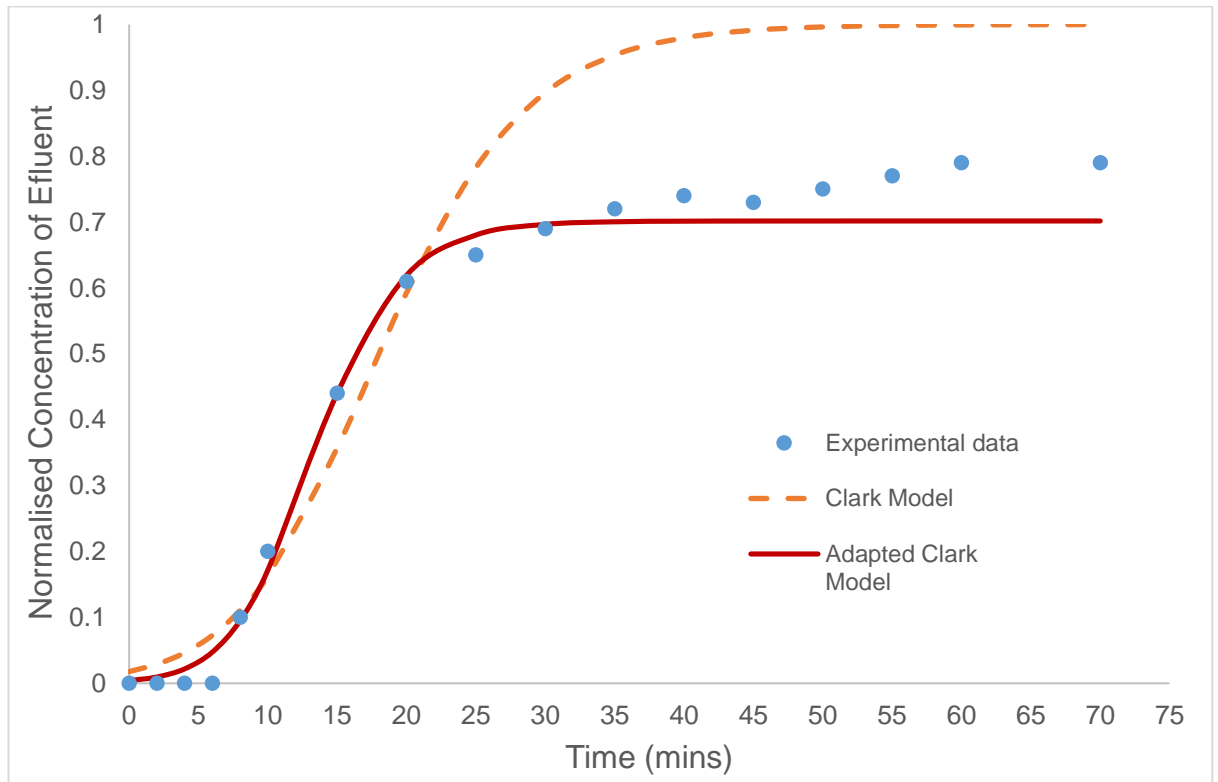


Figure 5.20: Breakthrough characteristics of cell recovery onto Nyex™ particles ($h = 10$ cm, $C_0 = 0.2$ OD, $Q = 5$ mL/min), predicted with the original and adapted Clark models.

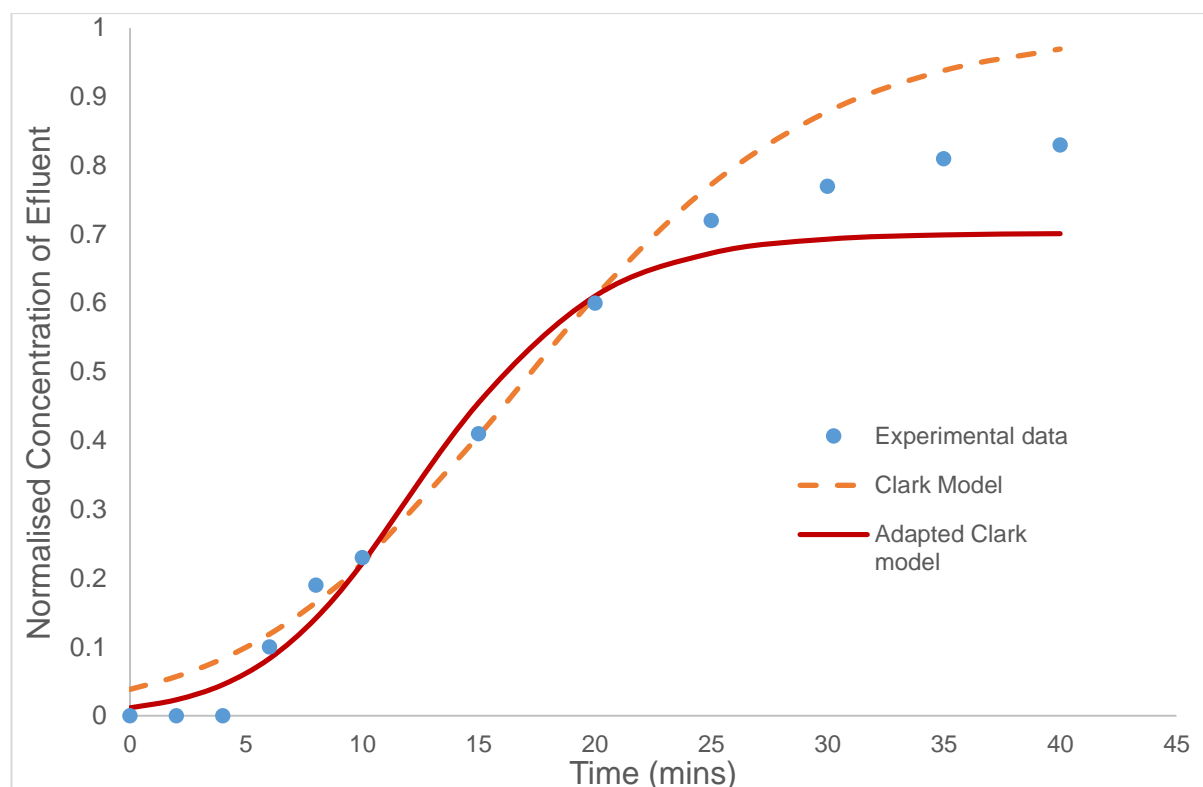


Figure 5:21: Breakthrough characteristics of cell recovery onto Nyex™ at ($h = 20$ cm, $C_0 = 0.2$ OD, $Q = 10$ mL/min), predicted with the original and adapted Clark models.

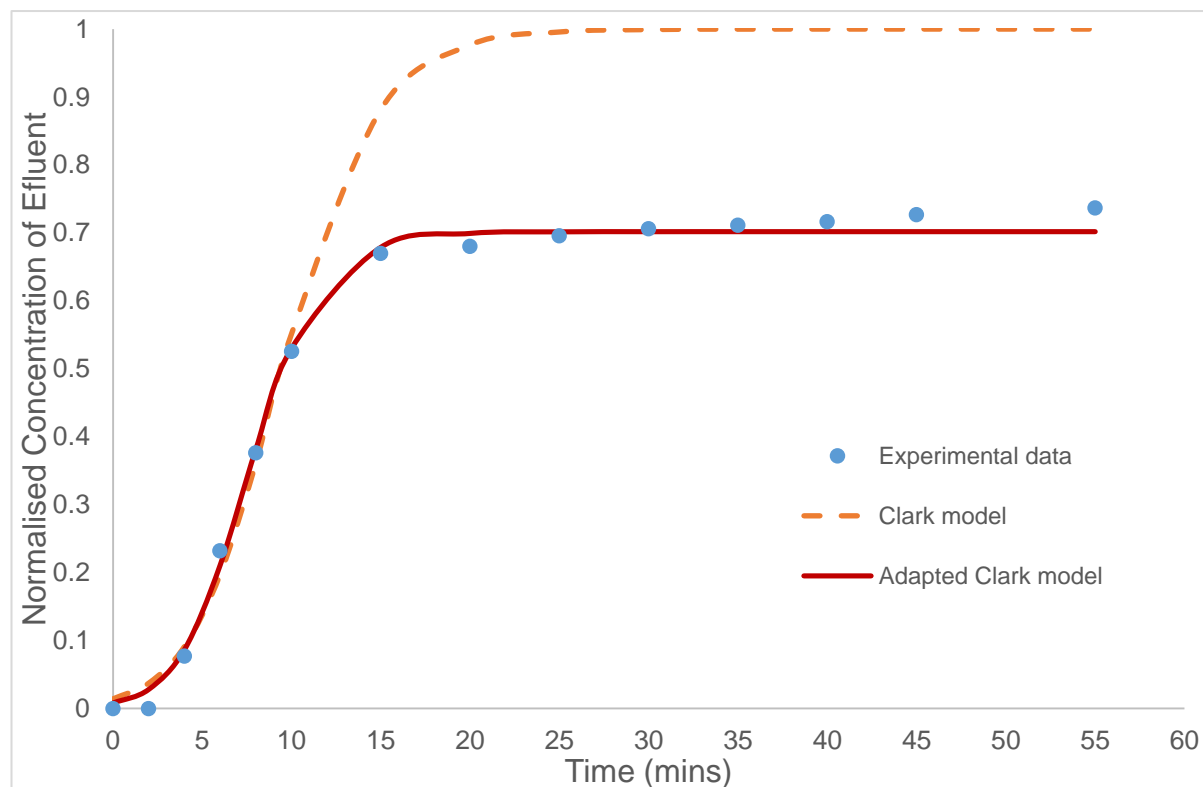


Figure 5:22: Breakthrough characteristics of cell recovery onto Nyex™ particles at ($h = 20$ cm, $C_0 = 0.4$ OD, $Q = 10$ mL/min), predicted with the Original and adapted Clark models.

Table 5.13: Clark parameters in the original and adapted forms to predict breakthrough characteristics of cell recovery onto Nyex™ particles.

Scenario	r	I	R^2	SSE
2				
Original	0.17	11.69	0.965	0.458
Adapted	0.29	24.78	0.99	0.03
4				
Original	0.15	6.79	0.984	0.0632
Adapted	0.25	12.29	0.983	0.045
5				
Original	0.34	13.83	0.966	0.62
Adapted	0.44	16.10	0.998	0.004

Apart from figure 5.21, the adapted Clark model was also a better fit at the higher times of the breakthrough curves. As shown in Table 5.13, the correlation coefficients were 0.99 and 0.998 for scenarios 2 and 3 respectively. In addition, the SSE was much smaller with the adapted models for all of the scenarios. In the same vein, the adapted Clark model was a better fit of the experimental data than the MDR model in terms of the R^2 and SSE values. In comparison to the Clark model, the parameters of the adapted Clark model increased for all the scenarios considered.

5.6 Summary

The suitability of a number of mathematical models to describe the recovery of microalgae cells onto Nyex™ particles within a fixed bed system has been studied. The use of mathematical models is economically desirable and more straightforward in comparison to laborious experimentation. The models considered for the research reported in this thesis were the Bohart-Adams, bed depth service time (BDST), Thomas, Clark and the modified dose response (MDR) models.

A number of scenarios were investigated, which took into account changes in the bed height, flow rate and the initial concentration of the microalgae suspension. Based on the accuracy of predictions of the experimental bed capacity as well as the statistical parameters evaluated, the MDR model was found consistently most

suited to describe the dynamics of cell recovery in the fixed bed. In this study, the Bohart-Adams and the Thomas models, as presently used, were shown to be mathematically identical. Findings based on the research reported in this thesis suggest that the Thomas model, as widely used in the literature, is the limiting form of the Bohart-Adams model. Hence, both models should not be used separately to describe column dynamics let alone when comparing their performance.

For all the models considered in this research, the linear regression analysis of the models was found to be unsuitable to predict column dynamics. An exception was the MDR model, which performed similarly to when non-linear regression analysis was used to fit the model to the experimental data.

For the first time, the logistic characteristics of the fixed bed models was adapted in order to account for the depressed breakthrough curves experienced in the research reported in this thesis. The adapted models especially the adapted Clark was shown to be more suitable to predict the depressed breakthrough curves. With respect to statistical analysis, the newly introduced adaptations were found to significantly improve the accuracy of predictions (Typical R^2 values > 0.99). However, this is based on the assumption that the maximum C_t/C_0 was 0.8. At pilot or industrial scale, it remains to be seen if this assumed value is reliable. Furthermore, the adapted Bohart-Adams model failed to accurately predict the bed capacity of the column.

The modified dose response model, based on the research reported in this thesis, appears to be more robust in predicting the recovery of microalgae cells onto NyexTM particles in a fixed bed column.

6 Conclusions and Future Perspectives

6.1 Conclusions

The research reported in this thesis has shown, for the first time, the potential of recovering microalgae cells onto a non-porous adsorbent, NyexTM. Furthermore, the research has achieved the objectives set out at the beginning of this thesis. The contributions that this research makes to the field of knowledge are outlined below.

First, batch studies were carried out to evaluate the adsorption equilibrium characteristics of NyexTM particles in the recovery of microalgae cells from suspension. This study showed that a very rapid uptake of the microalgae cells by the adsorbent particles. The extent of fast adsorption was evident such that within one minute of contact with the NyexTM particles, about 90% of the microalgae cells were recovered from suspension. It is argued in this thesis that the non-porous characteristics of the adsorbent, where cells were recovered onto the external surface of NyexTM, was responsible for the fast adsorption.

This research also showed that the Freundlich isotherm, with a correlation coefficient $R^2 = 0.99$, gave a better description of the recovery of microalgae cells onto NyexTM particles than the Langmuir isotherm. It is concluded that the inadequacy of the Langmuir isotherm is due to the cell coverage onto the NyexTM particles not being a simple monolayer adsorption. This research, for the first time, estimated the adsorptive capacity of NyexTM particles for *C. reinhardtii* as 0.55 mg/g. The equilibrium data were used to show that this low adsorptive capacity was mainly due to the relatively small surface area of the non-porous adsorbent. Specifically, the Freundlich isotherm parameter ($1/n$), estimated as 0.61, was well within the range of 0 and 1, which suggests a favourable adsorption between the microalgae cells and NyexTM particles.

One of the key findings of the batch studies, shown in this research, were the mechanisms involved in the recovery of microalgae cells from suspension. For the first time, the acidic characteristics of the NyexTM particles were found to play a major role in the cell recovery; an observation not previously reported. Unlike previous studies, it was shown that recovery of cells using adsorption was achievable at all pH and zeta potential values investigated. From very acidic (pH 3) to neutral (pH 7) to very alkaline (pH 11), at least 75% of the microalgae cells were

recovered onto the adsorbent. This outcome revealed that a host of mechanisms could be involved in the recovery of microalgae cells. Based on the results reported in this thesis, it is concluded that the mechanisms of adsorption were; hydrophobic-hydrophobic interaction and electrostatic forces of attraction between the cells and Nyex™ particles as well as the flocculating behaviour of the adsorbent. Hence this research also demonstrated that within a batch system, a combination of these mechanisms were simultaneously driving the recovery of cells onto the adsorbent; depending on the microalgae suspension conditions.

Fixed bed continuous flow studies showed that the effects of flow rate, bed height and initial suspension concentration limit the recovery of cells onto the adsorbent. Due to the lack of pores, breakthrough times were observed to occur as early as 2 minutes; in addition to relatively short exhaustion times. Unlike most studies, this research showed that parameters such as breakthrough and exhaustion times are less relevant with respect to the overarching objective of this study. Thus, it was revealed that the bed capacity was a more valuable parameter to appreciate the effects of flow conditions and to identify the best scenarios.

This research demonstrated that the upward flow mode of feeding the column was unsuitable for the recovery of microalgae cells. Depressed breakthrough curves, where bed exhaustion never attained $C/C_0 = 1.0$, were also experienced. However, it was established, through the use of control studies with acid violet 17 dye, that these observations were peculiar to microalgae suspensions. It was also shown that it is of insignificant benefit to operate the bed in the submerged mode to recover the cells. Another key finding was that cell recovery could be as a result of the combined effects of adsorption and filtration within the bed of Nyex™ particles. The advantages of operating the fixed bed as a continuous system and the difficulties experienced in the Arvia Y-cell led to the conclusion that microalgae cell recovery within a fixed bed column has distinctive advantages over the batch system.

Of the mathematical models considered, the modified dose response (MDR) model was the best to predict the experimental bed capacity (percentage deviation was less than 11% for all scenarios) as well as the unique feature of depressed breakthrough curves experienced in this research. Statistical parameters, such as

the correlation coefficients and sum of the squared error, were used to validate the suitability of the MDR model.

For the first time, this research exploited the logistic characteristics of the fixed bed models to better fit the Bohart-Adams and the Clark models, through some adaptation, to the column experimental data. The adapted models, especially the adapted Clark model, were shown to significantly improve accuracy of predictions (Typical R^2 values > 0.99). The limitation of such adaptation, however, was in the assumption that the maximum C_t/C_0 attainable was a fixed value. As a consequence, this research considered the relative accuracy and reliability of the Modified Dose Response model, to conclude that it is the most suitable model to predict the recovery of microalgae cells onto NyexTM particles in a fixed bed column.

This research exploited the conductive characteristics of the NyexTM particles to regenerate the adsorbent by electrochemical means and more importantly to understand the effects on the adsorbed microalgae cells. Unlike the complete destruction of adsorbed organics, this research revealed that during electrochemical regeneration of the adsorbent, complete destruction of microalgae cells could not be achieved. It was established that a current density of 32 mA.cm^{-2} was sufficient to inactivate the cells, regenerate the adsorbent particles and reuse them to achieve a maximum recovery of the microalgae cells from suspension.

The electrochemically treated adsorbent particles were found to possess better adsorption characteristics than fresh particles. This finding also demonstrates the beneficial effects of electrochemically regenerating NyexTM; as the process promotes adsorbent degradation and surface chemistry modification which in turn enhance the recovery of microalgae cells. However, such enhanced recovery was found to be peculiar to batch systems, as fewer cells were recovered in column systems with regenerated NyexTM particles. Based on the scenarios considered, it was also found that the electrical charge was the driving force to regenerate the adsorbent particles and cause microalgae cell inactivation.

Another key finding in this research was that the use of smaller size fractions of NyexTM enhanced the recovery of microalgae cells. Contrary to the long held opinion that smaller size fractions of Nyex particles are undesirable for adsorption, this research demonstrated their suitability to recover microalgae cells from suspension.

As expected, the smaller size fractions gave much better cell recovery, attaining 99% percent recovery, in comparison to the widely used 'washed' Nyex™ particles. Furthermore, this research showed that the smaller size fractions settled much more quickly in microalgae suspension and did not colourise the suspension media. In addition, it was argued that the better adsorption characteristics of smaller fractions was due to greater surface area available for adsorption. As a consequence, it is suggested that there is no need to wash Nyex™ particles before using them to recover microalgae cells.

Using SEM micrographs, it was shown that the cell wall/membrane of the adsorbed microalgae cells was ruptured and intracellular materials were released during the electrochemical regeneration of Nyex™ particles. With the aid of hexane solvent, this study revealed that lipids could be washed off the surface of the Nyex™ particles. The maximum recovery, *circa* 30 µg/mL of lipids was estimated at a current density of 64 mA.cm⁻². This research, for the first time, uncovered the potential of rupturing the membranes of the adsorbed microalgae cells using electrochemical method; thus resulting in the potential recovery of lipids.

Through these findings, the objectives set at the beginning of the research reported in this thesis have been achieved. This supports the implicit hypothesis that the non-porous characteristics of Nyex™ particles offer the opportunity to use adsorption as a technique to recover microalgae cells from suspension for potential biofuel applications. Additionally, these findings provide the platform on which further investigations can be undertaken to develop a novel technology where microalgae biomass recovery and wet extraction of lipids can be achieved within a single stage process.

6.2 Future Perspectives

6.2.1 Recovery of Variety of Microalgae Strains

The use of adsorption to recover a variety of microalgae strains depending on their size was established in this research. However, there are more microalgae strains being considered for biofuel applications which have different characteristics. For instance, some microalgae cells are cultivated and thrive in either saline, brackish or wastewater media. As established in this research, suspension conditions do affect cell recovery and it will be interesting to understand how those cells not grown

on TAP media behave with Nyex™ particles. Furthermore, larger microalgae strains, circa 70 µm for *spirulina platensis*, would require some studies. This is especially relevant within a fixed bed column where such large cells can easily cause biofouling as observed with cells with average size of about 8 µm. In addition, some cells lack a membrane/wall, for instance *Botryococcus braunii*, hence a study on how this might affect the adsorption characteristics with Nyex™ particles would be of particular interest.

Whilst the microalgae strain employed in this research is a good model, it is not a high lipid producer. Hence, further studies should be conducted with other strains to provide some insight into the efficiency of the electrochemical aspects of the technique to recover lipids from such strains.

6.2.2 Choice of Adsorbent Material

A number of research initiatives have been undertaken to improve the adsorption characteristics of Nyex™ particles. An improved type of Nyex™ material with a much better adsorptive capacity is under development. Hence, the use of such adsorbents will no doubt improve the recovery efficiency of microalgae cells from suspension. New types of conductive nanomaterials are also surfacing, which implies that they can be electrochemically regenerated when used to recover microalgae cells. The morphology of the adsorbent material is also of importance. An exhaustive study on the use of Nyex™ granules, rather than flakes could provide more insight and might offer explanation(s) for the depressed breakthrough curves experienced in this research.

6.2.3 Effects of electrode materials/catholyte

The performance of an electrochemical cell depends on the choice of electrode material. A number of electrodes such as iridium oxide, platinum and boron-doped diamond electrodes are known to use different mechanisms to achieve anodic oxidation of adsorbates. In addition, the type of electrodes used determines the stability in electrolysis media, uniformity of current distribution as well as the oxidation reactions formed. The latter are important because the type of radicals formed and the quantity of oxygen evolution can influence the oxidation mechanism. While a graphite anode was used in this research, further investigations are needed to establish the advantage of using other anodic materials. In this research, there

was no evidence that uniform cell membrane disruption was achieved. Hence, the use of aforementioned electrode materials could shed light on their capability to achieve identical membrane disruption on the adsorbed cells.

Furthermore, the choice of catholyte determines the chemicals produced during electrolysis. These chemicals influence the sort of mechanisms that lead to adsorbent regeneration and their effects on the adsorbed microalgae cells. For instance, production of Ozone and Chlorine dioxide are known to be effective for the disruption of cell membranes. Hence, the need to consider other catholytes such as sodium sulphate to regenerate the adsorbent. Besides, the effects of by-products generated on the released intracellular materials would require some investigation. For instance, through transesterification reaction, the extracted lipids is converted to biodiesel, where contamination from the by-products may be undesirable.

6.2.4 Development of a protocol to estimate total lipids released

The quantity of total lipids extracted requires a robust and standardised protocol. This is because the lipids estimation reported in this thesis was limited to the lipids washed off from the Nyex™ surface. The lipids estimated does not include any potential polar lipids released into the supernatant, which could underestimate the actual total lipids released. Hence, an extraction protocol that takes into account the various forms of lipids would ensure an accurate analysis of lipids released as a result of cell disruption. In addition, the use of gas chromatography will be valuable in determining the fatty acid composition of the extracted lipids.

Furthermore, microalgae cells are known to accumulate other products such as β -carotene and chemicals like docosahexaenoic acid (DHA). The latter are high value intracellular materials with potential application in nutritional supplements and aquaculture. The fact that cell membrane disruption implies a number of these bio-products are also exposed, which can then be recovered. Hence, the development of standardised protocols to extract these valuable products should be of interest.

6.2.5 Dual use of technique for bioremediation

Microalgae cells are increasingly being exploited for the dual function of treating wastewater and providing biomass for biofuel applications. Hence, wastewater companies see microalgae cells as a biological material to remove nitrate and phosphate pollutants from their system. However, conventional techniques are still

being considered to recover such microalgae cells. Thus, the technique being investigated in this research could also be a treatment technology to remove microalgae cells grown on wastewater media due to its capability to inactivate the cells. However, this research has not considered a mixed culture of microorganisms which could be present in a wastewater stream. Hence, further work using this technology will provide an opportunity to investigate how such a wastewater system can be utilised.

In addition, the recovery of microbial cells onto an adsorbent are known to increase the negative charge density of the latter. Hence, such an adsorbent with surface modification can be used, depending on the system conditions, to remove heavy metal pollutants such as lead. At present, Nyex™ particles have not been reported to remove heavy metals from waste streams. Hence, further studies on the potential application of this technique can open up more opportunities.

6.2.6 Energy and cost implications

The capability of a non-porous adsorbent to recover microalgae cells from suspension as well as the membrane disruption of adsorbed cells during electrochemical regeneration of the adsorbent has been demonstrated in this research. However, as with a number of methods, energy and cost implications of a technology especially at industrial scale pose some challenges towards commercialisation. As it is possible to rupture cell membranes without the need for a separate dewatering and biomass drying stage, the energy and cost implications are expected to be relatively low. Nonetheless, a techno-economic and energy assessment of the process will still be of significant value to appreciate the energetic and cost associated with the technology. Parameters such as the energy and economic return on investment will be valuable in order to realise energy and cost savings, if any. This could also inform decisions on its advantages over existing technologies as well as identify aspects of the technology that require additional refinement.

References

- Aksu, Z. and Gönen, F. (2004) Biosorption of phenol by immobilized activated sludge in a continuous packed bed: prediction of breakthrough curves, *Process Biochemistry*, **39**(5), pp. 599–613, [online] Available from: <http://www.sciencedirect.com/science/article/pii/S0032959203001328>.
- Al-Degs, Y. S., El-Barghouthi, M. I., El-Sheikh, A. H. and Walker, G. M. (2008) Effect of solution pH, ionic strength, and temperature on adsorption behavior of reactive dyes on activated carbon, *Dyes and Pigments*, **77**(1), pp. 16–23, [online] Available from: <http://www.sciencedirect.com/science/article/pii/S0143720807000538>.
- Alfafara, C. G., Nakano, K., Nomura, N., Igarashi, T. and Matsumura, M. (2002) Operating and scale-up factors for the electrolytic removal of algae from eutrophied lakewater, *Journal of Chemical Technology & Biotechnology*, John Wiley & Sons, Ltd., **77**(8), pp. 871–876, [online] Available from: <http://dx.doi.org/10.1002/jctb.649>.
- Amaro, H. M., Guedes, A. C. and Malcata, F. X. (2011) Advances and perspectives in using microalgae to produce biodiesel, *Applied Energy*, **88**(10), pp. 3402–3410, [online] Available from: <http://www.sciencedirect.com/science/article/pii/S0306261910005210>.
- Anirban, B., Rohit, S., Yusuf, C. and Banerjee, U. C. (2002) Botryococcus braunii: A Renewable Source of Hydrocarbons and Other Chemicals, *Critical Reviews in Biotechnology*, **22**(3), pp. 245–279, [online] Available from: <http://www.ingentaconnect.com/content/apl/bbtn/2002/00000022/00000003/art00002>.
- Aragón, A. B., Padilla, R. B. and Ros de Ursinos, J. A. F. (1992) Experimental study of the recovery of algae cultured in effluents from the anaerobic biological treatment of urban wastewaters, *Resources, Conservation and Recycling*, **6**(4), pp. 293–302, [online] Available from: <http://www.sciencedirect.com/science/article/pii/0921344992900535>.
- Araujo, G. S., Matos, L. J. B. L., Gonçalves, L. R. B., Fernandes, F. A. N. and Farias, W. R. L. (2011) Bioprospecting for oil producing microalgal strains: Evaluation of oil and biomass production for ten microalgal strains, *Bioresource Technology*, **102**(8), pp. 5248–5250, [online] Available from: <http://www.sciencedirect.com/science/article/pii/S0960852411001830>.
- Asghar, H. M. A., Roberts, E. P. L., Hussain, S. N., Campen, A. K. and Brown, N. W. (2012) Wastewater treatment by adsorption with electrochemical regeneration using graphite-based adsorbents, *Journal of Applied Electrochemistry*, Springer Netherlands, **42**(9), pp. 797–807, [online] Available from: <http://dx.doi.org/10.1007/s10800-012-0439-8>.
- Asrafuzzaman, M., Fakhruddin, A. N. M. and Hossain, M. A. (2011) Reduction of Turbidity of Water Using Locally Available Natural Coagulants, *ISRN Microbiology*, **2011**, p. 6, [online] Available from: <http://dx.doi.org/10.5402/2011/632189>.

Azapagic, A. and Perdan, S. (2010) *Sustainable Development in Practice [electronic resource]: Case Studies for Engineers and Scientists*, 2nd ed, Chichester, John Wiley & Sons, [online] Available from: <http://www.ncl.ebllib.com/patron/FullRecord.aspx?p=624644>.

Azarian, G. H., Mesdaghinia, A. R., Vaezi, F., Nabizadeh, R. and Nematollahi, D. (2007) Algae removal by electro-coagulation process, application for treatment of the effluent from an industrial wastewater treatment plant, *Iranian journal of public health*, **36**(4).

Barbosa-Canovas, G. V, Pothakamury, U. R., Gongora-Nieto, M. M. and Swanson, B. G. (1999) *Preservation of Foods with Pulsed Electric Fields*, *Food Science and Technology*, Elsevier Science, [online] Available from: <https://books.google.co.uk/books?id=Z2sSYy5mVWUC>.

Barros, A. I., Gonçalves, A. L., Simões, M. and Pires, J. C. M. (2015) Harvesting techniques applied to microalgae: A review, *Renewable and Sustainable Energy Reviews*, **41**, pp. 1489–1500, [online] Available from: <http://www.sciencedirect.com/science/article/pii/S1364032114008107>.

Basha, H. A. and Culligan, P. J. (2010) Modeling particle transport in downward and upward flows, *Water Resources Research*, **46**(7), p. n/a-n/a, [online] Available from: <http://dx.doi.org/10.1029/2009WR008133>.

Bazan, J. C. and Bisang, J. M. (2004) Electrochemical Removal of Tin from Dilute Aqueous Sulfate Solutions using a Rotating Cylinder Electrode of Expanded Metal, *Journal of Applied Electrochemistry*, **34**(5), pp. 501–506, [online] Available from: <http://dx.doi.org/10.1023/B:JACH.0000021894.86112.63>.

Beach, E. S., Eckelman, M. J., Cui, Z., Brentner, L. and Zimmerman, J. B. (2012) Preferential technological and life cycle environmental performance of chitosan flocculation for harvesting of the green algae *Neochloris oleoabundans*, *Bioresource Technology*, **121**, pp. 445–449, [online] Available from: <http://www.sciencedirect.com/science/article/pii/S0960852412009169>.

van Beilen, J. B. (2010) Why microalgal biofuels won't save the internal combustion machine, *Biofuels, Bioproducts and Biorefining*, **4**(1), pp. 41–52, [online] Available from: <http://dx.doi.org/10.1002/bbb.193>.

Belash, I. T., Zharikov, O. V and Palnichenko, A. V (1989) Synthesis, stability and structure of GIC with Li, Na and K, *Synthetic Metals*, **34**(1), pp. 47–52, [online] Available from: <http://www.sciencedirect.com/science/article/pii/0379677989903627>.

Bernhardt, H., Schell, H., Hoyer, O. and Lüsse, B. (1991) Influence of algogenic organic substances on flocculation and filtration, In *WISA*, pp. 41–57.

Bitton, G. and Marshall, K. C. (1980) *Adsorption of microorganisms to surfaces*, John Wiley and Sons, Inc.

Bligh, E. G. and Dyer, W. J. (1959) A rapid method of total lipid extraction and purification, *Canadian journal of biochemistry and physiology*, NRC Research Press, **37**(8), pp. 911–917.

Boelee, N., Temmink, H., Janssen, M., Buisman, C. and Wijffels, R. (2011) Nitrogen and phosphorus removal from municipal wastewater effluent using microalgal biofilms, *Water Res*, **45**, [online] Available from: <http://dx.doi.org/10.1016/j.watres.2011.08.044>.

Bohart, G. S. and Adams, E. Q. (1920) Some aspects of the behavior of charcoal with respect to chlorine.1, *Journal of the American Chemical Society*, **42**(3), pp. 523–544, [online] Available from: <http://dx.doi.org/10.1021/ja01448a018>.

Borba, C. E., Guirardello, R., Silva, E. A., Veit, M. T. and Tavares, C. R. G. (2006) Removal of nickel(II) ions from aqueous solution by biosorption in a fixed bed column: Experimental and theoretical breakthrough curves, *Biochemical Engineering Journal*, **30**(2), pp. 184–191, [online] Available from: <http://www.sciencedirect.com/science/article/pii/S1369703X0600091X>.

Borba, C. E., Silva, E. A. da, Fagundes-Klen, M. R., Kroumov, A. D. and Guirardello, R. (2008) Prediction of the copper (II) ions dynamic removal from a medium by using mathematical models with analytical solution, *Journal of Hazardous Materials*, **152**(1), pp. 366–372, [online] Available from: <http://www.sciencedirect.com/science/article/pii/S0304389407009879>.

Borowitzka, M. A. (1992) Algal biotechnology products and processes — matching science and economics, *Journal of Applied Phycology*, **4**(3), pp. 267–279, [online] Available from: <http://dx.doi.org/10.1007/BF02161212>.

Boussiba, S., Vonshak, A., Cohen, Z., Avissar, Y. and Richmond, A. (1987) Lipid and biomass production by the halotolerant microalga *Nannochloropsis salina*, *Biomass*, **12**(1), pp. 37–47, [online] Available from: <http://www.sciencedirect.com/science/article/pii/0144456587900060>.

Brennan, L. and Owende, P. (2010) Biofuels from microalgae--A review of technologies for production, processing, and extractions of biofuels and co-products, *Renewable and Sustainable Energy Reviews*, **14**(2), pp. 557–577, [online] Available from: <http://www.sciencedirect.com/science/article/pii/S1364032109002408>.

Brown, N. W., Campen, A. K., Wickenden, D. A. and Roberts, E. P. L. (2013) On-site destruction of radioactive oily wastes using adsorption coupled with electrochemical regeneration, *Chemical Engineering Research and Design*, **91**(4), pp. 713–721, [online] Available from: <http://www.sciencedirect.com/science/article/pii/S0263876212004583>.

Brown, N. W. and Roberts, E. P. L. (2007) Electrochemical pre-treatment of effluents containing chlorinated compounds using an adsorbent, *Journal of Applied Electrochemistry*, **37**(11), pp. 1329–1335, [online] Available from: <http://link.springer.com/article/10.1007/s10800-007-9376-3>.

- Brown, N. W., Roberts, E. P. L., Chasiotis, A., Cherdron, T. and Sanghrajka, N. (2004) Atrazine removal using adsorption and electrochemical regeneration, *Water Research*, **38**(13), pp. 3067–3074, [online] Available from: <http://www.sciencedirect.com/science/article/pii/S0043135404002052>.
- Brown, N. W., Roberts, E. P. L., Garforth, A. A. and Dryfe, R. A. W. (2004) Electrochemical regeneration of a carbon-based adsorbent loaded with crystal violet dye, *Electrochimica Acta*, **49**(20), pp. 3269–3281, [online] Available from: <http://www.sciencedirect.com/science/article/pii/S0013468604002804>.
- Bruhn, A., Dahl, J., Nielsen, H. B., Nikolaisen, L., Rasmussen, M. B., Markager, S., Olesen, B., Arias, C. and Jensen, P. D. (2011) Bioenergy potential of *Ulva lactuca*: Biomass yield, methane production and combustion, *Bioresource Technology*, **102**(3), pp. 2595–2604, [online] Available from: <http://www.sciencedirect.com/science/article/pii/S0960852410016585>.
- Calero, M., Hernáinz, F., Blázquez, G., Tenorio, G. and Martín-Lara, M. A. (2009) Study of Cr (III) biosorption in a fixed-bed column, *Journal of Hazardous Materials*, **171**(1–3), pp. 886–893, [online] Available from: <http://www.sciencedirect.com/science/article/pii/S0304389409010164>.
- Campbell, D. A., Dalrymple, I. M., Sunderland, J. G. and Tilston, D. (1994) The electrochemical recovery of metals from effluent and process streams, *Resources, Conservation and Recycling*, Elsevier, **10**(1), pp. 25–33.
- Canteli, A. M. D., Carpiné, D., Scheer, A. de P., Mafra, M. R. and Igarashi-Mafra, L. (2014) Fixed-bed column adsorption of the coffee aroma compound benzaldehyde from aqueous solution onto granular activated carbon from coconut husk, *LWT - Food Science and Technology*, **59**(2, Part 1), pp. 1025–1032, [online] Available from: <http://www.sciencedirect.com/science/article/pii/S0023643814003685>.
- Cartens, M., Grima, E. M., Medina, A. R., Giménez, A. G. and González, J. I. (1996) Eicosapentaenoic acid (20:5n-3) from the marine microalga *Phaeodactylum tricornutum*, *Journal of the American Oil Chemists' Society*, **73**(8), pp. 1025–1031, [online] Available from: <http://dx.doi.org/10.1007/BF02523411>.
- Carvalho, A. P. and Malcata, F. X. (2005) Preparation of fatty acid methyl esters for gas-chromatographic analysis of marine lipids: insight studies, *Journal of agricultural and food chemistry*, ACS Publications, **53**(13), pp. 5049–5059.
- Cassidy, M. B., Lee, H. and Trevors, J. T. (1996) Environmental applications of immobilized microbial cells: A review, *Journal of Industrial Microbiology*, **16**(2), pp. 79–101, [online] Available from: <http://dx.doi.org/10.1007/BF01570068>.
- Cerff, M., Morweiser, M., Dillschneider, R., Michel, A., Menzel, K. and Posten, C. (2012) Harvesting fresh water and marine algae by magnetic separation: Screening of separation parameters and high gradient magnetic filtration, *Bioresource Technology*, **118**(0), pp. 289–295, [online] Available from: <http://www.sciencedirect.com/science/article/pii/S0960852412007638>.

- Charlier, A., Charlier, M. F. and Fristot, D. (1989) Binary graphite intercalation compounds, *Journal of Physics and Chemistry of Solids*, **50**(10), pp. 987–996, [online] Available from: <http://www.sciencedirect.com/science/article/pii/0022369789904988>.
- Chen, C.-Y. Y., Yeh, K.-L. L., Aisyah, R., Lee, D.-J. J. and Chang, J.-S. S. (2011) Cultivation, photobioreactor design and harvesting of microalgae for biodiesel production: A critical review, *Bioresource Technology*, **102**(1), pp. 71–81, [online] Available from: <http://www.scopus.com/inward/record.url?eid=2-s2.0-77957343168&partnerID=40&md5=6dfe442daf31f044dea5c5b35f24517b>.
- Chen, G., Wu, D., Weng, W. and Wu, C. (2003) Exfoliation of graphite flake and its nanocomposites, *Carbon*, **41**(3), pp. 619–621.
- Chen, Y., Tang, X., Kapoore, R. V., Xu, C. and Vaidyanathan, S. (2015) Influence of nutrient status on the accumulation of biomass and lipid in *Nannochloropsis salina* and *Dunaliella salina*, *Energy Conversion and Management*, **106**, pp. 61–72, [online] Available from: <http://www.sciencedirect.com/science/article/pii/S0196890415008602>.
- Cheng, Y.-L., Juang, Y.-C., Liao, G.-Y., Tsai, P.-W., Ho, S.-H., Yeh, K.-L., Chen, C.-Y., Chang, J.-S., Liu, J.-C., Chen, W.-M. and Lee, D.-J. (2011) Harvesting of *Scenedesmus obliquus* FSP-3 using dispersed ozone flotation, *Bioresource Technology*, **102**(1), pp. 82–87, [online] Available from: <http://www.sciencedirect.com/science/article/pii/S0960852410007698>.
- Chern, J.-M. and Chien, Y.-W. (2002) Adsorption of nitrophenol onto activated carbon: isotherms and breakthrough curves, *Water Research*, **36**(3), pp. 647–655, [online] Available from: <http://www.sciencedirect.com/science/article/pii/S0043135401002585>.
- Cheung, P. C. K. (1999) Temperature and pressure effects on supercritical carbon dioxide extraction of n-3 fatty acids from red seaweed, *Food Chemistry*, **65**(3), pp. 399–403, [online] Available from: <http://www.sciencedirect.com/science/article/pii/S0308814698002106>.
- Chini Zittelli, G., Lavista, F., Bastianini, A., Rodolfi, L., Vincenzini, M. and Tredici, M. R. (1999) Production of eicosapentaenoic acid by *Nannochloropsis* sp. cultures in outdoor tubular photobioreactors, *Journal of Biotechnology*, **70**(1–3), pp. 299–312, [online] Available from: <http://www.sciencedirect.com/science/article/pii/S0168165699000826>.
- Chinnasamy, S., Ramakrishnan, B., Bhatnagar, A. and Das, K. C. (2009) Biomass production potential of a wastewater alga *Chlorella vulgaris* ARC 1 under elevated levels of CO₂ and temperature, *Int J Mol Sci*, **10**, [online] Available from: <http://dx.doi.org/10.3390/ijms10020518>.
- Chisti, Y. (2007) Biodiesel from microalgae, *Biotechnology Advances*, **25**(3), pp. 294–306, [online] Available from: <http://www.sciencedirect.com/science/article/pii/S0734975007000262>.

Chisti, Y. (2008a) Biodiesel from microalgae beats bioethanol, *Trends in Biotechnology*, **26**(3), pp. 126–131, [online] Available from: <http://www.sciencedirect.com/science/article/pii/S0167779908000218>.

Chisti, Y. (2010) Fuels from microalgae, *Biofuels*, **1**(2), pp. 233–235.

Chisti, Y. (2008b) Response to Reijnders: Do biofuels from microalgae beat biofuels from terrestrial plants?, *Trends in Biotechnology*, **26**(7), pp. 351–352, [online] Available from: <http://www.sciencedirect.com/science/article/pii/S0167779908001169>.

Chisti, Y. and Yan, J. (2011) Energy from algae: Current status and future trends: Algal biofuels - A status report, *Applied Energy*, **88**(10), pp. 3277–3279, [online] Available from: <http://www.sciencedirect.com/science/article/pii/S030626191100273X>.

Christensen, P., Stryhn, H. and Hansen, C. (2005) Discrepancies in the determination of sperm concentration using Bürker-Türk, Thoma and Makler counting chambers, *Theriogenology*, **63**(4), pp. 992–1003, [online] Available from: <http://www.sciencedirect.com/science/article/pii/S0093691X04001852>.

Christenson, L. B. and Sims, R. C. (2012) Rotating algal biofilm reactor and spool harvester for wastewater treatment with biofuels by-products, *Biotechnology and Bioengineering*, **109**(7), pp. 1674–1684, [online] Available from: <http://dx.doi.org/10.1002/bit.24451>.

Chu, K. H. (2010) Fixed bed sorption: Setting the record straight on the Bohart–Adams and Thomas models, *Journal of Hazardous Materials*, **177**(1–3), pp. 1006–1012, [online] Available from: <http://www.sciencedirect.com/science/article/pii/S030438941000035X>.

Chu, K. H. (2004) Improved fixed bed models for metal biosorption, *Chemical Engineering Journal*, **97**(2–3), pp. 233–239, [online] Available from: <http://www.sciencedirect.com/science/article/pii/S1385894703002146>.

Chung, D. D. L. (2002) Review Graphite, *Journal of Materials Science*, **37**(8), pp. 1475–1489, [online] Available from: <http://dx.doi.org/10.1023/A:1014915307738>.

Clark, R. M. (1987) Evaluating the cost and performance of field-scale granular activated carbon systems, *Environmental Science & Technology*, **21**(6), pp. 573–580, [online] Available from: <http://dx.doi.org/10.1021/es00160a008>.

Clément, C., Lonchamp, D., Rebeller, M., Van Landeghem, H., Clement, C., Lonchamp, D., Rebeller, M. and Van Landeghem, H. (1980) The development of Spirulina algae cultivation, *Chemical Engineering Science*, **35**(1–2), pp. 119–126, [online] Available from: <http://www.sciencedirect.com/science/article/pii/0009250980800789>.

Conte, A. A. (1983) Graphite Intercalation Compounds as Solid Lubricants, *ASLE Transactions*, **26**(2), pp. 200–208, [online] Available from: <http://dx.doi.org/10.1080/05698198308981494>.

Conti-Ramsden, M. G., Brown, N. W. and Roberts, E. P. L. (2012) Towards an odour control system combining slurry sorption and electrochemical regeneration, *Chemical Engineering Science*, **79**(0), pp. 219–227, [online] Available from: <http://www.sciencedirect.com/science/article/pii/S0009250912003302>.

Conti-Ramsden, M. G., Nkrumah-Amoako, K., Brown, N. W. and Roberts, E. P. L. (2013) The oxidation of aqueous thiols on a graphite intercalation compound adsorbent, *Adsorption*, **19**(5), pp. 989–996, [online] Available from: <http://dx.doi.org/10.1007/s10450-013-9514-7>.

Cooney, M., Young, G. and Nagle, N. (2009) Extraction of Bio-oils from Microalgae, *Separation & Purification Reviews*, **38**(4), pp. 291–325, [online] Available from: <http://dx.doi.org/10.1080/15422110903327919>.

Coughlin, R. W., Ezra, F. S. and Tan, R. N. (1968) Influence of chemisorbed oxygen in adsorption onto carbon from aqueous solution, *Journal of Colloid and Interface Science*, **28**(3), pp. 386–396, [online] Available from: <http://www.sciencedirect.com/science/article/pii/0021979768900696>.

Couto, R. M., Simões, P. C., Reis, A., Da Silva, T. L., Martins, V. H. and Sánchez-Vicente, Y. (2010) Supercritical fluid extraction of lipids from the heterotrophic microalga *Cryptocodinium cohnii*, *Engineering in Life Sciences*, **10**(2), pp. 158–164, [online] Available from: <http://dx.doi.org/10.1002/elsc.200900074>.

Crini, G. and Badot, P. M. (2010) *Sorption Processes and Pollution: Conventional and Non-conventional Sorbents for Pollutant Removal from Wastewaters*, *Environnement et développement durable*, Presses universitaires de Franche-Comté, [online] Available from: https://books.google.co.uk/books?id=y06b_mOOrVwC.

Crittenden, B. and Thomas, W. J. (1998) *Adsorption Technology and Design*, Elsevier Science, [online] Available from: <https://books.google.co.uk/books?id=ipDjl2tyXfkC>.

Curtain, C. (2000) Plant Biotechnology—the growth of Australia's algal B-carotene industry, *Australas Biotechnol*, **10**, p. 18.

Curtain, C. C. and Snook, H. (1983) Method for harvesting algae, United States.

Curtain, C. C. and Snook, H. (1985) Method for harvesting algae, Google Patents, [online] Available from: <https://www.google.com/patents/US4554390>.

Curtain, C. C., West, S. M. and Schlipalius, M. (1986) Manufacture of β -carotene from the salt lake alga *Dunaliella salina*; the scientific and technical background, *Australian Journal of Biotechnology*, **1**(3), p. 6.

Dai, M. (1994) The Effect of Zeta Potential of Activated Carbon on the Adsorption of Dyes from Aqueous Solution: I. The Adsorption of Cationic Dyes: Methyl Green and Methyl Violet, *Journal of Colloid and Interface Science*, **164**(1), pp. 223–228, [online] Available from: <http://www.sciencedirect.com/science/article/pii/S002197978471160X>.

Danquah, M. K., Ang, L., Uduman, N., Moheimani, N. and Forde, G. M. (2009) Dewatering of microalgal culture for biodiesel production: exploring polymer flocculation and tangential flow filtration, *Journal of Chemical Technology & Biotechnology*, **84**(7), pp. 1078–1083, [online] Available from: <http://dx.doi.org/10.1002/jctb.2137>.

Danquah, M. K., Gladman, B., Moheimani, N. and Forde, G. M. (2009) Microalgal growth characteristics and subsequent influence on dewatering efficiency, *Chemical Engineering Journal*, **151**(1–3), pp. 73–78, [online] Available from: <http://www.sciencedirect.com/science/article/pii/S1385894709000783>.

Davis, R., Aden, A. and Pienkos, P. T. (2011) Techno-economic analysis of autotrophic microalgae for fuel production, *Applied Energy*, **88**(10), pp. 3524–3531, [online] Available from: <http://www.sciencedirect.com/science/article/pii/S0306261911002406>.

Department of Energy and Climate Change (DECC), (2011) *UK Renewable Energy Roadmap*, [online] Available from: <http://www.decc.gov.uk/assets/decc/11/meeting-energy-demand/renewable-energy/2167-uk-renewable-energy-roadmap.pdf>.

Department of Energy and Climate Change (DECC), (2016) Third Progress Report on the Promotion and Use of Energy from Renewable Sources for the United Kingdom. Article 22 of the Renewable Energy Directive 2009/28/EC, Department of Energy and Climate Change, [online] Available from: https://www.gov.uk/government/uploads/system/uploads/attachment_data/file/493857/3RD_UK_PROGRESS_REPORT_ON_RENEWABLE_ENERGY.pdf.

Demirbaş, A. (2001) Biomass resource facilities and biomass conversion processing for fuels and chemicals, *Energy Conversion and Management*, **42**(11), pp. 1357–1378, [online] Available from: <http://www.scopus.com/inward/record.url?eid=2-s2.0-0035400999&partnerID=40&md5=355144dfd21b0d0fd425f06100990b46>.

Demirbas, M. F. (2011) Biofuels from algae for sustainable development, *Applied Energy*, **88**(10), pp. 3473–3480, [online] Available from: <http://www.sciencedirect.com/science/article/pii/S0306261911000778>.

Diao, H. F., Li, X. Y., Gu, J. D., Shi, H. C. and Xie, Z. M. (2004) Electron microscopic investigation of the bactericidal action of electrochemical disinfection in comparison with chlorination, ozonation and Fenton reaction, *Process Biochemistry*, **39**(11), pp. 1421–1426, [online] Available from: <http://www.sciencedirect.com/science/article/pii/S0032959203002747>.

Dierkes, H., Steinhagen, V., Bork, M., LÜTGE, C. and Knez, Z. (2012) Cell lysis of plant or animal starting materials by a combination of a spray method and decompression for the selective extraction and separation of valuable intracellular materials, Google Patents, [online] Available from: <http://www.google.com/patents/EP2315825B1?cl=en>.

Domínguez, J. R., Beltrán de Heredia, J., González, T. and Sanchez-Lavado, F. (2005) Evaluation of Ferric Chloride as a Coagulant for Cork Processing

Wastewaters. Influence of the Operating Conditions on the Removal of Organic Matter and Settleability Parameters, *Industrial & Engineering Chemistry Research*, American Chemical Society, **44**(17), pp. 6539–6548, [online] Available from: <http://dx.doi.org/10.1021/ie0487641>.

Ebersson, L. (1982) Electron-Transfer Reactions in Organic Chemistry, In Chemistry, V. G. and D. B. B. T.-A. in P. O. (ed.), Academic Press, pp. 79–185, [online] Available from: <http://www.sciencedirect.com/science/article/pii/S0065316008601392>.

Edenhofer, O., Pichs-Madruga, R., Sokona, Y., Kadner, S., Minx, J. C. and Brunner, S. (2014) Technical Summary. In: Climate Change 2014: Mitigation of Climate Change. Contribution of Working Group III to the Fifth Assessment Report of the Intergovernmental Panel on Climate Change, Cambridge University Press, Cambridge, United Kingdom and New York, NY, USA., [online] Available from: http://www.ipcc.ch/pdf/assessment-report/ar5/wg3/ipcc_wg3_ar5_technical-summary.pdf.

Edzwald, J. K. (1993) Coagulation in drinking water treatment: particles, organics and coagulants, *Water Science and Technology*, IWA Publishing, **27**(11), pp. 21–35.

Fajardo, A. R., Cerdan, L. E., Medina, A. R., Fernández, F. G. A., Moreno, P. A. G. and Grima, E. M. (2007) Lipid extraction from the microalga *Phaeodactylum tricornutum*, *European Journal of Lipid Science and Technology*, Wiley Online Library, **109**(2), pp. 120–126.

Faust, S. D. and Aly, O. M. (1998) *Chemistry of Water Treatment, Second Edition*, Taylor & Francis, [online] Available from: <https://books.google.co.uk/books?id=ivLiNH-NjOcC>.

Fehrenbach, R., Comberbach, M. and Petre, J. O. (1992) On-line biomass monitoring by capacitance measurement, *Journal of biotechnology*, Elsevier, **23**(3), pp. 303–314.

Feng, C., Suzuki, K., Zhao, S., Sugiura, N., Shimada, S. and Maekawa, T. (2004) Water disinfection by electrochemical treatment, *Bioresource Technology*, **94**(1), pp. 21–25, [online] Available from: <http://www.sciencedirect.com/science/article/pii/S0960852403003511>.

Fischer, J. E. (1980) Graphite intercalation compounds: Electronic properties and their correlation with chemistry, *Physica B+C*, **99**(1), pp. 383–394, [online] Available from: <http://www.sciencedirect.com/science/article/pii/037843638090265X>.

Foppen, J. W., van Herwerden, M. and Schijven, J. (2007) Measuring and modelling straining of *Escherichia coli* in saturated porous media, *Journal of Contaminant Hydrology*, **93**(1–4), pp. 236–254, [online] Available from: <http://www.sciencedirect.com/science/article/pii/S0169772207000381>.

Frenz, J., Largeau, C., Casadevall, E., Kollerup, F. and Daugulis, A. J. (1989) Hydrocarbon recovery and biocompatibility of solvents for extraction from cultures

of *Botryococcus braunii*, *Biotechnology and Bioengineering*, **34**(6), pp. 755–762, [online] Available from: <http://dx.doi.org/10.1002/bit.260340605>.

Furdin, G. (1998) Exfoliation process and elaboration of new carbonaceous materials, *Fuel*, Elsevier, **77**(6), pp. 479–485.

Gao, S., Yang, J., Tian, J., Ma, F., Tu, G. and Du, M. (2010) Electro-coagulation–flotation process for algae removal, *Journal of Hazardous Materials*, **177**(1–3), pp. 336–343, [online] Available from: <http://www.sciencedirect.com/science/article/pii/S0304389409020081>.

Garnett, P. J. and Treagust, D. F. (1992) Conceptual difficulties experienced by senior high school students of electrochemistry: Electric circuits and oxidation–reduction equations, *Journal of Research in Science Teaching*, Wiley Online Library, **29**(2), pp. 121–142.

Gencer, M. A. and Mutharasan, R. (1979) Determination of biomass concentration by capacitance measurement, *Biotechnology and Bioengineering*, **21**(6), pp. 1097–1103, [online] Available from: <http://dx.doi.org/10.1002/bit.260210616>.

George, N. and Davies, J. T. (1988) Adsorption of microorganisms on activated charcoal cloth: A material with potential applications in biotechnology, *Journal of Chemical Technology & Biotechnology*, **43**(2), pp. 117–129, [online] Available from: <http://dx.doi.org/10.1002/jctb.280430205>.

Gerardo, M. L., Van Den Hende, S., Vervaeren, H., Coward, T. and Skill, S. C. (2015) Harvesting of microalgae within a biorefinery approach: A review of the developments and case studies from pilot-plants, *Algal Research*, **11**, pp. 248–262, [online] Available from: <http://www.sciencedirect.com/science/article/pii/S2211926415300059>.

Ghayal, M. S. and Pandya, M. T. (2013) Microalgae Biomass: A Renewable Source of Energy, *Energy Procedia*, **32**, pp. 242–250, [online] Available from: <http://www.sciencedirect.com/science/article/pii/S1876610213000337>.

Gheraout, D., Naceur, M. W. and Aouabed, A. (2011) On the dependence of chlorine by-products generated species formation of the electrode material and applied charge during electrochemical water treatment, *Desalination*, **270**(1–3), pp. 9–22, [online] Available from: <http://www.sciencedirect.com/science/article/pii/S001191641100021X>.

Goel, J., Kadirvelu, K., Rajagopal, C. and Kumar Garg, V. (2005) Removal of lead(II) by adsorption using treated granular activated carbon: Batch and column studies, *Journal of Hazardous Materials*, **125**(1–3), pp. 211–220, [online] Available from: <http://www.sciencedirect.com/science/article/pii/S0304389405002712>.

Goldemberg, J. (2008) The Brazilian biofuels industry, *Biotechnology for Biofuels*, **1**(1), pp. 1–7, [online] Available from: <http://dx.doi.org/10.1186/1754-6834-1-6>.

Goldemberg, J., Coelho, S. T. and Guardabassi, P. M. (2008) The sustainability of ethanol production from sugarcane BT - Energy Policy, In.

- Goldemberg, J., Coelho, S. T., Lucon, O. S. and Nastari, P. M. (2003) Ethanol learning curve – the Brazilian experience, *Biomass and Bioenergy*, **26**, [online] Available from: [http://dx.doi.org/10.1016/S0961-9534\(03\)00125-9](http://dx.doi.org/10.1016/S0961-9534(03)00125-9).
- Gomathi Priya, P., Ahmed Basha, C. and Ramamurthi, V. (2011) Removal of Ni(II) Using Cation Exchange Resins in Packed Bed Column: Prediction of Breakthrough Curves, *CLEAN – Soil, Air, Water*, WILEY-VCH Verlag, **39**(1), pp. 88–94, [online] Available from: <http://dx.doi.org/10.1002/clen.200900178>.
- Gonçalves, A. L., Ferreira, C., Loureiro, J. A., Pires, J. C. M. and Simões, M. (2015) Surface physicochemical properties of selected single and mixed cultures of microalgae and cyanobacteria and their relationship with sedimentation kinetics, *Bioresources and Bioprocessing*, **2**(1), pp. 1–10, [online] Available from: <http://dx.doi.org/10.1186/s40643-015-0051-y>.
- González-Fernández, C. and Ballesteros, M. (2012) Microalgae autoflocculation: an alternative to high-energy consuming harvesting methods, *J Appl Phycol*, **25**.
- Goshadrou, A. and Moheb, A. (2011) Continuous fixed bed adsorption of C.I. Acid Blue 92 by exfoliated graphite: An experimental and modeling study, *Desalination*, **269**(1–3), pp. 170–176, [online] Available from: <http://www.sciencedirect.com/science/article/pii/S0011916410007733>.
- Greenspan, P., Mayer, E. P. and Fowler, S. D. (1985) Nile red: a selective fluorescent stain for intracellular lipid droplets, *The Journal of cell biology*, **100**(3), p. 965.
- Greenwell, H. C., Laurens, L. M. L., Shields, R. J., Lovitt, R. W. and Flynn, K. J. (2010) Placing microalgae on the biofuels priority list: a review of the technological challenges, *Journal of The Royal Society Interface*, **7**(46), p. 703.
- Grossman, A. R., Croft, M., Gladyshev, V. N., Merchant, S. S., Posewitz, M. C., Prochnik, S. and Spalding, M. H. (2007) Novel metabolism in *Chlamydomonas* through the lens of genomics, *Current opinion in plant biology*, **10**(2), pp. 190–198.
- Günerken, E., D'Hondt, E., Eppink, M. H. M., Garcia-Gonzalez, L., Elst, K. and Wijffels, R. H. (2015) Cell disruption for microalgae biorefineries, *Biotechnology Advances*, **33**(2), pp. 243–260, [online] Available from: <http://www.sciencedirect.com/science/article/pii/S073497501500021X>.
- Gutzeit, G., Lorch, D., Weber, A., Engels, M. and Neis, U. (2005) Bioflocculent algal–bacterial biomass improves low-cost wastewater treatment, *Water science and technology*, IWA Publishing, **52**(12), pp. 9–18.
- Hadjoudja, S., Deluchat, V. and Baudu, M. (2010) Cell surface characterisation of *Microcystis aeruginosa* and *Chlorella vulgaris*, *J Colloid Interface Sci*, **342**(2), pp. 293–299, [online] Available from: <http://www.sciencedirect.com/science/article/pii/S0021979709014143>.
- Halim, R., Danquah, M. K. and Webley, P. A. (2012) Extraction of oil from microalgae for biodiesel production: A review, *Biotechnology Advances*, **30**(3), pp.

709–732, [online] Available from: <http://www.sciencedirect.com/science/article/pii/S0734975012000031>.

Halim, R., Gladman, B., Danquah, M. K. and Webley, P. A. (2011) Oil extraction from microalgae for biodiesel production, *Bioresource Technology*, **102**(1), pp. 178–185, [online] Available from: <http://www.sciencedirect.com/science/article/pii/S0960852410011399>.

Hall, K. R., Eagleton, L. C., Acrivos, A. and Vermeulen, T. (1966) Pore- and Solid-Diffusion Kinetics in Fixed-Bed Adsorption under Constant-Pattern Conditions, *Industrial & Engineering Chemistry Fundamentals*, **5**(2), pp. 212–223, [online] Available from: <http://dx.doi.org/10.1021/i160018a011>.

Hamdaoui, O. (2006) Dynamic sorption of methylene blue by cedar sawdust and crushed brick in fixed bed columns, *Journal of Hazardous Materials*, **138**(2), pp. 293–303, [online] Available from: <http://www.sciencedirect.com/science/article/pii/S0304389406006285>.

Hammer, M. J. (2008) *Water and Wastewater Technology, Pearson international edition*, Pearson/Prentice Hall, [online] Available from: <https://books.google.co.uk/books?id=XVdGAAAYAAJ>.

Han, R., Ding, D., Xu, Y., Zou, W., Wang, Y., Li, Y. and Zou, L. (2008) Use of rice husk for the adsorption of congo red from aqueous solution in column mode, *Bioresource Technology*, **99**(8), pp. 2938–2946, [online] Available from: <http://www.sciencedirect.com/science/article/pii/S0960852407005202>.

Han, R., Wang, Y., Zou, W., Wang, Y. and Shi, J. (2007) Comparison of linear and nonlinear analysis in estimating the Thomas model parameters for methylene blue adsorption onto natural zeolite in fixed-bed column, *Journal of Hazardous Materials*, **145**(1–2), pp. 331–335, [online] Available from: <http://www.sciencedirect.com/science/article/pii/S0304389406014853>.

Han, R., Zou, L., Zhao, X., Xu, Y., Xu, F., Li, Y. and Wang, Y. (2009) Characterization and properties of iron oxide-coated zeolite as adsorbent for removal of copper(II) from solution in fixed bed column, *Chemical Engineering Journal*, **149**(1–3), pp. 123–131, [online] Available from: <http://www.sciencedirect.com/science/article/pii/S1385894708006645>.

Han, Y., Quan, X., Ruan, X. and Zhang, W. (2008) Integrated electrochemically enhanced adsorption with electrochemical regeneration for removal of acid orange 7 using activated carbon fibers, *Separation and Purification Technology*, **59**(1), pp. 43–49, [online] Available from: <http://www.sciencedirect.com/science/article/pii/S1383586607002572>.

Hand, D., Crittenden, J. and Thacker, W. (1984) Simplified Models for Design of Fixed-Bed Adsorption Systems, *Journal of Environmental Engineering*, **110**(2), pp. 440–456, [online] Available from: [http://dx.doi.org/10.1061/\(ASCE\)0733-9372\(1984\)110:2\(440\)](http://dx.doi.org/10.1061/(ASCE)0733-9372(1984)110:2(440)).

Hanova, J., Benemann, J., McMillan, J., Saddler, J. and Agency, I. E. (2010) *Algal Biofuels Status and Prospects, Annual Report 2010 IEA Bioenergy*, Prospects, A. B. S. and (ed.), International Energy Agency.

Hartog, C. den. (1959) *The epilithic algal communities occurring along the coast of the Netherlands*, North Holland Publishing, Amsterdam, [online] Available from: <http://trove.nla.gov.au/work/10253821?q&versionId=11929363>.

Hartono, T., Wang, S., Ma, Q. and Zhu, Z. (2009) Layer structured graphite oxide as a novel adsorbent for humic acid removal from aqueous solution, *Journal of Colloid and Interface Science*, **333**(1), pp. 114–119, [online] Available from: <http://www.sciencedirect.com/science/article/pii/S0021979709001659>.

Hashim, M. A. and Chu, K. H. (2007) Prediction of protein breakthrough behavior using simplified analytical solutions, *Separation and Purification Technology*, **53**(2), pp. 189–197, [online] Available from: <http://www.sciencedirect.com/science/article/pii/S1383586606003169>.

Heasman, M., Diemar, J., O'Connor, W., Sushames, T. and Foulkes, L. (2000) Development of extended shelf-life microalgae concentrate diets harvested by centrifugation for bivalve molluscs – a summary, *Aquaculture Research*, **31**(8–9), pp. 637–659, [online] Available from: <http://dx.doi.org/10.1046/j.1365-2109.2000.318492.x>.

Henderson, R. K., Baker, A., Parsons, S. A. and Jefferson, B. (2008) Characterisation of algogenic organic matter extracted from cyanobacteria, green algae and diatoms, *Water Research*, **42**(13), pp. 3435–3445, [online] Available from: <http://www.sciencedirect.com/science/article/pii/S0043135407006744>.

Henderson, R. K., Parsons, S. A. and Jefferson, B. (2008) Successful Removal of Algae through the Control of Zeta Potential, *Separation Science and Technology*, **43**(7), pp. 1653–1666, [online] Available from: <http://dx.doi.org/10.1080/01496390801973771>.

Henderson, R. K., Parsons, S. A. and Jefferson, B. (2010) The impact of differing cell and algogenic organic matter (AOM) characteristics on the coagulation and flotation of algae, *Water Research*, **44**(12), pp. 3617–3624, [online] Available from: <http://www.sciencedirect.com/science/article/pii/S0043135410002563>.

Henderson, R., Parsons, S. A. and Jefferson, B. (2008) The impact of algal properties and pre-oxidation on solid–liquid separation of algae, *Water Research*, **42**(8–9), pp. 1827–1845, [online] Available from: <http://www.sciencedirect.com/science/article/pii/S004313540700704X>.

Henniges, O. and Zeddies, J. (2004) Competitiveness of Brazilian ethanol in the EU, *FO Licht's World Ethanol and Biofuels Report*, **2**.

Henriques, M., Silva, A. and Rocha, J. (2007) Extraction and quantification of pigments from a marine microalga: a simple and reproducible method, *Communicating Current Research and Educational Topics and Trends in Applied Microbiology*, **2**, pp. 586–593.

- Herrero, M., Cifuentes, A. and Ibanez, E. (2006) Sub-and supercritical fluid extraction of functional ingredients from different natural sources: Plants, food-by-products, algae and microalgae:: A review, *Food chemistry*, **98**(1), pp. 136–148.
- Hibbert, D. B. (1993) *Introduction to Electrochemistry*, Macmillan physical science series, Macmillan, [online] Available from: <https://books.google.co.uk/books?id=80Z4QgAACAAJ>.
- Hoffmann, J. P. (1998) Wastewater treatment with suspended and non-suspended algae, *Journal of Phycology*, **34**(5), pp. 757–763, [online] Available from: <http://dx.doi.org/10.1046/j.1529-8817.1998.340757.x>.
- Hu, Q., Sommerfeld, M., Jarvis, E., Ghirardi, M., Posewitz, M., Seibert, M. and Darzins, A. (2008) Microalgal triacylglycerols as feedstocks for biofuel production: Perspectives and advances, *Plant Journal*, **54**(4), pp. 621–639, [online] Available from: <http://www.scopus.com/inward/record.url?eid=2-s2.0-43549102657&partnerID=40&md5=a79ff2e05b6c8072bc2b71baf3a9ac06>.
- Hu, Y.-R., Wang, F., Wang, S.-K., Liu, C.-Z. and Guo, C. (2013) Efficient harvesting of marine microalgae *Nannochloropsis maritima* using magnetic nanoparticles, *Bioresource Technology*, (0), [online] Available from: <http://www.sciencedirect.com/science/article/pii/S0960852413006202>.
- Huang, G.-H., Chen, G. and Chen, F. (2009) Rapid screening method for lipid production in alga based on Nile red fluorescence, *Biomass and Bioenergy*, **33**(10), pp. 1386–1392, [online] Available from: <http://www.sciencedirect.com/science/article/pii/S0961953409001111>.
- Huang, Y., Holzel, R., Pethig, R. and Wang, X.-B. (1992) Differences in the AC electrodynamics of viable and non-viable yeast cells determined through combined dielectrophoresis and electrorotation studies, *Physics in medicine and biology*, IOP Publishing, **37**(7), p. 1499.
- Hunter, R. J., Ottewill, R. H. and Rowell, R. L. (2013) *Zeta Potential in Colloid Science: Principles and Applications*, Colloid science, Elsevier Science, [online] Available from: <https://books.google.co.uk/books?id=9I3-BAAAQBAJ>.
- Hutchins, R. (1973) New method simplifies design of activated carbon systems., *Chemical Engineering*, **80**(19), pp. 133–138.
- International Energy Agency (IEA), (2015) *World Energy Outlook*, France, [online] Available from: http://www.iea.org/publications/freepublications/publication/WEB_WorldEnergyOutlook2015ExecutiveSummaryEnglishFinal.pdf.
- International Energy Agency (IEA), (2009) *Bioenergy – a sustainable and reliable energy source: A review of status and prospects*, International Energy Agency, [online] Available from: <http://www.ieabioenergy.com/LibItem.aspx?id=6479>.
- Inman, M., Taylor, E. J., McCrabb, H., Kell, J. and Stuart, B. (2012) ElectroConcentration and ElectroFlotation for Dewatering/Water Purification, In *Meeting Abstracts*, The Electrochemical Society, p. 80.

Iverson, S. J., Lang, S. L. C. and Cooper, M. H. (2001) Comparison of the bligh and dyer and folch methods for total lipid determination in a broad range of marine tissue, *Lipids*, **36**(11), pp. 1283–1287, [online] Available from: <http://dx.doi.org/10.1007/s11745-001-0843-0>.

Ives, K. J. (1959) The significance of surface electric charge on algae in water purification, *Journal of Biochemical and Microbiological Technology and Engineering*, Interscience Publishers, Inc., **1**(1), pp. 37–47, [online] Available from: <http://dx.doi.org/10.1002/jbmte.390010105>.

Jarvis, E. E. (2008) *Aquatic Species Program (ASP): Lessons Learned*, National Renewable Energy Laboratory (NREL), Golden, CO.

Jeong, I., Yi, M., Zhao, H. and Dockko, S. (2015) Characteristics of DBPs reduction of AOM by dissolved air flotation, *Desalination and Water Treatment*, **54**(4–5), pp. 1436–1444, [online] Available from: <http://dx.doi.org/10.1080/19443994.2014.917990>.

John, R. P., Anisha, G. S., Nampoothiri, K. M. and Pandey, A. (2011) Micro and macroalgal biomass: A renewable source for bioethanol, *Bioresource Technology*, **102**(1), pp. 186–193, [online] Available from: <http://www.sciencedirect.com/science/article/pii/S0960852410011429>.

Johnson, M. and Wen, Z. (2010) Development of an attached microalgal growth system for biofuel production, *Applied Microbiology and Biotechnology*, Springer-Verlag, **85**(3), pp. 525–534, [online] Available from: <http://dx.doi.org/10.1007/s00253-009-2133-2>.

Jones, C. S. and Mayfield, S. P. (2012) Algae biofuels: versatility for the future of bioenergy, *Current Opinion in Biotechnology*, **23**(3), pp. 346–351, [online] Available from: <http://www.sciencedirect.com/science/article/pii/S0958166911007099>.

Kanda, H. and Li, P. (2011) Simple extraction method of green crude from natural blue-green microalgae by dimethyl ether, *Fuel*, **90**(3), pp. 1264–1266, [online] Available from: <http://www.sciencedirect.com/science/article/pii/S0016236110005971>.

Karunaratne, H. D. S. S. and Amarasinghe, B. M. W. P. K. (2013) Fixed Bed Adsorption Column Studies for the Removal of Aqueous Phenol from Activated Carbon Prepared from Sugarcane Bagasse, *Energy Procedia*, **34**(0), pp. 83–90, [online] Available from: <http://www.sciencedirect.com/science/article/pii/S187661021300979X>.

Kates, M. and Work, T. S. (1972) *Techniques of lipidology: isolation, analysis and identification of lipids*, *Laboratory techniques in biochemistry and molecular biology*, North-Holland Pub. Co., [online] Available from: <https://books.google.co.uk/books?id=f8oAQAAMAAJ>.

Kawai, T., Saito, K., Sugita, K., Katakai, A., Seko, N., Sugo, T., Kanno, J. and Kawakami, T. (2000) Comparison of Amidoxime Adsorbents Prepared by Cografting Methacrylic Acid and 2-Hydroxyethyl Methacrylate with Acrylonitrile onto

Polyethylene, *Industrial & Engineering Chemistry Research*, **39**(8), pp. 2910–2915, [online] Available from: <http://dx.doi.org/10.1021/ie990474a>.

Kay, R. A. and Barton, L. L. (1991) Microalgae as food and supplement, *Critical Reviews in Food Science and Nutrition*, **30**(6), pp. 555–573, [online] Available from: <http://dx.doi.org/10.1080/10408399109527556>.

Khan, M. M. R., Rahman, M. W., Mozumder, M. S. I., Ferdous, K., Ong, H. R., Chan, K. M. and Prasad, D. M. R. (2016) Performance of a submerged adsorption column compared with conventional fixed-bed adsorption, *Desalination and Water Treatment*, **57**(21), pp. 9705–9717, [online] Available from: <http://dx.doi.org/10.1080/19443994.2015.1030779>.

Khoomrung, S., Chumnannpuen, P., Jansa-Ard, S., Ståhlman, M., Nookaew, I., Borén, J. and Nielsen, J. (2013) Rapid Quantification of Yeast Lipid using Microwave-Assisted Total Lipid Extraction and HPLC-CAD, *Analytical Chemistry*, **85**(10), pp. 4912–4919, [online] Available from: <http://dx.doi.org/10.1021/ac3032405>.

Kim, H.-C., Park, S.-J., Lee, C.-G., Kim, S.-B. and Kim, K.-W. (2009) Bacterial attachment to iron-impregnated granular activated carbon, *Colloids and Surfaces B: Biointerfaces*, **74**(1), pp. 196–201, [online] Available from: <http://www.sciencedirect.com/science/article/pii/S0927776509003166>.

Kim, S. G., Choi, A., Ahn, C. Y., Park, C. S., Park, Y. H. and Oh, H. M. (2005) Harvesting of *Spirulina platensis* by cellular flotation and growth stage determination, *Letters in Applied Microbiology*, **40**(3), pp. 190–194.

Klein, J. and Ziehr, H. (1990) Immobilization of microbial cells by adsorption, *Journal of biotechnology*, Elsevier, **16**(1), pp. 1–15.

Knothe, G. (2005) Dependence of biodiesel fuel properties on the structure of fatty acid alkyl esters, *Fuel Processing Technology*, **86**(10), pp. 1059–1070, [online] Available from: <http://www.sciencedirect.com/science/article/pii/S0378382004001894>.

Ko, D. C. K., Porter, J. F. and McKay, G. (2000) Optimised correlations for the fixed-bed adsorption of metal ions on bone char, *Chemical Engineering Science*, **55**(23), pp. 5819–5829, [online] Available from: <http://www.sciencedirect.com/science/article/pii/S0009250900004164>.

Koutinas, A. A., Vlysidis, A., Pleissner, D., Kopsahelis, N., Lopez Garcia, I., Kookos, I. K., Papanikolaou, S., Kwan, T. H. and Lin, C. S. K. (2014) Valorization of industrial waste and by-product streams via fermentation for the production of chemicals and biopolymers, *Chemical Society Reviews*, The Royal Society of Chemistry, **43**(8), pp. 2587–2627, [online] Available from: <http://dx.doi.org/10.1039/C3CS60293A>.

Kraft, A. (2008) Electrochemical Water Disinfection: A Short Review, *Platinum Metals Review*, **52**(3), pp. 177–185, [online] Available from: <http://www.ingentaconnect.com/content/matthey/pmr/2008/00000052/00000003/ar.t00008>.

Kundu, S. and Gupta, A. K. (2007) As(III) removal from aqueous medium in fixed bed using iron oxide-coated cement (IOCC): Experimental and modeling studies, *Chemical Engineering Journal*, **129**(1–3), pp. 123–131, [online] Available from: <http://www.sciencedirect.com/science/article/pii/S1385894706004475>.

Laine, D. F. and Cheng, I. F. (2007) The destruction of organic pollutants under mild reaction conditions: A review, *Microchemical Journal*, **85**(2), pp. 183–193, [online] Available from: <http://www.sciencedirect.com/science/article/pii/S0026265X06001421>.

Largeau, C., Casadevall, E., Berkloff, C. and Dhamelincourt, P. (1980) Sites of accumulation and composition of hydrocarbons in *Botryococcus braunii*, *Phytochemistry*, **19**(6), pp. 1043–1051, [online] Available from: <http://www.sciencedirect.com/science/article/pii/0031942280830548>.

Lee, A. K., Lewis, D. M. and Ashman, P. J. (2009) Microbial flocculation, a potentially low-cost harvesting technique for marine microalgae for the production of biodiesel, *Journal of Applied Phycology*, **21**(5), pp. 559–567, [online] Available from: <http://dx.doi.org/10.1007/s10811-008-9391-8>.

Lee, C.-G., Kim, J.-H., Kang, J.-K., Kim, S.-B., Park, S.-J., Lee, S.-H. and Choi, J.-W. (2014) Comparative analysis of fixed-bed sorption models using phosphate breakthrough curves in slag filter media, *Desalination and Water Treatment*, pp. 1–11, [online] Available from: <http://dx.doi.org/10.1080/19443994.2014.930698>.

Lee, J.-Y., Yoo, C., Jun, S.-Y., Ahn, C.-Y. and Oh, H.-M. (2010) Comparison of several methods for effective lipid extraction from microalgae, *Bioresource Technology*, **101**(1, Supplement 1), pp. S75–S77, [online] Available from: <http://www.sciencedirect.com/science/article/pii/S0960852409003149>.

Lee, S. H., Oh Hm Fau - Jo, B.-H., Jo Bh Fau - Lee, S.-A., Lee Sa Fau - Shin, S.-Y., Shin Sy Fau - Kim, H.-S., Kim Hs Fau - Lee, S.-H., Lee Sh Fau - Ahn, C.-Y. and Ahn, C. Y. (2014) Higher biomass productivity of microalgae in an attached growth system, using wastewater, *Journal of Microbiology and Biotechnology*, Environmental Biotechnology Research Center, Korea Research Institute of Bioscience and Biotechnology (KRIBB), Daejeon 305-806, Republic of Korea. FAU - Oh, Hee-Mock, **24**(11), pp. 1566–1573.

Lee, Y.-C., Lee, K. and Oh, Y.-K. (2015) Recent nanoparticle engineering advances in microalgal cultivation and harvesting processes of biodiesel production: A review, *Bioresource Technology*, **184**, pp. 63–72, [online] Available from: <http://www.sciencedirect.com/science/article/pii/S0960852414015776>.

Lee, Kim, Kwon, Yoon and Oh (1998) Effects of harvesting method and growth stage on the flocculation of the green alga *Botryococcus braunii*, *Letters in Applied Microbiology*, Blackwell Science Ltd, **27**(1), pp. 14–18, [online] Available from: <http://dx.doi.org/10.1046/j.1472-765X.1998.00375.x>.

Leermakers, F., Eriksson, J. C. and Lyklema, H. (2005) Chapter 4 - Association Colloids and their Equilibrium Modelling, In *Soft Colloids*, Science, J. L. B. T.-F. of

I. and C. (ed.), Academic Press, p. 4.1-4.123, [online] Available from: <http://www.sciencedirect.com/science/article/pii/S187456790580008X>.

Lehmann, M., Zouboulis, A. I. and Matis, K. A. (2001) Modelling the sorption of metals from aqueous solutions on goethite fixed-beds, *Environmental Pollution*, **113**(2), pp. 121–128, [online] Available from: <http://www.sciencedirect.com/science/article/pii/S0269749100001743>.

Lepage, G. and Roy, C. C. (1984) Improved recovery of fatty acid through direct transesterification without prior extraction or purification., *Journal of Lipid Research*, ASBMB, **25**(12), pp. 1391–1396.

Li, H., Zhu, X. and Ni, J. (2011) Comparison of electrochemical method with ozonation, chlorination and monochloramination in drinking water disinfection, *Electrochimica Acta*, **56**(27), pp. 9789–9796, [online] Available from: <http://www.sciencedirect.com/science/article/pii/S0013468611012965>.

Li, L., Quinlivan, P. A. and Knappe, D. R. U. (2002) Effects of activated carbon surface chemistry and pore structure on the adsorption of organic contaminants from aqueous solution, *Carbon*, **40**(12), pp. 2085–2100, [online] Available from: <http://www.sciencedirect.com/science/article/pii/S0008622302000696>.

Li, Y.-G., Gao, H.-S., Li, W.-L., Xing, J.-M. and Liu, H.-Z. (2009) In situ magnetic separation and immobilization of dibenzothiophene-desulfurizing bacteria, *Bioresource Technology*, **100**(21), pp. 5092–5096, [online] Available from: <http://www.sciencedirect.com/science/article/pii/S0960852409006336>.

Li, Y., Lian, S., Tong, D., Song, R., Yang, W., Fan, Y., Qing, R. and Hu, C. (2011) One-step production of biodiesel from *Nannochloropsis* sp. on solid base Mg-Zr catalyst, *Applied Energy*, **88**(10), pp. 3313–3317, [online] Available from: <http://www.sciencedirect.com/science/article/pii/S0306261910005775>.

Lin, S. H., Shyu, C. T. and Sun, M. C. (1998) Saline wastewater treatment by electrochemical method, *Water Research*, **32**(4), pp. 1059–1066, [online] Available from: <http://www.sciencedirect.com/science/article/pii/S0043135497003278>.

Lin, Z., Xu, Y., Zhen, Z., Fu, Y., Liu, Y., Li, W., Luo, C., Ding, A. and Zhang, D. (2015) Application and reactivation of magnetic nanoparticles in *Microcystis aeruginosa* harvesting, *Bioresource Technology*, **190**, pp. 82–88, [online] Available from: <http://www.sciencedirect.com/science/article/pii/S0960852415005751>.

Liu, C.-Z., Zheng, S., Xu, L., Wang, F. and Guo, C. (2013) Algal oil extraction from wet biomass of *Botryococcus braunii* by 1,2-dimethoxyethane, *Applied Energy*, **102**, pp. 971–974, [online] Available from: <http://www.sciencedirect.com/science/article/pii/S0306261912005867>.

Van Loosdrecht, M. C., Lyklema, J., Norde, W., Schraa, G. and Zehnder, A. J. (1987) Electrophoretic mobility and hydrophobicity as a measured to predict the initial steps of bacterial adhesion, *Applied and Environmental Microbiology*, **53**(8), pp. 1898–1901.

Lubián, L., Montero, O., Moreno-Garrido, I., Huertas, I. E., Sobrino, C., González-del Valle, M. and Parés, G. (2000) Nannochloropsis (Eustigmatophyceae) as source of commercially valuable pigments, *Journal of Applied Phycology*, **12**(3–5), pp. 249–255, [online] Available from: <http://dx.doi.org/10.1023/A:1008170915932>.

Maeda, Y., Okemoto, Y. and Inagaki, M. (1985) Electrochemical Formation of Graphite-Sulfuric Acid Intercalation Compounds on Carbon Fibers, *Journal of The Electrochemical Society*, **132**(10), pp. 2369–2372, [online] Available from: <http://jes.ecsdl.org/content/132/10/2369.abstract> N2 - The cyclic voltammograms in 98%25 were measured on the mesophase-pitch-based carbon fibers heat-treated at various temperatures. They showed a marked dependence on the heat-treatment temperature of the c.

Maeda, Y., Touzain, P. and Bonnetain, L. (1988) Electrochemical formation of graphite intercalation compound in magnesium chloride-dimethylsulphoxide solution, *Synthetic Metals*, **24**(3), pp. 267–270, [online] Available from: <http://www.sciencedirect.com/science/article/pii/0379677988902652>.

Maji, S. K., Pal, A., Pal, T. and Adak, A. (2007) Modeling and fixed bed column adsorption of As(III) on laterite soil, *Separation and Purification Technology*, **56**(3), pp. 284–290, [online] Available from: <http://www.sciencedirect.com/science/article/pii/S1383586607001165>.

Malvern, I. (2001) Zeta Potential Training Manual, Malvern Instruments, p. 106.

Martínez-Huitle, C. A. and Brillas, E. (2008) Electrochemical Alternatives for Drinking Water Disinfection, *Angewandte Chemie International Edition*, WILEY-VCH Verlag, **47**(11), pp. 1998–2005, [online] Available from: <http://dx.doi.org/10.1002/anie.200703621>.

Mata, T. M., Martins, A. A. and Caetano, N. S. (2010) Microalgae for biodiesel production and other applications: A review, *Renewable and Sustainable Energy Reviews*, **14**(1), pp. 217–232, [online] Available from: <http://www.scopus.com/inward/record.url?eid=2-s2.0-70349505956&partnerID=40&md5=34818fe089d910705a48ee06adafb5c6>.

Matsunaga, T., Nakasono, S., Kitajima, Y. and Horiguchi, K. (1994) Electrochemical disinfection of bacteria in drinking water using activated carbon fibers, *Biotechnology and Bioengineering*, Wiley Subscription Services, Inc., A Wiley Company, **43**(5), pp. 429–433, [online] Available from: <http://dx.doi.org/10.1002/bit.260430511>.

Matsunaga, T., Nakasono, S., Takamuku, T., Burgess, J. G., Nakamura, N. and Sode, K. (1992) Disinfection of drinking water by using a novel electrochemical reactor employing carbon-cloth electrodes, *Applied and Environmental Microbiology*, **58**(2), p. 686.

McKay, G. (1981) Design models for adsorption systems in wastewater treatment, *Journal of Chemical Technology and Biotechnology*, Wiley Online Library, **31**(1), pp. 717–731.

McKay, G. (1995) *Use of Adsorbents for the Removal of Pollutants from Wastewater*, Taylor & Francis, [online] Available from: <https://books.google.co.uk/books?id=ep5bLsOs4lwC>.

McKendry, P. (2002) Energy production from biomass (part 2): conversion technologies, *Bioresource Technology*, **83**(1), pp. 47–54, [online] Available from: <http://www.sciencedirect.com/science/article/pii/S0960852401001195>.

McMillan, J. R., Watson, I. A., Ali, M. and Jaafar, W. (2013) Evaluation and comparison of algal cell disruption methods: Microwave, waterbath, blender, ultrasonic and laser treatment, *Applied Energy*, **103**, pp. 128–134, [online] Available from: <http://www.sciencedirect.com/science/article/pii/S0306261912006605>.

Meng, X., Yang, J., Xu, X., Zhang, L., Nie, Q. and Xian, M. (2009) Biodiesel production from oleaginous microorganisms, *Renewable Energy*, **34**(1), pp. 1–5, [online] Available from: <http://www.sciencedirect.com/science/article/pii/S0960148108001468>.

Mercer, P. and Armenta, R. E. (2011) Developments in oil extraction from microalgae, *European Journal of Lipid Science and Technology*, **113**(5), pp. 539–547, [online] Available from: <http://dx.doi.org/10.1002/ejlt.201000455>.

Merchant, S. S., Prochnik, S. E., Vallon, O., Harris, E. H., Karpowicz, S. J., Witman, G. B., Terry, A., Salamov, A., Fritz-Laylin, L. K., Maréchal-Drouard, L., Marshall, W. F., Qu, L.-H., Nelson, D. R., Sanderfoot, A. A., Spalding, M. H., Kapitonov, V. V., Ren, Q., Ferris, P., Lindquist, E., Shapiro, H., Lucas, S. M., Grimwood, J., Schmutz, J., Cardol, P., Cerutti, H., Chanfreau, G., Chen, C.-L., Cognat, V., Croft, M. T., Dent, R., Dutcher, S., Fernández, E., Fukuzawa, H., González-Ballester, D., González-Halphen, D., Hallmann, A., Hanikenne, M., Hippler, M., Inwood, W., Jabbari, K., Kalanon, M., Kuras, R., Lefebvre, P. A., Lemaire, S. D., Lobanov, A. V., Lohr, M., Manuell, A., Meier, I., Mets, L., Mittag, M., Mittelmeier, T., Moroney, J. V., Moseley, J., Napoli, C., Nedelcu, A. M., Niyogi, K., Novoselov, S. V., Paulsen, I. T., Pazour, G., Purton, S., Ral, J.-P., Riaño-Pachón, D. M., Riekhof, W., Rymarquis, L., Schroda, M., Stern, D., Umen, J., Willows, R., Wilson, N., Zimmer, S. L., Allmer, J., Balk, J., Bisova, K., Chen, C.-J., Elias, M., Gendler, K., Hauser, C., Lamb, M. R., Ledford, H., Long, J. C., Minagawa, J., Page, M. D., Pan, J., Pootakham, W., Roje, S., Rose, A., Stahlberg, E., Terauchi, A. M., Yang, P., Ball, S., Bowler, C., Dieckmann, C. L., Gladyshev, V. N., Green, P., Jorgensen, R., Mayfield, S., Mueller-Roeber, B., Rajamani, S., Sayre, R. T., Brokstein, P., Dubchak, I., Goodstein, D., Hornick, L., Huang, Y. W., Jhaveri, J., Luo, Y., Martínez, D., Ngau, W. C. A., Otilar, B., Poliakov, A., Porter, A., Szajkowski, L., Werner, G., Zhou, K., Grigoriev, I. V., Rokhsar, D. S. and Grossman, A. R. (2007) The *Chlamydomonas* Genome Reveals the Evolution of Key Animal and Plant Functions, *Science*, **318**(5848), pp. 245–250, [online] Available from: <http://science.sciencemag.org/content/318/5848/245.abstract>.

Miao, X. and Wu, Q. (2006) Biodiesel production from heterotrophic microalgal oil, *Bioresource Technology*, **97**(6), pp. 841–846, [online] Available from:

<http://www.scopus.com/inward/record.url?eid=2-s2.0-29944435261&partnerID=40&md5=31996d42f9543ae5f7f72c0ba3c487ce>.

Milledge, J. and Heaven, S. (2012) A review of the harvesting of micro-algae for biofuel production, *Reviews in Environmental Science and Biotechnology*, pp. 1–14, [online] Available from: <http://dx.doi.org/10.1007/s11157-012-9301-z>.

Mitchnick, M. (2012) *An Overview of the Zeta Potential*, [online] Available from: <http://www.particlesciences.com/news/technical-briefs/2012/overview-of-zeta-potential.html>.

Mohammed, F. M., Roberts, E. P. L., Hill, A., Campen, A. K. and Brown, N. W. (2011) Continuous water treatment by adsorption and electrochemical regeneration, *Water Research*, **45**(10), pp. 3065–3074, [online] Available from: <http://www.sciencedirect.com/science/article/pii/S0043135411001345>.

Mohan, D. and Pittman Jr, C. U. (2007) Arsenic removal from water/wastewater using adsorbents—A critical review, *Journal of Hazardous Materials*, **142**(1–2), pp. 1–53, [online] Available from: <http://www.sciencedirect.com/science/article/pii/S0304389407000349>.

Molina Grima, E., Belarbi, E. H., Acien Fernandez, F. G., Robles Medina, A. and Chisti, Y. (2003) Recovery of microalgal biomass and metabolites: process options and economics, *Biotechnology Advances*, **20**(7–8), pp. 491–515.

Mollah, M. Y. A., Morkovsky, P., Gomes, J. A. G., Kesmez, M., Parga, J. and Cocke, D. L. (2004) Fundamentals, present and future perspectives of electrocoagulation, *Journal of Hazardous Materials*, **114**(1–3), pp. 199–210, [online] Available from: <http://www.sciencedirect.com/science/article/pii/S0304389404004170>.

Moreno-Garrido, I. (2008) Microalgae immobilization: Current techniques and uses, *Bioresource Technology*, **99**(10), pp. 3949–3964, [online] Available from: <http://www.sciencedirect.com/science/article/pii/S0960852407004567>.

Mueller, W. (n.d.) Logistic Functions, [online] Available from: http://wmueller.com/precalculus/families/1_80.html (Accessed 20 April 2016).

Mungasavalli, D. P., Viraraghavan, T. and Jin, Y.-C. (2007) Biosorption of chromium from aqueous solutions by pretreated *Aspergillus niger*: Batch and column studies, *Colloids and Surfaces A: Physicochemical and Engineering Aspects*, **301**(1–3), pp. 214–223, [online] Available from: <http://www.sciencedirect.com/science/article/pii/S0927775706009939>.

Mutanda, T., Ramesh, D., Karthikeyan, S., Kumari, S., Anandraj, A. and Bux, F. (2011) Bioprospecting for hyper-lipid producing microalgal strains for sustainable biofuel production, *Bioresource Technology*, **102**(1), pp. 57–70, [online] Available from: <http://www.sciencedirect.com/science/article/pii/S0960852410010588>.

Nagle, N. and Lemke, P. (1990) Production of methyl ester fuel from microalgae, *Applied Biochemistry and Biotechnology*, Springer, **24**(1), pp. 355–361.

- Naik, S. N., Goud, V. V, Rout, P. K. and Dalai, A. K. (2010) Production of first and second generation biofuels: A comprehensive review, *Renewable and Sustainable Energy Reviews*, **14**(2), pp. 578–597, [online] Available from: <http://www.sciencedirect.com/science/article/pii/S1364032109002342>.
- Namasivayam, C. and Kavitha, D. (2002) Removal of Congo Red from water by adsorption onto activated carbon prepared from coir pith, an agricultural solid waste, *Dyes and Pigments*, **54**(1), pp. 47–58, [online] Available from: <http://www.sciencedirect.com/science/article/pii/S0143720802000256>.
- Narbaitz, R. M. and Cen, J. (1994) Electrochemical regeneration of granular activated carbon, *Water Research*, **28**(8), pp. 1771–1778, [online] Available from: <http://www.sciencedirect.com/science/article/pii/004313549490250X>.
- Newcombe, G. and Drikas, M. (1997) Adsorption of NOM onto activated carbon: Electrostatic and non-electrostatic effects, *Carbon*, **35**(9), pp. 1239–1250, [online] Available from: <http://www.sciencedirect.com/science/article/pii/S000862239700078X>.
- Nitta, N., Wu, F., Lee, J. T. and Yushin, G. (2015) Li-ion battery materials: present and future, *Materials Today*, **18**(5), pp. 252–264, [online] Available from: <http://www.sciencedirect.com/science/article/pii/S1369702114004118>.
- Nkrumah-Amoako, K., Roberts, E. P. L., Brown, N. W. and Holmes, S. M. (2014) The effects of anodic treatment on the surface chemistry of a Graphite Intercalation Compound, *Electrochimica Acta*, **135**(0), pp. 568–577, [online] Available from: <http://www.sciencedirect.com/science/article/pii/S0013468614010470>.
- Noel, M. and Santhanam, R. (1998) Electrochemistry of graphite intercalation compounds, *Journal of Power Sources*, **72**(1), pp. 53–65, [online] Available from: <http://www.sciencedirect.com/science/article/pii/S037877539702675X>.
- Olanipekun, O., Oyefusi, A., Neelgund, G. M. and Oki, A. (2014) Adsorption of lead over Graphite Oxide, *Spectrochimica acta. Part A, Molecular and biomolecular spectroscopy*, **118**, pp. 857–860, [online] Available from: <http://www.ncbi.nlm.nih.gov/pmc/articles/PMC4123955/>.
- Olsson, P., Holmbäck, J. and Herslöf, B. (2012) Separation of lipid classes by HPLC on a cyanopropyl column, *Lipids*, **47**(1), pp. 93–99.
- Olu-Owolabi, B. I., Diagboya, P. N. and Ebaddan, W. C. (2012) Mechanism of Pb²⁺ removal from aqueous solution using a nonliving moss biomass, *Chemical Engineering Journal*, **195–196**(0), pp. 270–275, [online] Available from: <http://www.sciencedirect.com/science/article/pii/S138589471200575X>.
- Oss, C. J., Good, R. J. and Chaudhury, M. K. (1988) Additive and nonadditive surface tension components and the interpretation of contact angles, *Langmuir*, **4**, [online] Available from: <http://dx.doi.org/10.1021/la00082a018>.
- Othman, M. Z., Roddick, F. A. and Snow, R. (2001) Removal of dissolved organic compounds in fixed-bed columns: Evaluation of low-rank coal adsorbents, *Water*

Research, **35**(12), pp. 2943–2949, [online] Available from: <http://www.sciencedirect.com/science/article/pii/S0043135400005789>.

Oulman, C. S. (1980) The Logistic Curve as a Model for Carbon Bed Design, *Journal (American Water Works Association)*, American Water Works Association, **72**(1), pp. 50–53, [online] Available from: <http://www.jstor.org/stable/41269892>.

Ozkan, A. and Berberoglu, H. (2013) Adhesion of algal cells to surfaces, *Biofouling*, Taylor & Francis, **29**(4), pp. 469–482, [online] Available from: <http://dx.doi.org/10.1080/08927014.2013.782397>.

Ozkan, A. and Berberoglu, H. (2013) Cell to substratum and cell to cell interactions of microalgae, *Colloids Surf B Biointerfaces*, **112**, [online] Available from: <http://dx.doi.org/10.1016/j.colsurfb.2013.08.007>.

Packer, M. (2009) Algal capture of carbon dioxide; biomass generation as a tool for greenhouse gas mitigation with reference to New Zealand energy strategy and policy, *Energy Policy*, **37**(9), pp. 3428–3437, [online] Available from: <http://www.sciencedirect.com/science/article/pii/S0301421508007623>.

Pandey, A., Lee, D. J., Chisti, Y. and Soccol, C. R. (2013) *Biofuels from Algae*, Elsevier Science, [online] Available from: <https://books.google.co.uk/books?id=2bZhJlq7-N0C>.

Papanikolaou, S. and Aggelis, G. (2011) Lipids of oleaginous yeasts. Part I: Biochemistry of single cell oil production, *European Journal of Lipid Science and Technology*, **113**(8), pp. 1031–1051, [online] Available from: <http://dx.doi.org/10.1002/ejlt.201100014>.

Pastrana-Martínez, L. M., López-Ramón, M. V, Fontecha-Cámara, M. A. and Moreno-Castilla, C. (2010) Batch and column adsorption of herbicide fluroxypyr on different types of activated carbons from water with varied degrees of hardness and alkalinity, *Water Research*, **44**(3), pp. 879–885, [online] Available from: <http://www.sciencedirect.com/science/article/pii/S0043135409006368>.

Patermarakis, G. and Fountoukidis, E. (1990) Disinfection of water by electrochemical treatment, *Water Research*, **24**(12), pp. 1491–1496, [online] Available from: <http://www.sciencedirect.com/science/article/pii/0043135490900831>.

Patravale, V. B., Kulkarni, R. M. and Date, A. A. (2004) Nanosuspensions: a promising drug delivery strategy, *Journal of pharmacy and pharmacology*, Wiley Online Library, **56**(7), pp. 827–840.

Perez, N. (2004) *Electrochemistry and Corrosion Science, Information Technology: Transmission, Processing & Storage*, Springer US, [online] Available from: <https://books.google.co.uk/books?id=k-RaskQEnHMC>.

Phukan, M. M., Chutia, R. S., Konwar, B. K. and Kataki, R. (2011) Microalgae *Chlorella* as a potential bio-energy feedstock, *Applied Energy*, **88**(10), pp. 3307–3312, [online] Available from: <http://www.sciencedirect.com/science/article/pii/S0306261910004897>.

- Pienkos, P. T. and Darzins, A. (2009) The promise and challenges of microalgal derived biofuels, *Biofuels, Bioproducts and Biorefining*, **3**(4), pp. 431–440.
- Pittman, J. K., Dean, A. P. and Osundeko, O. (2011) The potential of sustainable algal biofuel production using wastewater resources, *Bioresource Technology*, **102**(1), pp. 17–25, [online] Available from: <http://www.sciencedirect.com/science/article/pii/S0960852410010163>.
- Poelman, E., De Pauw, N. and Jeurissen, B. (1997) Potential of electrolytic flocculation for recovery of micro-algae, *Resources, Conservation and Recycling*, **19**(1), pp. 1–10, [online] Available from: <http://www.sciencedirect.com/science/article/pii/S0921344996011561>.
- Prabakaran, P. and Ravindran, A. D. (2011) A comparative study on effective cell disruption methods for lipid extraction from microalgae, *Letters in Applied Microbiology*, **53**(2), pp. 150–154, [online] Available from: <http://dx.doi.org/10.1111/j.1472-765X.2011.03082.x>.
- Pragya, N., Pandey, K. K. and Sahoo, P. K. (2013) A review on harvesting, oil extraction and biofuels production technologies from microalgae, *Renewable and Sustainable Energy Reviews*, **24**(0), pp. 159–171, [online] Available from: <http://www.sciencedirect.com/science/article/pii/S1364032113001937>.
- Prathalingam, N. S., Holt, W. W., Revell, S. G., Jones, S. and Watson, P. F. (2006) The precision and accuracy of six different methods to determine sperm concentration, *Journal of andrology*, **27**(2), p. 257.
- Prochazkova, G., Safarik, I. and Branyik, T. (2013) Harvesting microalgae with microwave synthesized magnetic microparticles, *Bioresource Technology*, **130**(0), pp. 472–477, [online] Available from: <http://www.sciencedirect.com/science/article/pii/S0960852412019189>.
- Proctor, A. and Sherwood, P. M. A. (1983) X-ray photoelectron spectroscopic studies of carbon fibre surfaces—II: The effect of electrochemical treatment, *Carbon*, **21**(1), pp. 53–59, [online] Available from: <https://www.scopus.com/inward/record.uri?eid=2-s2.0-0020547224&partnerID=40&md5=632630ac3e8961497374162265f9e72d>.
- Pudipeddi, M., Zannou, E. A., Vasanthavada, M., Dontabhaktuni, A., Royce, A. E., Joshi, Y. M. and Serajuddin, A. T. M. (2016) Measurement of Surface pH of Pharmaceutical Solids: A Critical Evaluation of Indicator Dye-Sorption Method and its Comparison With Slurry pH Method, *Journal of Pharmaceutical Sciences*, Elsevier, **97**(5), pp. 1831–1842, [online] Available from: <http://dx.doi.org/10.1002/jps.21052>.
- Pulz, O. (2001) Photobioreactors: production systems for phototrophic microorganisms, *Appl Microbiol Biotechnol*, **57**, [online] Available from: <http://dx.doi.org/10.1007/s002530100702>.
- Quinlivan, P. A., Li, L. and Knappe, D. R. U. (2005) Effects of activated carbon characteristics on the simultaneous adsorption of aqueous organic micropollutants

and natural organic matter, *Water Research*, **39**(8), pp. 1663–1673, [online] Available from: <http://www.sciencedirect.com/science/article/pii/S0043135405000606>.

Rajkumar, D. and Palanivelu, K. (2004) Electrochemical treatment of industrial wastewater, *Journal of Hazardous Materials*, **113**(1–3), pp. 123–129, [online] Available from: <http://www.sciencedirect.com/science/article/pii/S0304389404003619>.

Rao, A. R., Dayananda, C., Sarada, R., Shamala, T. R. and Ravishankar, G. A. (2007) Effect of salinity on growth of green alga *Botryococcus braunii* and its constituents, *Bioresource Technology*, **98**(3), pp. 560–564, [online] Available from: <http://www.sciencedirect.com/science/article/pii/S0960852406000502>.

Rashid, N., Ur Rehman, M. S., Sadiq, M., Mahmood, T. and Han, J.-I. (2014) Current status, issues and developments in microalgae derived biodiesel production, *Renewable and Sustainable Energy Reviews*, **40**, pp. 760–778, [online] Available from: <http://www.sciencedirect.com/science/article/pii/S1364032114005565>.

Ratlidge, C. and Cohen, Z. (2008) Microbial and algal oils: Do they have a future for biodiesel or as commodity oils, *Lipid Technol*, **20**(7), pp. 155–160.

Rawat, I., Ranjith Kumar, R., Mutanda, T. and Bux, F. (2013) Biodiesel from microalgae: A critical evaluation from laboratory to large scale production, *Applied Energy*, **103**, pp. 444–467, [online] Available from: <http://www.sciencedirect.com/science/article/pii/S0306261912007088>.

Reijnders, L. (2008) Do biofuels from microalgae beat biofuels from terrestrial plants?, *Trends in Biotechnology*, **26**(7), pp. 349–350, [online] Available from: <http://www.sciencedirect.com/science/article/pii/S0167779908001157>.

Reijnders, L. (2009) Microalgal and Terrestrial Transport Biofuels to Displace Fossil Fuels, *Energies*, **2**(1), pp. 48–56, [online] Available from: <http://www.mdpi.com/1996-1073/2/1/48/>.

Richter, B. E., Jones, B. A., Ezzell, J. L., Porter, N. L., Avdalovic, N. and Pohl, C. (1996) Accelerated solvent extraction: a technique for sample preparation, *Analytical Chemistry*, ACS Publications, **68**(6), pp. 1033–1039.

Rittmann, B. E. (2008) Opportunities for renewable bioenergy using microorganisms, *Biotechnology and Bioengineering*, **100**(2), pp. 203–212.

Rivera-Utrilla, J., Bautista-Toledo, I., Ferro-García, M. A. and Moreno-Castilla, C. (2001) Activated carbon surface modifications by adsorption of bacteria and their effect on aqueous lead adsorption, *Journal of Chemical Technology & Biotechnology*, John Wiley & Sons, Ltd., **76**(12), pp. 1209–1215, [online] Available from: <http://dx.doi.org/10.1002/jctb.506>.

Rodolfi, L., Chini Zittelli, G., Bassi, N., Padovani, G., Biondi, N., Bonini, G. and Tredici, M. R. (2009) Microalgae for oil: Strain selection, induction of lipid synthesis and outdoor mass cultivation in a low-cost photobioreactor, *Biotechnology and*

Bioengineering, **102**(1), pp. 100–112, [online] Available from: <http://dx.doi.org/10.1002/bit.22033>.

Rodríguez-Ruiz, J., Belarbi, E.-H., Sánchez, J. L. G. and Alonso, D. L. (1998) Rapid simultaneous lipid extraction and transesterification for fatty acid analyses, *Biotechnology techniques*, Springer, **12**(9), pp. 689–691.

Roeselers, G., Loosdrecht, M. and Muyzer, G. (2008) Phototrophic biofilms and their potential applications, *J Appl Phycol*, **20**, [online] Available from: <http://dx.doi.org/10.1007/s10811-007-9223-2>.

Rosegrant, M. W. (2008) *Biofuels and grain prices: impacts and policy responses*, International Food Policy Research Institute Washington, DC.

Rosenberg, M., Gutnick, D. and Rosenberg, E. (1980) Adherence of bacteria to hydrocarbons: a simple method for measuring cell-surface hydrophobicity, *FEMS Microbiology letters*, Wiley Online Library, **9**(1), pp. 29–33.

Rosenberg, M. and Kjelleberg, S. (1986) Hydrophobic interactions: role in bacterial adhesion, In *Advances in microbial ecology*, Springer, pp. 353–393.

Rouquerol, J., Rouquerol, F., Llewellyn, P., Maurin, G. and Sing, K. S. W. (2013) *Adsorption by powders and porous solids: principles, methodology and applications*, Academic press.

Rozada, F., Calvo, L. F., García, A. I., Martín-Villacorta, J. and Otero, M. (2003) Dye adsorption by sewage sludge-based activated carbons in batch and fixed-bed systems, *Bioresource Technology*, **87**(3), pp. 221–230, [online] Available from: <http://www.sciencedirect.com/science/article/pii/S0960852402002432>.

Saadi, Z., Saadi, R. and Fazaeli, R. (2013) Fixed-bed adsorption dynamics of Pb (II) adsorption from aqueous solution using nanostructured γ -alumina, *Journal of Nanostructure in Chemistry*, Springer, **3**(1), pp. 1–8.

Salim, S., Bosma, R., Vermuë, M. H. and Wijffels, R. H. (2011) Harvesting of microalgae by bio-flocculation, *J Appl Phycol*, **23**(5), pp. 849–855, [online] Available from: <http://dx.doi.org/10.1007/s10811-010-9591-x>.

Salim, S., Shi, Z., Vermuë, M. H. and Wijffels, R. H. (2013) Effect of growth phase on harvesting characteristics, autoflocculation and lipid content of *Ettlia texensis* for microalgal biodiesel production, *Bioresource Technology*, **138**(0), pp. 214–221, [online] Available from: <http://www.sciencedirect.com/science/article/pii/S0960852413005774>.

Salim, S., Vermuë, M. H. and Wijffels, R. H. (2012) Ratio between autoflocculating and target microalgae affects the energy-efficient harvesting by bio-flocculation, *Bioresource Technology*, **118**, pp. 49–55, [online] Available from: <http://www.sciencedirect.com/science/article/pii/S0960852412007493>.

Satyanarayana, K. G., Mariano, A. B. and Vargas, J. V. C. (2011) A review on microalgae, a versatile source for sustainable energy and materials, *International*

Journal of Energy Research, **35**(4), pp. 291–311, [online] Available from: <http://dx.doi.org/10.1002/er.1695>.

Schäfer, K. (1998) Accelerated solvent extraction of lipids for determining the fatty acid composition of biological material, *Analytica Chimica Acta*, **358**(1), pp. 69–77, [online] Available from: <http://www.sciencedirect.com/science/article/pii/S0003267097005874>.

Schenk, P. M., Thomas-Hall, S. R., Stephens, E., Marx, U. C., Mussgnug, J. H., Posten, C., Kruse, O. and Hankamer, B. (2008) Second generation biofuels: high-efficiency microalgae for biodiesel production, *Bioenergy research*, Springer, **1**(1), pp. 20–43.

Sciences, P. N. V.-2 (2012) *Technical Brief, An Overview of the Zeta Potential*.

Scragg, A. H., Morrison, J. and Shales, S. W. (2003) The use of a fuel containing *Chlorella vulgaris* in a diesel engine, *Enzyme and Microbial Technology*, **33**(7), pp. 884–889, [online] Available from: <http://www.sciencedirect.com/science/article/pii/S0141022903002746>.

Senthilkumar, R., Vijayaraghavan, K., Thilakavathi, M., Iyer, P. V. R. and Velan, M. (2006) Seaweeds for the remediation of wastewaters contaminated with zinc(II) ions, *Journal of Hazardous Materials*, **136**(3), pp. 791–799, [online] Available from: <http://www.sciencedirect.com/science/article/pii/S0304389406000288>.

Sharma, K. K., Garg, S., Li, Y., Malekizadeh, A. and Schenk, P. M. (2013) Critical analysis of current Microalgae dewatering techniques, *Biofuels*, **4**(4), pp. 397–407, [online] Available from: <http://www.tandfonline.com/doi/abs/10.4155/bfs.13.25>.

Sheehan, J. (1998) *A look back at the US Department of Energy's aquatic species program: biodiesel from algae*, National Renewable Energy Laboratory Golden, CO.

Sheintuch, M. and Matatov-Meytal, Y. I. (1999) Comparison of catalytic processes with other regeneration methods of activated carbon, *Catalysis Today*, **53**(1), pp. 73–80, [online] Available from: <http://www.sciencedirect.com/science/article/pii/S0920586199001042>.

Shelef, G., Sukenik, A., Green, M. and Institute, S. E. R. (1984) *Microalgae Harvesting and Processing: A Literature Review*, SERI/STR-2, Golden Colorado, Solar Energy Research Institute.

Sing, K. S. W. (1995) Physisorption of nitrogen by porous materials, *Journal of Porous Materials*, Springer, **2**(1), pp. 5–8.

Singh, J. and Gu, S. (2010) Commercialization potential of microalgae for biofuels production, *Renewable and Sustainable Energy Reviews*, Elsevier, **14**(9), pp. 2596–2610.

Singh, A., Chisti, Y. and Banerjee, U. C. (2011) Production of carbonyl reductase by *Metschnikowia koreensis*, *Bioresource Technology*, **102**(22), pp. 10679–10685, [online] Available from: <http://www.sciencedirect.com/science/article/pii/S0960852411013010>.

- Singh, A., Nigam, P. S. and Murphy, J. D. (2011a) Mechanism and challenges in commercialisation of algal biofuels, *Bioresource Technology*, **102**(1), pp. 26–34, [online] Available from: <http://www.sciencedirect.com/science/article/pii/S0960852410010382>.
- Singh, A., Nigam, P. S. and Murphy, J. D. (2011b) Renewable fuels from algae: An answer to debatable land based fuels, *Bioresource Technology*, **102**(1), pp. 10–16, [online] Available from: <http://www.sciencedirect.com/science/article/pii/S0960852410010138>.
- Singh, A. and Olsen, S. I. (2011) A critical review of biochemical conversion, sustainability and life cycle assessment of algal biofuels, *Applied Energy*, **88**(10), pp. 3548–3555, [online] Available from: <http://www.sciencedirect.com/science/article/pii/S0306261910005192>.
- Singh, M., Singh, S., Singh, R. S., Chisti, Y. and Banerjee, U. C. (2008) Transesterification of primary and secondary alcohols using *Pseudomonas aeruginosa* lipase, *Bioresource Technology*, **99**(7), pp. 2116–2120, [online] Available from: <http://www.sciencedirect.com/science/article/pii/S0960852407004580>.
- Singh, T. S. and Pant, K. K. (2006) Experimental and modelling studies on fixed bed adsorption of As (III) ions from aqueous solution, *Separation and Purification Technology*, Elsevier, **48**(3), pp. 288–296.
- Sirmerova, M., Prochazkova, G., Siristova, L., Kolska, Z. and Branyik, T. (2013) Adhesion of *Chlorella vulgaris* to solid surfaces, as mediated by physicochemical interactions, *Journal of Applied Phycology*, Springer Netherlands, pp. 1–9, [online] Available from: <http://dx.doi.org/10.1007/s10811-013-0015-6>.
- Sliwinska-Bartkowiak, M., Drozdowski, H., Kempinski, M., Jazdzewska, M., Long, Y., Palmer, J. C. and Gubbins, K. E. (2012) Structural analysis of water and carbon tetrachloride adsorbed in activated carbon fibres, *Physical Chemistry Chemical Physics*, **14**(19), pp. 7145–7153, [online] Available from: <http://dx.doi.org/10.1039/C2CP22111J>.
- Soto Ayala, R. and Luque de Castro, M. D. (2001) Continuous subcritical water extraction as a useful tool for isolation of edible essential oils, *Food Chemistry*, **75**(1), pp. 109–113, [online] Available from: <http://www.sciencedirect.com/science/article/pii/S0308814601002126>.
- Spolaore, P., Joannis-Cassan, C., Duran, E. and Isambert, A. (2006) Commercial applications of microalgae, *Journal of bioscience and bioengineering*, **101**(2), pp. 87–96, [online] Available from: <http://www.sciencedirect.com/science/article/pii/S1389172306705497>.
- Stoner, G. E., Cahen, G. L., Sachyani, M. and Gileadi, E. (1982) The mechanism of low frequency a.c. electrochemical disinfection, *Bioelectrochemistry and Bioenergetics*, **9**(3), pp. 229–243, [online] Available from: <http://www.sciencedirect.com/science/article/pii/0302459882800135>.

- Subhadra, B. and Grinson, G. (2011) Algal biorefinery-based industry: an approach to address fuel and food insecurity for a carbon-smart world, *Journal of the Science of Food and Agriculture*, **91**(1), pp. 2–13, [online] Available from: <http://dx.doi.org/10.1002/jsfa.4207>.
- Sukenik, A., Bilanovic, D. and Shelef, G. (1988) Flocculation of microalgae in brackish and sea waters, *Biomass*, **15**(3), pp. 187–199, [online] Available from: <http://www.sciencedirect.com/science/article/pii/0144456588900844>.
- Tan, C. H., Show, P. L., Chang, J.-S., Ling, T. C. and Lan, J. C.-W. (2015) Novel approaches of producing bioenergies from microalgae: A recent review, *Biotechnology Advances*, **33**(6, Part 2), pp. 1219–1227, [online] Available from: <http://www.sciencedirect.com/science/article/pii/S0734975015000385>.
- Tang, H., Abunasser, N., Garcia, M. E. D., Chen, M., Simon Ng, K. Y. and Salley, S. O. (2011) Potential of microalgae oil from *Dunaliella tertiolecta* as a feedstock for biodiesel, *Applied Energy*, **88**(10), pp. 3324–3330, [online] Available from: <http://www.sciencedirect.com/science/article/pii/S0306261910003788>.
- Taty-Costodes, V. C., Fauduet, H., Porte, C. and Ho, Y.-S. (2005) Removal of lead (II) ions from synthetic and real effluents using immobilized *Pinus sylvestris* sawdust: Adsorption on a fixed-bed column, *Journal of Hazardous Materials*, **123**(1–3), pp. 135–144, [online] Available from: <http://www.sciencedirect.com/science/article/pii/S0304389405001512>.
- Tchobanoglous, G., Burton, F. L. and Stensel, D. H. (2003) *Wastewater Engineering: Treatment and Reuse/ Metcalf & Eddy Inc*, Fourth (Re, New York, McGraw Hill Higher Education.
- Tenney, M. W., Echelberger Jr, W. F., Schuessler, R. G. and Pavoni, J. L. (1969) Algal flocculation with synthetic organic polyelectrolytes, *Applied and Environmental Microbiology*, **18**(6), p. 965.
- Thatipamala, R. and Hill, G. A. (1991) Spectrophotometric method for high biomass concentration measurements, *Biotechnology and Bioengineering*, **38**(9), pp. 1007–1011, [online] Available from: <http://dx.doi.org/10.1002/bit.260380908>.
- Thomas, H. C. (1948) CHROMATOGRAPHY: A PROBLEM IN KINETICS, *Annals of the New York Academy of Sciences*, **49**(2), pp. 161–182, [online] Available from: <http://dx.doi.org/10.1111/j.1749-6632.1948.tb35248.x>.
- Thomas, H. C. (1944) Heterogeneous Ion Exchange in a Flowing System, *Journal of the American Chemical Society*, **66**(10), pp. 1664–1666, [online] Available from: <http://dx.doi.org/10.1021/ja01238a017>.
- Trzcinski, A. P., Hernandez, E. and Webb, C. (2012) A novel process for enhancing oil production in algae biorefineries through bioconversion of solid by-products, *Bioresource Technology*, **116**, pp. 295–301, [online] Available from: <http://www.sciencedirect.com/science/article/pii/S0960852412005421>.

Tumsri, K. and Chavalparit, O. (2011) Optimizing Electrocoagulation-electroflotation Process for Algae Removal, In *2nd International Conference on Environmental Science and Technology: IPCBEE*.

United States Department of Energy (USDOE), (2010) *National Algal Biofuels Technology Roadmap*, U.S. Department of Energy, Office of Energy Efficiency and Renewable Energy, Biomass Program, [online] Available from: http://www1.eere.energy.gov/biomass/pdfs/algal_biofuels_roadmap.pdf.

Ubbelohde, A. R. (1979) Intercalation Compounds, In *Intercalated Layered Materials*, Lévy, F. (ed.), Dordrecht, Springer Netherlands, pp. 1–31, [online] Available from: http://dx.doi.org/10.1007/978-94-009-9415-7_1.

Uduman, N., Bourniquel, V., Danquah, M. K. and Hoadley, A. F. A. (2011) A parametric study of electrocoagulation as a recovery process of marine microalgae for biodiesel production, *Chemical Engineering Journal*, **174**(1), pp. 249–257, [online] Available from: <http://www.sciencedirect.com/science/article/pii/S1385894711010709>.

Uduman, N., Qi, Y., Danquah, M. K., Forde, G. M. and Hoadley, A. (2010) Dewatering of microalgal cultures: A major bottleneck to algae-based fuels, *Journal of Renewable and Sustainable Energy*, **2**, p. 12701.

Vadivelan, V. and Kumar, K. V. (2005) Equilibrium, kinetics, mechanism, and process design for the sorption of methylene blue onto rice husk, *Journal of Colloid and Interface Science*, **286**(1), pp. 90–100, [online] Available from: <http://www.sciencedirect.com/science/article/pii/S0021979705000081>.

Vandamme, D., Foubert, I. and Muylaert, K. (2013) Flocculation as a low-cost method for harvesting microalgae for bulk biomass production, *Trends Biotechnol*, **31**, [online] Available from: <http://dx.doi.org/10.1016/j.tibtech.2012.12.005>.

Vandamme, D., Muylaert, K., Fraeye, I. and Foubert, I. (2014) Floc characteristics of *Chlorella vulgaris*: Influence of flocculation mode and presence of organic matter, *Bioresource Technology*, **151**(0), pp. 383–387, [online] Available from: <http://www.sciencedirect.com/science/article/pii/S0960852413015447>.

Vandamme, D., Pontes, S. C. V., Goiris, K., Foubert, I., Pinoy, L. J. J. and Muylaert, K. (2011) Evaluation of electro-coagulation–flocculation for harvesting marine and freshwater microalgae, *Biotechnology and Bioengineering*, **108**(10), pp. 2320–2329, [online] Available from: <http://dx.doi.org/10.1002/bit.23199>.

Vieira, F., Cisneros, I., Rosa, N. G., Trindade, G. M. and Mohallem, N. D. S. (2006) Influence of the natural flake graphite particle size on the textural characteristic of exfoliated graphite used for heavy oil sorption, *Carbon*, **44**(12), pp. 2590–2592, [online] Available from: <http://www.sciencedirect.com/science/article/pii/S0008622306003113>.

Wahlen, B. D., Morgan, M. R., McCurdy, A. T., Willis, R. M., Morgan, M. D., Dye, D. J., Bugbee, B., Wood, B. D. and Seefeldt, L. C. (2013) Biodiesel from Microalgae,

Yeast, and Bacteria: Engine Performance and Exhaust Emissions, *Energy & Fuels*, **27**(1), pp. 220–228, [online] Available from: <http://dx.doi.org/10.1021/ef3012382>.

Walker, D. (2009) Biofuels, facts, fantasy, and feasibility, *Journal of Applied Phycology*, **21**(5), pp. 509–517, [online] Available from: <http://dx.doi.org/10.1007/s10811-009-9446-5>.

Walker, G. M. and Weatherley, L. R. (1997) Adsorption of acid dyes on to granular activated carbon in fixed beds, *Water Research*, **31**(8), pp. 2093–2101, [online] Available from: <http://www.sciencedirect.com/science/article/pii/S0043135497000390>.

Wan, C., Alam, M. A., Zhao, X.-Q., Zhang, X.-Y., Guo, S.-L., Ho, S.-H., Chang, J.-S. and Bai, F.-W. (2015) Current progress and future prospect of microalgal biomass harvest using various flocculation technologies, *Bioresource Technology*, **184**, pp. 251–257, [online] Available from: <http://www.sciencedirect.com/science/article/pii/S0960852414016939>.

Wang, F., Yi, J., Wang, Y., Wang, C., Wang, J. and Xia, Y. (2014) Graphite Intercalation Compounds (GICs): A New Type of Promising Anode Material for Lithium-Ion Batteries, *Advanced Energy Materials*, Wiley Online Library, **4**(2).

Weber, T. W. and Chakravorti, R. K. (1974) Pore and solid diffusion models for fixed-bed adsorbers, *AIChE Journal*, **20**(2), pp. 228–238, [online] Available from: <http://dx.doi.org/10.1002/aic.690200204>.

Weng, C.-H. and Hsu, M.-C. (2008) Regeneration of granular activated carbon by an electrochemical process, *Separation and Purification Technology*, **64**(2), pp. 227–236, [online] Available from: <http://www.sciencedirect.com/science/article/pii/S1383586608003870>.

Wiley, P. E., Campbell, J. E. and McKuin, B. (2011) Production of Biodiesel and Biogas from Algae: A Review of Process Train Options, *Water Environment Research*, **83**(4), pp. 326–338, [online] Available from: <http://www.ingentaconnect.com/content/wef/wer/2011/00000083/00000004/art00004>.

Wilson, R. J. and Danner, R. P. (1983) Adsorption of synthesis gas-mixture components on activated carbon, *Journal of Chemical & Engineering Data*, **28**(1), pp. 14–18, [online] Available from: <http://dx.doi.org/10.1021/je00031a005>.

Winsconsin, U. of and Wisconsin, U. of (n.d.) Virtual Microbiology, University of Wisconsin, [online] Available from: http://inst.bact.wisc.edu/inst/index.php?module=Book&func=displayarticle&art_id=107.

Wolborska, A. (1989) Adsorption on activated carbon of p-nitrophenol from aqueous solution, *Water Research*, **23**(1), pp. 85–91, [online] Available from: <http://www.sciencedirect.com/science/article/pii/0043135489900663>.

Wu, Z., Zhu, Y., Huang, W., Zhang, C., Li, T., Zhang, Y. and Li, A. (2012) Evaluation of flocculation induced by pH increase for harvesting microalgae and reuse of

flocculated medium, *Bioresource Technology*, **110**, pp. 496–502, [online] Available from: <http://www.sciencedirect.com/science/article/pii/S0960852412001253>.

Xia, L., Li, H. and Song, S. (2015) Cell surface characterization of some oleaginous green algae, *Journal of Applied Phycology*, pp. 1–10, [online] Available from: <http://dx.doi.org/10.1007/s10811-015-0768-1>.

Xu, H., Miao, X. and Wu, Q. (2006) High quality biodiesel production from a microalga *Chlorella protothecoides* by heterotrophic growth in fermenters, *Journal of Biotechnology*, **126**(4), pp. 499–507, [online] Available from: <http://www.sciencedirect.com/science/article/pii/S0168165606003853>.

Xu, L., Guo, C., Wang, F., Zheng, S. and Liu, C. Z. (2011) A simple and rapid harvesting method for microalgae by in situ magnetic separation, *Bioresource Technology*, **102**(21), pp. 10047–10051.

Xu, L., Wang, F., Li, H.-Z., Hu, Z.-M., Guo, C. and Liu, C.-Z. (2010) Development of an efficient electroflocculation technology integrated with dispersed-air flotation for harvesting microalgae, *Journal of Chemical Technology and Biotechnology*, **85**(11), pp. 1504–1507.

Xu, Z., Cai, J. and Pan, B. (2013) Mathematically modeling fixed-bed adsorption in aqueous systems, *Journal of Zhejiang University SCIENCE A*, Springer, **14**(3), pp. 155–176.

Yahi, H., Elmaleh, S. and Coma, J. (1994) Algal flocculation-sedimentation by pH increase in a continuous reactor, *Water Science and Technology*, **30**(8), pp. 259–267.

Yan, G. and Viraraghavan, T. (2001) Heavy metal removal in a biosorption column by immobilized *M. rouxii* biomass, *Bioresource Technology*, **78**(3), pp. 243–249, [online] Available from: <http://www.sciencedirect.com/science/article/pii/S0960852401000207>.

Yan, G., Viraraghavan, T. and Chen, M. (2001) A New Model for Heavy Metal Removal in a Biosorption Column, *Adsorption Science & Technology*, **19**(1), pp. 25–43, [online] Available from: <http://adt.sagepub.com/content/19/1/25.abstract>.

Yoo, G., Yoo, Y., Kwon, J.-H., Darpito, C., Mishra, S. K., Pak, K., Park, M. S., Im, S. G. and Yang, J.-W. (2014) An effective, cost-efficient extraction method of biomass from wet microalgae with a functional polymeric membrane, *Green Chemistry*, The Royal Society of Chemistry, **16**(1), pp. 312–319, [online] Available from: <http://dx.doi.org/10.1039/C3GC41695J>.

Yoshida, H., Jitsukawa, H. and Galinada, W. A. (2004) Breakthrough and Elution Curves for Adsorption of Phosphates on an OH-Type Strongly Basic Ion Exchanger, *Industrial & Engineering Chemistry Research*, American Chemical Society, **43**(13), pp. 3394–3402, [online] Available from: <http://dx.doi.org/10.1021/ie030547x>.

Zhang, W., Dong, L., Yan, H., Li, H., Jiang, Z., Kan, X., Yang, H., Li, A. and Cheng, R. (2011) Removal of methylene blue from aqueous solutions by straw based adsorbent in a fixed-bed column, *Chemical Engineering Journal*, **173**(2), pp. 429–

436, [online] Available from: <http://www.sciencedirect.com/science/article/pii/S1385894711009296>.

Zhang, X., Amendola, P., Hewson, J. C., Sommerfeld, M. and Hu, Q. (2012) Influence of growth phase on harvesting of *Chlorella zofingiensis* by dissolved air flotation, *Bioresource Technology*, **116**(0), pp. 477–484, [online] Available from: <http://www.sciencedirect.com/science/article/pii/S0960852412005925>.

Zhang, X., Hu, Q., Sommerfeld, M., Puruhito, E. and Chen, Y. (2010) Harvesting algal biomass for biofuels using ultrafiltration membranes, *Bioresource Technology*, **101**(14), pp. 5297–5304, [online] Available from: <http://www.sciencedirect.com/science/article/pii/S0960852410002786>.

Zhong, C., Cao, Y.-X., Li, B.-Z. and Yuan, Y.-J. (2010) Biofuels in China: past, present and future, *Biofuels, Bioproducts and Biorefining*, **4**(3), pp. 326–342, [online] Available from: <http://dx.doi.org/10.1002/bbb.207>.

Zhou, W., Min, M., Hu, B., Ma, X., Liu, Y., Wang, Q., Shi, J., Chen, P. and Ruan, R. (2013) Filamentous fungi assisted bio-flocculation: A novel alternative technique for harvesting heterotrophic and autotrophic microalgal cells, *Separation and Purification Technology*, **107**, pp. 158–165, [online] Available from: <http://www.sciencedirect.com/science/article/pii/S1383586613000452>.